TOWARDS A SMALL MOLECULE INHIBITOR OF LACTATE DEHYDROGENASE-A

Thesis submitted by:
Andrew Philip Lomas
Brasenose College

For the Degree of:
Doctor of Philosophy
Department of Pharmacology
Trinity Term 2011
University of Oxford

Supervisors:
Professor Adrian L. Harris
Doctor Angela J. Russell

For Mum and Dad, you pair of old gits.

ABSTRACT

Lactate Dehydrogenase-A (LDH-A) is up-regulated in a broad array of cancers and is associated with poor prognosis. Involved in the hypoxic response, LDH-A is a HIF-1 target and is responsible for the enzymatic reduction of pyruvate to lactate. This is important for several reasons, chiefly (1) the regeneration of NAD^+ which feeds back into earlier glycolytic stages and (2) the depletion of intracellular pyruvate concentrations. High intracellular pyruvate is known to inhibit HDACs and is associated with increased apoptosis. LDH-A is also known to be controlled by oncogenes such as c-Myc suggesting an oncogenic role. Studies have shown that the knock-out of LDH-A reduces proliferation and tumourgenicity, and stimulates the mitochondria. This thesis therefore had three aims: firstly, to validate LDH-A inhibition and elucidate its full nature in terms of the implications for tumour survival; secondly, to ascertain the role of LDH-B in order to determine whether selectivity towards LDH-A would be a necessary feature of any small molecule; lastly, to recapitulate siRNA mediated LDH-A inhibition with small molecule inhibitors that had the potential for clinical application. The thesis examined both clinical data and a broad panel of cultured cancer cell types in order to select appropriate model in which to validate siRNA mediated inhibition of LDH-A and LDH-B. After it was demonstrated that LDH-A inhibition reduced the growth of cultured cells, a range of techniques were used to quantify this reduced growth in terms of cell death and changes in metabolism. Further to this, literature studies had proposed a role for LDH-B in maintaining lactate fuelled tumour growth; however, this thesis shows that in the cell lines studied, lactate-fuelled tumour

growth was an LDH-A dependent phenomenon. Finally, a high throughput assay system was designed and validated and a library of small molecules was selected, synthesized, and screened in order to identify selective inhibitors of LDH-A.

Submitted for the degree of Doctor of Philosophy in Pharmacology by:

Andrew Philip Lomas

Brasenose College, University of Oxford

Trinity Term 2011

Supervisors:

Professor Adrian L. Harris

Department of Medical Oncology

Weatherall Institute of Molecular Medicine

John Radcliffe Hospital, Headington, OX3 9DS

Doctor Angela J. Russell

Chemistry Research Laboratory

Mansfield Road

Oxford, OX1 3TA

ACKNOWLEDGMENTS

The first thank you must be to Cancer Research UK, and the countless number of volunteers who raise money across the country; without them, this thesis would not have gotten off the ground.

Beyond this, special thanks must go to: Brasenose College for generously providing me with both a Senior Cheetham and Senior Hulme scholarship; Professor Adrian Harris and Doctor Angela Russell, for consistently showing good humour and bags of patience; and Professor Len Seymour who was always free when I needed to have a moan.

I must also thank my friends and colleagues in the Weatherall Institute of Molecular Medicine, the Department of Pharmacology, and Chemistry Research Laboratory. Special mentions in particular are due to Dr Simon Wigfield for sharing a sense of humour as warped as mine, teaching me a huge number of the techniques I used in this thesis, and for his forensic proof-reading; Dr Anna Ramachandran for never failing to bring a ray of sunshine into the lab and providing much needed second pair of eyes; Dr Helen Sheldon for putting up with sitting next to Simon and me; Dr Elena Favaro for being such a byoootifull-a-laydee and for having the patience of a saint; Dr Alan McIntyre for being an Image-J geek and taking my inquiries as to his legitimacy in good part; Dr Dean Singleton for his 'motivational' words of encouragement and boundless cynicism;Dr Karim Bensaad for confirming everything I already thought about the French; Dr Helen Turley for being possibly the nicest person alive; Dr Camillo Quevedo for showing me how to

use GOLD; Dr Killian Huber for help overcoming some of the more intractable synthetic problems; Chris Blick for introducing me to the dark and stormy; Dr Simon Lord for his regular words of wisdom; Rose and Linda for being Rose and Linda; and the Beard for not getting in the way when it mattered. Thanks must also go to the vending machines in the WIMM for pushing me closer to obesity and caffeine dependence than I ever thought possible and the paramedics of South Central Ambulance Service for dealing with the consequences.

Final thanks must go to: my parents for their unending support and checking I was 'eating plenty of fruit' and my sister for her regular encouragement to eat cake instead; Our Old Friend for giving me the opportunity to let my hair down once in a while and the Duke of Marlborough for not pressing charges; and lastly, the electors of Wycombe for making a decision which, whilst obviously misguided, allowed me to finish writing this thesis...

ABBREVIATIONS

%	Percentage
5-FU	5-Fluorouracil
AAT	Aspartate Aminotransferase
ACC	Acetyl-CoA Carboxylase
ACCA	Alpha-Cyano-4-hydroxy Cinnamic Acid
ACL	ATP Citrate Lyase
ADP	Adenosine Diphosphate
Akt	A proto-oncogenic serine/threonine kinase
ALD	Aldolase
ANT	Adenine Nucleotide Transporter
ATP	Adenosine Triphosphate
Bad	Bcl-2 Homologous Antagonist/Killer
Bax	Bcl-2 Associated Protein X
Bcl-2	A regulator of apoptosis
CA9	Carbonic Anhydrase 9
DCA	Dichloro Acetic Acid
DHFR	Dihydrofolate Reductase
DMEM	Dulbecco's Modified Eagle's Medium
DMSO	Dimethyl Sulfoxide
EDTA	Ethylene Diamine Tetra-acetic Acid
ENO	Enolase
ER	Estrogen Receptor

FAS	Fatty Acid Synthase
FCS	Foetal Calf serum
FX11	3-dihydroxy-6-methyl-7-(phenylmethyl)-4-propylnaphthalene-1-carboxylic acid
GAPDH	Glyceraldehyde 3-Phosphate Dehydrogenase
GLS	Glutaminase
GLUT	Glucose Transporter
H&E	Haematoxylin and Eosin
HCl	Hydrochloric Acid
HIF	Hypoxia Inducible Factor
HK	Hexokinase
KCl	Potassium Chloride
KI67	A protein associated with proliferation
LDH	Lactate Dehydrogenase
MCT	Mono Carboxylate Transporter
MDH	Malate Dehydrogenase
ME	Malic Enzyme
MPTP	Mitochondrial Permeability Transition Pore
mTOR	Mammalian Target of Rapamycin
Myc	A proto-oncogenic transcription factor that drives proliferation
NAD+	Nicotinamide Adenine Dinucleotide
NADH	Nicotinamide Adenine Dinucleotide Hydride
OXPHOS	Oxidative Phosphorylation

p53	p53, a tumour suppressor protein
PC	Pyruvate Carboxylase
PDH	Pyruvate Dehydrogenase
PDK	Pyruvate Dehydrogenase Kinase
PEP	Phospho Enol Pyruvate
PFK	Phosphofructokinase
PGI	Phospho Glucose Isomerase
PGK	Phosphoglycerate Kinase
PGM	Phosphoglucomutase
PHD	Prolyl Hydroxylase
PI3K	Phosphoinositide 3-Kinase
PK	Pyruvate Kinase
Ras	A GTPase involved in cell signalling
RB	Retino Blastoma protein, a tumour suppressor protein
Src	A proto-oncogenic tyrosine kinase
TCA Cycle	Tri Carboxylic Acid Cycle
TIGAR	A p53 inducible regulator of glycolysis and apoptosis
TKTL	Transketolase
TPI	Triose Phosphate Isomerase
Tris	Tris(hydroxymethyl)aminomethane
VDAC	Voltage Dependent Anion Channel

TABLE OF CONTENTS

LIST OF FIGURES

LIST OF TABLES AND SCHEMES

CHAPTER 1: GENERAL INTRODUCTION

1.1: CANCER AND CHEMOTHERAPY

Cancer is a disease affecting multiple tissue types which is at heart a pathology of hyperproliferation. In 2001, cancer overtook heart disease as the number one cause of death in men and women in the United Kingdom[1].Globally, cancer accounts for more fatalities than HIV/AIDS, tuberculosis and malaria combined with predictions of 15 million new cases a year by 2020[2].

There are three principal means of treating cancer: surgery, radiotherapy, or chemotherapy. Of these, chemotherapy is used in instances where the disease is unable to be removed by surgery, as an adjuvant (or neo-adjuvant) to surgery, or is otherwise disseminated about the body.

1.2: FROM CYTOTOXICS TO SELECTIVE INHIBITORS; A BRIEF HISTORY OF CANCER CHEMOTHERAPY

The history of medicine is littered with serendipitous discoveries where sharp-eyed investigators have sought to explain an unexpected or counterintuitive result. The field of cancer chemotherapy is no different, and two examples in particular illustrate the broader genesis and evolution of anti-cancer treatments.

[1]http://info.cancerresearchuk.org/news/pressreleases/2003/may/39431 accessed at 1700, 15/07/07
[2]http://www.admin.ox.ac.uk/po/070508.shtml accessed at 1701, 15/07/07

The nitrogen mustards (**Figure 1.1**), a class of compounds more commonly known as mustard gas and developed initially as chemical weapons, were observed to suppress haematopoiesis and as a result used to treat a range of haematological malignancies (Krumbhaar, E.B., 1919).

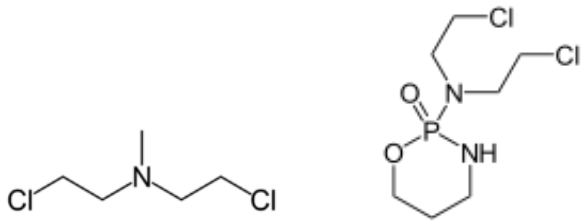

Figure 1.1: the simple nitrogen mustard mustine ((bis(2-chloroethyl)methylamine) and its derivative cyclophosphamide.

Likewise, the discovery of platins (**Figure 1.2**) as a class of anti-cancer agents happened by chance; researchers noticed that *Escherichia coli* grown near platinum electrodes failed to divide, instead reaching up to three hundred times their normal length (Rosenberg, B., *et al*, 1965). This was revealed to be the result of the platinum at the electrode being converted to the compound cis-platin by electrolysis. This use of platins as agents inducing cell-cycle arrest found clinical utility fairly quickly, and platins are still used to treat a wide range of malignancies, particularly testicular and ovarian tumours.

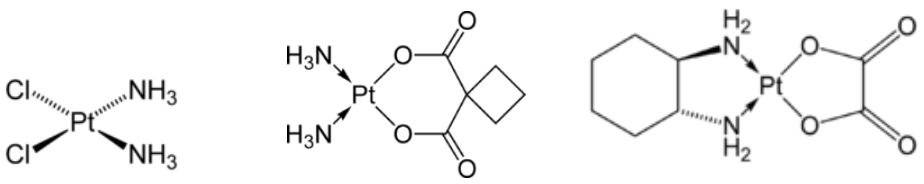

Figure 1.2: cisplatin, carboplatin and oxaliplatin.

Whilst the platins and the nitrogen mustards have been refined and derivatised in order to improve their efficacy, their mode of action is remarkably similar in that they both induce DNA damage by cross-linking nucleotide bases. This occurs via an alkylation reaction (strictly alkylation-like in the case of cisplatin due to the absence of an alkyl group) that results in two nucleotide bases being linked together.

Nitrogen mustards target the nucleophilic N-7 of guanine whilst platins crosslink purines, again commonly guanine (this time in a 1,2 intrastrand manner), though adenine-guanine linkages are also possible. The net effect of this cross-linking is a deformation in the structure of DNA that leads to the inhibition of replication and the arrest of the cell cycle, causing the cell to undergo programmed cell-death.

Aside from alkylating agents, naturally occurring antibiotics such as the anthracyclines epirubicin and daunorubicin, also act directly on nucleic acids (**Figure 1.3**). The mode of action of these compounds arises from their ability to intercalate themselves between strands of DNA, thereby inhibiting replication and potentially inducing cell-death (Minotti G., *et al*, 2004).

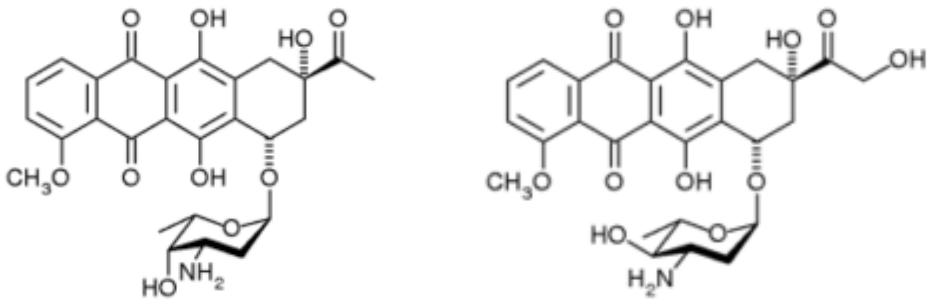

Figure 1.3: the anthracylcines daunorubicin and epirubicin.

Other strategies pursued by early chemotherapeutics had the same goal of general cytotoxicity towards dividing/proliferating cells. In brief these strategies encompass anti-metabolites such as 5-fluorouracil (**Figure 1.4**), a modified nucleotide that combines *in situ* with a cofactor to covalently inactivate dihydrofolate reductase (DHFR), an enzyme critical in nucleotide synthesis, (thereby directly affecting the ability of cells to maintain a proliferative phenotype) (Heidelberger, C., *et al*, 1957); the vinca alkaloids (**Figure 1.5**) that prevent tubulin polymerisation (Starling, D., 1976) and the taxanes (**Figure 1.6**) that prevent tubulin depolymerisation (Wani, N., *et al*, 1977), disrupting cell division through effects on the cytoskeleton; and hormone-based therapies such as tamoxifen (**Figure 1.7**) that antagonise those receptors responsible for the aberrant growth signals responsible for driving many cancers (Terenius, L., 1971).

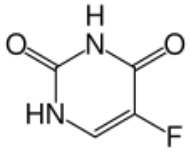

Figure 1.4: 5-fluorouracil, an antimetabolite that acts through inhibiting DHFR.

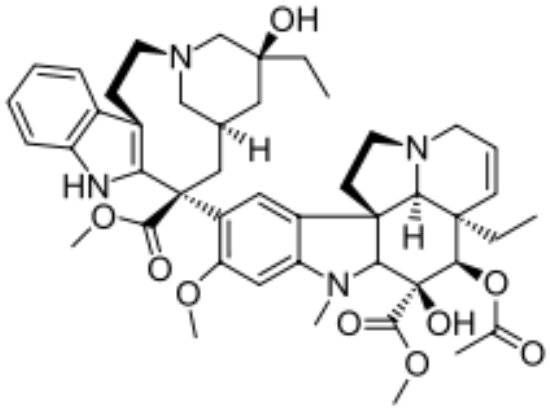

Figure 1.5: the vinca alkaloid vinblastine prevents microtubule polymerisation.

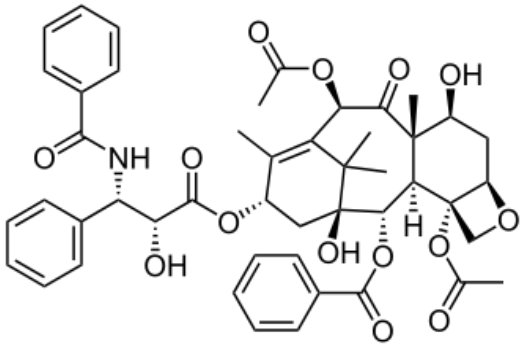

Figure 1.6: the taxane taxol prevents microtubule depolymerisation.

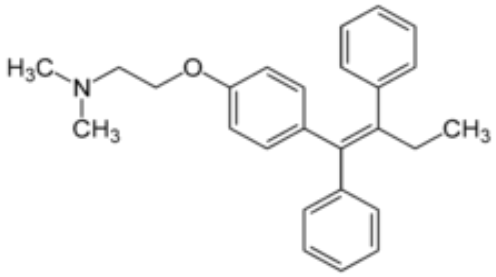

Figure 1.7: tamoxifen antagonises the estrogen receptor.

In short, the experience of these early drugs demonstrated that it is possible to target the higher rate of proliferation of transformed cells vis-à-vis healthy tissue. This approach is not without drawbacks; the direct risk to patients from side-effects such as nephrotoxicity and immunosuppresion, in addition to indirect problems such as reduced patient compliance, combine to maintain a pressure upon medicinal chemistry to produce more selective drugs that, as a result of their greater selectivity, have fewer side effects.

1. 3: THE DRUG DISCOVERY PARADIGM

The shift within medicinal chemistry towards the search for selective compounds can been formalized into a flow diagram otherwise known as the drug discovery paradigm representing the progress from unvalidated target through to screening compounds and finally preclinical trials (**Figure 1.8**).

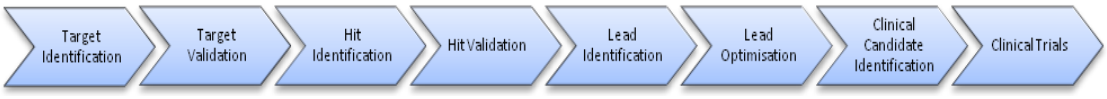

Figure 1.8: the drug discovery paradigm.

This paradigm of course represents an idealised form of an imperfect, messy, and expensive process. The reality is that drug discovery remains more than gently sprinkled with findings that owe much to serendipity and luck. This notwithstanding, the general point remains; anti-cancer drug discovery today focuses on identifying and validating molecular targets before reaching for a round-bottom flask and synthetic chemistry journals.

It is in this context that this thesis set out to find not only a pathway associated with cancer and oncogenesis but also a discrete target within it that if inhibited with a small molecule would elicit a highly selective cytotoxic effect upon cancer cells.

1.4: THE HALLMARKS OF CANCER

The twin problems of side-effects and resistance alone were not sufficient to drive a change in strategy in anti-cancer drug discovery. The catalyst for change has come from a much greater understanding of the molecular basis of oncogenesis and the individual pathways responsible for regulating and controlling cancer.

The boom in genetic science, particularly since the sequencing of the human genome, has opened up whole new fields of research; cancer, as a disease of the genome, has particularly benefited from this.

Whilst the breadth and depth of most cancer research is beyond the scope of this thesis, the most pertinent point that will be of benefit to the reader is that it is possible to categorise the main phenotypic elements of cancer into 'hallmarks' (**Figure 1.9**) (Hanahan, .D, *et al*, 2000).

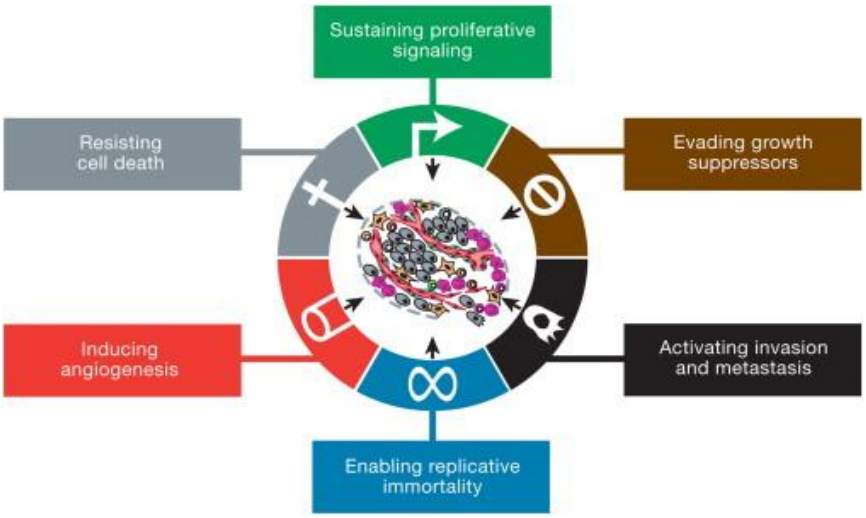

Figure 1.9: the six original hallmarks of cancer (Hanahan, .D, *et al*, 2000).

Recently, the orginal hallmarks have been added to and now include two characteristics that are thought to enable tumour progression and two 'emergent' hallmarks (**Figure 1.10**) (Hanahan, D., *et al*, 2011).

The first hallmark of cancer is the ability to sustain proliferative signalling: cancer as a pathology of hyper-proliferation requires mutations to genes that will drive and sustain this proliferation. There are a variety of strategies that cancers can pursue to achieve this deregulation including the cell manufacturing its own growth factors, over-expressing extracellular growth receptors, or switching the type of receptor expressed. Precedent exists for all of these strategies (Hanahan, D., *et al*, 2000).

Coupled to sustained proliferative signalling is the second hallmark of evading growth suppressors. These factors combined are key to a cancer cell becoming independent of the normal constraints and controls placed upon a healthy cell's growth. The two most commonly documented tumour suppressor proteins are Retinoblastoma (RB) associated protein (Goodrich, D., 2006) and p53 (Levine, A., *et al*, 2009), both of which are documented as being mutated in a broad range of cancers. Many tumours also suffer mutations to the Transforming Growth Factor-β (TGF-β) pathway, a known anti-proliferative pathway (Shi, Y., 2003) further limiting their ability to suppress abnormal growth.

The loss of p53 function also leads to the third hallmark of evading apoptosis; over 50% of human tumours possess a mutation to the tumour suppressor gene *p53* which results in the cell losing a key part of its pro-apoptotic machinery (Harris, C., 1996). This is an important acquired characteristic in that a nascent tumour cell may well acquire the ability to sustain proliferation and be insensitive to those

signals that suppress proliferation, but it will still be vulnerable to programmed cell death. In this instance, either a loss of function in the means to sense those slights to a cell that would ordinarily trigger programmed cell death (DNA damage, hypoxia) or a loss of function in the pathways through which a cell would usually carry out cell death can overcome this.

Fourthly, tumours acquire the ability to maintain telomere length which enables replicative immortality (Shay, J.W., 1997). This effectively delimits the number of replications a cell can perform and therefore further fuels a proliferative phenotype.

In order to grow beyond a certain diameter, it is critical for tumour cells to attract new blood supplies. To do this, tumour cells acquire the ability to induce angiogenesis (Hanahan, D., 1996), often mediated through increased expression of Vascular Endothelial Growth Factor (VEGF).

Invasion and metastasis is also a well established hallmark (Talmadge, J.E., *et al*, 2010) given that over 90% of fatalities from cancer arise from secondary tumours (Sporn, M.B., 1996). For these secondary tumours to arise, cells must not only acquire the ability to invade neighbouring tissues but also to colonise distant sites; whilst these secondary tumours will of course have acquired the preceding 5 hallmarks, they will have additionally acquired the ability for anchorage independent growth.

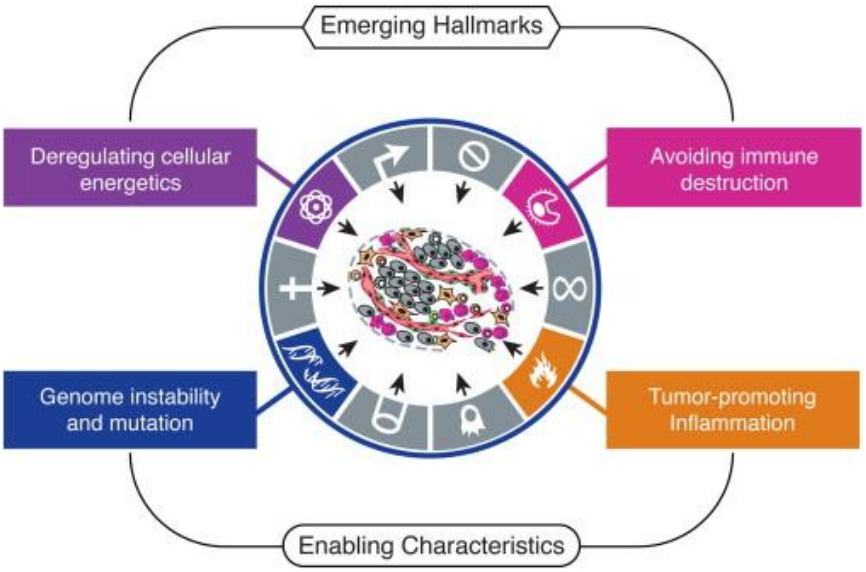

Fig 1.10: emergent hallmarks and enabling characteristics (Hanahan, D., *et al*, 2011).

Beyond the six original hallmarks, reprogrammed cellular metabolism, specifically an increase in aerobic glycolysis, is now seen to be an emergent hallmark (Hanahan, D., *et al*, 2011). As this hallmark provides the focus for this thesis, the key aspects will be covered in greater detail shortly. The second emergent hallmark is the role of the immune system; it seems in many cases that tumours are able to evade immune destruction.

Lastly, two enabling characteristics have now been identified which allow cells to acquire the other hallmarks. Firstly, genomic instability is a driver of mutations. Whilst many mutations may have no effect (or indeed may be detrimental to survival), the existence of increased genomic instability creates the environment for advantageous mutations to occur and the hallmarks to be acquired.

Secondly, an inflammatory microenvironment underpins many of the pre-existing hallmarks in that it provides growth and survival factors whilst generating signals that promote angiogenesis, invasion and metastasis.

1.4.1: TUMOUR HYPOXIA

Alongside the hallmarks of cancer, it is important to consider the phenomenon of tumour hypoxia.

Hypoxia is defined as an oxygen concentration of less than 1% and is associated with a variety of cellular responses (Harris, A.L., 2002). These responses are necessary if a tumour is to grow above 80 μm in diameter as the cell must activate transcriptional pathways that allow it to initially cope with low oxygen and also attract new blood supplies that will go some way to reverse tumour hypoxia.

Many of these pathways are mediated through Hypoxia Inducible Factor-1 (HIF-1), a heterodimer composed of α and β subunits. HIF-1 is the best characterized of the HIF family which also contains HIF-2 and HIF-3. Whilst HIF-1 is expressed across a range of tissue types, HIF-2 expression is restricted to endothelial cells, glial cells, type II pneumocytes, cardiomyocytes, fibroblasts of the kidney, interstitial cells of the pancreas and duodenum, and hepatocytes (Rankin, E.B., *et al*, 2008).Little is known about HIF-3.

The β subunit is also known as the aryl hydrocarbon receptor nuclear translocator (ARNT) and is located in the nucleus.The α subunit is located in the cytosol and under normoxic conditions is post-translationally hydroxylated by prolyl hydroxylases (PHDs) (McNeill, L.A., 2002), allowing it to associate with the Von

Hippel-Lindau (VHL) complex. This in turn causes the α subunit to be ubliquitinylated and leads to its eventual degradation.

In hypoxic cells, the drop in oxygen tension results in PHD being unable to hydroxylate HIF-1α; as a result HIF-1α is not targeted for degradation and remains stably expressed. In this stable form it can translocate to the nucleus where it dimerises with ARNT and binds to hypoxia responsive elements (HREs) within the genome. This in turn leads to the up-regulation of hypoxia related genes and the activation of hypoxia regulated pathways.

1.5: Deregulated Cellular Energetics: the Warburg Effect

As a greater understanding of the molecular basis of cancer has developed, a simultaneous and interrelated shift in the philosophy and methodology of anti-cancer therapeutics has occurred. In short there has been a movement away from general cytotoxic drugs such as the platins and nitrogen mustards towards targeted molecular therapeutics. The emergence of the kinome (Knight, Z.A., 2010) has cemented this paradigm shift with kinases in particular not only underpinning many of the hallmarks of cancer but also offering a rich seam of molecular targets for the medicinal chemist to pursue.

The pursuit of novel, biomolecular anti-cancer targets has been a major factor in driving renewed interest in the Warburg effect (Vander Heiden, M.G., *et al*, 2009). Moreover, it now seems clear that metabolic reconfiguration is integral to oncogenesis in some tumour types (Hanahan, D., *et al*, 2011). This relationship is

underscored by the implication of many oncogenes in this metabolic change with roles for the tumour suppressor p53 (Bensaad, K., 2007) as well as the oncoproteinsPhosphoinositide 3-kinase (PI3K)/Akt, Myc, and Ras(Vander Heiden, M.G., *et al*, 2009) (Kim, J., 2006).

All told then, the changes in cellular carbon flux that alter the molecular fate of pyruvate have sufficient implications in tumour survival and progression to suggest that the tumour metabolome offers biological targets with potential clinical utility.

1.6: TUMOUR METABOLISM; AN OVERVIEW

The Warburg Effect is the phenomenon of elevated aerobic glycolysis in many tumour types and can be defined as an increase in the flux of glucose to lactatewhich is accompanied by a change in the fate of pyruvate (Warburg, O. 1956). Indeed, carbon labeling studies have shown that 90% of glucose is converted to lactate in this way in transformed cells (De Berardinis, R.J., *et al*, 2007). The enzymes of glycolysis convert one molecule of glucose to two molecules of pyruvate using the oxidative potential of NAD^+ to generate 2 molecules of ATP. In the majority of healthy cells pyruvate is then trafficked into the mitochondria and decarboxylated to acetyl coenzyme-A which is cycled through the tricarboxylic acid (TCA) cycle. The TCA cycle generates another 2 molecules of ATP alongside succinate and NADH which are oxidised to fumarate and NAD^++H^+ respectively by oxidative phosphorylation (OXPHOS) generating a further 34 molecules of ATP per glucose. Carbon can be diverted out of glycolysis

into the biosynthetic pentose phosphate pathway whilst TCA cycle intermediates can feed lipid biosynthesis (**Figure 1.11**).

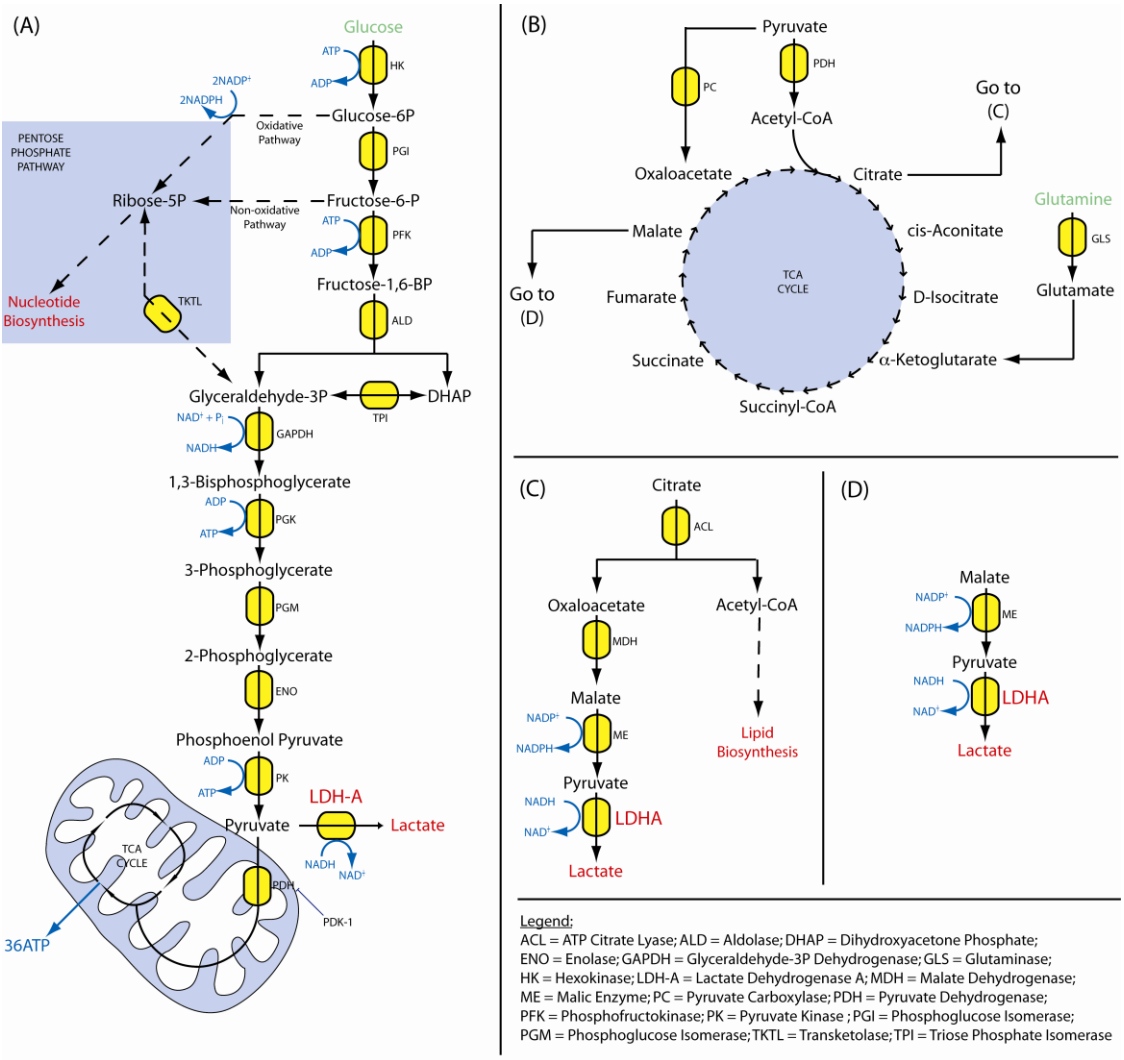

Figure 1.11: [A] glycolysis is the flux of glucose to pyruvate; this pyruvate can then be trafficked into the TCA cycle or reduced to lactate by LDH-A; [B] the TCA cycle sees oxaloacetate combine with acetyl co-A to undergo several interconversions that liberate CO_2, generate reductive intermediates to drive OXPHOS, and ultimately regenerate oxaloacetate. Glutamine can also feed the TCA cycle; [C] citrate can exit the TCA cycle to drive lipid synthesis or produce lactate; [D] Malate can exit the TCA cycle to produce lactate. Green represents metabolic inputs whilst red represents metabolic outputs (and their mediators).

In transformed cells Pyruvate Dehydrogenase Kinase 1 (PDK-1) is upregulated, inactivating Pyruvate Dehydrogenase (PDH) and redirecting pyruvate to lactate via lactate dehydrogenase (LDH) away from the TCA cycle (Wigfield, S.M., *et al*, 2008). This observation is further supported by evidence that shows some tumour cells have a higher mitochondrial membrane potential (Chen, L.B., 1988) which is thought to stem from the lower levels of electron transport (and by extension, OXPHOS) occurring in those tumour cells.

However, from this it cannot be inferred, as originally thought (Warburg, O., 1956), that the Warburg effect arises from mitochondrial defects; many cancers display unaltered mitochondrial physiology and active TCA cycles fed by glutamine and other carbon sources (De Berardinis, R.J., *et al*, 2008). Given that ordinary aerobic metabolism yields 36 molecules of ATP per molecule of glucose, it is readily apparent that the switch away from OXPHOS is not occurring for reasons of increased metabolic efficiency. Why, then, are cells that have competent mitochondria adopting a phenotype that is much less efficient? The answer to this, it seems, must lie beyond bioenergetics and cellular demand for ATP.

1.6.1: Warburg Explained; Acidity or Biomass?

In energetic terms aerobically glycolytic cells do not appear to suffer from the metabolic shift to a Warburg phenotype. Indeed, ATP:ADP ratios remain high as do NADH:NAD^+ ratios (Vander Heiden, M.G., *et al*, 2009). Rather than producing less ATP, the cells have an aggressively increased glucose demand (Gattenby, R.A., *et al*, 2004).

Two of the hallmarks of cancer are increased invasion and increased proliferation; viewed through this prism two theories as to the nature of the Warburg Effect

emerge. The first such theory suggests that increased glycolysis allows enhanced acid production (Gattenby, R.A., *et al*, 2004). This in turn has two effects; it selects for hardier phenotypes amongst the transformed population, specifically towards cells that are resistant to acid toxicity and also facilitates invasion by damaging adjacent healthy tissue. The lowering of extracellular pH (pH_e) is an established phenomenon, evidence that suggests that acidity in the extra-cellular space arises chiefly from carbonic acid and not lactate production (Yamagata, M., *et al*, 1998) though it is likely that both play equally important roles.

The other theory is that it is the increased requirement for proliferation, and by corollary biosynthesis, that drives selection towards the Warburg phenotype (De Berardinis, R.J., *et al*, 2008). This seems to be born out by fact that early glycolysis feeds into the pentose phosphate pathway responsible for nucleotide biosynthesis (**Figure 1.11A**) whilst the TCA cycle feed lipid biosynthesis via citrate. With this in mind, increasing cellular biosynthesis would seem critical to maintaining a proliferative phenotype.

1.6.2: Oncogenic Signaling and Metabolism

Oncogenic signalling and a Warburg-type phenotype are highly integrated (**Figure1.12**). To an extent this is to be expected in the light of transformed cells requiring greater biosynthesis to fuel proliferation. However, in the context of de-convoluting complex pathways with multiple redundancies, it is important to understand this integration in order to better understand weak points in the tumour metabolome.

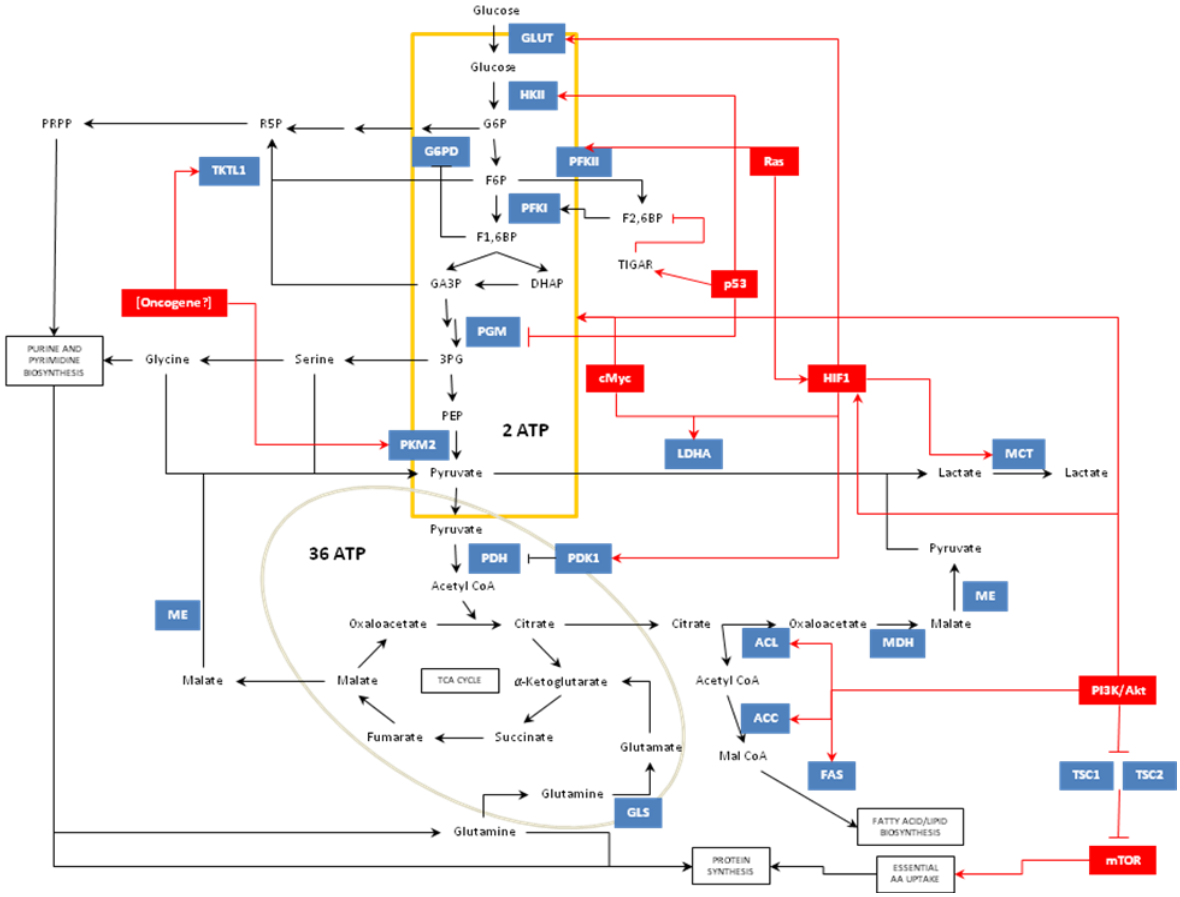

Figure 1.12: metabolism and oncogenic signalling are highly integrated. HIF-1 is responsible for the up-regulation of the enzymes of glycolysis as well as glucose transporters, mono-carboxylate transporters and PDK-1. Oncogenes such as PI3K/Akt, Ras, and c-Myc can promote this response through HIF stabilization and have direct control over the expression of some metabolic enzymes. p53, which is involved in DNA repair, traffics carbon flow away from glycolysis and into the pentose phosphate pathway, promoting nucleotide synthesis, by up-regulating HKII and inactivating PFKI via the TIGAR mediated inhibition of PFKII.

Given that glycolysis is often an adaptive response to low oxygen levels, it is perhaps unsurprising that there is a link between hypoxia inducible factor 1 (HIF-1) (Ke, Q., *et al*, 2006), a transcription factor responsible for upregulating cellular

responses to low oxygen and many metabolic enzymes. HIF-1 up-regulates many of the enzymes involved in glucose metabolism (**Table 1.1)**.

Table 1.1
Glucose metabolism enzymes up-regulated as HIF-1 target genes
Aldolase-A, Aldolase-C, Carbonic anhydrase-9, Enolase-1, Glucose transporter-1, Glucose transporter-3, Hexokinase I, Hexokinase II, Lactate dehydrogenase-A, Pyruvate Kinase M, Phosphofructokinase L, Phosphoglycerate kinase 1, 6-phosphofructo-2-kinase/fructose-2,6-bisphosphatase 3.

Beyond HIF, studies have shown roles for the tumour supressors p53 and VHL as well as the oncoproteins Myc (Semenza, G.L., et al, 1996), Ras and Src (Chan, D.A., *et al*, 2002). Akt, the most frequently activated oncoprotein in human cancer (Bhaskar, P.T., *et al*, 2007) promotes normoxic HIF-1 activation through mTORC1 (Robey, R.B., *et al*, 2009). The broader control of glucose transporters, allosteric regulators of glycolysis, and mitochondrial association of hexokinase by Akt has led some to postulate that Akt may in fact be the 'Warburg kinase' (Robey, R.B., *et al*, 2009).

This view must been seen within the context of other oncogenes that are also implicated in reconfiguring metabolism in transformed cells. Ras operates through PI3K and ultimately through Akt (Lim, K.H., et al, 2005) whilst there is evidence of cooperativity between c-Myc and HIF-1 (Gordan, J.D., *et al*, 2007). Lastly, TIGAR, a p53 inducible gene has been shown to regulate glycolysis (Bensaad, K., *et al*, 2006).

1.6.3: Reconfiguring Metabolism; the Fate of Pyruvate

1.6.3.1: Pyruvate Kinase (PK)

The changing fate of pyruvate is central to the Warburg effect. Pyruvate is formed from the dephosphorylation of Phospho-Enol Pyruvate (PEP) by PK, a reaction that is coupled to the generation of a further molecule of ATP. PEP can also act as a precursor for shikimate metabolism. There are four PK isoforms coded by two separate genes; PKL, PKR, PKM1 and PKM2. PKM1 is almost exclusively expressed in adult tissue whilst the latter's expression is usually restricted to embryonic development (Jurica, M.S., *et al*, 1998). However, transformed cells see a marked change in PK expression, from PKM1 to PKM2 (Mazurek, S., *et al*, 2005).

PK activity is up-regulated by fructose-1,6-bisphosphate leading to greater activity (and therefore greater glycolytic flux) when there is more substrate present. Pyruvate Kinase is also a regulatory enzyme in gluconeogenesis: the phosphorylation of PK inhibits it, causing an accumulation of PEP which is instead converted to glucose (Feliu, J.E., *et al*, 1976). PKM2 is a phospho-tyrosine binding protein; this binding regulates the activity of PKM2 via fructose-1,6-bisphosphate release (Christofk, H.R., *et al*, 2008). PKM2 is the only isoform that exhibits this ability to be allosterically regulated, suggesting that controlling intracellular pyruvate levels is important in transformed cells.

This ability to switch between more and less active forms would seem to have two distinct advantages. Firstly, there is some evidence that high intracellular pyruvate concentrations can trigger apoptosis (Thangaraju, M., *et al*, 2009), so minimizing this possibility is an obvious evolutionary advantage to the transformed cell.

Secondly, in preventing the flow of glucose through to either lactate or the mitochondria, PKM2 control redirects carbon flux to the biosynthetic processes fed by early-stage glycolysis (Mazurek, S, *et al*, 2003),

Given the apparent importance of PKM2 to maintaining a glycolytic phenotype, there are now attempts to selectively target PKM2 with small molecule therapies. The Cantley group in particular has achieved a measure of success (Christofk, H.R., *et al*, 2008) in identifying compounds with low micromolar IC_{50}s.

1.6.3.2: Pyruvate Dehydrogenase (PDH), Pyruvate Dehydrogenase Kinase (PDK), and Mitochondrial Inactivation

In addition to being able to control pyruvate concentrations it is necessary for transformed cells to be able to redirect pyruvate towards Lactate Dehydrogenase (LDH) and away from the mitochondria. PDH catalyses the first step of the conversion of pyruvate to acetyl-coA. The activity of PDH is modulated by two enzymes. PDK phosphorylates PDH, inactivating it, whereas pyruvate dehydrogenase phosphatase (PDP) de-phosphorylates the enzyme back to the active form (Kolobova, E., *et al*, 2001).

There are 4 mammalian isoforms of PDK (Gudi, R., *et al*, 1995). PDK-2 is the most common form, PDK-3 has the highest specific activity and PDK-4 is up-regulated in response to starvation. PDK-1 is a HIF-1 target (Kim, J., *et al*, 2006), with expression increased under hypoxia- normally the expression of PDK-1 is limited to the heart muscle (Bowker-Kinley, M.M., *et al*, 1998).

The up regulation of PDK-1 prevents the conversion of pyruvate to acetyl coA and promotes the pyruvate to lactate reaction catalysed by LDH; high levels of lactate

further promote and activate HIF (Koukourakis, M.I., *et al*, 2001). It can therefore be postulated that inhibiting PDK-1 would have the effect of both improving PDH activity in normoxic cells and reducing cellular lactate thereby reducing the aggressive growth of a tumour; work with siRNA has begun to validate this approach (Wigfield, S.M., *et al*, 2008). Dichloroacetate (DCA) is currently in Phase II trials as a PDK-1 inhibitor after showing a marked effect on tumour growth in earlier studies (Tennant, D.A., *et al*, 2010).

1.7: Metabolic Choke Points as Potential Therapeutic Targets

If metabolic pathways are complex and interconnected, the focus for drug discovery must arguably be on the biological targets whose role is critically implicated in tumour survival. In short, to have a global effect with a small molecule therapeutic, one must seek out not only important pathways, but choke points on those pathways in order to have a sufficient impact. PKM2 and PDK-1 are already described examples of targets that are critically important to tumour survival.

Where broader tumour metabolism is concerned, a focus on choke points would appear to yield three distinct strategies; blocking metabolite transport, blocking early stage metabolism and disrupting cellular redox competence.

1.7.1: BLOCKING TRANSPORT

In terms of glucose influx and lactate efflux, there are two main targets; glucose transporters and mono-carboxylate transporters which taken together form parentheses around the metabolism of glucose to lactate. Glutamine transporters may also be considered as worthy of investigation given the high rate of glutamine utilisation (DeBerardinis, R.J., *et al*, 2007) by many tumours. However, given the role of glutamine transport in sustaining neurotransmitter synthesis and maintaining nervous processes, glutamine transporters are probably precluded for the forseeable future from drug development.

1.7.1.1: GLUCOSE TRANSPORTER (GLUT)

Whilst the switch to glycolysis reduces the demand for oxygen, there is a cost in terms of metabolic efficiency: glycolysis produces 2 ATP molecules per glucose as opposed to the 38 molecules of ATP per glucose that aerobic respiration can potentially yield. To cope with these energy demands the growing tumour cell must take up much more glucose than healthy tissue: *in vivo*, tumours show an increase in glucose uptake compared to normal tissue of approximately one order of magnitude (Younes, M., *et al*, 1996).

GLUTs are integral transmembrane proteins with several isoforms (**Table 1.2**) (Gould, G.W., *et al*, 1993). Tumours experience an up-regulation of GLUTs, specifically GLUT1 and GLUT3, with high levels of GLUT1 expression associated with increased proliferative activity**,** decreased differentiation and poor prognosis (Macheda, M., *et al*, 2005).

Table 1.2		
Mammalian isoforms of GLUT		
Isoform	**Isoenzyme**	**Tissue**
GLUT1	erythrocyte-type glucose transporter	placenta; brain; blood-tissue barrier; adipose and muscle tissue (low levels); tissue culture cells; transformed cells
GLUT2	liver-type glucose transporter	liver; pancreatic β-cell; kidney proximal tubule and small intestine (basolateral membrane)
GLUT3	brain-type glucose transporter	brain; nerve; kidney, liver and heart (low levels)
GLUT4	insulin-responsive glucose transporter	muscle, heart and adipose tissue
GLUT5	small-intestine sugar transporter	small intestine(apical membranes); brain, muscle (both low levels) and adipose tissue

GLUT1 is stimulated by most if not all mitogens and by low glucose levels (Gould, G.W., *et al*, 1993). Up-regulation of GLUT1 and GLUT3 under hypoxic conditions is controlled by HIF-1α (Chen, C., *et al*, 2001) whilst Ras and Src have also been shown to increase GLUT1 expression (Murakami, T., et al, 1992). The expression of GLUT1 in tumour cells promotes tumour survival whilst knocking down glucose transport with phloretin has been shown to overcome drug resistance (Cao, X., *et al*, 2007).

GLUT1 and GLUT3 have a high affinity for glucose and this may provide a rationale for their up-regulation in transformed cells opposed to GLUT2 and GLUT5, which have lower affinities (very low affinity in the case of GLUT5) and which are suppressed in transformed cells (Baron-Delage, S., *et al*, 1996). Furthermore, GLUT1 experiences kinetic asymmetry, that is to say that glucose influx exceeds

efflux: it has been proposed that this allows GLUT1 to effectively act as a unidirectional transporter (Gould, G.W., *et al*, 1993).

There is evidence that different cancers may increase the expression of different isoforms: for example, not all cancers up-regulate GLUT1: GLUT12, a novel isoform, was recently discovered as being expressed in these tissues as an alternate or complementary glucose transporter (Rogers, S., *et al*, 2002). Furthermore GLUT5, which is a high affinity fructose/low affinity glucose transporter is expressed in some breast cancer cell lines but not in healthy breast tissue (Zamora-Leon, S.P., *et al*, 1996) suggesting a possible demand for fructose in some tumours.

GLUT1 deficiency syndrome has been characterised and is a rare autosomal dominant disorder (Seidner, G., *et al*, 1998) resulting in poor glucose transport across the blood-brain barrier. The problem of selectively targeting only tumour GLUT expression is not easily resolved. Additionally, there is a requirement to avoid GLUT1 deficiency syndrome-like side effects should any drug based on GLUT be developed. These points notwithstanding, there is potentially utility to be derived in investigating strategies to inhibit GLUTs providing sufficient selectivity between isoforms can be leveraged.

1.7.1.2: MONO CARBOXYLATE TRANSPORTERS (MCT)

MCTs are transmembrane transporters that allow the diffusion of small organic acids bearing a carboxyl moiety (lactic acid, pyruvic acid, butyric acid). Genomic analysis has revealed 14 putative MCT isoforms yet only MCT1-4 have been functionally identified as lactate transporters (Price, N.T., *et al*, 1998). MCTs are upregulated in a broad range of cancers (Pinheiro, C., *et al*, 2010). MCT1 and MCT4

are upregulated under hypoxic conditions by HIF-1 (Perez de Heredia, F., *et al*, 2009).

What is of further interest is the emergent idea of cooperativity between different MCT isoforms. In short, there is evidence to suggest that lactate produced by glycolysis in the poorly oxygenated tumour core is being exported by MCT-4 before being taken up by MCT-1 in cells on the periphery for use in OXPHOS to fuel growth (Sonveaux, P., *et al*, 2008).

This revelation has sparked interest in targeting this lactate-fuelled cancer growth. Several studies utilizing α-cyano-4-hydroxy cinnamic acid (ACCA), a non-specific MCT inhibitor, have shown this approach to have promise (Sonveaux, P., *et al*, 2008). The question moving forward will be whether there is significant room for generating selectivity between isoforms. Moreover, which isoform will prove the best target will depend on whether lactate-uptake is more critical to survival or whether the toxic accumulation of lactate in cells is a better strategy.

1.7.2: BLOCKING EARLY STAGE METABOLISM

1.7.2.1: HEXOKINASE (HK)

HK catalyses the first step of glycolysis, the conversion of glucose to glucose-6-phosphate (G6P), a step which is coupled to the dephosphorylation of ATP to ADP. HK levels are amplified up to five times in hepatoma cell lines (Rempel, A., *et al*, 1996). There are 4 isoforms of HK with HKII being the predominant isoform up-regulated in cancer (Mathupala, S.P., *et al*, 2006). HKI-III have a high affinity for glucose whereas HKIV (glucokinase) has a low affinity.

Normal mammalian tissues express very little HKII. During tumourigenesis those tissues that express HKIV see a suppression of HKIV and an up-regulation of HKII (and to some extent HKI) (Rempel, A., *et al*, 1994) (Mathupala, S.P., *et al*, 1997) (Pederson, P.L., *et al*, 2002). This up-regulation is at the transcriptional level and occurs via activation and up-regulation of the HKII gene promoter. Activation of the HK gene promoter is mediated by glucose, insulin, glucagons and cAMP analogues(Mathupala, S.P., *et al*, 2006). HKII is also a HIF-1α target indicating that HKII is upregulated in response to hypoxia (Ke, Q., *et al*, 2006).

A mutated p53 allele can stimulate the transcription of HKII promoter (Mathupala, S.P., *et al*, 1997) suggesting a role for mutant p53 in tumour metabolism whilst p53 may also act as a direct hypoxia responsive transcription factor given that it is stabilised by, and interacts with, HIF-1α (An, W., *et al*, 1998).

An important feature of HKs is that they are coupled to partner molecules. The first partner molecule to consider is GLUT, which is unsurprising given that GLUT facilitates the cellular availability of HK's substrate. A second partner molecule is the mitochondrial membrane protein voltage dependent anion channel (VDAC) which binds HK and has the effect of localising most HK at the mitochondrial membrane, especially in highly glycolytic tumours (Mathupala, S.P., *et al*, 2006). Two final partners are ATP synthase which is bound to the inner mitochondrial membrane and the adenine nuclear translocator (ANT) which transports ATP to the VDAC-HKII complex. ANT exists in three isoforms (I-III) but it is ANTII that is primarily over-expressed in malignant tissues (Chevrollier, A., *et al*, 2005). VDAC and ANT form what is referred to as the mitochondrial permeability transition pore (MPTP) complex: the MPTP is implicated in apoptotic pathways.

The binding of HK to the VDAC allows HK direct access to ATP synthesised by mitochondrial ATP synthase as VDACs are the primary means for adenine nucleotides to cross the outer mitochondrial membrane (Arora, K.K., *et al*, 1998). There is evidence to suggest that some cancers experience enhanced VDAC expression (Shinohara, Y., *et al*, 2000). Though there are several VDAC isoforms, VDAC-1 is by far the most abundant and provides the binding site for many mitochondrial associated proteins including HK.

Furthermore, the binding of HKs to VDAC has been implicated in preventing apoptosis (Pastorino, J.G., *et al*, 2003) with disruption of HK-VDAC binding shown to enhance apoptosis in tumours (Zaid, H. *et al*, 2005). This arises due to HK competing with the protein Bax for binding to VDAC causing the MPTP to remain closed; this in turn prevents cytochrome C release and apoptosis. Several factors have been identified in regulating the HK-VDAC interaction including lactate, ATP/ADP, glucose/glucose-6P, pH, and signalling cascades involving protein kinase B (Gauthier, T., *et al*, 1990) (Miccoli, L., *et al*, 1996).

VDAC bound HK prevents apoptosis by inhibiting the formation of MPTP (Cheng, E.H.Y., *et al*, 2003). HK binding to VDAC prevents the localisation of pro-apoptotic proteins at the mitochondrial membrane (Pastorino, J.G., *et al*, 2003). The binding of pro-apoptotic proteins such as Bax or Bad has been described in the literature as causing an opening of the MPTP. This causes a release of cytochrome c which activates caspases resulting in cell death. On the other hand, the binding of Bcl-XL, a member of the same family of proteins as Bax and Bad, has the effect of closing the VDAC and preventing apoptosis (Halestrap, A.P., *et al*, 2000).

Given that HK-VDAC binding prevents apoptosis, the HK-VDAC interaction presents itself as an attractive target for an anti-cancer strategy. A range of small molecule drugs that inhibit HK activity (lonidamine) or interfere with HK-VDAC binding (clotrimazole, bifonazole) exist(Mathupala, S.P., *et al*, 2006). Another strategy is that employed by 3-bromopyruvate, an anti-metabolite, which is highly effective against rat hepatoma cells as a substrate analogue against advanced cancers but without adverse side effects (Ko, Y.H., *et al*, 2004).

1.7.2.2: THE PHOSPHOFRUCTOKINASES

Phosphofructokinase-1 (PFK-1)

PFK-1 catalyses the irreversible conversion of fructose-6-phosphate (F6P) to fructose-1,6-bisphosphate (F1,6BP). Whilst not the first step of glycolysis, the conversion of F6P to F1,6BP is the first irreversible step and marks a metabolic commitment to glycolysis. PFK-1 is therefore a key enzymatic control point dictating the rate of glycolytic flux (Weber, G., *et al*, 1977). Alternate metabolic paths for F6P include entry into the pentose phosphate pathway and nucleotide synthesis, or entry into fructose and mannose metabolism.

There are five PFK-1 isoenzymes, composed of a tetrameric assembly of M (muscle-type) or L (liver-type) subunits. Muscle and liver cells exclusively express the homotetrameric M_4 and L_4 isoforms respectively whereas erythrocytes express all five possible combinations (M_4, L_3M_1, L_2M_2, M_1L_3, L_4) (Vora, S., *et al*, 1985). PFK-1 is inhibited by citrate (from the TCA cycle), low pH, glucagon, and ATP. PFK-1 activity is notably increased in transformed cells (Sanchez-Martinez, C., *et al*, 1997) (Hennipman, A., *et al*, 1987) (Hennipman, A., *et al*, 1988) and PFK-1 is activated by oncogenicRas and Src (Kole, H.K., *et al*, 1991) (Bosca, L., *et al*,1996).

Phosphofructokinase-2

PFK-2 is a bi-functional enzyme better described as 6-phosphofructo-2-kinase/fructose-2,6-bisphosphatase (PFKFB). PFKFBs are responsible for maintaining a steady-state concentration of fructose-2,6-bisphospate (F2,6BP) via the phosphorylation of F6P to F2,6BP and the dephosphorylation of F2,6BP back to F6P (Okar, D.A., *et al*, 2004) (Okar, D.A., *et al*, 2001) (Okar, D.A., *et al*, 2004).

F2,6BP is an allosteric activator of PFK-1, increasing the affinity of PFK-1 for its substrate on binding (Van Schaftingen, E., *et al*, 1980). F2,6BP can also relieve PFK-1 of inhibition by ATP, allowing transformed cells to maintain a high rate of glycolytic flux in the presence of ATP (Chesney, J., *et al*, 2006) (**Figure 1.13**).

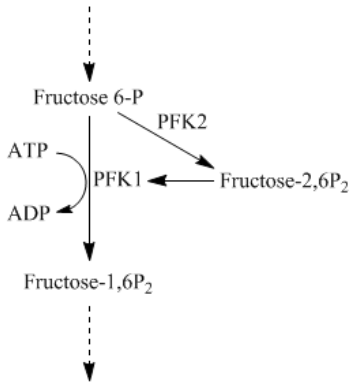

Figure 1.13: the interplay between PFK-1 and PFK-2

There are 4 PFKFB isoenzymes expressed in humans (**Table 1.3**) (Rider, M.H., *et al*, 2004). Studies have shown the hypoxia induced up-regulation of all four *PFKFB* mRNAs though the most marked upregulation is that of *PFKFB3* mRNA in the lungs, liver, kidney, brain heart and testes (Minchenko, O., *et al*, 2003).

Table 1.3		
Human PFKFB Variants		
Gene	Isoenzyme	Isoform
PFKFB1	Liver	L M
PFKFB2	Heart	Long Short
PFKFB3	Placenta	Ubiquitous Inducible
PFKFB4	Testis	T

PFKFB3 shows no bisphosphatase activity, suggesting a role for PFKFB3 in increasing the steady-state concentration of F2,6BP (Hue, L., *et al*, 1993). Furthermore, inducible PFKFB3 is expressed at very low levels in normal adult cells (Chesney, J., *et al*, 1999) but is over-expressed in leukeamias, solid tumours and *ras*-transformed cells in response to hypoxic, mitogenic and pro-inflammatory stimuli (Sakakibara, R., *et al*, 1997) (Minchenko, A., *et al*, 2002) (Atsumi, T., *et al*, 2002).

Experimental evidence has shown that oncogenic Ras increases the activity of PFK-1 by increasing the steady-state concentration of F2,6BP. Confusingly, another study has shown that whilst PFKFB3 expression increases in immortalized cells, the steady state concentration of F2,6BP *decreased* and, despite a slight increase after the introduction of oncogenic Ras, F2,6BP continued to be maintained at a lower level than that in healthy cells (Telang, S., *et al*, 2006). However, both studies show a clear role for PFKFB3 in *Ras* transformation.

Finally a study on *PFKFB3*$^{+/-}$ mice has demonstrated a role for F2,6BP in metastasis with lower F2,6BP suppressing the mediation of anchorage independent growth

by oncogenic Ras. Otherwise, reduced F2,6BP concentration caused no abnormalities in embryogenesis, development or growth (Telang, S., *et al*, 2006).

The role of PFKFBs as determinants of the rate of glycolytic flux, coupled to the fact that PFKFB3 is almost exclusively expressed in tumours makes PFKFB3 an attractive target for development. The further implication of F2,6BP in suppressing metastasis only serves to validate this assessment.

1.7.2.3: GLUTAMINASE (GLS)

The other input in carbon flux terms is glutamine. GLS converts glutamine to glutamate which ultimately becomes α-ketoglutarate in the TCA cycle. There are two GLS isoforms, liver (L), and kidney (K) (Curthoys, N.P. *et al*, 1995). The bulk of GLS is anchored to the inner mitochondrial membrane, which requires glutamine to be taken up by the mitochondria; studies show that malignant cells take up glutamine at a faster rate than non-malignant cells (DeBerardinis, R.J., *et al*, 2007).

The expression of phosphate-activated GLS can be correlated with malignancy in different tumours (Matsuno, T., *et al*, 1989). Different studies have shown that using RNA interference to knockdown GLS decreases growth and tumourigenicity (Lobo, C., *et al*, 2000).

1.7.3: DISRUPTING CELLULAR REDOX

1.7.3.1: GLYCERALDEHYDE 3-PHOSPHATE DEHYDROGENASE (GAPDH)

GAPDH catalyses the sixth step of glycolysis where glyceraldehyde-3-phosphate (GA3P) is oxidized to 1,3-disphosphoglycerate. The reaction requires NAD^+ which in turn accepts a hydride ion to be reduced to NADH; the NADH is recycled to NAD^+ by fuelling the reduction of pyruvate to lactate at the level of LDH. It is evident that

it is important for cells to regulate the intracellular means of controlling redox in order to remain viable; it is reflected in the fact that transformed cells maintain the high NADH:NAD^+ ratios of healthy cells (Vander Heiden, *et al*, 2009).

The expression of GAPDH is upregulated 6 fold by HIF-1α (Seagroves, T.N., *et al*, 2001). Furthermore, HIF-2α has been shown to upregulate GAPDH specifically in endothelial cells (ECs). The induction of GAPDH is highest in ECs and it is unclear why this should be the case given that the glycolytic step catalysed is not rate determining nor is the inhibition of the enzyme a primary cellular means of regulating glycolysis.

The answer may lie in the non-glycolytic functions of GAPDH. These can be split into two distinct areas: transcriptional and apoptotic. Dealing with the former first, GAPDH can bind DNA and RNA (Nagy, E., *et al*, 2000) (Perucho, M., *et al*, 1980). GAPDH is implicated in DNA repair complexes (Sirover, M.A., *et al*, 2005) though the full details of this remains to be elucidated. Furthermore, GAPDH has been shown to be implicated in binding at telomeres (Sunararaj, K.P., *et al*, 2004) possibly linking GAPDH to cancer cell immortalisation. GAPDH-RNA interactions constitute another area where further elucidation will shed light on the precise nature and role of these interactions.

GAPDH is a component of the OCA-S complex, an S-phase-dependent transactivator of the histone *H2B* gene (Zheng, L., *et al*, 2003). GAPDH has a key role in this complex, integrating the regulation of energy metabolism and the cell cycle.

GAPDH expression has been shown to be significantly increased during apoptosis (Saunders, P.A., *et al*, 1999). Results indicate that nitric oxide (NO) generated following apoptotic stimulatation induces the S-nitrosylation of GAPDH. This in turn makes GAPDH binding to Siah1 (a ubiquitin ligase) more favourable. The GAPDH-Siah1 complex then undergoes nuclear translocation with GAPDH stabilising Siah1 thereby facilitating the degradation of nuclear proteins. The result is apoptotic cell death mediated by GAPDH (Hara, M.R., *et al*, 2005).

The location of GAPDH in the cytosol or nucleus has led to the suggestion that there might be two specific isoforms, $GAPDH_C$ and $GAPDH_N$. It has been further suggested these isoforms arise from the reversible post translational phosphorylation of $GAPDH_C$ and $GAPDH_N$ has been further implicated in other processes including tubulin binding and membrane fusion (Sirover, M.A., *et al*, 1999).

Given the importance of DNA repair and apoptosis evasion to cancer cells, it is perhaps in the non-glycolytic roles of GAPDH that its importance lies.

1.7.3.2: LACTATE DEHYDROGENASE (LDH)

L-Lactate dehydrogenases (LDH) are a family of 2-hydroxy acid oxidoreductases that simultaneously and stereospecifically interconvert pyruvate to lactate, and NADH to NAD^+ (Read, J.A., *et al*, 2001). Five tetrameric LDH isozymes are present in mammalian tissues that are formed by combination of the two different polypeptide chains, M (muscle) and H (heart); LDH-A is a homotetramer composed of 4 M subunits and is responsible for the forward conversion of pyruvate to lactate. LDH-B is a homotetramer composed of all H subunits and is that favours the reverse oxidation of lactate to pyruvate (Pretsch, W. *et al*, 1998).

Cells lacking LDH-A have a markedly diminished glycolytic capacity (Yamagate, M., *et al*, 1998). LDH-A levels relate to levels of Myc expression in G1 of the cell cycle, and over-expression of LDH-A is sufficient to induce the Warburg effect (Shim, H. *et al*, 1997) as high concentrations of lactate inhibit Prolyl Hydroxylases (PHDs). This has the effect of maintaining and promoting HIF activity (Lu, H., *et al*, 2005) which can then up-regulate glycolysis under normoxic conditions.

The role of LDH-A in glycolysis and tumour maintenance has been studied with reference to changes in the mitochondrial membrane potentials (Fantin, V.R., *et al*, 2006). Aerobically glycolytic cells have a higher mitochondrial membrane potential ($\Delta\psi_m$) which is thought to arise from less ATP-synthase associated proton transport (and therefore less OXPHOS). Moreover, several studies now complement the idea of LDH-A knockdown affecting mitochondrial physiology, with literature reports of LDH-A knockdown increasing reactive oxygen species (ROS) levels and therefore oxidative stress (Le, A., *et al*, 2010). This increase in oxidative stress in turn accounts for an increase in programmed cell death.

Knocking down LDH-A not only reduces the mitochondrial membrane potential but it also significantly reduces the tumorigenic potential of tumour cells with LDH-A deficient cells implanted into mice showing markedly reduced markers of proliferation (Fantin, V.R., *et al*, 2006).

Lastly, LDH-A is important in redox cycling, regenerating NAD^+ for use at the level of GAPDH. This competition for NADH with the mitochondrial NADH/NAD^+ shuttle is also important in reducing mitochondrial metabolism; the relatively fast rate of pyruvate reduction to lactate, driven by greater glucose uptake and a faster flow through glycolysis, depletes NADH that would otherwise be used in the

mitochondria and therefore slows the rate at which mitochondrial respiration can operate(Greiner, E.F., *et al*, 1994).

The role of LDH-B in cancer is much less well-established though some work has emerged suggesting a role for LDH-B in mTOR-mediated tumorigenesis mediated through signal stransducer and activation of transcription 3 (STAT3) (Zha, X., *et al*, 2011). Tuberous Sclerosis Complexes 1 and 2 (TSC1 and TSC2) are known suppressors of the mTOR signaling pathway; experiments discovered that in TSC1 and TSC2 null mice there was an increase in LDH-B expression. The link between mTOR and LDH-B expression was confirmed as being mediated via STAT3. Moreover, shRNA knockdown of LDH-B in TSC2 null mice severly compromised tumour proliferation, though the exact mechanism of this has yet to be described. Whilst these findings are interesting, from a drug discovery point of view they present a challenge; until more comprehensive biological data is available, the utility of targeting LDH-B as a broad therapeutic strategy will be unclear.

In terms of major enzymopathies, both LDH-A and LDH-B have to be deficient in order to present in a patient as haemolytic anaemia. Otherwise, a patient who is deficient in only LDH-A suffers from exertional myoglobinuria, painful muscle stiffness and cramps, easy fatigue during extended periods of exercise, abnormalities at parturition and skin eruptions (Van Wijk, R., *et al*, 2005).

LDH-A can therefore be considered as a valid target for inhibition, as doing so would not only reduce tumour cells' ability to cope with hypoxia, but also reduce the aggressive nature of a tumour. In short, its position at the end of glycolysis makes it a choke point for several key processes including energy production, maintaining cellular redox status; there is also evidence that the expression of

LDH-A underpins proliferation. Coupled to this, the high rate of glucose uptake and subsequent flux of these carbon units through glycolysis makes LDH-A peculiarly sensitive to inhibition, leading to either an accumulation of pyruvate which is potentially toxic, or an increase in oxidative stress as a result of the reactivation of OXPHOS. Either of these eventualities are likely to trigger greater cell death and therefore make LDH-A a particularly attractive target.

It would appear therefore, that whilst there are many metabolic enzymes that have compelling cases to be considered as targets it is LDH-A that presents itself as the most promising. In particular, if the Warburg effect is about the changing fate of cellular pyruvate, then exploring and exploiting the chief mediator of this new fate is particularly attractive.

1.8: Lactate Dehydrogenase in Detail

If LDH-A is to be pursued as a target, it is desirable to characterise the enzyme in slightly more detail in terms of its genetic locus, structural biology, and expression patterns.

1.8.1: Genetics and Structural Biology

The human LDH-A subunit is located on chromosome 11 and has two splice variants. The splice variant differs from amino acids 230 to 274 where VHKQV…VHPVS is replaced by CRYTLGDPKGAAILKSSDVI SFHCLGYNRILGGGCACCPF YLICD. This change is in a region not associated with nucleotide binding and is not recorded as having an effect on function.

The human LDH-B subunit is located on chromosome 12. It is notable that the active sites between LDH-A and LDH-B are highly (75%) conserved. The notable residues are arginines (99/100, 106/107, 169/170), asparagine (138/139), threonine (248/249) and a criticial histidine (193/194) that is responsible for the proton transfer that reduces pyruvate to lactate.

However, whilst the residues might be similar there is a difference in pK_A for the active site histidine (H193/194) between LDH-A and LDH-B, with the pK_A lower in LDH-A. The net result of this is that the histidine is a stronger acid/weaker base in LDH-A than LDH-B and therefore LDH-A is more likely to favour the forward conversion of pyruvate to lactate with LDH-B favouring the reverse reaction of lactate to pyruvate. Beyond this, pH affects reaction kinetics markedly, with LDH-A displaying a K_M for pyruvate 3-10 fold higher at pH 6.0 (Read, J.A., *et al*, 2001). On a molecular basis, pyruvate is unable to bind to the active site when H193/194 is unprotonated resulting in the forward reaction being favoured at lower pH. The difference in pK_A is affected by net surface charge, which is –6 for LDH-B and +1 for LDH-A; it is this difference that tailors each isoform for the respective redox environment within which it is active.

There is a third isoform, LDH-C, that is exclusively expressed in the testes and is located at a different site on chromosome 11. Less is known about this isoform and given its tissue specific location it will be discounted for the time being.

In terms of similarity with other proteins, LDH-A belongs in a class of dehydrogenases that includes the other LDH isoforms and also the Malate Dehydrogenase (MDH) enzyme responsible for catalyzing the conversion of malate to oxaloacetate in the TCA cycle.

1.8.2: EXPRESSION AND UTILITY

In healthy tissue, LDH-A expression is largely restricted to skeletal muscle, liver and lymphatic tissue under hypoxic conditions and has little expression in its normoxic surroundings (Granchi, C., *et al*, 2010).

The over-expression of LDH-A in non-small cell lung cancer, colorectal cancer and squamous head and neck cancer has been observed (Koukourakis, M.I., *et al*, 2003) (Koukourakis, M.I., *et al*, 2006) (Koukourakis, M.I., *et al*, 2009) and is likely to arise due to hypoxia. However, as previously alluded to, a strong link exists between LDH-A expression and Myc levels.

To date, LDH-A inhibition has been proposed as a means of treating hereditary leiomyomatosis and renal cell cancer as these diseases display a fumarate hydratase (FH) deficiency with which LDH-A inhibition has been shown to work cooperatively with. FH catalyses the reversible hydration of fumarate to malate such that FH deficiency inhibits the TCA cycle. A lack of FH also stabilizes HIF due to fumarate accumulation, reinforcing a glycolytic phenotype. The mechanism of action of LDH-A inhibition in this model is one where the knockdown experiences increased ROS production (Xie, H., *et al*, 2009).

Implication of increased oxidative stress is borne out in another more recent study using RNA interference and a putative small molecule inhibitor; in this instance, the increase in ROS triggers apoptosis when LDH-A is knocked down (Le, A., *et al*, 2010).

1.9: AIMS

Given the background data on LDH-A, this thesis has three aims:

1. to validate LDH-A inhibition and elucidate its full nature in terms of the implications for tumour survival;

2. to ascertain the role of LDH-B in order to determine whether selectivity towards LDH-A would be a necessary feature of any small molecule inhibitor;

3. to recapitulate siRNA mediated LDH-A inhibition with small molecule inhibitors that have the potential for clinical application.

The thesis is explicitly interdisciplinary and will tackle these aims by using a range of techniques across synthetic organic chemistry, molecular pharmacology, and cell biology. Furthermore, clinical data will be exploited to put the data in its proper context.

CHAPTER 2: MATERIALS AND METHODS

2.1: MATERIALS

2.1.1: CELL LINES

MCF-7, MDA-MB-231, MDA-MB-468 and PC3 cells, were from Clare Hall laboratories, UK. HCT-116 +/+p53 and HCT116 -/-p53 cells were from Prof Bert Vogelstein's lab. RCC4 +/+VHL and RCC4 -/-VHL were from Dr Ioannis Ragoussis's lab and IGROV-1 and OC316 cells were from Stefano Indraccolo's lab. Fetal bovine serum (FBS) Gold was from PAA Laboratories. All variants ofDulbecco's Modified Eagle's Medium (DMEM) were from Gibco (Invitrogen), Oligofectamine™ and Optimem™ were from Invitrogen, whilst protease and phosphatase inhibitor cocktail tablets were from Roche.

2.1.2: CHEMICALS

The small molecule library was obtained from Chembridge. All other chemicals, unless specified, were obtained from Sigma-Aldrich.

2.1.3: ANTIBODIES

Rabbit anti-GLUT1, mouse anti-GLUT3 and rabbit anti-HIF-2α were from Abcam. Mouse anti-β-Actin was from Sigma, mouse anti-HIF-1α was from BD Biosciences, Goat anti-LDH-A was from Santa Cruz Biotechnology and mouse anti-LDH-B was from Abnova.Rabbit anti-MCT-1 and rabbit anti- MCT-4 were both from Millipore and rabbit anti-PARP was from Cell Signalling Technology. All HRP-conjugated secondary antibodies were from Dako.

2.1.4: PROTEIN

LDH-A and LDH-B were sourced from Lee Biosciences.

2.2: RNA EXTRACTION AND RT-PCR

2.2.1: RNA EXTRACTION AND CDNA SYNTHESIS

Cells were rinsed with PBS and drained thoroughly. RNA was extracted from the cells using Tri reagent (Sigma). The quantity and quality of RNA extracted were assessed using NanoDrop ND 1000 Spectrophotometer (NanoDrop Technologies). RNA samples were stored at –80°C. cDNA was synthesized by reverse transcribing RNA using the High Capacity cDNA Archive Kit (Applied Biosystems). Briefly a 2X mastermix was prepared (10 μL reverse transcription buffer, 4 μL 25X dTNPs, 10 μL of 10X random primers, 5 μL of reverse transcriptase and 21 μL of nuclease free H_2O). To this was added 50 μL of RNA sample; the reverse transcription was then completed on a thermal cycler (PTC-2000, MJ Systems) for 10 min at 25°C followed by 120 min at 37°C.

2.2.2: REAL-TIME QUANTITATIVE PCR

Real-time quantitative PCR (qPCR) reactions were performed in triplicate using the Corbett Research Rotor Gene RG-3000 (Sydney, Australia). Each reaction was performed in an individual tube and made up to 25 μL containing 10 μL cDNA, 12.5 μL TaqMan PCR Master Mix (Abgene, Epsom, UK), 0.25μL probe, 1μL of forward and reverse primer and 0.2μL H_2O. Conditions for the PCR reaction were 2 min at 50°C, 10 min at 95°C and then 40 cycles, each consisting of 15 s at 95°C, and 1 min at 60°C. β-Actin was used as a reference gene using primers (Invitrogen) 5'-

CCCAGCACAATGAAGATCAA-3' forward and 5'-CGATCCACACGGAGTACTTG-3' reverse with probe 63 (Roche, Lewes, UK). Primers against LDH-A (Invitrogen) 5'-GCAGATTTGGCAGAGAGTATAATGA-3' forward and 5'-GACATCATCCTTTATTCCGTAAAGA-3' reverse and against LDHB (Invitrogen)5'-GATGGATTTTGGGGGAACAT-3' forward and 5'-AACACCTGCCACATTCACAC-3' were used for qPCR. Relative quantitation of gene expression was performed using the method described by Pfaffl (Pfaffl, 2001). In brief, comparisons were made between the number of cycles required for the fluorescence of a sample to reach a predetermined threshold that lay within the exponential phase and above the non-specific background. The relative ratio of gene expression was calculated as follows:

$$\text{Relative ratio} = \frac{(\text{Etarget})^{\Delta\text{Ct TARGET (mean comparator}-\text{mean sample)}}}{(\text{Eref})^{\Delta\text{Ct REF (mean comparator}-\text{mean sample)}}}$$

Etarget=reaction efficiency of the gene of interest, Eref=reaction efficiency of the reference gene, ΔCt=the cycle difference between the comparator and the sample. All calculations are based on the mean value of PCRs performed in triplicate.

2.3: PROTEIN EXTRACTION AND ANALYSIS

2.3.1: PROTEIN EXTRACTION AND QUANTIFICATION

Cells were washed with 4^{o}C PBS and homogenised on ice in lysis buffer containing 6.2 M urea, 10% glycerol, 5 mM DTT, 1% SDS, protease inhibitors and phosphatase inhibitors.

2.3.2: PROTEIN POLYACRYLAMIDE ELECTROPHORESIS AND SEMI-DRY PROTEIN TRANSFER

An appropriate volume of 6X SDS-PAGE sample buffer (72 mM Tris pH 6.8, 20% glycerol, 4.5% SDS, 10% β-mercaptoethanol and 0.015% bromophenol blue) was added and samples were heated to 95^{o}C for 5 min. Proteins (typically 30 μg/lane), were separated by SDS-PAGE, using 12% Tris-HCL gels unless otherwise stated prior to semi-dry transfer to PVDF membranes.

2.3.3: ANTIBODY INCUBATION AND DETECTION

Blots were incubated overnight with an appropriate concentration of primary antibody in PBS containing 5% milk powder and 0.1% Tween-20. Membranes were incubated with the appropriate HRP-conjugated secondary at 1:1000 (Dako). Immunoreactivity was detected using Amersham ECL™ western blotting detection reagent and Hyperfilm™ (GE Healthcare).

2.4: CELL CULTURE AND *IN VITRO* TECHNIQUES

2.4.1: CULTURING AND PASSAGING CELLS

All work with cells was conducted in a laminar flow hood (Astec) with cells being grown in sterile flasks or on sterile plates (Corning). Cells were passaged by aspirating the medium, washing the cells with PBS, and then treating with 1 x trypsin-EDTA (Invitrogen) to detach. The cell mix was then spun for 4 minutes at 1000 rpm to generate a pellet from which the supernatant was aspirated. The pellet was then split 1:10 and reseeded. This process was carried out every 6-7 days.

2.4.2: PREPARATION AND RECOVERY OF CRYO-PRESERVED CELLS

To freeze cells down for storage, a pellet was prepared as above. The cell pellet was then resuspended in 1.5 mL FCS and 0.5 mL DMSO and divided between cryo-vials (Corning). Freezing down to -80^{o}C at the rate of 1^{o}C per minute was achieved by using a Mr Frosty (Nalgene) lined with isopropanol. To recover cells from storage, cryovials were rapidly defrosted to 37^{o}C and transferred to pre-warmed (37^{o}C) media.

2.4.3: COUNTING CELLS

Cells were counted using the Coulter Particle Counter Z2 (Beckman Coutler) according to manufacturer's instructions. Briefly, 400 μL of cell suspension were diluted with 19.6 mL of isoton buffer and a particle count take in the range of 9-22 μm.

2.4.4: HYPOXIC EXPOSURE

Hypoxic incubations (0.1% O_2, 5% CO_2) were performed using an INVIVO$_2$ 400 hypoxic workstation (Pro-Lab Diagnostics). All cells were allowed 6 hours to adhere and recover after being seeded in final densities before being exposed to hypoxia.

2.4.5: GENE SILENCING BY TRANSIENT SIRNA KNOCKDOWN

Cells were seeded on 10 cm^2 dishes at 8 x 10^5 per dish and left overnight to adhere. siRNA duplexes were transfected into cells at 20nM using Oligofectamine™ and then cultured in Optimem™ for 4 hours prior to the addition of serum for overnight recovery (8 μL siRNA, 120 μL Oligofectamine™, 7.872 mL Optimem™, 2 mL FCS). On the following day, the cells were reseeded as appropriate.

2.4.5.1: SCRAMBLE CONTROL SEQUENCE

Scrambled control (Scr) RNAi duplexes was designed using InvivoGen siRNA wizard™ and synthesised and annealed by Eurogentec. The oligonucleotide sense strand sequence was 5'-GGCUAAACGUAAGUUGACtt-3'; antisense 5'-GUCAACUUACGUUUAGCCtt-3'; were synthesised and annealed to form duplexes.

2.4.5.2: HIF1/2 SEQUENCES

The target sequences for HIF-1, and HIF-2 were selected from the relevant ORF region of the human cDNA sequence according to the manufacturer's recommendations (Cruachem Limited, Glasgow, UK) and submitted to a Basic Local Alignment Search Tool search (National Centre for Biotechnology Information database) to ensure targeting of a single gene. All siRNA duplexes were synthesised and annealed by Eurogentec. The oligonucleotide sense strand sequences were HIF-1 antisense, 5'-CUGAUGACCAGCAACUUGAdTdT-3'; HIF-1 sense, 5'-UCAAGUUGCUGGUCAUCAGdTdT-3'; HIF-2 antisense, 5'-CAGCAUCUUUGAUAGCAGUdTdT-3'; HIF-2 sense, 5'ACUGCUAUCAAAGAUGCUGdTdT-3'; were synthesised and annealed to form duplexes.

2.4.5.3: LDHA/B SEQUENCES

2 LDH-A RNAi duplexes were bought ready to use from Ambion. The oligonucleotide sense strand sequences were: LDH-A(1) 5'-GGGUCUUUACGGAAUAAAGtt-3'; anti-sense5'-CUUUAUUCCGUAAAGACCCtt-3'; LDH-A(2) sense 5'-GGCUACACAUCCUGGGCUAtt-3'; antisense UAGCCCAGGAUGUGUAGCCtt; a third, LDH-A(3) 5'-XXXXXXXXXAtt-3' was bought from Santa Cruz (SC-43893A).

LDH-B sequences were designed using InvivoGen siRNA wizard™ and synthesised and annealed by Eurogentec. The oligonucleotide sense strand sequences were LDH-B(1) 5'-GCUAAAAGGAUAUACCAACtt-3'; antisense 5'-GUUGGUAUAUCCUUUUAGCtt-3'; LDH-B(2) sense 5'-GGAUUCAUCCCGUGUCAACtt-3'; antisense: 5'-GUUGACACGGGAUGAAUCCtt-3'; LDH-B(3) sense 5'-GGAUAUACCAACUGGGCUAtt-3'; antisense: 5'-UAGCCCAGUUGGUAUAUCCtt-3'; were synthesised and annealed to form duplexes.

2.4.6: 3D SPHEROID FORMATION

MCF-7 and MDA-MB-231 cells were transfected according to the standard protocol to provide a scramble control, an LDH-A knockdown and an LDH-B knockdown. The cells were then reseeded the following day in 200μL DMEM in non-adherent 96 well plates at 5000 cells per well to generate 16 spheroids per condition used. The MDA-MB-231 cells required a further 5μL per 1mL of reconstituted basement membrane (RBM) which was defrosted on ice with cell pellets being kept on ice until plating. The plates were then spun at 2000 rpm for 10 min and left overnight for the spheroids to form. Microscope photographs were then taken at appropriate timepoints using a digital camera and AxioVision™ software at 5x magnification. After the final time point, the spheroids were fixed in formalin, embedded in wax, and sliced and mounted onto slides for immunohistochemical analysis.

2.4.6.1: Quantifying Spheroid Tumour Volume

The analysis software ImageJ was used to quantify spheroid tumour volume. In short, the 5x images were processed as JPEGs after a suitable threshold was set to exclude non-tumour mass. The surface area in pixels was then converted into

$\mu M^2$and then further converted into a radius of the equivalent circle. From these radii, it was possible to calculate the volume of the equivalent sphere.

2.4.7: SULFORHODAMINE B (SRB) ASSAY

Cells were seeded in 96 well plates and cultured as appropriate. At the required timepoint, the media was discarded and 200 μL of 10% trichloroacetic acid (TCA) and incubated at 4°C for 60 min. The TCA was then removed from the wells and the plate washed 3 times with tap water. The plates were then dried and 100 μL of 0.4% SRB was added too each well which were then incubated at room temperature for 30 min. The SRB was then removed and the wells washed 3 times with 1% acetic acid. To resolve the SRB, 200 μL of 10 mM Tris pH 9.5 and the plates incubated for 15 min at room temperature under shaking before the absorbance was read at 540 nM.

2.4.8: CLONOGENIC ASSAY

MCF-7 and MDA-MB-231 cells were seeded at 8 x 10^5 cells in 10cm plates and allowed to adhere overnight. The media was replaced with optimum and the cells transfected with siRNA according to the standard protocol to provide a scramble control, an LDH-A knockdown and an LDH-B knockdown. The cells were then reseeded the following day in DMEM at a 100, 1000, and 1000 (MCF-7 only) cells in 6cm plates and allowed to adhere overnight. The cells were then incubated under normoxic and hypoxic conditions for 5 days before being allowed to recover for 10 days in normoxia. The cells were then treated with a dual fixing/staining solution made up of 50% dH_2O, 49.8% ethanol, and 0.2% crystal violet. After several washes with tap water, the plates were air-dried and the stained colonies counted using an automated scanner (ColCount, Oxford Optronics).

2.4.9: LACTATE MEASUREMENT

MCF-7 and MDA-MB-231 cells were transfected with siRNA according to the standard protocol to provide a scramble control, an LDH-A knockdown and an LDH-B knockdown. The cells were then reseeded in 10 cm plates and at appropriate points 1 mL of media was harvested and the cell number recorded. This media was then measured for lactate using a Lactate Assay Kit (Instruchemie). Briefly, a lyophilized NAD+ solution was resuspended in buffer, distilled water and LDH in a ratio of 4:2:0.1. 10 μL of sample was plated in triplicate in a 96 well plate to which 290 μL of the resuspended reaction mix was added to initiate. The plate was then incubated at room temperate for 30 min before being read for absorbance at 340 nm. Values were normalized to cell number.

2.4.10: ATP MEASUREMENT

MCF-7 and MDA-MB-231 cells were transfected with siRNA according to the standard protocol to provide a scramble control, an LDH-A knockdown and an LDH-B knockdown. The cells were then reseeded in duplicate the following day in DMEM in 96 well plates. One replicate was seeded in a standard clear bottom 96 well plate and analysed according to standard SRB procedure after 48 hours. The other replicate was seeded in a white-bottomed 96 well plate for luminescence plate reading and ATP levels assessed using a Cell Titer-Glo Luminescent Cell Viability kit (Promega). Briefly, the media was aspirated and replaced with 100 μL of fresh media to which a further 100 μL of reaction mix was added. The plate was then incubated under skaing at room temperature for 15minutes before being

read for luminescence on a FluoSTAR OPTIMA (BMG Labtech). The ATP data was then normalised to the protein concentration values obtained by SRB.

2.4.11: Extracellular Acidification and Oxygen Consumption Experiments

MCF-7 cells were transfected with siRNA according to standard protocol and reseeded in duplicate at 3 x 10^5 cells in a custom 96-well plate (Seahorse Bioscience). Half of the population were treated with the hypoxia mimetic DMOG at 1 mM, which was also added to the trypsin and PBS that was used to culture these cells in order to keep them under pseudo-hypoxia for the duration of the experiment.

The cells were assayed using an XF96 extracellular flux analyser (Seahorse Bioscience) to perform non-destructive, time-resolved measurements of extracellular acidification rate (ECAR) and oxygen consumption rate (OCR).Each XF assay kit contains a disposable sensor cartridge, embedded with 96 pairs of fluorescent biosensors to measure oxygen and pH. The movement of the sensor cartridge into a measuring position over the 96-well plate produces a transient micro-chamber within which oxygen consumption and proton extrusion cause rapid, measurable changes in oxygen tension and pH. During this time, oxygen and mpH was measured every 10 s.

Further to the fluorescent biosensors, each sensor cartridge is equipped with two reagent delivery chambers per well for injecting testing agents into wells during an assay. To the first chamber for all wells was sufficient oligomycine to produce a final concentration of 1 μM. To the second chamber of the first replicate was added

sufficient FCCP to give a final concentration of 300 nM; to the second chamber of the second replicate was added sufficient rotenone to give a final concentration of 1 μM.

To facilitate rapid ECAR reading, medium was replaced immediately prior to measurement with non-buffered pH 7.4 custom glucose free DMEM (Seahorse Bioscience) that was supplemented with 4.5 g/L glucose where appropriate. After automatic calibration checks the experiment was started with 13 readings taken every 10 s to provide each rate point. After this was repeated another two times, the contents of the first reagent chamber were injected and a further three rate points were measured. The contents of the second chamber were then injected into the wells and a final 3 rate measurements were taken. After this, the results were automatically recorded on the inbuilt software and analysed according to standard protocol (**2.9**).

2.5: CLINICAL SAMPLES

2.5.1: ONCOMINE

Publically available clinical data was accessed using Oncomine and interpreted according to standard statistical procedures (**2.9**).

2.5.2: CLINICAL SAMPLES

The Oxf-IJB dataset, containing 152 breast cases, was analysed on a Affymetrix U133A array for clinical and molecular covariates. The demographics of this dataset are covered in detail by Higgins *et al* (Higgins, G.W. *et al,* 2010). Statistical

analysis was carried out by Dr. Francesca Buffa at the Weatherall Institute of Molecular Medicine.

The relative expression of LDH-A and LDH-B in the 152 cases is outlined in **Tables 2.1 and 2.2**.

Table 2.1

	Cases					
	Valid		Missing		Total	
	N	Percent	N	Percent	N	Percent
LDHA 200650_s_at	152	100.0%	0	.0%	152	100.0%
LDHB 201030_x_at	152	100.0%	0	.0%	152	100.0%
LDHB 213564_x_at	152	100.0%	0	.0%	152	100.0%

Table 2.2

Standardized expression		Statistic	Std. Error
LDHA 200650_s_at	Mean	0.046726	0.027685
	Median	0.014872	
	Std. Deviation	0.341329	
LDHB 201030_x_at	Mean	-0.05091	0.074193
	Median	-0.1316	
	Std. Deviation	0.914717	
LDHB 213564_x_at	Mean	-0.05121	0.074244
	Median	-0.0957	
	Std. Deviation	0.915348	

The clinical and molecular covariates that were analysed are represented in **Table 2.3** along with the raw data; the gene expression signatures are recorded elsewhere in the literature (Buffa, F.M. *et al*, 2010) (Wirapati, P., *et al*, 2008).

Table 2.3

Spearman correlation		Gene expression signatures						
		Hypoxia	Proliferation	ESR1 signalling	ERBB2 signaling	Invasion	Immune Response	Apoptosis
LDHA 200650_s_at	rho	0.5735	0.3689	-0.0160	0.0303	0.0685	0.0890	0.0556
	p (2-tailed)	<0.0001	<0.00001	0.8448	0.7107	0.4016	0.2757	0.4960
	N	152	152	152	152	152	152	152
LDHB 201030_x_at	rho	0.0805	0.0299	-0.5895	-0.0840	0.1616	0.2146	0.1066
	p (2-tailed)	0.3243	0.7145	<0.0001	0.3034	0.0467	0.0079	0.1912
	N	152	152	152	152	152	152	152
LDHB 213564_x_at	rho	0.0988	0.0348	-0.5907	-0.0737	0.1624	0.2166	0.1095
	p (2-tailed)	0.2260	0.6706	<0.0001	0.3669	0.0456	0.0074	0.1793
	N	152	152	152	152	152	152	152

Lastly, in order to assess relapse free survival a univariate analysis was carried out where samples were divided by median expression value.

2.6: Staining Techniques

2.6.1: Immunohistochemistry

The spheroids, having been prepared for immunohistochemistry as outlined in **2.4.6** and mounted on slides, were prepared for staining as follows. Firstly, the slides were dewaxed by heating in an oven at 60°C for 10 min.

Following this, the slides were washed sequentially (5 min for each wash); twice in histoclear (Fisher), twice in 100% ethanol, once in 50% ethanol, and then in water. The procedure for all staining but H&E staining is then as follows.

Following this, antigen retrieval was conducted by placing the slides in a pressure cooker for 45 min at 125^{o}C. The buffer that this was done in varied according to which primary antibody was to be used and is outlined in **Table 2.4**

Table 2.4

Antibody	**Antigen Retrieval**	**Primary Dilution**
kI67	Citrate pH6	1/50 in RPMI
Cleaved Caspase 3	Citrate pH6	1/2000 in RPMI
CA9	TRIS EDTA pH9	1/100 in RPMI

Following antigen retrieval, the slides were placed into PBS before being dried and blocked with 10% Bovine Serum Albumin (Invitrogen) for 15 min. The primary antibody was then added to the slide in the correct dilution and the slide was kept humidified for 45 minutes.

The slides were then washed in PBS for 5 min and the secondary antibody was added and the slide kept humidified for 30 min. The slides were then washed again for 5 min in PBS and parts B and C from a IHC kit (Dako) were mixed together with 60μL of C in 3 mL of B. 100μLwas added to each slide for 8 min, the slides were washed in PBS, stained for haematoxylin and washed in tap water before being mounted with coverslips for further examination.

Scoring was performed using ImageJ on 5x images captures JPEGs. Background was excluded and images deconvoluted to given an image for the specific staining and the nuclear staining. Scoring was then completed by expressing specific staining as a ratio of total nuclear stained cells.

2.6.1.1: HAEMATOXYLIN AND EOSIN (H&E) STAINING

Slides for H&E staining were dewaxed and rehydrated as above. They were then washed in Harris' haematoxylin for one minute followed by a wash in tap water. The slides were then washed in acid alcohol before being washed in tap water again. The slides were then washed sequentially in Scotts water, tap water, eosin for 90 s, followed by tap water. The final sequential washes were in 50% ethanol, 70% ethanol, 100% ethanol (twice), xylene (twice) before being fixed.

2.6.2: IMMUNOFLUORESCENCE

Briefly, after transfecting MDA-MB-231 according to standard protocol, cells were reseeded onto glass slips in 6-well plates at 1 x 10^5 cells per well and incubated overnight. The cells were rinsed briefly in PBS and fixed with 4% formaldehyde in PBS for 15 min at room temperature followed by rinsing three times in PBS for 5 min each. Cells were permeabilised with ice-cold 100% methanol and incubated for 10 min at –20°C before final rinse in PBS for 5 min. Following blocking of nonspecificbinding with 5% BSA in PBS for 1 h, sections were incubated with primary antibody for 1 h at room temperature. The breast cells were then incubated with goat anti-LDH-A N-14 (1:100, Santa Cruz) and rabbit anti-TOM20 (1:100, Cell Signalling Technology). After a 10 min wash in PBS, cells were incubated with secondary antibody Alexa-Fluor 633 donkey anti-goat (0.5 µg/mL, Molecular Probe, Invitrogen) and Alexa-Fluor 488 donkey anti-rabbit(0.5 µg/mL, Molecular Probe, Invitrogen) for 1 h at room temperature. Cells were then washed three times in PBS before mounting with fluorescent mounting medium with DAPI (Vectashield) and visualised under the fluorescent microscope.

2.7: PHARMACOLOGY

2.7.1: MOLECULAR DOCKING AND 3D STRUCTURES

The structure of LDH-A was accessed from the Protein Database (PDB ref 1I10) and was generated by Brady and coworkers (Read, J.A., *et al*, 2001). Before the docking analysis, the relevant compounds were drawn in ChemDraw and converted to 3D structures using ChemDraw 3D. The less energetic conformation of the 3D structure was calculated and saved as a mol2 file.

In order to analyse possible interactions between proteins and ligands the docking programme GOLD (Genetic Optimization for Ligand Docking) was used (Jones, G., *et al*, 1997) (Onodera, K., *et al*, 2007). GOLD allows analysis of possible interactions between docking partners and will predict preferred orientations of the ligand within the binding site as well as measuring the strength of interactions.

With 1I10 open in GOLD hydrogens were added to the structure of the protein and waters removed. A docking site was defined as a region of 10 Å around a key amino acid residue of the binding site (H193). The relevant compound mol2 files were then loaded and the programme was run sequentially for each compound. The computer program used a scoring function (GOLD Score Fitness function) to rank the generated binding modes. The best conformation as ranked by GOLD was use in each instance. To aid better visualisation of the results, the docking results were presented in a three-dimensional diagram using the computational program PyMOL.

2.7.2: ASSAY PRINCIPLES

The basic format of the assay was developed from a method outlined by Hewitt (Hewitt, C.O., et al, 1999). In short, it is possible to monitor the decay in absorbance of NADH as it is converted to NAD^+ at 340 nm. All experiments were conducted in buffered solution, where the buffer contained 20 mM tris-HCL and 50 mM KCl at pH 6.8.

To generate a decay curve, the absorbance of NADH and NAD^+ was measured at the following respective concentration ratios; 200:0 mM, 150:50 mM, 166:34 mM, 100:100 mM, 66:134 mM, 50:150 mM and 0:200 mM.

2.7.3: HIGH THROUGHPUT SCREEN

To the wells of an appropriate number of 96 well plates, the following was added: 5μL of library compound in neat DMSO at 100, 10 and 1μM concentrations; 20μL of buffer solution (50mM Tris, 20 mM KCl, pH 6.8); 25μL of sodium pyruvate in buffer at 400μM; 25μL of NADH in buffer at 800μM. To initiate the reaction, 25μL of LDH-A in buffer at 12nM was added after which the reaction kinetics were monitored using Soft Max Pro™ on a SpectraMax™ M2e plate reader for 3 mins. An endpoint was then taken and values normalised using positive control (no inhibitor, 5μL neat DMSO) and negative control (no sodium pyruvate, 25μL buffer for each inhibitor concentration) values. The data was then represented as a percentage of the normalised negative control at 500nM final concentration.

2.8: CHEMISTRY

All reactions involving organometallic or other moisture-sensitive reagents were carried out under a nitrogen or argon atmosphere using standard vacuum line techniques and glassware that was flame dried and cooled under nitrogen before use. Solvents were dried according to the procedure outlined by Grubbs and co-workers (Pangborn, A.B., *et al*, 1996). Water was purified by an Elix® UV-10 system. All other reagents were used as supplied (analytical or HPLC grade) without prior purification. Organic layers were dried over $MgSO_4$. Thin layer chromatography was performed on aluminium plates coated with 60 F_{254} silica. Plates were visualised using UV light (254 nm), iodine, 1% aq $KMnO_4$, or 10% ethanolic phosphomolybdic acid. Flash column chromatography was performed on Kieselgel 60 silica on a glass column.

Melting points were recorded on a Gallenkamp Hot Stage apparatus and are uncorrected. NMR spectra were recorded on Bruker Avance spectrometers in the deuterated solvent stated. Spectra were recorded at rt unless otherwise stated. The field was locked by external referencing to the relevant deuteron resonance. Low-resolution mass spectra were recorded on either a VG MassLab 20-250 or a Micromass Platform 1 spectrometer. Accurate mass measurements were run on either a Bruker MicroTOF internally calibrated with polyalanine, or a Micromass GCT instrument fitted with a Scientific Glass Instruments BPX5 column (15 m × 0.25 mm) using amyl acetate as a lock mass.

2.8.1: GENERAL SYNTHESIS OF BIS-OXIMES

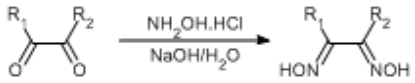

Hydroxylamine hydrochloride (2.0 eq) was dissolved in an ice-cold solution of sodium hydroxide (1.4 eq) in water. With the reaction mixture still on ice, the appropriate 1,2-dicarbonyl (1.0 eq) was added slowly and under stirring. The mixture was allowed to stand for 15 min on ice and then at room temperature overnight. The flask and contents were then cooled to 0^{o}C and the precipitate was filtered, washed with cold water, and dried under vacuum (Sheremetev, A.B., *et al*, 2003).

1-PHENYLPROPANE-1,2-DIONE DIOXIME

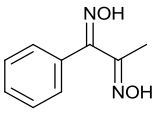

Isolated as a tan-coloured solid (0.43g, 70%); δ_H (400 MHz, $CDCl_3$) 2ppm (s, Me), 7.50-7.85ppm (m, Ph); mp 234-235^{o}C; MS(FI) 178.22(M^+).

2-(HYDROXYIMINO)-2-PHENYLACETALDEHYDE OXIME

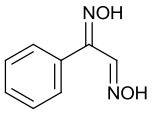

Isolated as a tan-coloured solid (0.45g, 81%); δ_H (400 MHz, $CDCl_3$) 7.80-8.50ppm (m, Ph), 8.35ppm (s, 1H); mp 146-148^{o}C; MS(FI) 164.06(M^+).

BIACETYL DIOXIME

Isolated as a white-coloured solid (7.2g, 77%); δ_H (400 MHz, $CDCl_3$) 1.95 ppm (s, 2Me); mp 237-238^oC; MS(FI) 116.06(M^+).

2.8.2: GENERAL SYNTHESIS OF FURAZANS

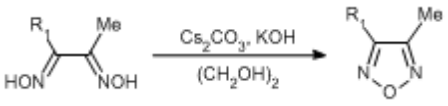

Bis-oxime (1.0 eq), ethylene glycol (0.15mL mM^{-1}), potassium hydroxide (0.04 eq), and caesium carbonate (0.008 eq) were placed in a round bottom flask with a stirrer. The resulting viscous substance was rapidly heated to 110^oC with stirring. Further heating to over 160^oC took place at ~1^oC min^{-1}. A dark solution was formed and the distillate was collected after which the residue was cooled to 80-90^oC. Water (80μL mM^{-1}) was added and the residue of the product was removed by azeotropic distillation with water. The combined distillates were extracted with dichloromethane and the mixture was washed with water. The organic layer was dried of magnesium sulphate and filtered. The dichloromethane was removed under vacuum and the remaining oil distilled at atmospheric pressure (Sheremetev, A.B., *et al*, 2003).

3-METHYL-4-PHENYL-1,2,5-OXADIAZOLE

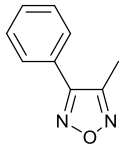

Isolated as a yellow oil; δ_H (400 MHz, $CDCl_3$) 2.55ppm (s, Me), 7.50-7.80ppm (m, Ph); bp 163-169^oC; MS(FI) 160.19(M^+).

3,4-DIMETHYL-1,2,5-OXADIAZOLE

Isolated as a yellow oil (0.60g, 20%); δ_H (400 MHz, $CDCl_3$) 2.35ppm (s, Me); bp 165-171^oC; MS(FI) 98.10(M^+).

2.8.3: GENERAL SYNTHESIS OF OXAMIC ESTERS

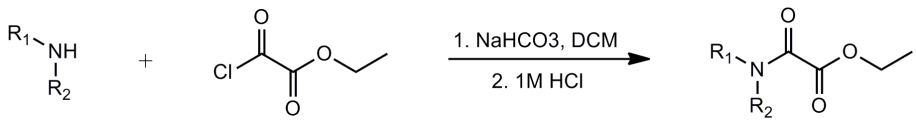

To a stirred 1M solution of ethyl chlorooxoacetate (2.0 eq) in DCM at 0^oC was added a 0.5M solution of amine (1.0 eq) in DCM and a 0.2M solution of sodium hydrogencarbonate (1.5 eq) in DCM. The mixture was stirred at 0^oC for 10 h.

On completion, the reaction mixture was treated with 1N hydrochloric acid until the reaction mixture was pH 2. The acid was then extracted with DCM and washed with brine (3 x 10 mL), dried ($MgSO_4$), and concentrated under vacuum(Choi, S-r., *et al*, 2007).

ETHYL 2-OXO-2-(4-P-TOLYPIPERAZIN-1-YL) ACETATE

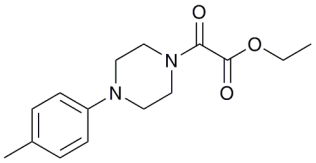

Isolated as a yellow oil (517mg, 69%); δ_H (400 MHz, $CDCl_3$) 1.27 (3H, t, ***J*** 7.24, C***H***$_3$), 2.29 (3H, s, C***H***3), 3.20-3.85 (8H, m, ***piperazine***), 4.34 (2H, q, ***J*** 7.12, C***H***$_2$), 6.86-7.13 (4H, m, ***Ph***); MS(ES) 299.14 (M^++Na).

ETHYL 2-(4-(4-FLUOROPHENYL)PIPERAZIN-1-YL)-2-OXOACETATE

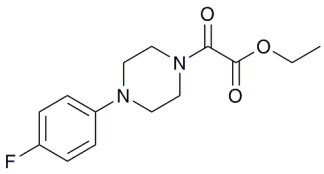

Isolated as a yellow oil (487mg, 58%); δ_H (400 MHz, $CDCl_3$) 1.39 (3H, t, ***J*** 7.23, C***H***$_3$),3.12-3.79 (8H, m, ***piperazine***), 4.33 (2H, q, ***J*** 7.19, C***H***$_2$), 6.78-7.02 (4H, m, ***Ph***); MS(ES) 303.11 (M^++Na).

ETHYL 2-(4-(2-FLUOROPHENYL)PIPERAZIN-1-YL)-2-OXOACETATE

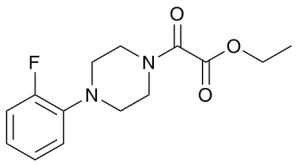

Isolated as a yellow oil (605mg, 72%); δ_H (400 MHz, $CDCl_3$) 1.40 (3H, t, ***J*** 7.32, C***H***$_3$), 3.15-3.85 (8H, m, ***piperazine***), 4.39 (2H, q, ***J*** 7.10, C***H***$_2$), 6.99-7.28 (4H, m, ***Ph***); MS(ES) 303.11 (M^++Na).

ETHYL 2-(4-(2-METHOXYPHENYL)PIPERAZIN-1-YL)-2-OXOACETATE

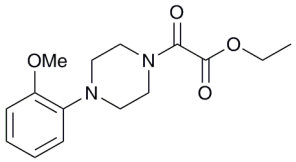

Isolated as a yellow oil (735mg, 84%); δ_H (400 MHz, $CDCl_3$) 1.39 (3H, t, ***J*** 7.31, C***H***$_3$), 3.08-3.83 (8H, m, ***piperazine***), 3.85 (3H, s, OC***H***$_3$), 4.37 (2H, q, ***J*** 7.07, C***H***$_2$), 6.87-7.05 (4H, m, ***Ph***); MS(ES) 315.13 (M^++Na).

ETHYL 2-(4-(3-METHOXYPHENYL)PIPERAZIN-1-YL)-2-OXOACETATE

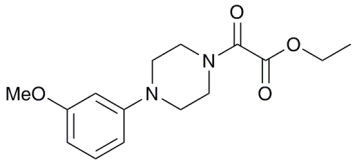

Isolated as a yellow oil (727g, 83%); δ_H (400 MHz, $CDCl_3$) 1.35 (3H, t, ***J*** 7.29, C***H***$_3$), 3.17-3.74 (8H, m, ***piperazine***), 3.75 (3H, s, OC***H***$_3$), 4.32 (2H, q, ***J*** 7.08, C***H***$_2$), 6.43-7.15 (4H, m, ***Ph***); MS(ES) 315.13 (M^++Na).

ETHYL 2-(4-(4-METHOXYPHENYL)PIPERAZIN-1-YL)-2-OXOACETATE

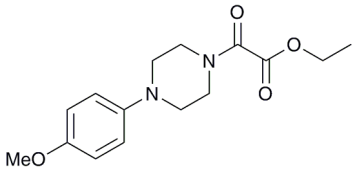

Isolated as an amber oil (675mg, 77%); δ_H (400 MHz, $CDCl_3$) 1.35 (3H, t, ***J*** 7.30, C***H***$_3$), 3.04-3.75 (8H, m, ***piperazine***), 3.75 (3H, s, OC***H***$_3$), 4.36 (2H, q, ***J*** 7.10, C***H***$_2$), 6.87 (4H, m, ***Ph***); MS(ES) 315.14 (M^++Na).

ETHYL 2-(4-(4-TRIFLUOROMETHYL)PIPERAZIN-1-YL)-2-OXOACETATE

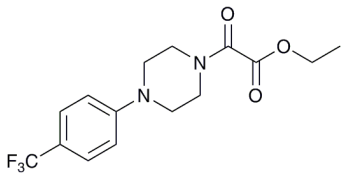

Isolated as a yellow oil (733mg, 74%); δ_H (400 MHz, $CDCl_3$) 1.39 (3H, t, ***J*** 7.23, C***H***$_3$),3.33-3.85 (8H, m, ***piperazine***), 4.36 (2H, q, ***J*** 7.14, C***H***$_2$), 6.97-7.55 (4H, m, ***Ph***);MS(ES) 353.26 (M^++Na).

2.9: STATISTICAL METHODS

All data analysis was performed using GraphPad Prism® v4.0 software. Statistical significance was determined using unpaired, two-tailed, t-tests with confidence intervals set at 95%.

CHAPTER 3: LACTATE DEHYDROGENASE, HYPOXIA, AND CANCER

3.1: INTRODUCTION

3.1.1: THE WARBURG EFFECT

The Warburg Effect, or elevated aerobic glycolysis in transformed cells, correlates with more malignant phenotypes and poor prognosis in patients (Kim, J.W., *et al*, 2006). To maintain a glycolytic phenotype it is necessary, amongst other things, for the cellular fate of pyruvate to change.

To metabolise this pyruvate out of the cell LDH-A reduces the pyruvate to lactate which is then exported from the cell by Mono-Carboxylate Transporters (MCTs). LDH-A achieves this reduction via the use of NADH as a cofactor which is simultaneously oxidised to NAD^+ which is in turn recycled by early stage glycolysis at the level of Glyceraldehyde Phosphate Dehydrogenase (GAPDH).

3.1.2: LDH-A AND TUMOUR HYPOXIA

LDH-A is over-expressed in a variety of tumour types and can be correlated with poor prognosis (Koukourakis, M.I., *et al*, 2003) (Koukourakis, M.I., *et al*, 2006) (Koukourakis, M.I., *et al*, 2009). It is also expressed in response to hypoxic conditions as a direct HIF-1 target gene (Ke, Q., *et al*, 2006).

As referred to in **Chapter 1**, hypoxia is defined as an oxygen concentration of less than 1% and is associated with a variety of cellular responses, many of which are mediated through HIF.

3.1.3: LDH-A EXPRESSION; ADAPTIVE OR ONCOGENIC PHENOTYPE?

The hypoxic expression of LDH-A suggests that the shift to glycolysis in many cases is an adaptive change in response to low oxygen. However, increasing evidence suggests an oncogenic role for LDH-A (Hanahan, D., *et al*, 2011).

The literature suggests a correlation between c-Myc and LDH-A expression (Shim, H. *et al*, 1997) whilst more broadly there is a great deal of speculation as to the existence or otherwise of a 'Warburg Kinase' (Robey, R.B., *et al*, 2009). Moreover, over-expressing LDH-A is sufficient to induce the Warburg effect (Shim, H. *et al*, 1997) whilst several studies have pointed to the efficacy of knocking out LDH-A as a clinical approach that reduces invasion and tumourigenicity (Fantin, V.R., *et al*, 2006) (Le, A., *et al*, 2010).

3.1.4: AIMS

The challenge then is to identify cell lines and tumour types particularly sensitive to LDH-A inhibition in order to validate LDH-A as an anti-cancer target. In parallel to this, LDH-B will be explored in order to ascertain whether selectivity towards LDH-A will be required in any potential small molecule inhibitor.In the first instance it is important to uncover any interplay between tumour hypoxia and the role of LDH-A in order to shed further light on whether LDH-A expression in tumours is an adaptive or oncogenic phenotype, or both.

3.2: RESULTS

3.2.1: THE EXPRESSION OF LDH VARIES BETWEEN HEALTHY TISSUE AND TUMOUR TISSUE

Before analyzing proprietary datasets, an opensource serach was conducted of clinical data in the public realm on Oncomine in order to generate a general impression of the nature of LDH-A expression in healthy versus tumour tissue.

The data was filtered to select those cases that compared normal versus tumour tissue expression (unpaired). Following this, key tissue types were selected. Finally, for each tissue type, the data that was downloaded was the most significant.

Analysing gene expression data and comparing the difference in mean LDH-A expression between healthy and tumour tissue, the broad pattern was that mean LDH-A was more highly expressed in tumour tissue (**Figures3.1-3.3**). This was the case in ovarian cancers, prostate cancer, renal cancer, and cancers of colon and the rectum where the difference was statistically significant. In breast cancer, the difference was not statistically significant, though whether this was as a result of high basal levels in healthy tissue or low levels of induction remains to be determined; there is evidence in the literature of up-regulation in some breast tissue sections (Balinsky, D., *et al*, 1983).

The picture with LDH-B was more mixed with up-regulation in colorectal adenocarcinoma, down regulation in renal clear cell carcinoma, and again no statistical difference in breast tissue. (**Figure 3.4**).

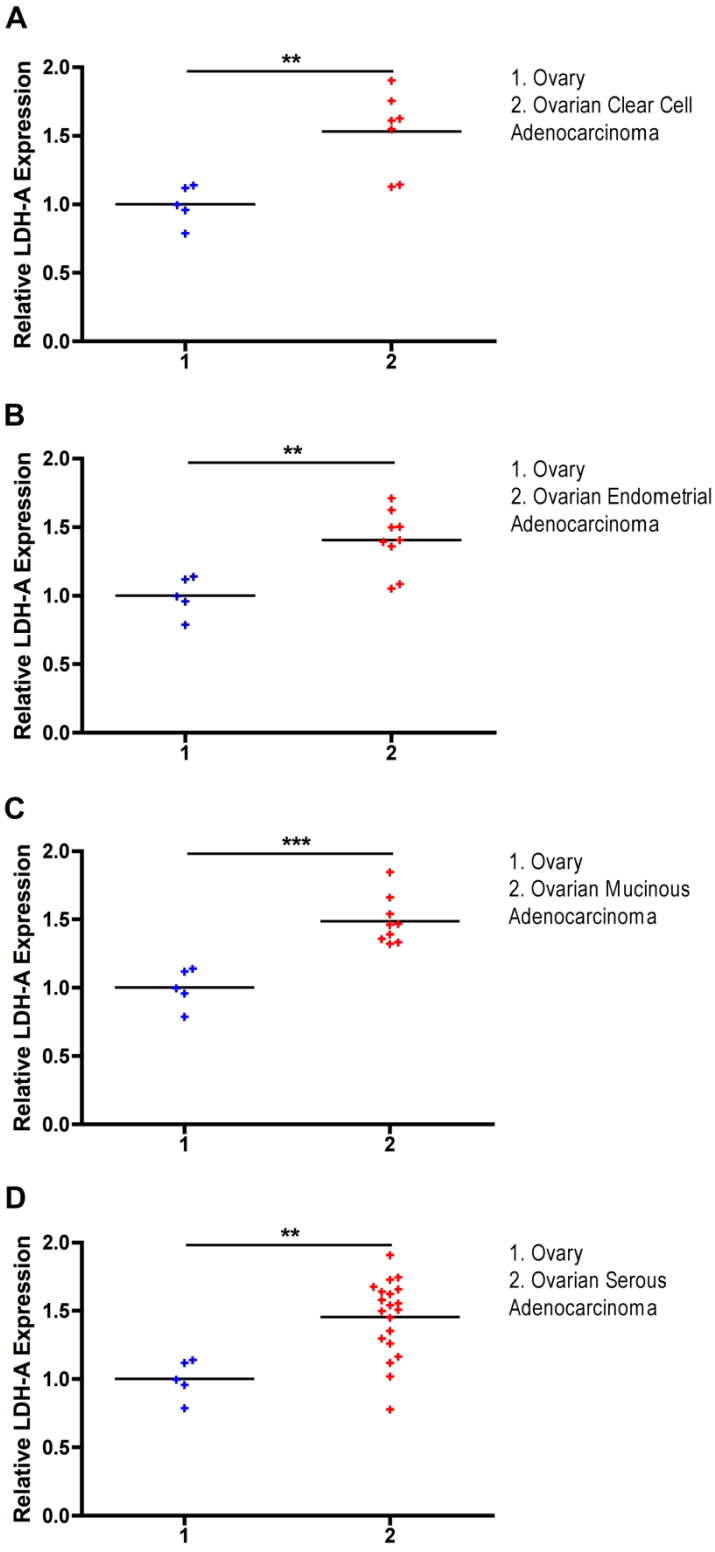

Figure 3.1: Expression of LDH-A in normal ovarian tissue versus [A] Ovarian Clear Cell Carcinoma; [B] Ovarian Endometrial Adenocarcinoma; [C] Ovarian Mucous Adenocarcinoma; [D] Ovarian Serous Adenocarcinoma. * = P <0.05; ** = P<0.01; *** = P<0.001. (50 patients in total).

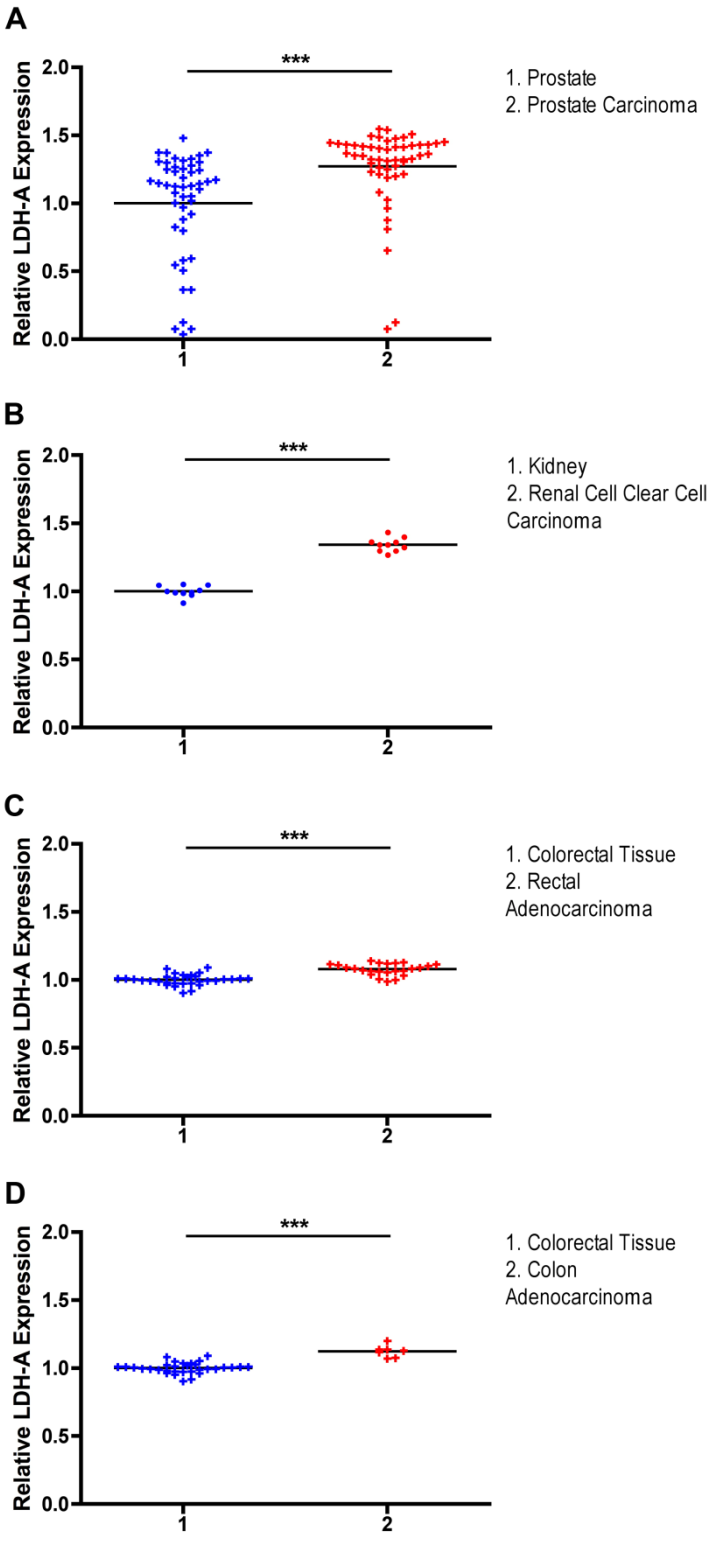

Figure 3.2: Expression of LDH-A in normal tissue versus [A] Prostate Carcinoma (102 patients); [B] Renal Clear Cell Carcinoma (20 patients); [C] Rectal Adenocarcinoma; [D] Colon Adenocarcinoma. * = P <0.05; ** = P<0.01; *** = P<0.001 (32 patients for [C] and [D] combined).

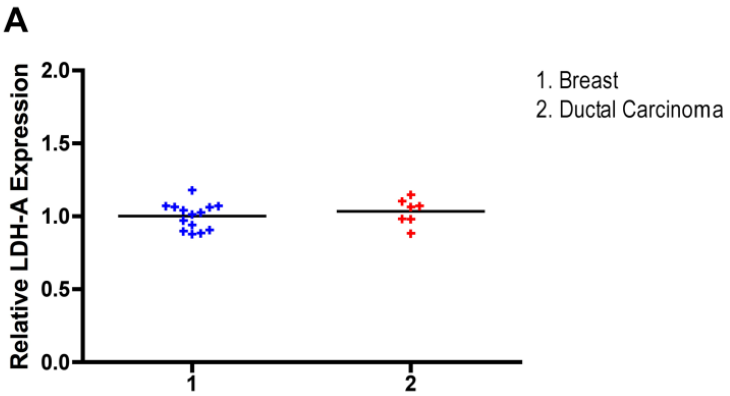

Figure 3.3: Expression of LDH-A in normal breast tissue versus [A] Ductal Carcinoma. * = P <0.05; ** = P<0.01; ** = P<0.001 (22 patients).

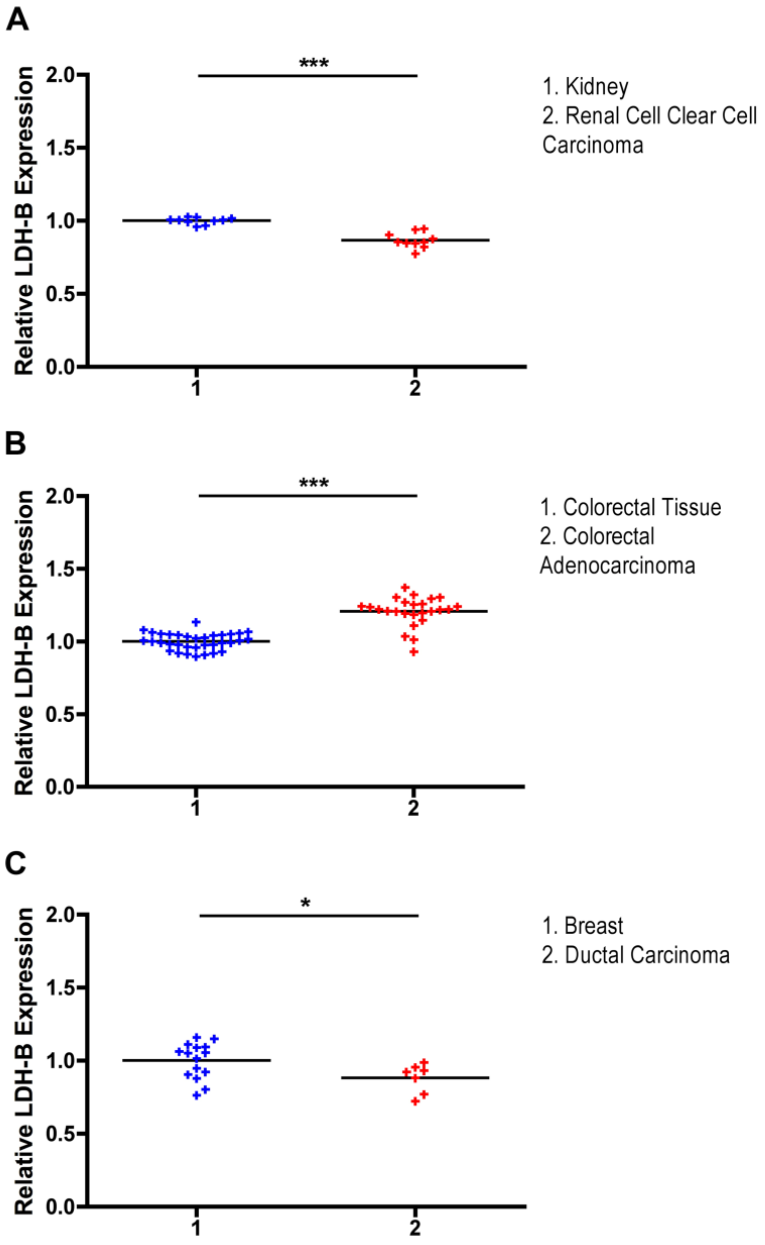

Figure 3.4: Expression of LDH-B in normal tissue versus [A] Renal Clear Cell Carcinoma (32 patients); [B] Colorectal Adenocarcinoma (32 patients); [C] Ductal Carcinoma (22 patients). * = P <0.05; ** = P<0.01; *** = P<0.001.

3.2.2: THE EXPRESSION OF LDH-A CORRELATES WITH INVASIVE, HYPOXIC TUMOURS WITH POOR PROGNOSIS WHILST THE EXPRESSION OF LDH-B DISPLAYS AN INVERSE RELATIONSHIP WITH ER EXPRESSION IN BREAST CANCER

Once analysis of the open source clinical data had been performed, the focus moved to more comprehensive data held in the group.152 clinical breast cancer cases were analysed to determine whether the expression of either LDH-A or LDH-B showed a significant degree of correlation with broader tumour phenotypes or patient prognosis.

The method used to analyse the data was chosen so as to normalize the results as much as possible to the background. For example, LDH-A is hypoxically up-regulated so one would therefore expect that, without such a correction, LDH-A expression could be linked to a broad range of characteristics associated with a hypoxic phenotype in which it was in fact a simple bystander. By taking into account this background phenotype the results account for a correlation between the LDH isoforms and a particular phenotype with the bystander problem minimized as much as possible. The characteristic genetic signatures that allowed this correction to take place have been identified elsewhere (Buffa, F.M. *et al*, 2010) (Wirapati, P., *et al*, 2008).

It was therefore interesting to note that the data shows that LDH-A expression correlates with two main characteristics, notably tumour hypoxia but also with more invasive tumour types (**Figure 3.5**). This correlation, as previously explained, takes into account the invasion score normally associated with hypoxia is important and whilst not demonstrating a causal link between LDH-A

expression and invasion, perhaps points to a link between LDH-A and more aggressive cancers worth further investigation.

Taking this a step further, patients were grouped into above or below median LDH-A expression in order to determine whether there was a link between expression and prognosis. As the data shows, patients expressing greater than the median levels of LDH-A have a poorer prognosis as measured in terms of recurrence free survival(**Figure 3.5D**).

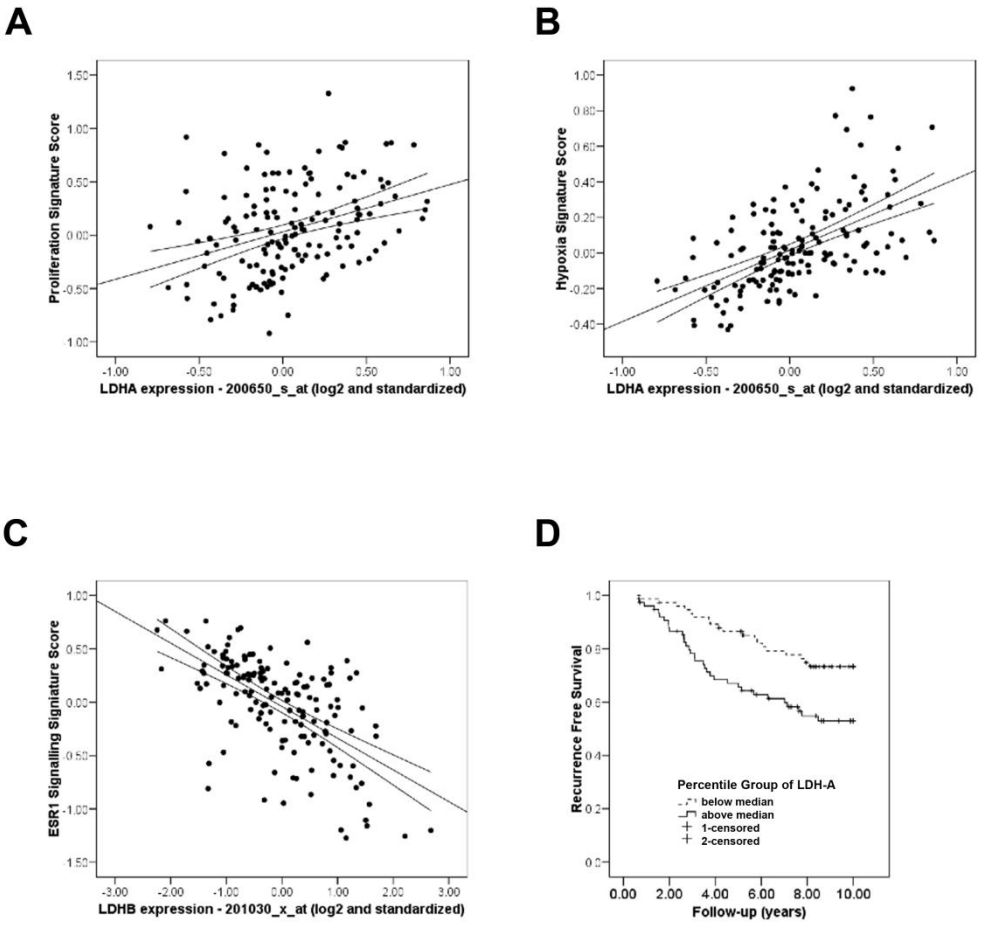

Figure 3.5: LDH-A expression: [A] correlates with proliferation (score = 0.3689); [B] correlates with hypoxia (score = 0.5735); [C] LDH-B expression inversely correlates with ER status (score = -0.5907); [D] is linked to lower recurrence free survival.

The only significant relationship demonstrated in correlation with LDH-B expression was where LDH-B expression showed an inverse relationship with estrogen receptor (ER) status. An easy explanation of this was not forthcoming and it was decided to probe this relationship further.

3.2.3: CONSTITUTIVE AND INDUCIBLE LDH-A AND LDH-B EXPRESSION VARIES IN DIFFERENT CANCER TYPES

The clinical data presented an interesting enough story to proceed with an investigation of the behaviour of tumour cells *in vitro* to better elucidate the interplay between LDH-A expression, hypoxia (given the strong correlation with LDH-A expression), and other characteristics of transformed cells.

A broad panel of cancer cell types were selected from a variety of different tissues, taking the ovarian (IGROV-1 and OC-316), prostate (PC3), renal ($^{+}$VHL and WTRCC4), colorectal ($^{+/+}$p53 and $^{-/-}$p53 HCT-116) and breast (MCF-7, MDA-MB-231, MDA-MB-361, MDA-MB-468) cancers that were looked at in the previous clinical analyses for the sake of consistency.

With the exception of the PC3 cells, the other lines were paired to specifically look at different mutations or surface receptor states. A full list of the mutations in the cell lines used is provided in **Table 3.1**.The key mutations of interest however are elaborated upon in the text below.

Table 3.1

Cell Line	Tissue	Mutations	Comments
IGROV-1	Ovarian	*MLH1* *MSH6* *p53*	*MLH1*, or MutL homolog 1, is a DNA mismatch repair gene. Codes for a G-T mismatch binding protein implicated in DNA repair. Codes for the tumour suppressor protein p53.
OC-316	Ovarian	*p53*	-
PC-3	Prostate	*PTEN* *p53*	Codes for phophatase and tensin homolog (PTEN), a tumour suppressor protein. -
RCC4	Kidney	*VHL*	Codes for Von Hippel Lindau complex responsible for degrading HIF.
HCT-116	Colon	*CDKN2a(p16)* *CDKN2a(p14)* *CTNNB1* *KRAS* *MLH1* *PI3KCA*	Cell cycle dependent kinase- a tumour suppressor gene coding for proteins p16 and p14, normally involved in cell cycle regulation. Involved in the control of cell adhesion and implicated in the regulation of anchorage dependent growth. Codes for V-Ki-ras2 Kirsten rat sarcoma viral oncogene homolog (KRAS), a GTPase involved in multiple cell signaling pathways. - Codes for the Phosphatidylinositol 3-kinasep110α, a catalytic kinase involved in multiple cell signaling pathways.
MCF-7	Breast	*CDKN2a(p16)* *CDKN2a(p14)* *PI3KCA*	- - -
MDA-MB-231	Breast	*BRAF* *CDKN2a(p16)* *CDKN2a(p14)* *KRAS* *NF2* *p53*	Gene codes for the serine/threonine protein kinase v-Raf murine sarcoma viral oncogene homolog B1- implicated in cell signaling and growth - - - Neurofibromatosis type 2, ordinarily an inheritable genetic condition- gene mutated in some cancers -
MDA-MB-361	Breast	*CDKN2a(p16)* *PI3KCA*	- -
MDA-MB-468	Breast	*PTEN* *RB1* *SMAD4* *p53*	- Codes for the retinoblastoma tumour suppressor protein Codes for the tumour suppressor protein SMAD4 -

The oncoprotein p53 is associated with many cancer types (Bensaad, K., *et al*, 2007). Many of the cell lines selected possess a p53 mutation; in glycolytic terms its interaction with the phosphofructokinases via TIGAR offers an opportunity to see if p53 affects expression of LDH. To this end, and to allow direct comparison within a cell line, HCT-116 cells (a cell-line normally without a p53 mutation) were used with $^{+/+}$p53 representing the wild-type and the knockout representing a p53 mutant.

A mutation in the gene coding for the Von Hippel Lindau complex is characteristic of renal clear cell carcinomas; as such, $^{-/-}$VHL RCC4 is the wild-type cell and lacks the ability to ubiquitinylate HIF-1α. As a result HIF-1α is not degraded and the wild-type therefore displays a pseudo-hypoxic phenotype. The pairing of this cell line with RCC4 with VHL knocked back in provides a pseudo-normoxic phenotype against which to compare the wild-type.

Lastly, four breast cell lines were selected to probe LDH expression further. These were paired according to their Estrogen Receptor (ER) status, given the earlier interesting indications from the clinical data of an inverse relationship between ER status and LDH-B expression. In brief, MCF-7 and MDA-MB-361 cells are ER-positive and therefore present estrogen receptors whereas MDA-MB-231 and MDA-MB-468 are ER-negative and do not.

ER is a nuclear hormone binding receptor that binds estradiol (estrogen), stimulating proliferation. Some 70% of breast tumours are ER-positive and ER status is linked to prognosis and age of occurrence. Specifically, ER-positive tumours are more likely to occur post-menopause and are not generally as aggressive as ER-negative tumours (Gelbfish, G.A., *et al*, 1988).

Taking this panel as representative of a broad spectrum, it is clear that there was a degree of variance in both LDH-A and LDH-B expression both between and within cancer types(**Figure 3.6**). This not withstanding, the following observations can be made. Firstly, despite a difference in constitutive levels of LDH-A expression, LDH-A was hypoxia-induced in all of the cell lines with the exception of the paired $^{+/+}$p53 and $^{-/-}$p53 HCT-116 which instead demonstrated a relatively high constitutive normoxic level of LDH-A expression (**Figure 3.6A**).

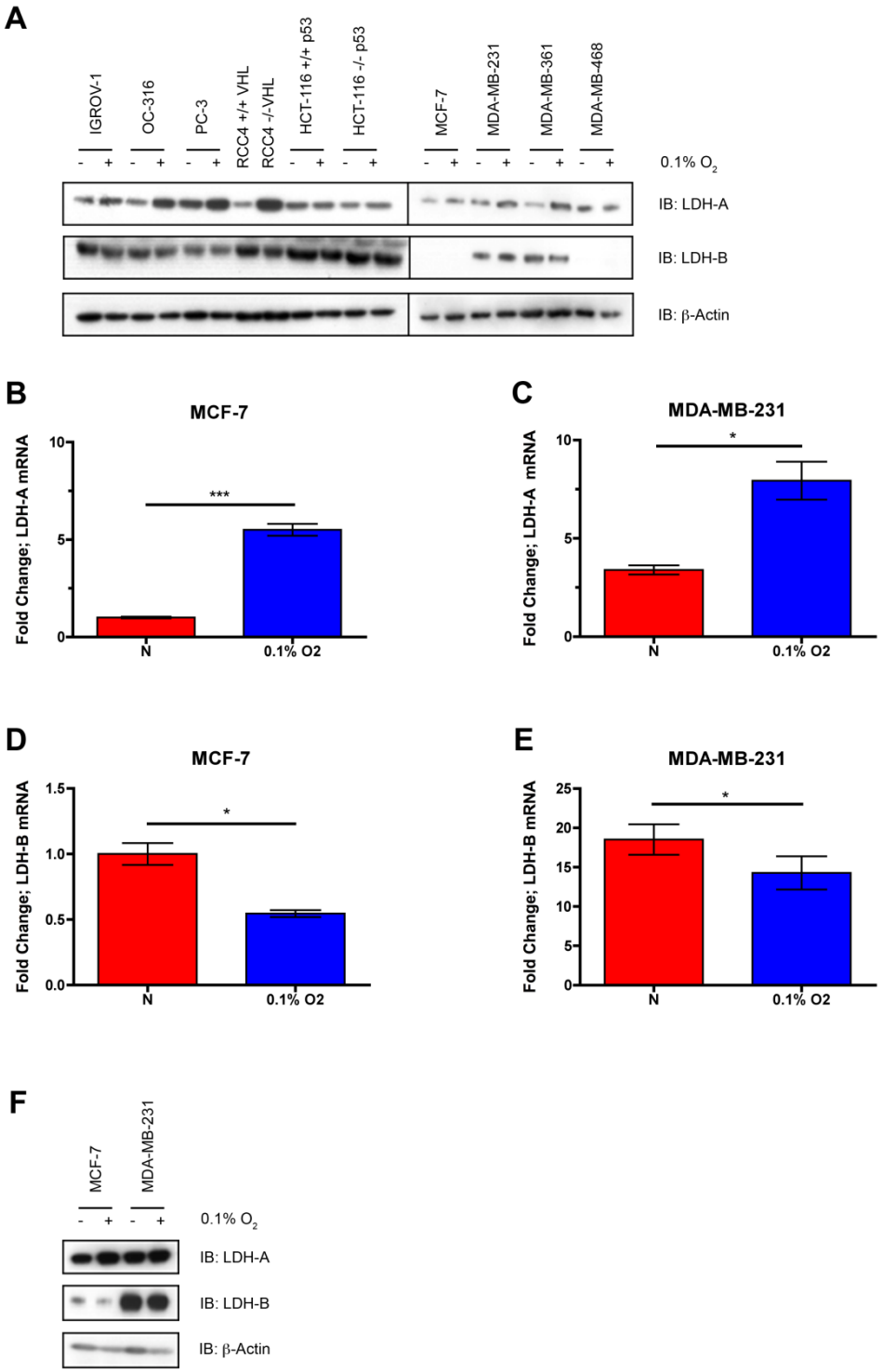

Figure 3.6: LDH-A and LDH-B expression under normoxia and hypoxia: [A] protein levels across a broad panel of cell lines; [B]-[D] RNA levels in MCF-7 and MDA-MB-231; [F] a higher exposure of MCF-7 and MDA-MB-231 reveals LDH-B is constitutively expressed by MCF-7. t = 48h. N=3. * = P <0.05; ** = P<0.01; *** = P<0.001.

Secondly, there appeared to be limited differences in LDH-B expression after hypoxic exposure in the non-breast cell lines on a protein level.

The picture in the breast lines was less clear due to large variances in constitutive expression levels. In particular, the relationship between ER status and LDH-B expression only held in half of the breast cancer cell lines, with MDA-MB-361 and MDA-MB-468 showing the inverse relationship of what was expected.

To explore LDH-A further and investigate the inverse relationship between ER status and LDH-B identified in MCF-7 and MDA-MB-231**Figure 3.5C**it was decided to look at both LDH-A and LDH-B expression in more detail in these cell lines as they showed large differences in constitutive LDH-A and LDH-B expression.

The relative mRNA levels in MCF-7 and MDA-MB-231 (**Figure 3.6B-E**) showed that there was again a difference in constitutive levels between cell lines with MDA-MB-231 expressing 3.4 times more LDH-A mRNA and 18.5 times more LDH-B mRNA under normoxia than MCF-7. This higher constitutive level of expression in MDA-MB-231 led to less hypoxic control than in MCF-7 with the latter seeing a 5.5 fold increase in LDH-A mRNA (**Figure 3.6B**) compared to the former's 2.3 fold increase (**Figure 3.6C**). The story was repeated for LDH-B mRNA with hypoxia in MCF-7 reducing levels by 45% (**Figure 3.6D**) compared to 23% in MDA-MB-231 (**Figure 3.6E**).

This data was reinforced by re-running the protein gels for MCF-7 and MDA-MB-231 and then over-exposing the resulting film (**Figure 3.6F**); this supported the mRNA data. It also demonstrated that whilst the differences in constitutive LDH-B expression between MCF-7 and MDA-MB-231 in **Figure 3.6A** are correct, that the

levels of LDH-B in MCF-7 are so low compared to MDA-MB-231 that they were virtually undetectable at a normal film exposure.

With this data in mind, the third observation is that in MCF-7 and MDA-MB-231 cells there was an inverse relationship between ER status and LDH-B expression which correlates to the previous clinical data; in particular the MDA-MB-231 cells which are ER-negative showed markedly higher LDH-B levels on both a protein and mRNA level as opposed to the ER-positive MCF-7 though this relationship was not mirrored in ER-negative MDA-MB-468 which instead showed no LDH-B expression.

Lastly, there was a higher constitutive level of expression of LDH-A in MDA-MB-231 than MCF-7. This difference in LDH-A expression reflects the difference between MCF-7 and MDA-MB-231 with the latter being recognised as a more glycolytic cell line than the former (Gattenby, R.A., *et al*, 2004).

These findings considered, it was decided that MCF-7 and MDA-MB-231 represented a good pair of cell lines to continue experimental work in given their differing ER statuses, LDH-A and LDH-B expression levels and glycolytic rates.

3.2.4: Exposure to hypoxia reveals a reciprocal relationship between LDH-A and LDH-B Expression in MCF-7 and MDA-MB-231

Given the link between LDH-A and hypoxia, it was important to establish the point at which LDH-A is induced, understand the importance of differencesin constitutive levels of expression, and also to probe further the relationship between LDH-B and hypoxia. As can be seen in **Figure 3.7**, exposing MCF-7 and

MDA-MB-231 cells to hypoxia at 0.1% oxygen uncovers a reciprocal relationship between LDH-A and LDH-B expression.

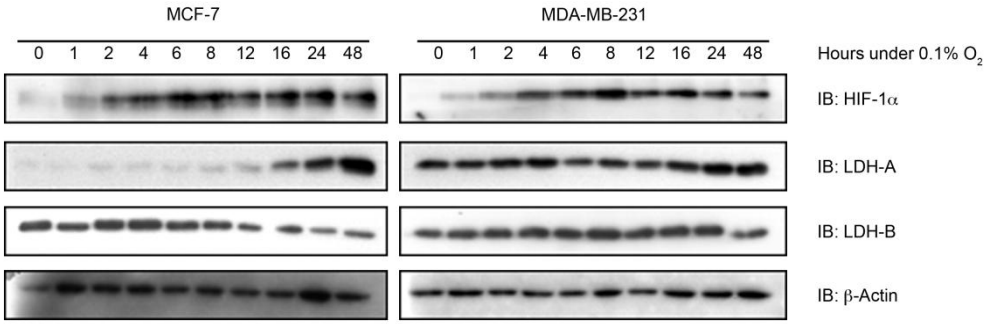

Figure 3.7:changes to the expression of HIF-1α, LDH-A and LDH-B upon prolonged exposure to hypoxia. N=3.

This inversion in expression levels was clearest in the MCF-7, with a point of inflexion occurring between 8 and 12 hours whilst in MDA-MB-231 this takes place later between 24 and 48 hours.

The more highly glycolytic MDA-MB-231 had a higher level of constitutive expression of both proteins and therefore a less marked hypoxic induction of LDH-A or down-regulation of LDH-B, though in the case of LDH-B it was starting from a markedly higher basal level than the MCF-7 cells. In short, evidence of a reciprocal relationship in MDA-MB-231 was less clear-cut.

Taken as a whole, the data not only shows differential response to hypoxia in terms of LDH-A and LDH-B expression but crucially also suggests a possible role for LDH-B that necessitates its down regulation in both cell lines that studies to date have failed to uncover.

3.2.5: THE HYPOXIC UP-REGULATION OF LDH-A AND DOWN-REGULATION OF LDH-B IS MEDIATED BY HIF-1

Following on from the previous data exposing a relationship between LDH-A/B expression and hypoxia it was important to determine the nature of hypoxic control and demonstrate whether it was dependent on a known hypoxia-regulated transcription factor.

The approach chosen used RNA interference to knock down HIF-1 and HIF-2.In MCF-7 the effects were clear at both the RNA and protein levels (**Figure 3.8A, C and E**). LDH-A up-regulation under hypoxia was HIF-1 dependent and HIF-2 independent with LDH-A mRNA levels reduced by 64% compared to the hypoxic control when HIF-1 was knocked down. The down-regulation of LDH-B in MCF-7 under hypoxia showed a similar HIF-1 dependence with a 1.6 fold increase in mRNA levels compared to the hypoxic control.

In MDA-MB-231, (**Figure 3.8B, D and E**) there was a higher constitutive level of expression of both isoforms; whilst HIF-1 and HIF-2 played a similar role, their effect on global levels of LDH-A and LDH-B as a consequence were much less marked; HIF-1 knockdown reduced LDH-A mRNA levels by 21% and led to a 1.4 fold increase in LDH-B mRNA.However, in MDA-MB-231 cells, there was a disconnect between HIF-2 and LDH-A with mRNA suggesting no HIF-2 control of LDH-A whilst the protein data was less conclusive.

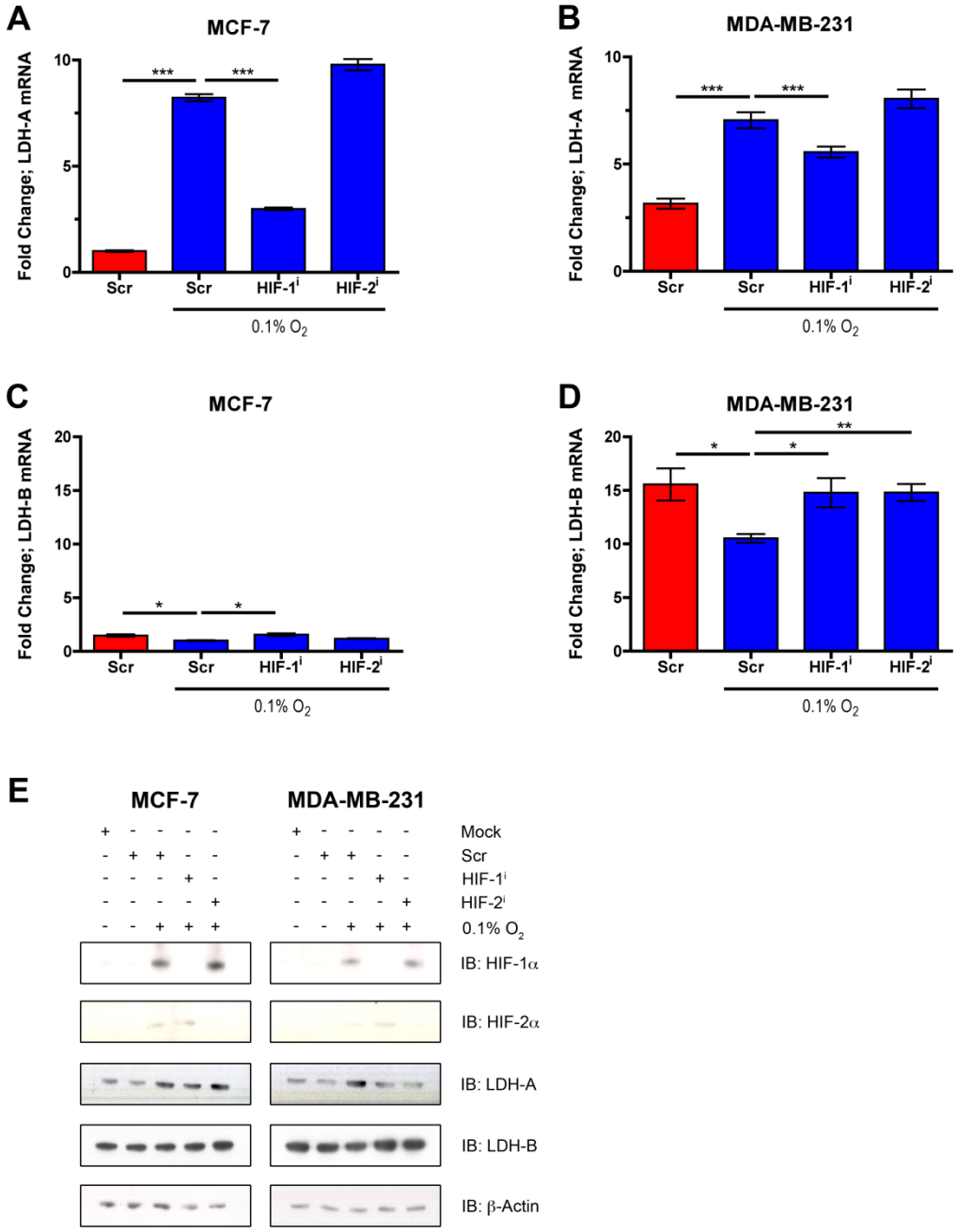

Figure 3.8: LDH-A expression is HIF-1 dependent in [A] MCF-7 and [B] MDA-MB-231; LDH-B expression is negatively regulated by [C] HIF-1 in MCF-7 and [D] HIF-1 and HIF-2 in MDA-MB-231. t = 48h. N=3. * = P <0.05; ** = P<0.01; *** = P<0.001.

3.2.6: RNA INTERFERENCE OF LDH-A AND LDH-B REDUCES CONSTITUTIVE EXPRESSION AFTER 48 HOURS

In order to further understand the role of LDH-A and LDH-B it was important to select and validate siRNA to both proteins. In both cases, three siRNA sequences were designed and synthesized; alongside these three, a pool of the three was also evaluated. With both LDH-A and LDH-B all three sequences were successful in knocking down their target protein; in neither was there an additive effect from the siRNA pool that in any way demonstrated an improved level of down-regulation (**Figure 3.9**).

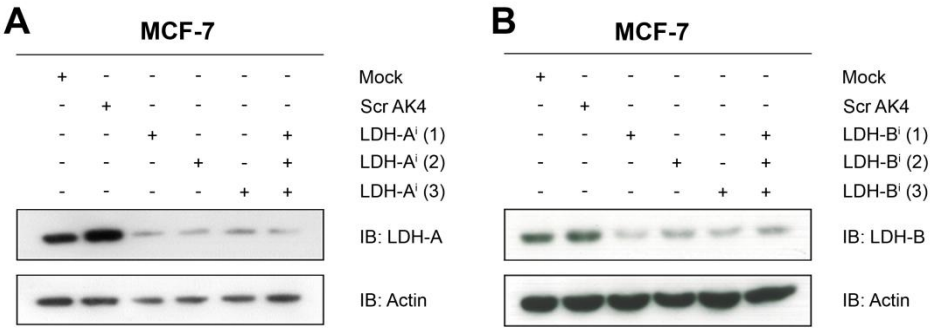

Figure 3.9: siRNA to [A] LDH-A and [B] LDH-B. t = 48h. N=3.

With the siRNA validated this provided a tool to knock out the expression of LDH-A and LDH-B in order to further study their function. With that in mind, LDH-A(1) and LDH-B(1) respectively were selected for further experimental use.

3.2.7: siRNA MEDIATED KNOCKDOWN OF LDH-A REDUCES THE GROWTH OF MCF-7 AND MDA-MB-231 CELLS GROWN IN 2D

Cells were transfected in duplicate according to standard protocol and allowed to recover before being exposed to 5 days hypoxia or being cultured in normoxia (control). Average cell counts were then analysed across all repeats and presented graphically.

In terms of cell growth over time MDA-MB-231 cells, as a more glycolytic and proliferative cell type than the MCF-7 cells, grew more quickly. However, in both cell lines, LDH-A knockdown had a significant effect on reducing growth when compared to the scramble control (**Figure 3.10**) (which itself demonstrated a reduction in growth when compared to a mock control, indicating the intrinsic toxicity of RNA interference). In MCF-7 cells there was a 61% reduction in growth in normoxia (**Figure 3.10A**) and a 93% reduction in growth in hypoxia (**Figure 3.10C**) when LDH-A was knocked down compared to the control.

In MDA-MB-231 there was a 60% reduction in growth in normoxia (**Figure 3.10B**) and a 52% reduction in growth in hypoxia (**Figure 3.10D**) when LDH-A was knocked down compared to the control. That the knockdown reduced growth in both normoxia and hypoxia demonstrates that there is a constitutive level of LDH-A activity that may correlate to the Warburg effect in both cell lines.

The story with LDH-B also seems clear inasmuch as the effect of LDH-B knockdown has no significant effect (**Figure 3.11**). Nevertheless, the role of LDH-B may be more subtle and it is naïve to expect dramatic global effects from every

protein knocked down. For this reason alone, the role of LDH-B deserves further exploration.

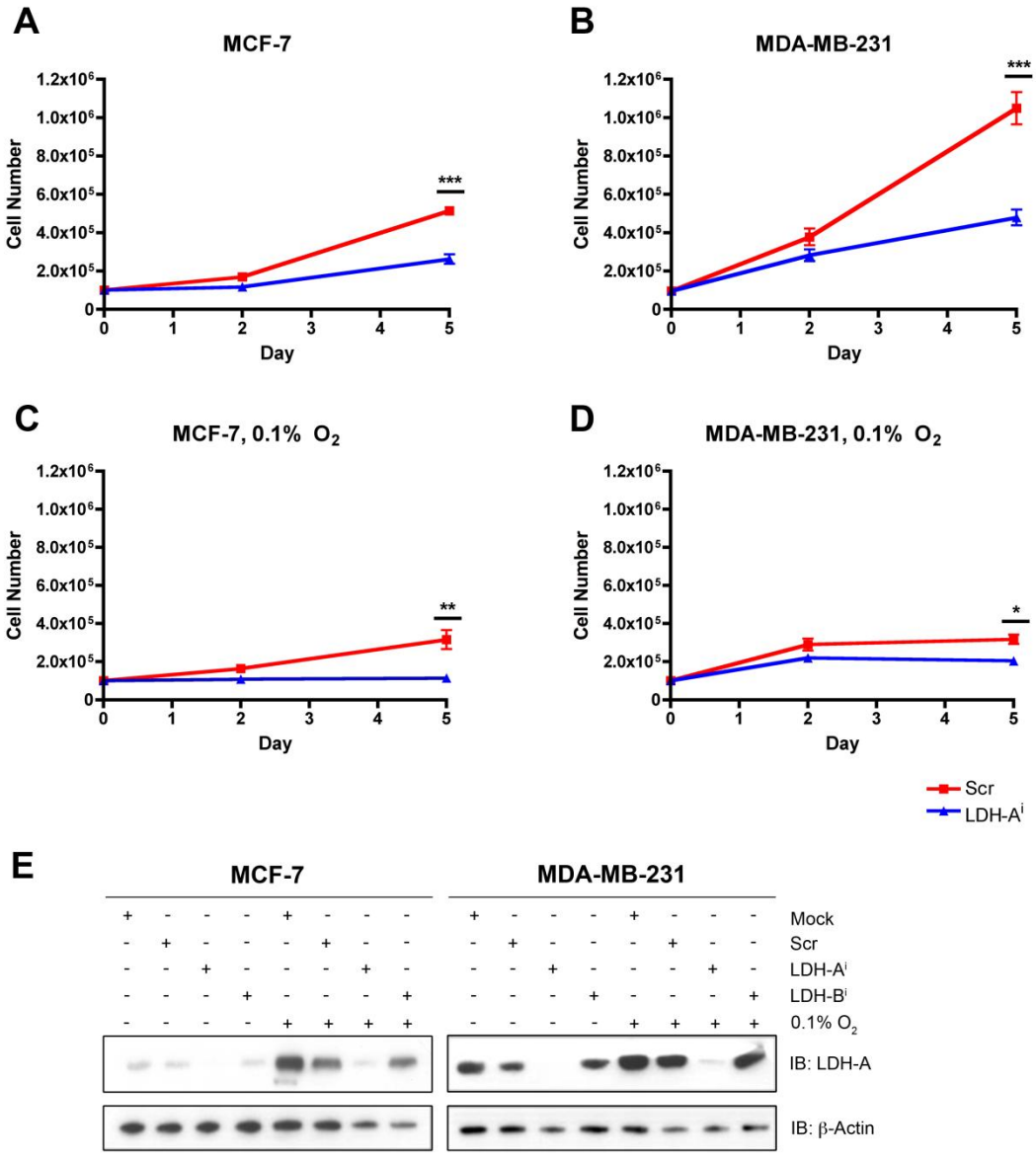

Figure 3.10: siRNA knockdown of LDH-A reduces the growth of [A] MCF-7 and [B] MDA-MB-231 in normoxia and [C]-[D] hypoxia; [E] immunoblot analysis demonstrates an efficient knockdown of LDH-A at day 5. N=3. * = P <0.05; ** = P<0.01; *** = P<0.001.

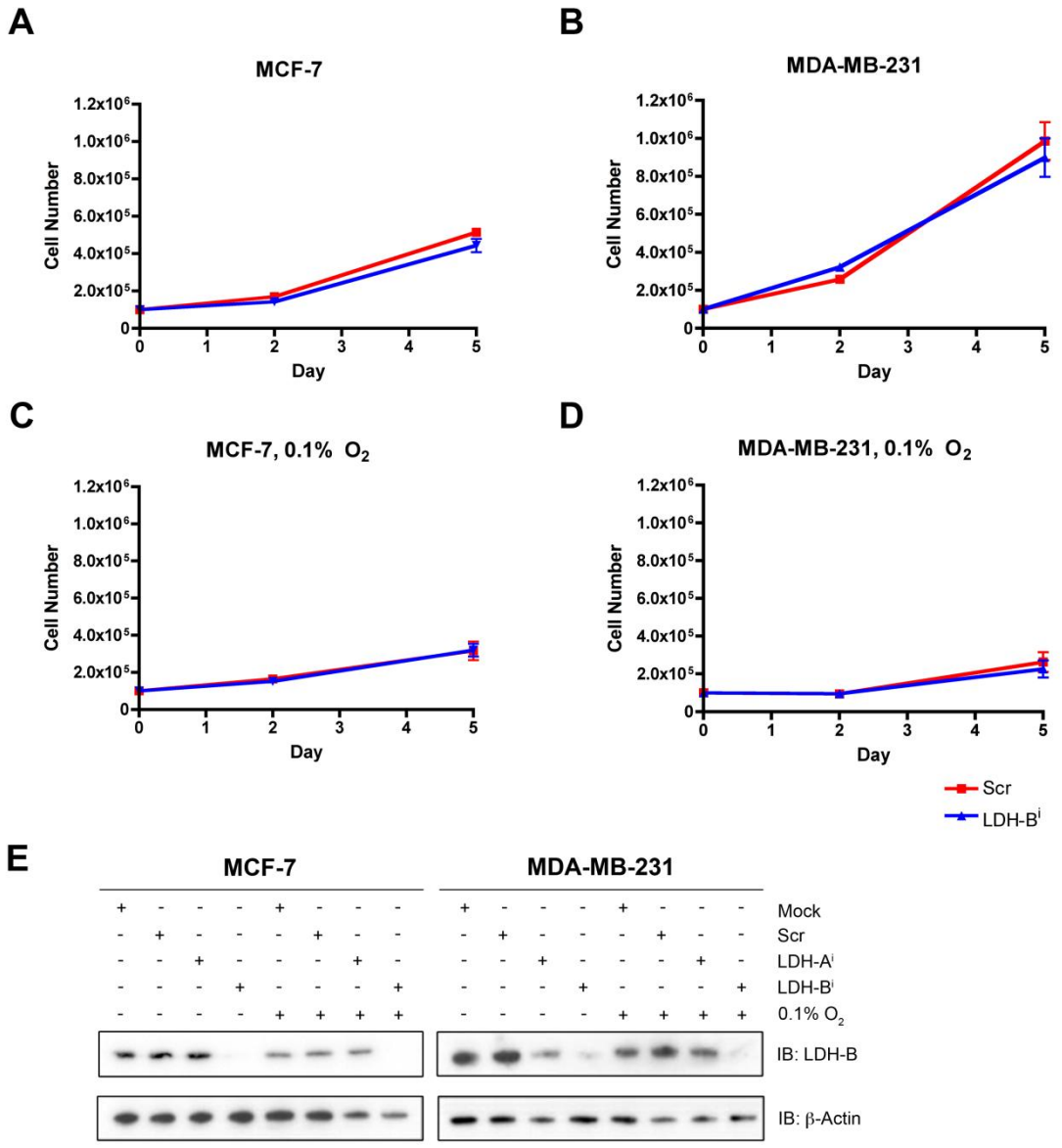

Figure 3.11: siRNA knockdown of LDH-B does not affect the growth of [A] MCF-7 and [B] MDA-MB-231 in normoxia and [C]-[D] hypoxia; [E] immunoblot analysis demonstrates an efficient knockdown of LDH-B at day 5. N=3. * = P <0.05; ** = P<0.01; *** = P<0.001.

3.3: DISCUSSION

3.3.1: LDH-A IS A VALID TARGET FOR FURTHER INVESTIGATION IN MCF-7 AND MDA-MB-231

LDH-A levels are elevated across a broad range of cancers and are upregulated under hypoxia in HIF-1 dependent manner. Despite there being a clear indication of differences between LDH-A and LDH-B levels in breast cancer cells, the data showing significant levels of both in some breast cancer cell lines indicates that this lack of significance on a clinical level derives in part from high constitutive levels of expression in healthy tissue.

The most important finding, within the context of validating LDH-A as a molecular target for small molecule inhibition, is that LDH-A is critical to tumour growth in normoxia and hypoxia.

Interestingly, LDH-A knockdown in normoxia in the less glycolytic MCF-7 impairs growth almost as significantly as knockdown in the more glycolytic MDA-MB-231 in hypoxia. This data perhaps uncovers several findings. Firstly, the role of hypoxia is not critical in determining the effect of LDH-A knockdown. Secondly, and following on from this, is the conclusion that LDH-A expression (and as a corollary aerobic glycolysis in general) is maintaining a phenotype that has more to it than a simply adaptive bioenergetic response to low oxygen levels. Lastly, on a practical level, is the supposition that confluent cells can generate pericellular hypoxia under normoxic conditions that cannot be completely factored out of experiments.

It would be expected that there would be a significant bioenergetic loss for cells to adopt an aerobic glycolytic phenotype; oxidative phosphorylation (OXPHOS) is a

much more efficient means of generating ATP. For every molecule of glucose, glycolysis produces 2 molecules of ATP whilst OXPHOS can produce up to 34 molecules of ATP. However, glycolytic cells appear to compensate for this shift to a less efficient pathway by aggressively increasing their glucose uptake (Vander Heiden, M.G., *et al*, 2009).

By trafficking pyruvate towards LDH instead of PDH and onwards into the mitochondrial Tri-Carboxylic Acid (TCA) cycle, loses a key substrate for conversion to oxaloacetate. Other sources of carbon feed the TCA cycle to maintain its biosynthetic role exist such as glutamine; indeed, evidence suggests that 40% of glutamine in some cell lines cells ends up incorporated into lactate, demonstrating an active TCA cycle feeding pyruvate back into the cytosol (DeBerardinis, R.J., *et al*, 2007). However, whilst the TCA cycle retains a certain degree of activity, studies have shown that the ATP generating potential of the mitochondria is severally compromised in aerobically glycolytic cells, with an increase in the mitochondrial membrane potential reflecting lower levels of ATP synthase proton transport across the membrane and therefore less ATP being synthesized via OXPHOS (Fantin, V.R., *et al*, 2006). This shift from a bioenergetic role for the mitochondria to a biosynthetic role is supported in the literature (DeBerardinis, R.J., *et al*, 2007).

Furthermore, the literature shows that murine cancer cells suffer reduced tumourigenicity and invasiveness when LDH-A expression was attenuated (Fantin, V.R., *et al*, 2006). There was also a reactivation of OXPHOS in cells where LDH-A expression was knocked down reflecting a link between LDH-A and mitochondrial metabolism. Aerobic glycolysis and LDH-A expression therefore plays a part in reducing oxidative stress by reducing the potential for the formation of reactive

oxygen species **(**ROS); in keeping with this, initial studies seem to show that LDH-A inhibition increases oxidative stress in tumour cells (Le, A., *et al*, 2010).In the first instance then, it is important to validate and quantify the effects of LDH-A inhibition in MCF-7 and MDA-MB-231 cells in order to explore whether the effects seen so far are the result of LDH-A inhibition producing a cytotoxic effect or whether it is merely slowing growth/cytostatic. Induced cytotoxicity would make LDH-A an attractive target; it is therefore important to establish the nature of LDH-A inhibition.

3.3.2: THE ROLE OF LDH-B NEEDS FURTHER ELUCIDATION

It remains unclear why LDH-B is down-regulated under hypoxia. There is a suggestion in the literature that pyruvate accumulation is cytotoxic and triggers apoptosis through the inhibition of Histone Deacetylase Complexes (HDACs). Without LDH-B, cells are unable to reflux lactate to pyruvate and as pyruvate is toxic, this would prevent a potentially lethal accumulation.

This notwithstanding, the question that needs addressing with respect to LDH-B centres on whether LDH-B is playing a role in maintaining growth or survival and future work should focus on unpicking this role further.

CHAPTER 4: LDH-A AS A TARGET FOR SELECTIVE ANTI-CANCER CHEMOTHERAPY

4.1: INTRODUCTION

Having established in the previous chapter that there is a reduction in growth when LDH-A is knocked down, it is important in terms of the central aim of this thesis- namely to explore targets with a view to drug discovery- to gain a better understanding of LDH-A as an anti-cancer target. To do this, it is necessary to reiterate the concepts that allow a molecular target to be judged as 'good' (or indeed, not 'good').

4.1.1: WHAT CONSTITUTES A 'GOOD' MOLECULAR TARGET?

The history of anti-cancer chemotherapeutics has been discussed at great length in an earlier chapter. With this in mind, it is sufficient highlight the shift in strategy from general cytotoxics that broadly inhibit all proliferating cells (with the attendant heavy side-effects that would be expected of such an approach) to more selective inhibitors of pathways that have been particularly implicated in maintaining transformed cells.

These targets can be found in a diverse array of pathways, from cell signalling to angiogenesis; it was with selective chemotherapeutics in mind that **Chapter 1** introduced LDH-A as a target due to it acting as a choke-point in maintaining bioenergetic, biosynthetic and bioreductive pathways. This notwithstanding, the

desired outcome is the samewhatever the target; to selectively kill tumour cells whilst minimizing the damage to healthy tissue, thereby increasing the potency of the treatment and reducing unwanted side-effects.

The key to a target being considered good then is that the pathway must either be one that is heavily or exclusively used in transformed cells (and as such is normally down-regulated or silenced in healthy tissue) or one where a redundancy exists in healthy tissue that is not present in the transformed cell. LDH-A could be placed in either the former category, given the up-regulation of aerobic glycolysis associated with many cancers, or the latter, considering that mitochondrial respiration is down-regulated in transformed cells (thereby removing an escape pathway for pyruvate that remains available in healthy cells).

Alongside this, it is important to consider whether any healthy tissues are over-reliant on a particular pathway; not least, the complex physiology and biochemistry of the heart cannot be overlooked. In this vein, the existence of LDH-B as a heart isoform needs to be probed in order to uncover whether selectivity towards LDH-A is essential.

Lastly, considering the aim to kill tumour cells, it is important that inhibiting the target of choice achieves this outcome; cytostatic agents may have a desirable effect and arrest tumour growth during the course of the treatment but once the chemotherapy is removed the potential remains for proliferation to resume. With this in mind, it is important to quantify whether inhibition of the target induces cell-cycle arrest or programmed cell death.

4.1.2: AIMS

Having established that LDH-A knockdown reduces the growth of MCF-7 and MDA-MB-231 cells, it is necessary to quantify this effect in terms of direct effects on metabolic outputs (ATP and lactate) and also more global effects on proliferation and cell death. In so doing, it should also be possible to arrive at a mechanistic explanation for any observations.

4.2: RESULTS

4.2.1: SIRNA MEDIATED KNOCKDOWN OF LDH-A AND LDH-B HAS DIFFERENT EFFECTS ON MCF-7 AND MDA-MB-231 CELLS IN A 3D MODEL

In order to develop a better idea of the effect both LDH-A and LDH-B knockdown, MCF-7 and MDA-MB-231 cells were grown as 3D tumour spheroids according to established procedures (Ivascu, A., *et al*, 2006). This model was adopted to give a more realistic idea of tumour growth in 3D; it was expected that over a given size the spheroid would develop a hypoxic core and therefore an oxygen gradient, something that the limitations of 2D culture cannot mimic.

The difference in growth rates between MCF-7 and MDA-MB-231 seen in 2D culture in the previous chapter (**Figure 3.10**) was exaggerated with MCF-7 cells growing much more slowly than MDA-MB-231 in the spheroid model.

In MCF-7 cells, neither LDH-A or LDH-B knockdown had a discernible effect (**Figure 4.1**). What was notable though was that the LDH-A knockdown produced much less round spheroids (**Figure 4.1 C**) that were more prone to disaggregation than the scramble control. This diminished roundness and increased propensity to disaggregate is indicative of peripheral cell death. These patches proved difficult to exclude when the imaging software was quantifying spheroid volume and subsequently may account for the slightly larger volume seen in the LDH-A knockdown throughout and in the control at day 1.

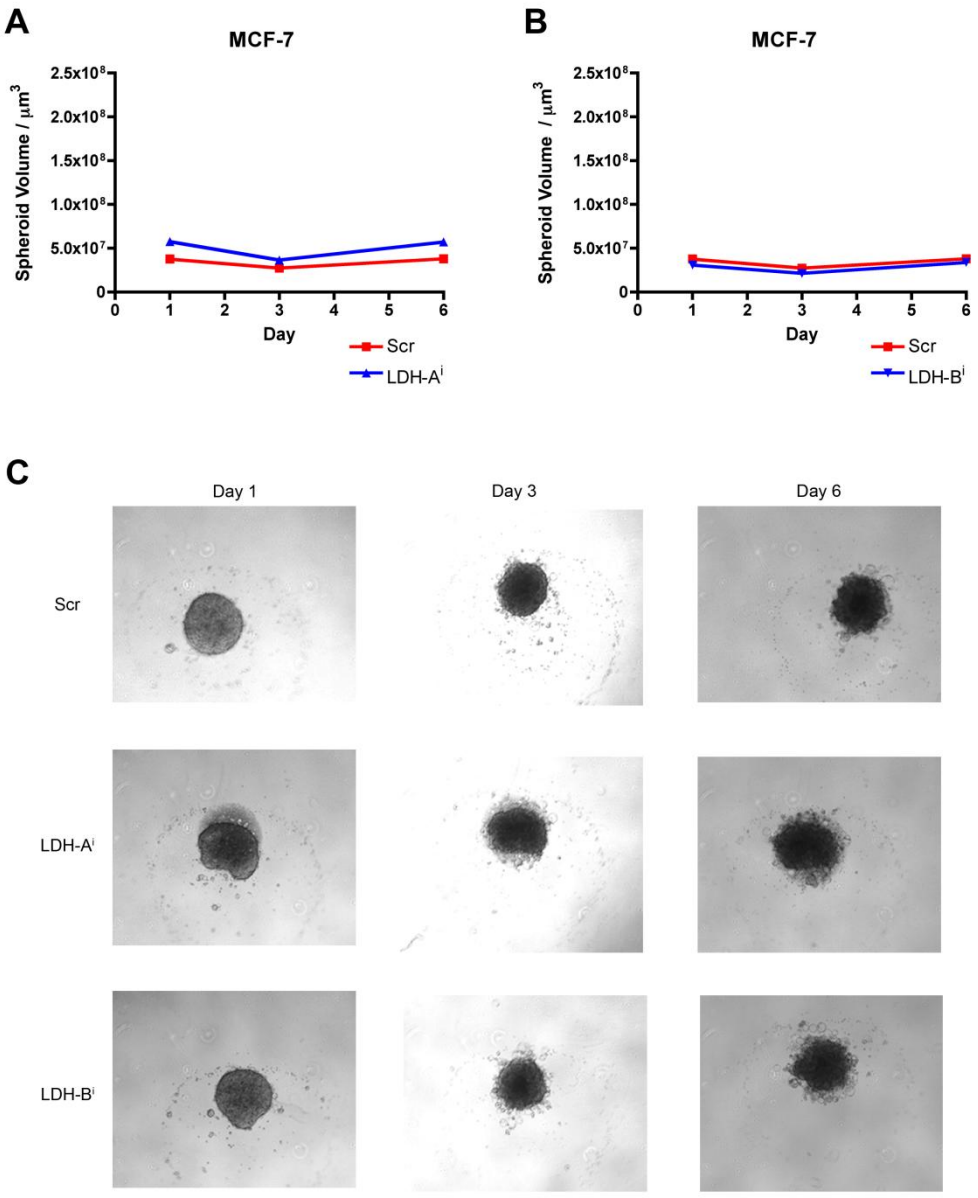

Figure 4.1: MCF-7 cells grow poorly in 3D spheroids; the result is that [A] LDH-A knockdown and [B] LDH-B knockdown have no effect compared to the scramble control; [C] LDH-A knockdown reduces the roundness of tumour spheroids. t = 144h. N=3. * = P <0.05; ** = P<0.01; *** = P<0.001.

In the MDA-MB-231 cells the results were more striking (**Figure 4.2**). The difference in growth between the LDH-A knockdown and the control was very large, with a 90% reduction in spheroid volume in the LDH-A knockdown at day 6.

The LDH-B knockdown had no effect on volume. However, on the basis of the data for both cell lines for the LDH-A knockdown there was sufficient basis for investigating any underlying mechanisms further.

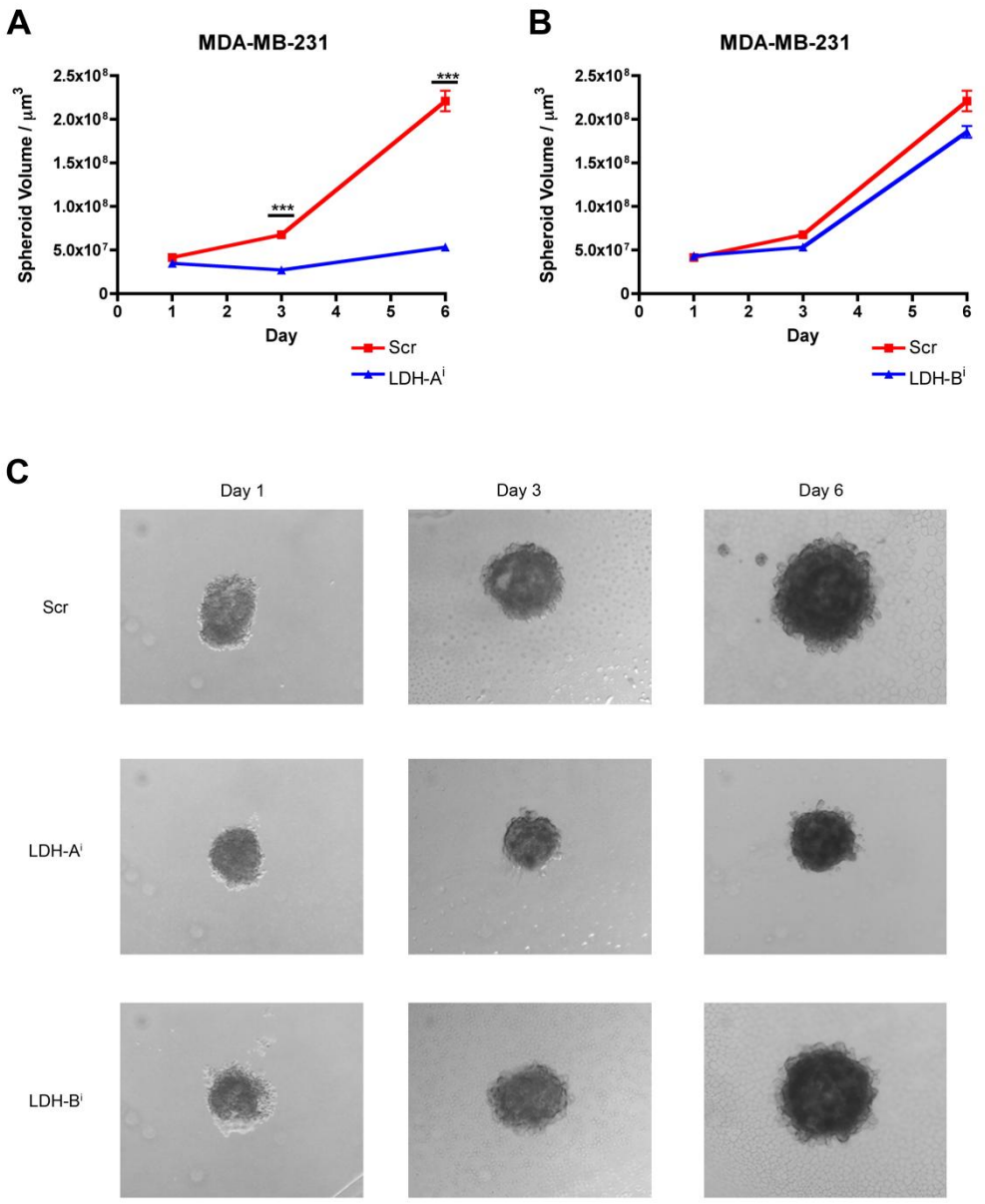

Figure 4.2: MDA-MB-231 growth in 3D spheroids is robust; [A] LDH-A knockdown reduces spheroid growth; [B] LDH-B knockdown has no significant effect compared to the scramble control; [C] spheroid images. t = 144h. N=3. * = P <0.05; ** = P<0.01; *** = P<0.001.

4.2.2: Immunohistochemical staining of 3D MDA-MB-231 spheroids reveals the effect of LDH-A knockdown on proliferation, hypoxia, necrosis and cell death

In order to further establish why LDH-A knockdown reduced spheroid volume in MDA-MB-231, the above experiment was repeated and the spheroids fixed, embedded and sliced ready for immunohistochemical analysis at day 6. MCF-7 were not taken forward at this point as the sluggish growth produced spheroids of insufficient size for a proper immunohistochemical analysis.

The stains used were specifically to look at changes to; the necrotic region at the centre of the spheroid (H&E); hypoxic areas (carbonic anhydrase 9 (CA9)); proliferation (KI67); and cell death (cleaved-caspase 3).

In terms of LDH-A knockdown, there was a 70% decrease in proliferation as measured by percentage cells staining positive for ki67 (**Figure 4.3**). LDH-B knockdown showed a 1.3 fold increase in proliferation though this is likely to be due to the decrease in cells in the core of the spheroid in this knockout (thereby reducing total number of cells) rather than an increase in proliferation *per se*. This interpretation is supported by the previous data in **Figure 4.2B** with no difference in spheroid volumes between the control and the LDH-B knockdown. Indeed, looking at the raw results (**Figure 4.3A**) the staining in the control and the LDH-B knockdown is similar in that KI67 is restricted to the leading edge of both spheroids where as in the LDH-A knockdown the KI67 staining is more diffuse the spheroid periphery appearing to disaggregate.

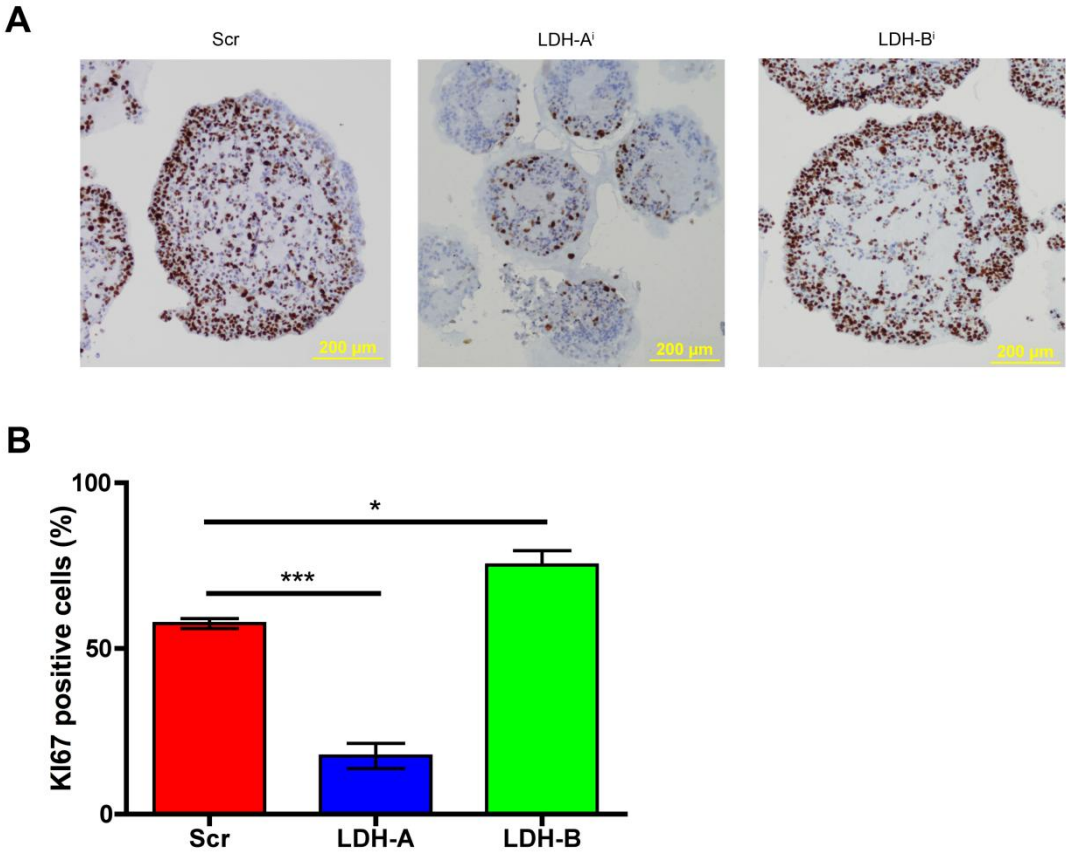

Figure 4.3: [A] MDA-MB-231 spheroids stained for KI67; [B] LDH-A knockdown reduces the number of ki67 positive cells; LDH-B knockdown slightly increases the number of ki67 positive cells. t = 144h. N=1. * = P <0.05; ** = P<0.01; *** = P<0.001.

In addition to this, there was a marked increase in cell death as measured by cleaved caspase-3 staining with the LDH-A knockdown showing 4.9 fold increase in positive staining. The LDH-B knockdown had no effect (**Figure 4.4**).

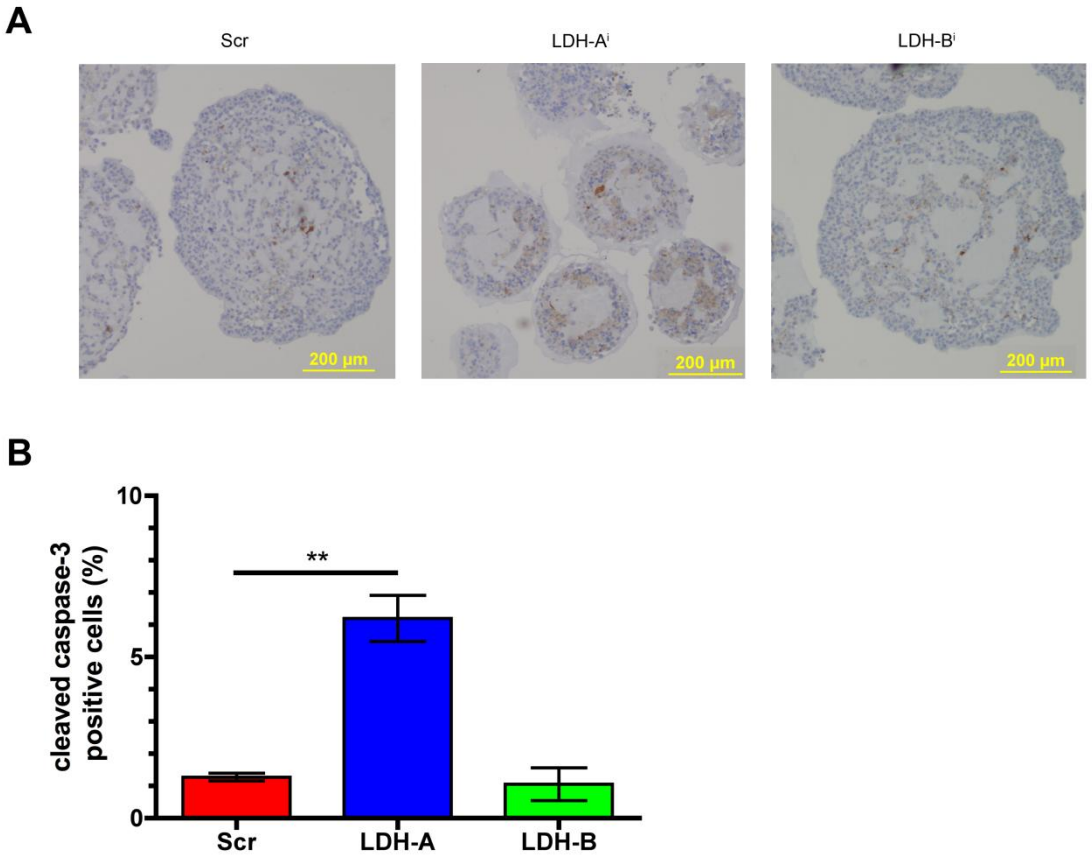

Figure 4.4: [A] MDA-MB-231 spheroids stained for cleaved caspase-3; [B] LDH-A knockdown increases the number of cleaved caspase-3 positive cells; LDH-B knockdown has no effect. t = 144h. N=1. * = P <0.05; ** = P<0.01; *** = P<0.001.

Measuring hypoxia and necrosis was achieved by staining and scoring for CA9, pimonidazole and H&E respectively. Hypoxia staining (**Figure 4.5 and 4.6**) showed that the LDH-A knockdown cells did not get to a sufficient size to generate a hypoxic core. Again, the fewer number of cells in the hypoxic core of the LDH-B knockdown perhaps skewed this result, with a recorded reduction in hypoxia as measured by CA9 staining.

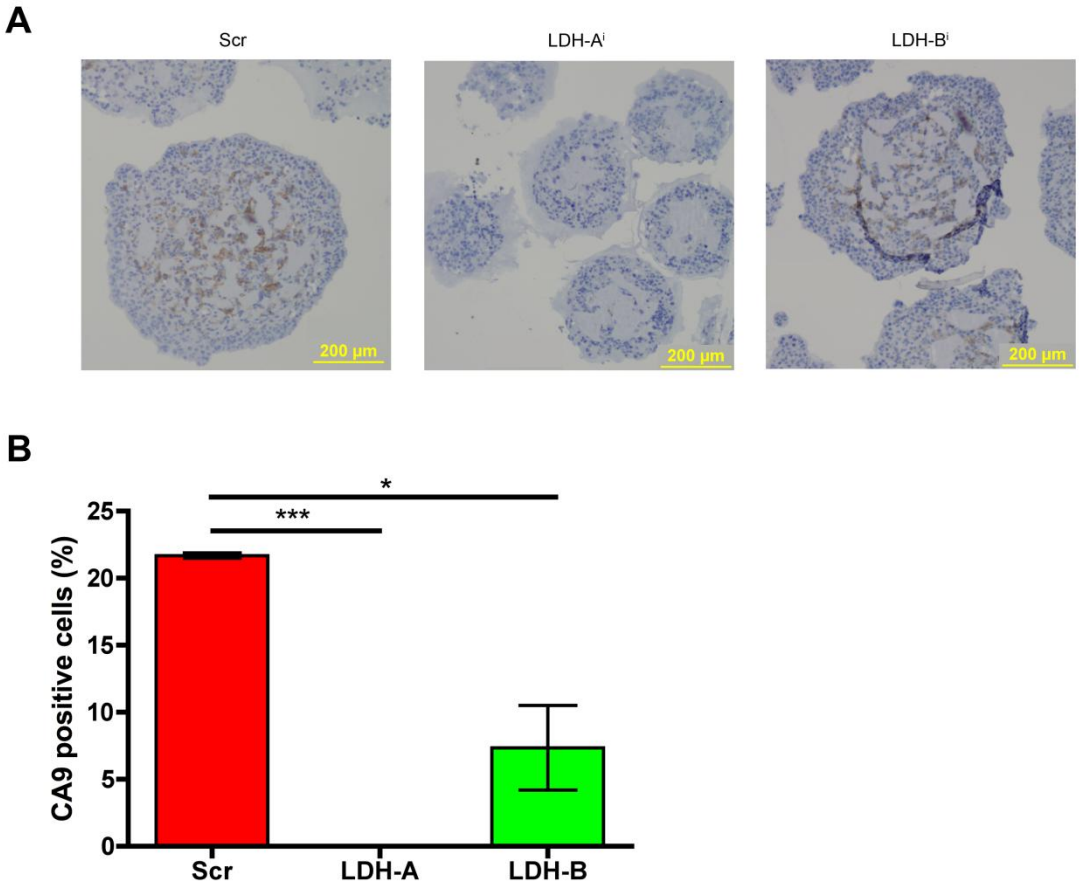

Figure 4.5: [A] MDA-MB-231 spheroids stained for CA9; [B] LDH-A knockdown reveals tumour spheroids do not reach a sufficient size to stain positively for CA9; LDH-B knockdown produces an apparent reduction in CA9 staining. t = 144h. N=1. * = P <0.05; ** = P<0.01; *** = P<0.001.

CA9 staining alone was not sufficient to understand changes in hypoxia due to the potential of cross talk between CA9 and LDH-A expression and change in acidity. With this in mind pimonidazole staining was conducted in parallel (**Figure 4.6**). The results corroborated the CA9 data with regards to hypoxia. However, the LDH-B staining was restricted by the recovery of only one spheroid at this timepoint for this experiment and would bear repeating in future experiments.

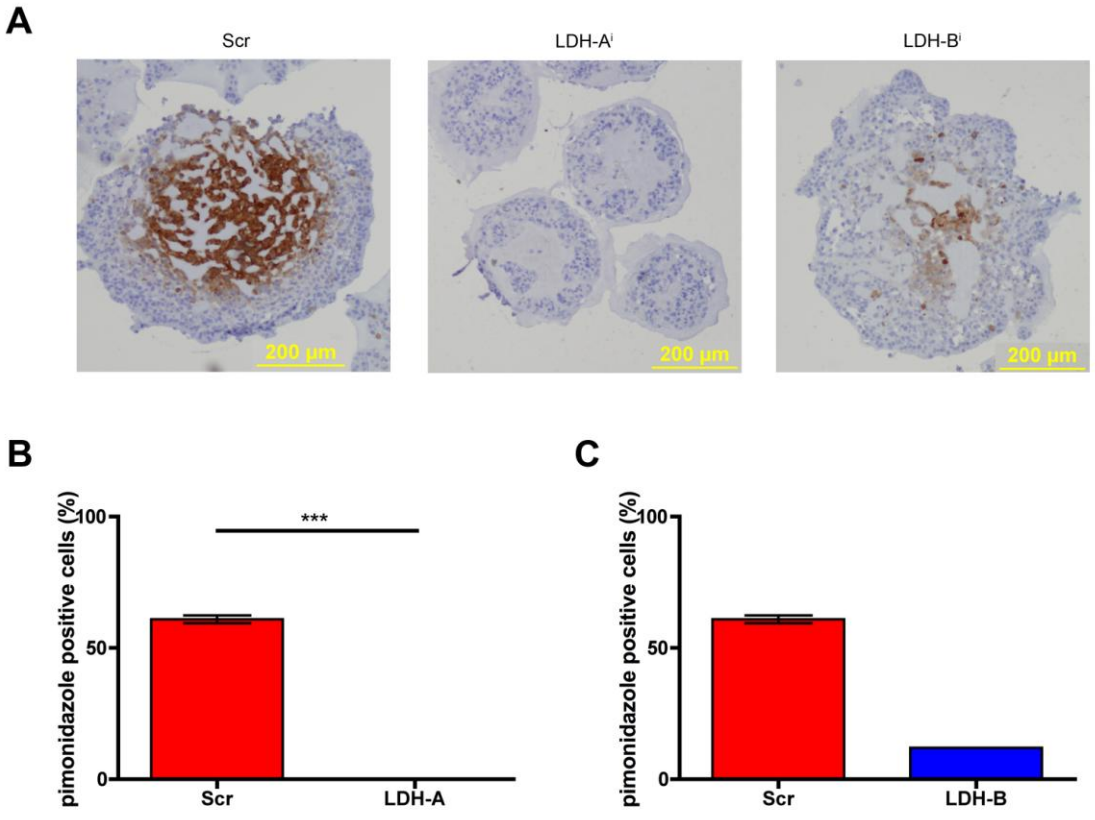

Figure 4.6: [A] MDA-MB-231 spheroids stained for pimonidazole; [B] LDH-A knockdown reveals tumour spheroids do not reach a sufficient size to stain positively for pimonidazole; [C] LDH-B knockdown produces an apparent reduction in pimonidazole staining. t = 144h. N=1. * = P <0.05; ** = P<0.01; *** = P<0.001.

Looking at necrosis (**Figure 4.7**) what is interesting is that the LDH-A knockdown, despite being small, has a necrotic region at the centre. Whilst this could be speculated as being in part deriving from the reconstituted basement membrane used to generate the spheroids, the ring of cleaved caspase-3 staining around this region would suggest that it is genuinely necrotic. LDH-B knockdown does not generate a significant difference in necrosis.

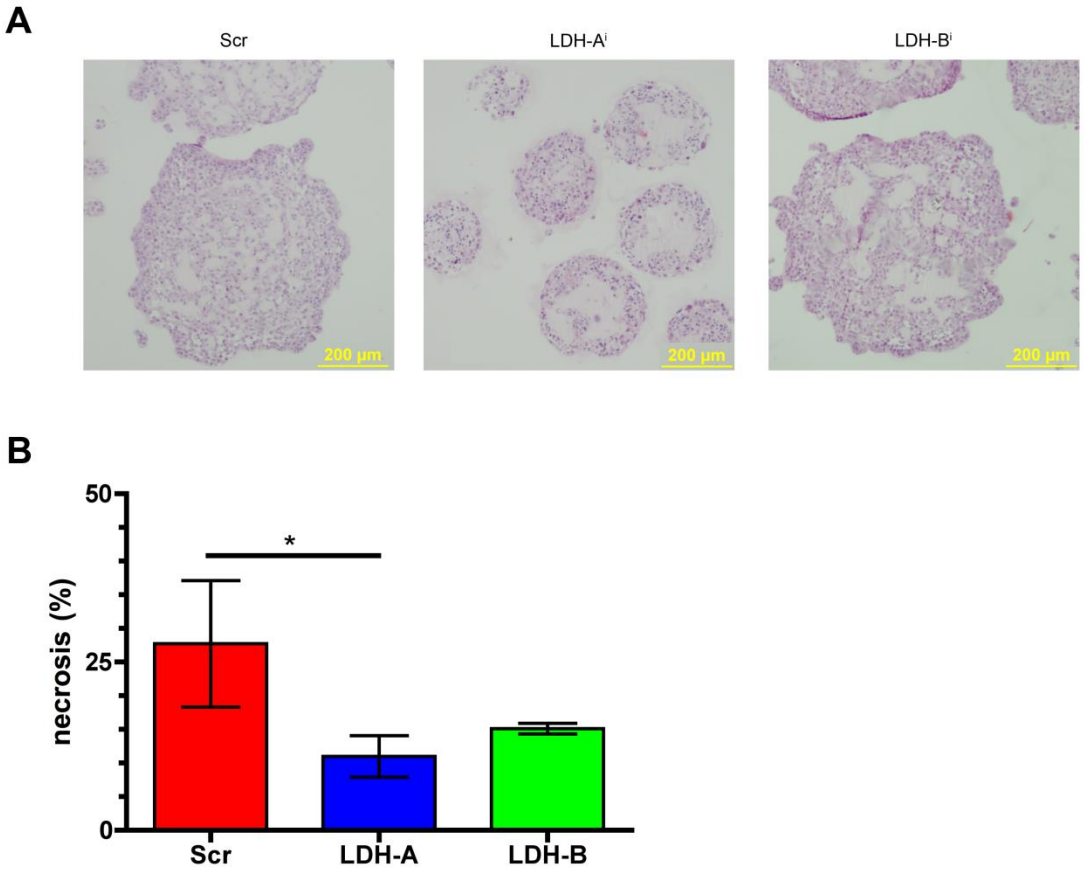

Figure 4.7: [A] MDA-MB-231 spheroids stained for H&E; [B] LDH-A knockdown reduces necrosis; [C] LDH-B knockdown produces no significant difference. t = 144h. N=1. * = P <0.05; ** = P<0.01; *** = P<0.001.

4.2.3: siRNA MEDIATED KNOCKDOWN OF LDH-A RESULTS IN THE ACTIVATION OF CELL DEATH PATHWAYS IN MCF-7 CELLS

Given the difficulty in reliably growing MCF-7 cells in 3D spheroids, the investigation returned to 2D culture for further investigation into the roles of LDH-A and LDH-B.

Poly (ADP-Ribose) Polymerase (PARP) is a protein involved in DNA repair and cell death pathways. PARP binds to DNA to repair DNA damage through two zinc

finger domains; this activity is inhibited by PARP cleavage which is initiated by pro-apoptotic factors. As a result, an increase in the ratio of cleaved PARP to total PARP is one indicator of increased cell death.

After 48 hours, MCF-7 cells show an increase in PARP cleavage under hypoxia (**Figure 4.8**), an effect that is magnified when LDH-A is knocked down. However, in MDA-MB-231 there is no difference in PARP cleavage under either normoxia or hypoxia when either LDH-A or LDH-B is knocked out.

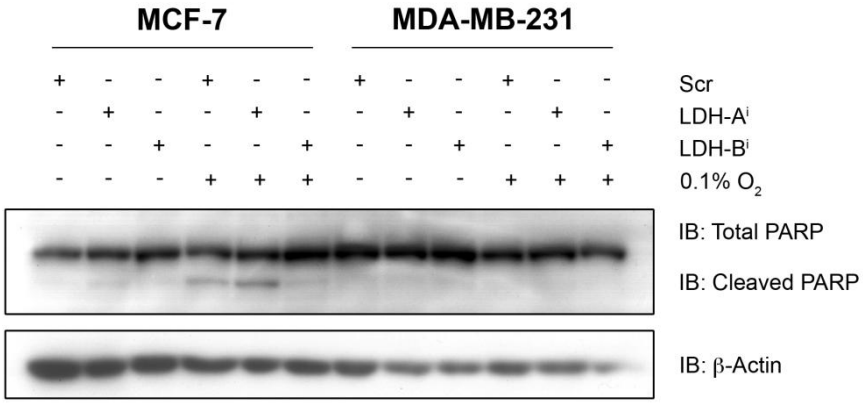

Figure 4.8:MCF-7 and MDA-MB-231 cells after 48 hours growth in 2D culture; MCF-7 cells show an increase in PARP cleavage under normoxia and hypoxia whilst MDA-MB-231 show no change. t = 48 h. N=3.

Further attempts were made to reinforce this data usingflow cytometry to quantify annexin V and Propidium Iodid (PI) levels as wellas plate-based caspase assays. However, the results were noisy and did not prove repeatable.

.

4.2.4: SIRNA MEDIATED KNOCKDOWN OF LDH-A SUPRESSES GROWTH AND REDUCES THE NUMBER OF CLONES IN A COLONY FORMING ASSAY

Clonogenics were performed in order to ascertain the level of cytotoxicity in a quantitative way. By exposing the cells to a transient slight such as siRNA mediated LDH-A and LDH-B knockdown and/or hypoxia and then allowing the cells to recover the number and size of colonies cangive a further indication as to whether a cytotoxic or cytostatic effect is being observed.

In both the case of LDH-A and LDH-B knockdown, cells were transfected according to standard procedure, allowed to recover, then exposed to hypoxia or normoxia (control) for 5 days before being allowed 10 days to recover prior to fixing and staining.

Knocking out LDH-A reduced the clonogenicity of MCF-7 with 68% fewer colonies forming (**Figure 4.9**) under normoxia and 66% fewer under hypoxia reinforcing the idea that LDH-A knockdown is cytotoxic.

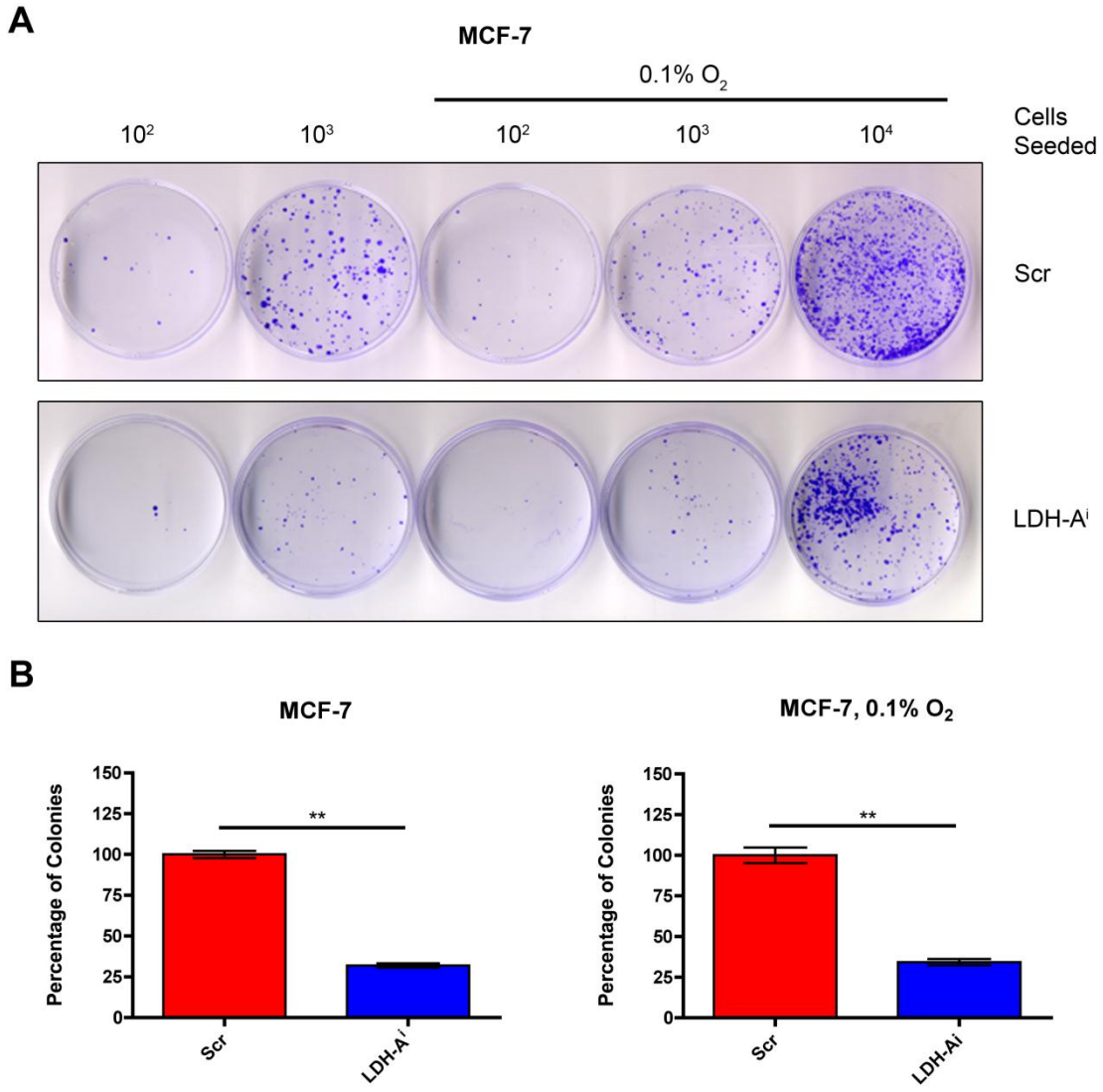

Figure 4.9: [A] a clonogenic assay in MCF-7 cells shows that LDH-A knockdown reduces colony formation which can be quantified in [B] normoxia and [C] hypoxia. t = 360h. N=3. * = P <0.05; ** = P<0.01; *** = P<0.001.

Repeating the LDH-A knockdown in MDA-MB-231 produced an effect similar to that already observed in MCF-7 with the clonogenic data for MDA-MB-231 also showing LDH-A knockdown as being cytotoxic under normoxic and hypoxic conditions with reductions of 33% and 82% respectively (**Figure 4.10**).

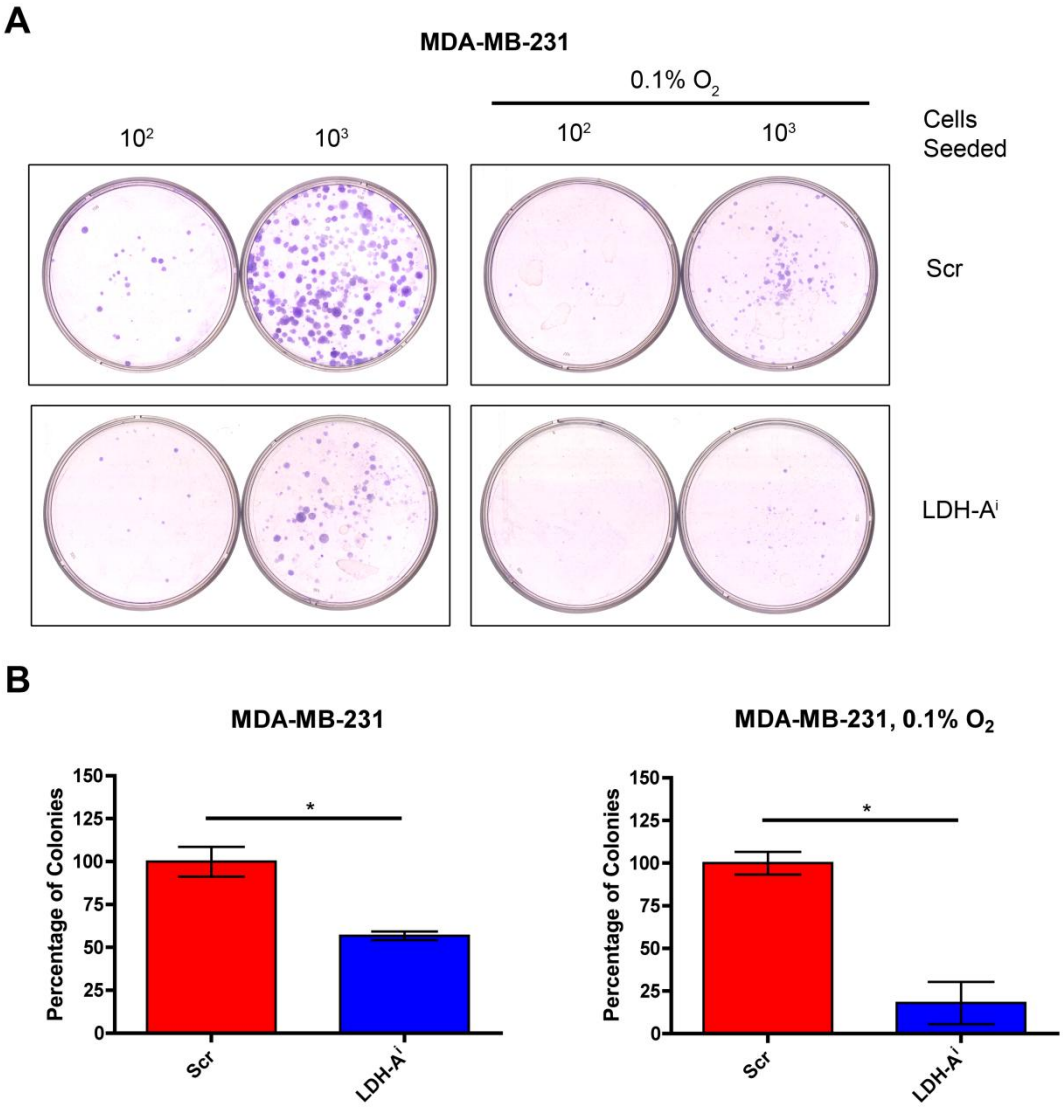

Figure 4.10: [A] a clonogenic assay in MDA-MB-231 cells shows that LDH-A knockdown reduces colony formation which can be quantified in [B] normoxia and [C] hypoxia. t = 360h. N=3. * = P <0.05; ** = P<0.01; *** = P<0.001.

4.2.5: SIRNA MEDIATED KNOCKDOWN OF LDH-B HAS VARIABLE EFFECTS ON GROWTH

When LDH-B was knocked down the effect was less clear cut. In MCF-7 (**Figure 4.11**) under normoxia, there was a 22% reduction in the number of colonies wheras under hypoxic conditions, there was no significant change.

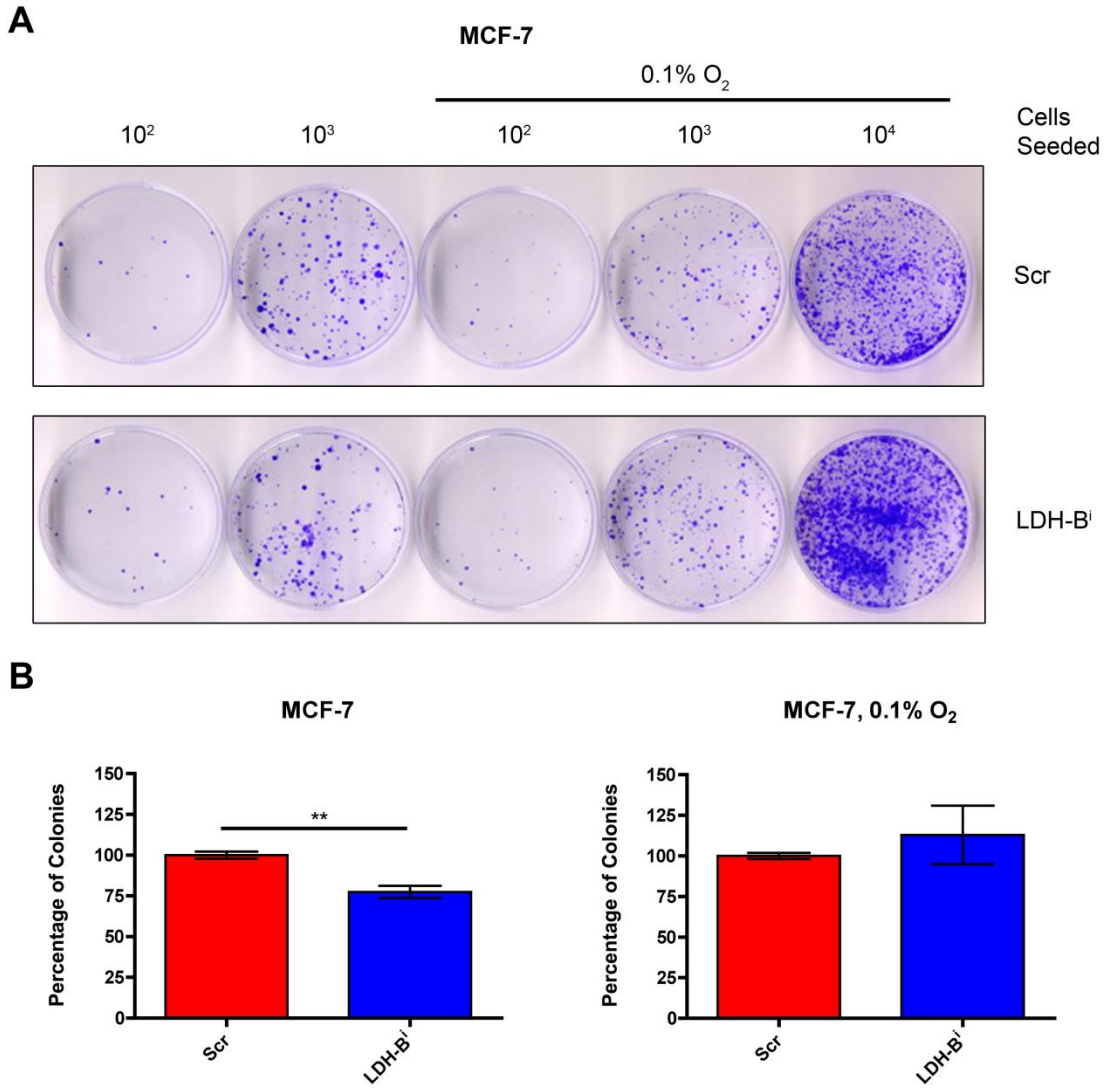

Figure 4.11: [A] a clonogenic assay in MCF-7 cells shows that LDH-B knockdown [B] reduces colony formation in normoxia and [C] has no effect in hypoxia. t = 360h. N=3. * = P <0.05; ** = P<0.01; *** = P<0.001.

In MDA-MB-231 cellsthe clonogenic data (**Figure 4.12**) shows no difference in normoxia and a 1.5 fold increase in colonies with LDH-B knockdown compared to the control in hypoxia.

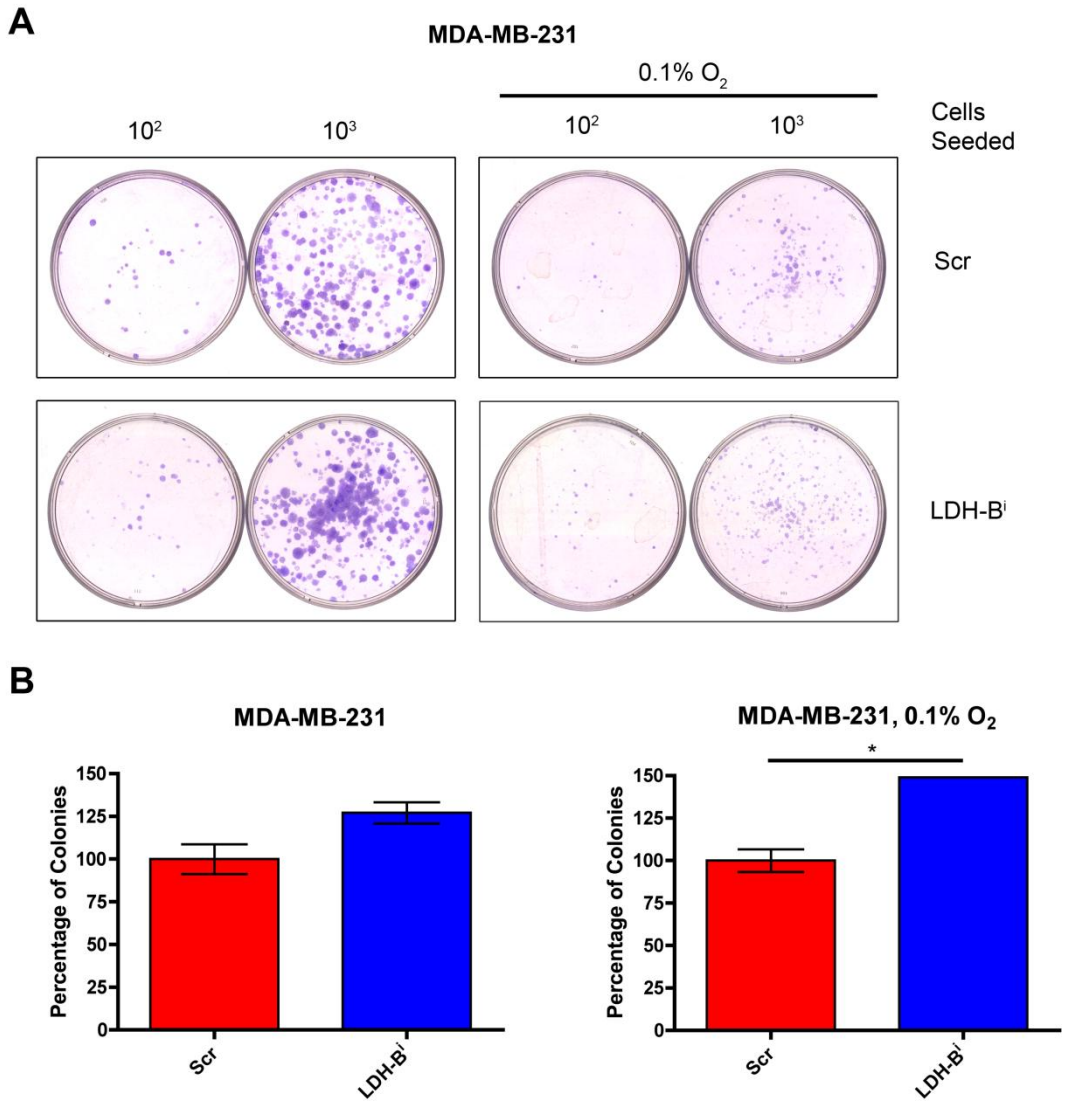

Figure 4.12: [A] a clonogenic assay in MDA-MB-231 cells shows that LDH-B knockdown increases colony formation in [B] normoxia and [C] hypoxia. t = 360h. N=3. * = P <0.05; ** = P<0.01; *** = P<0.001.

4.2.6: siRNA mediated knockdown of LDH-A results in a fall in lactate production and ATP depletion

Approaches that interfere with cellular metabolism also require an understanding of the subsequent changes to metabolic outputs. In the case of LDH-A and LDH-B knockdown, the two outputs that bear most relevance are lactate, the product of the enzymatic reaction in question, and ATP, a more global indicator of what is occurring on a bioenergetic level. Lactate levels were normalised to cell number to account for difference in proliferation whilst ATP levels were normalised to protein concentrations obtained from a parallel SRB assay as detailed in **Chapter 2**.

For LDH-A knockdown in both MCF-7 and MDA-MB-231 there was a reduction compared to the scramble in both the level of lactate and the level of ATP production (**Figures 4.13 and 4.14**). MCF-7 cells saw a 23% reduction in lactate production (**Figure 4.13A**) and a 48% reduction of ATP (**Figure 4.13C**) in normoxia when LDH-A was knocked down. Under hypoxia, lactate production fell by 39% (**Figure 4.13B**) whilst ATP dropped by 40% (**Figure 4.13D**).

In MDA-MB-231 cells, the reductions in lactate were 51% (**Figure 4.14A**) and 48% (**Figure 4.14B**) in normoxia and hypoxia respectively with the corresponding drops in ATP coming in at 26% (**Figure 4.14C**) and 31% (**Figure 4.14D**).

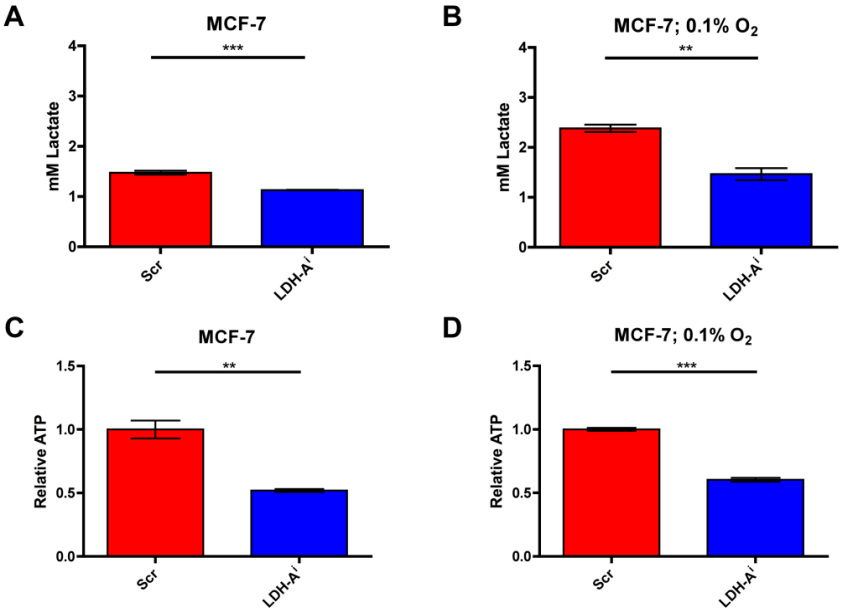

Figure 4.13: lactate levels are reduced in MCF-7 cells upon LDH-A knockdown under [A] normoxia and [B] hypoxia. ATP levels are reduced in MCF-7 cells upon LDH-A knockdown under [C] normoxia and [D] hypoxia. t = 120 h. N = 3. * = P <0.05; ** = P<0.01; *** = P<0.001.

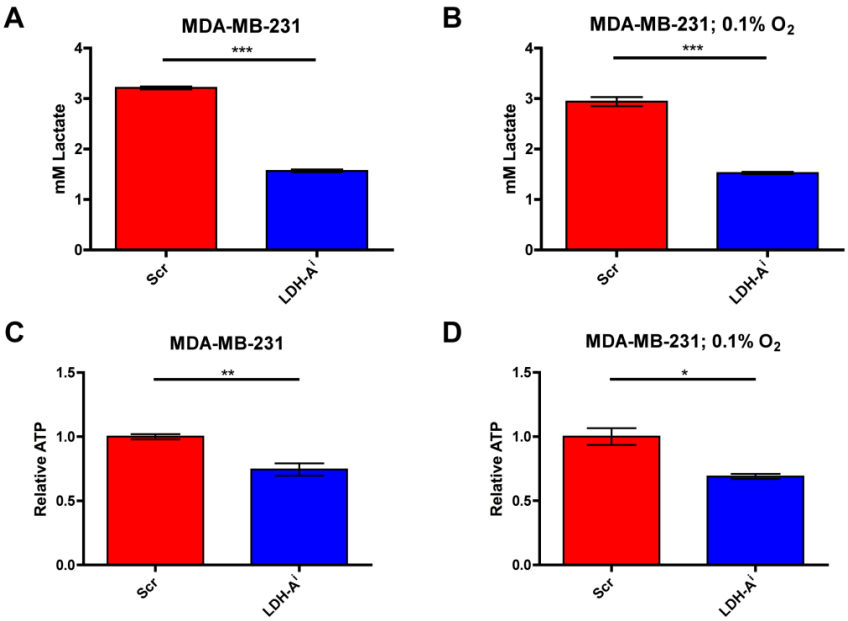

Figure 4.14: lactate levels are reduced in MDA-MB-231 cells upon LDH-A knockdown under [A] normoxia and [B] hypoxia. ATP levels are reduced in MDA-MB-231 cells upon LDH-A knockdown under [C] normoxia and [D] hypoxia. t = 120 h. N = 3. * = P <0.05; ** = P<0.01; *** = P<0.001.

When LDH-B was knocked down, there was a divergence between MCF-7 and MDA-MB-231. The former cell line showed no change in lactate or ATP levels between the control and LDH-B knockdown (**Figure 4.15**) except for a 15% drop in lactate production under hypoxia (**Figure 4.15B**). However, with MDA-MB-231 (**Figure 4.16**) there was a 1.15 fold increase in media lactate when LDH-B was knocked down under hypoxia which was repeated under both normoxia and hypoxia with ATP concentrations rising 1.17 and 1.23 fold respectively, agreeing with and reinforcing the more clear-cut clonogenic data for LDH-B knockdown in this cell line.

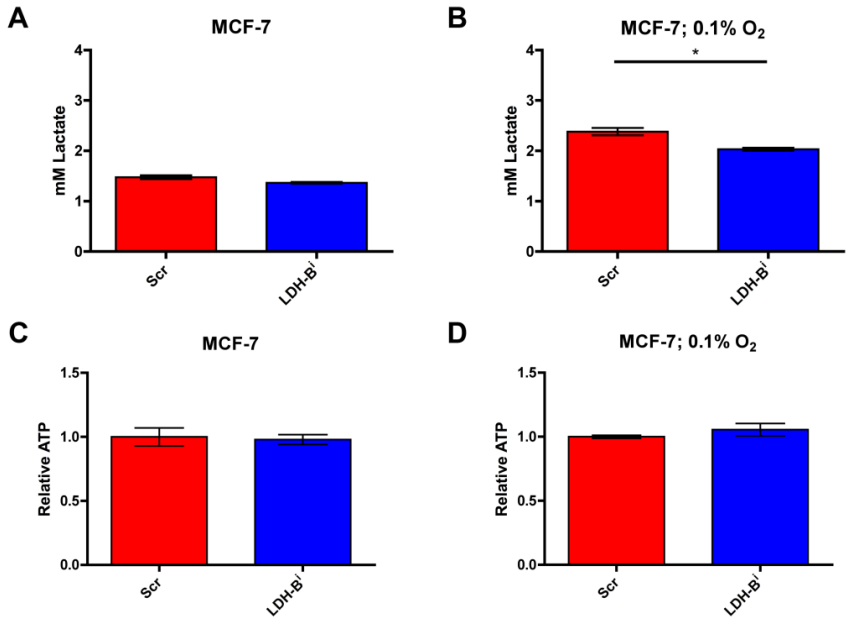

Figure 4.15: lactate levels MCF-7 cells upon LDH-B knockdown [A] show no change under normoxia and [B] are reduced under hypoxia. ATP levels in MCF-7 cells upon LDH-B knockdown show no change under [C] normoxia and [D] hypoxia. t = 120 h. N = 3. * = P <0.05; ** = P<0.01; *** = P<0.001.

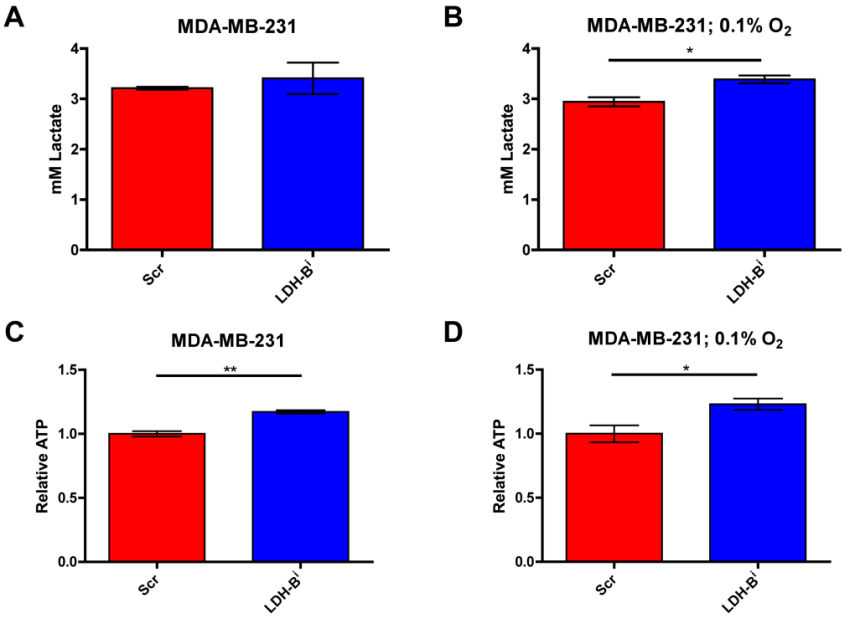

Figure 4.16: lactate levels MDA-MB-231 cells upon LDH-B knockdown [A] show no change under normoxia and [B] are increased under hypoxia. ATP levels in MCF-7 cells upon LDH-B knockdown are increased under [C] normoxia and [D] hypoxia. t = 120 h. N = 3. * = P <0.05; ** = P<0.01; *** = P<0.001.

4.2.7: siRNA MEDIATED KNOCKDOWN OF LDH-A RESULTS IN AN INCREASE IN EXTRA-CELLULAR ACIDIFICATION AND OXYGEN CONSUMPTION

The existence of technologies and techniques to allow the real-time quantification of the extracellular acidification rate (ECAR) and the oxygen consumption rate (OCR) of cells in culture allowed the activity of the mitochondria to be probed further.

Due to pressures of time and equipment availability, the experiment was initially performed in MCF-7 with an LDH-A knockdown. Nine discrete rate measurements were taken, each itself representative of 13 individual measurements of mpH (ECAR) or oxygen concentration (OCR). After rate point 3, all samples were treated with 1μM of oligomycin, a mitochondrial inhibitor targeting complex V. This had the effect of suppressing OXPHOS. Then, after rate point 6, half of the samples were treated with 300nM of FCCP which decouples ATPase activity and gives a maximal rate of respiration. The other half were treated with 1μM rotenone, a complex I inhibitor which in concert with oligomycin acts to suppress all mitochondrial activity.

In order to validate whether the system was returning realistic rates, and to explore whether there was any utility in repeating the experiment under hypoxia-like conditions, the hypoxia mimetic DMOG was used as it was not possible to conduct the experiment in a closed system. This returned a substantially lower rate of acidification for the hypoxia-like environment (**Figure 4.17A**). At first glance this looks to be contrary to what would be expected given that hypoxic regions are associated with a lower pH. However, when any single rate point was dissected (in the case of **Figure 4.17A**, rate point 1), it was clear that whilst the

rate under hypoxia-like conditions was substantially lower, this was because the starting pH was lower than that for normoxia and varies little over the time point whereas the normoxic pH moved between a greater range from a higher starting point. Given the suppression of ECAR under DMOG, this condition was not used to validate the effect of LDH-A knockdown on ECAR under hypoxia.

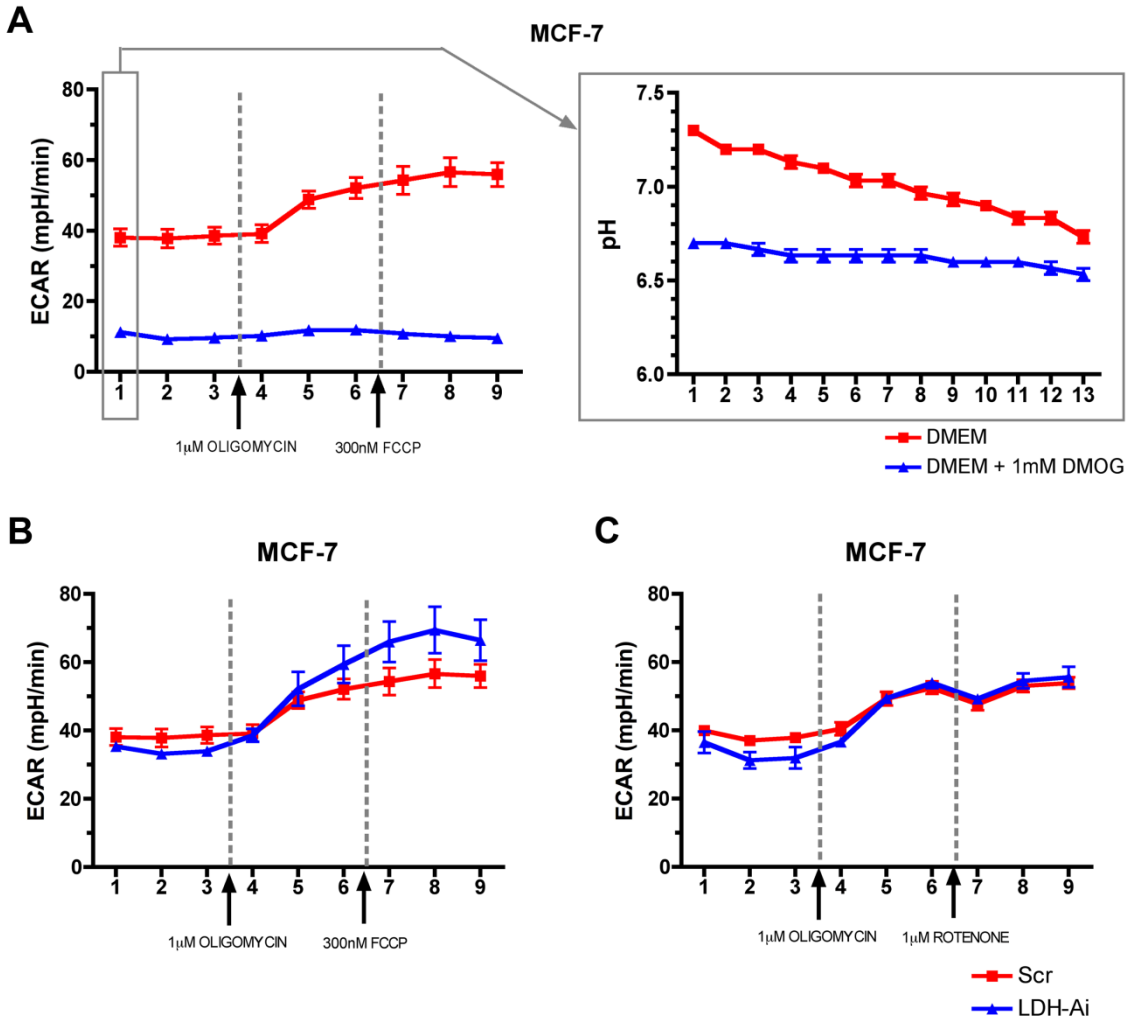

Figure 4.17: ECAR for MCF-7 cells:[A] the hypoxia mimetic DMOG suppresses ECAR; [B] shows an increase in ECAR on LDH-A knockdown on treatment with FCCP and [C] no change on treatment with rotenone. N = 1.

Looking at ECAR in normoxia, there was a difference between LDH-A knockdown and the scramble control upon treatment with FCCP (**Figure 4.17B**) whereas there was no difference when the experiment was repeated with rotenone treatment after rate point 6 (**Figure 4.17C**) validating that LDH-A knockdown has an effect on MCF-7 in normoxia.

In terms of mitochondrial activity, OCR is interesting as it is directly relatable to the amount of OXPHOS occurring. In interpreting OCR data, the difference between the mean of the first three points and the mean of the second three points represents the amount of ATP turnover. The difference between zero and the mean of the last three points when treated with rotenone represents non-mitochondrial respiration; subtracting non-mitochondrial respiration from the mean of the first three points represents basal respiration, whilst subtracting it from ATP turnover gives the amount of proton leakage occurring to drive the proton gradient. Finally, subtracting non-mitochondrial respiration from the mean of the last three points when treated with FCCP gives the respiratory capacity.

Again, to check the validity of the data, the hypoxia-mimetic DMOG was used (**Figure 4.18A**). In this instance, the results were as expected; the normoxic cells were greater oxygen consumers with a greater rate than was corroborated by raw data where the concentration of oxygen over the hypoxia-like cells was static but reduced markedly over time in the normoxic cells. However, the level of OCR was suppressed to almost zero restricting OCR measurements to normoxia.

What was clear as an overall point looking at the data in **Figure 4.18** is that there was more oxygen consumption when LDH-A is knocked down in terms of basal respiration, ATP turnover, and maximum respiratory capacity. However, in neither

case was there any particular difference in proton leakage. Significantly, when mitochondrial activity was completely disrupted with rotenone, there was also no difference (**Figure 4.18C**).

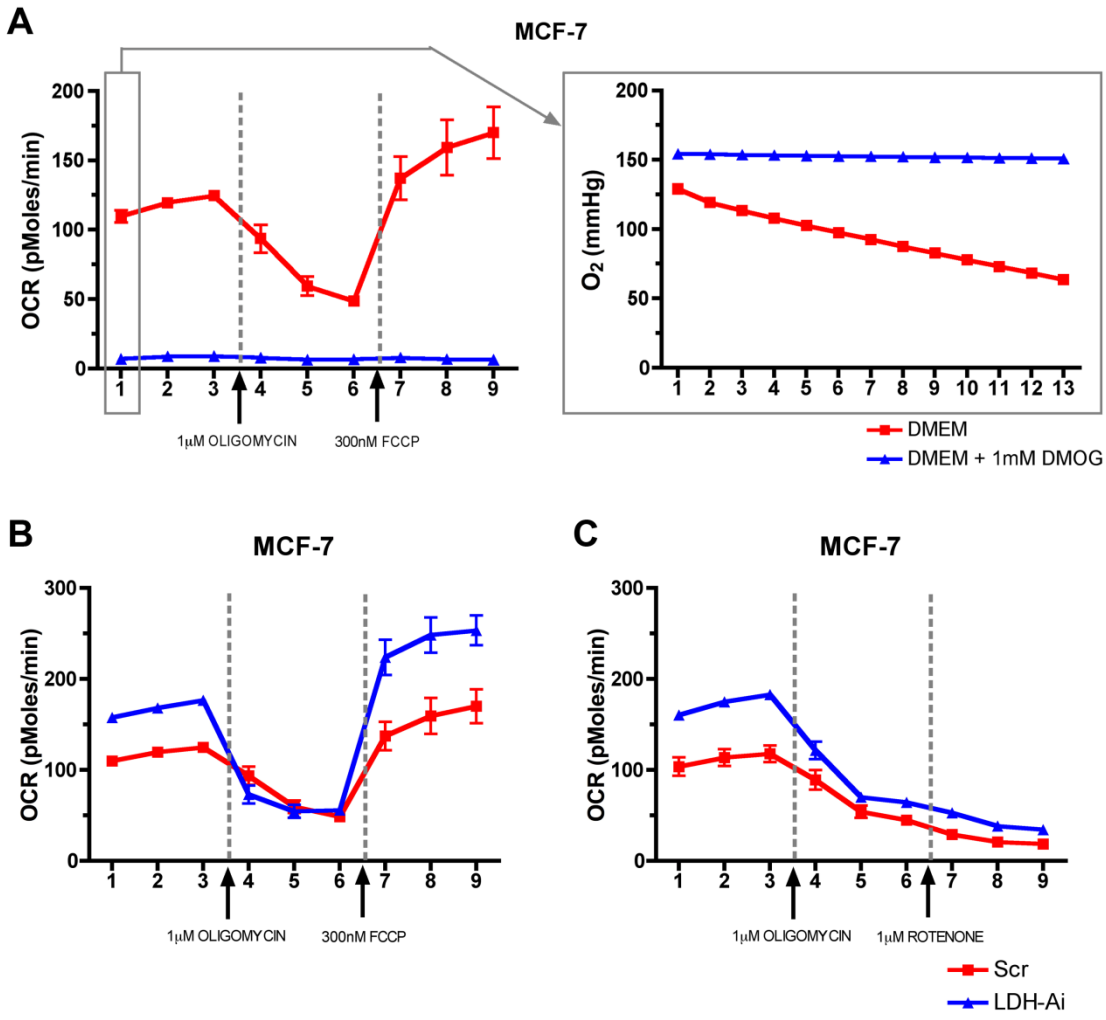

Figure 4.18: OCR for MCF-7 cells [A] the hypoxia mimetic DMOG suppresses OCR; [B] shows an increase in OCR on LDH-A knockdown on treatment with oligomicyn FCCP and [C] a change after treatment with oligomycin which is suppressed on treatment with rotenone. N=1.

4.3: DISCUSSION

4.3.1: LDH-A KNOCKDOWN IS CYTOTOXIC

The differences in spheroid volume between MCF-7 and MDA-MB-231 are interesting and most likely reflect the different glycolytic capacities of the respective cell lines with MDA-MB-231 growing much more strongly. In MDA-MB-231, the effect of LDH-A knockdown is proportionally much larger than the effect in 2D culture. This points to LDH-A playing a role in maintaining 3D growth, perhaps cooperatively with other pathways. This exact nature can only be explored by studying the effect of LDH-A knockdown under a further range of metabolic conditions (i.e., low glucose, low glutamine).

The immunohistochemical data adds to a picture of LDH-A being a potentially good anti-cancer target. The tumour spheroid volumes were reduced and this was due to two factors. Firstly, there was an increase in programmed cell death measured either by an increase in cleaved caspase-3 staining in MDA-MB-231 cells, or an increase in PARP cleavage in MCF-7 cells when LDH-A was knocked down. Secondly, proliferation was markedly reduced as measured by KI67 staining.

The clonogenic data reinforces the idea that LDH-A knockdown is cytotoxic; the data for LDH-B is less clear cut, but the potential that down-regulating LDH-B promotes growth and survival under hypoxia at least would agree with the earlier data in **Chapter 3** that sees LDH-B protein levels reduced after hypoxic exposure.

It is interesting that both lactate and ATP levels are reduced when LDH-A is knocked down. Whilst the former is predictable- with less LDH-A, there will be

fewer reductions of pyruvate occurring- the latter is perhaps indicative of aberrant mitochondrial function. This in itself might begin to explain the existence of the Warburg phenotype as a defensive mechanism against either reactive oxygen species (ROS) which damage DNA and can trigger apoptosis, or indeed a defence against the broader apoptotic role that competent mitochondria can play.

Returning to the depletion of ATP levels upon LDH-A knockdown, it would be normal to suppose that the TCA cycle and OXPHOS would act as a redundancy pathway in the absence of an LDH-A catalysed escape for pyruvate; in this instance ATP would be expected to remain at least static, or (more likely) increase due to the greater efficiency of OXPHOS. However, the data seems to show that whatever escape pathways exist are not sufficient to overcome a significant ATP depletion when LDH-A is knocked down. This is particularly encouraging in a drug discovery context.

The central question when it comes to the biology of ECAR is which factor can be expected to dominate this function; will it be lactic acid (and therefore prove to be a marker of glycolysis), or will it be dominated by carbonic acid generated from CO_2 in the TCA cycle? The results tend to favour the latter; when LDH-A is knocked down, there is a moderate increase in ECAR or no change whereas if ECAR were a true measurement of glycolysis then a dramatic drop in ECAR should be expected upon LDH-A inhibition.

The moderate increase in ECAR for the LDH-A knockdown when treated with the decoupler FCCP then is indicative of an increase in CO_2 production. This is corroborated by the oxygen consumption data which shows an increase in oxygen consumption and therefore an increase in mitochondrial activity. This

corroborates the ATP data inasmuch as a metabolic 'choice' seems to have been made by transformed cells that disfavours the mitochondria resulting in a heavy reliance upon LDH-A and a subsequent vulnerability to it's inhibition.

More broadly assessing mitochondrial activity, either by simply looking at changes to morphology by electron-microscopy or repeating the work of Fantin (Fantin, V.R., *et al*, 2006) on changes to mitochondrial membrane potential, could yield further answers in this regard.

4.3.2: FUTURE WORK

The first issue to be addressed given the data suggesting an increase in oxidative stress would be to verify this by measuring ROS concentration. Several methods have already been tried from colorimetric techniques using the dye dichlorofluorescin diacetate (DCF-DA) through to more complex FACS approaches. Problems encountered with both centred on repeatability, no doubt in large part due to the transient nature of such species. Nevertheless, it would be beneficial to tie the data together that shows increased oxygen consumption to programmed cell death via an intermediary mechanism.

Beyond this, the difference in growth between 2D and 3D models highlights the inadequacies of cell culture as a model. The existence of concentration gradients across tumours means that in reality hypoxia may be intermittent, and other stresses experienced such as low glucose. In order to reconcile the difference in 2D and 3D data, it is therefore important to consider the effect of LDH-A inhibition under low glucose conditions to determine whether it supports growth and inhibition is detrimental or otherwise. Moreover, it is important to uncover any

non-glyoclytic roles from a drug-discovery perspective so that LDH-A as a target can be properly assessed.

CHAPTER 5: LACTATE DEHYDROGENASE, METABOLITE WITHDRAWL, AND LACTATE

5.1: INTRODUCTION

The results in the previous chapters indicate a difference between the effects of LDH-A knockdown in 2-D versus 3-D growth models. That the siRNA knockdown had a greater effect in the latter in the more glycolytic MDA-MB-231 cells is indicative of LDH-A and its role in maintaining glycolysis being important in supporting 3-D growth above and beyond the other effects observed in 2-D. The question arising therefore, is what changes when transitioning to a 3-D model from 2-D culture.

5.1.1: GRADIENTS EXIST ACROSS TUMOURS

This question is answered in large part when considering the nature of gradients existing across solid tumours; the oxygen gradient is characterized by the hypoxic response, chiefly mediated by HIF-1, that allows tumours to grow beyond a certain size. Indeed, it has been calculated that a tumour mass cannot exceed 80 μM in diameter without recruiting the new blood supplies to alleviate these gradients at the core of the tumour, not only of oxygen, but also key metabolites such as glucose.

High interstitial pressures emanating from the centre of the tumour make it incredibly difficult for these metabolites to reach the centre of the tumour mass,

and must also be considered as a barrier to overcome in terms of delivering a drug to the whole tumour. Furthermore, given that LDH-A is notably up-regulated in hypoxia, corresponding to a greater degree of glycolysis, there will not only be a greater demand for glucose at the hypoxic core but also a greater production of lactate. This greater demand requires in some sense that the well-oxygenated cells on the periphery preferentially metabolise other substrates in favour of glucose, but also that there exists some mechanism for rapidly clearing lactate and preventing it from accumulating.

5.1.2: TUMOURS CAN USE LACTATE AS A FUEL SOURCE

Both of these problems seem to have been resolved to a certain extent with studies showing that lactate can not only fuel tumour metabolism, but that it also used as a substrate preferentially in the presence of glucose (Sonveaux, P., *et al*, 2008). The model proposed (Semenza, G.L., 2008) is one where LDH-A in the core is producing lactate from glucose-intensive glycolysis whilst LDH-B on the periphery is oxidizing this lactate back to pyruvate to ultimately produce ATP in the TCA cycle (**Figure 5.1**).

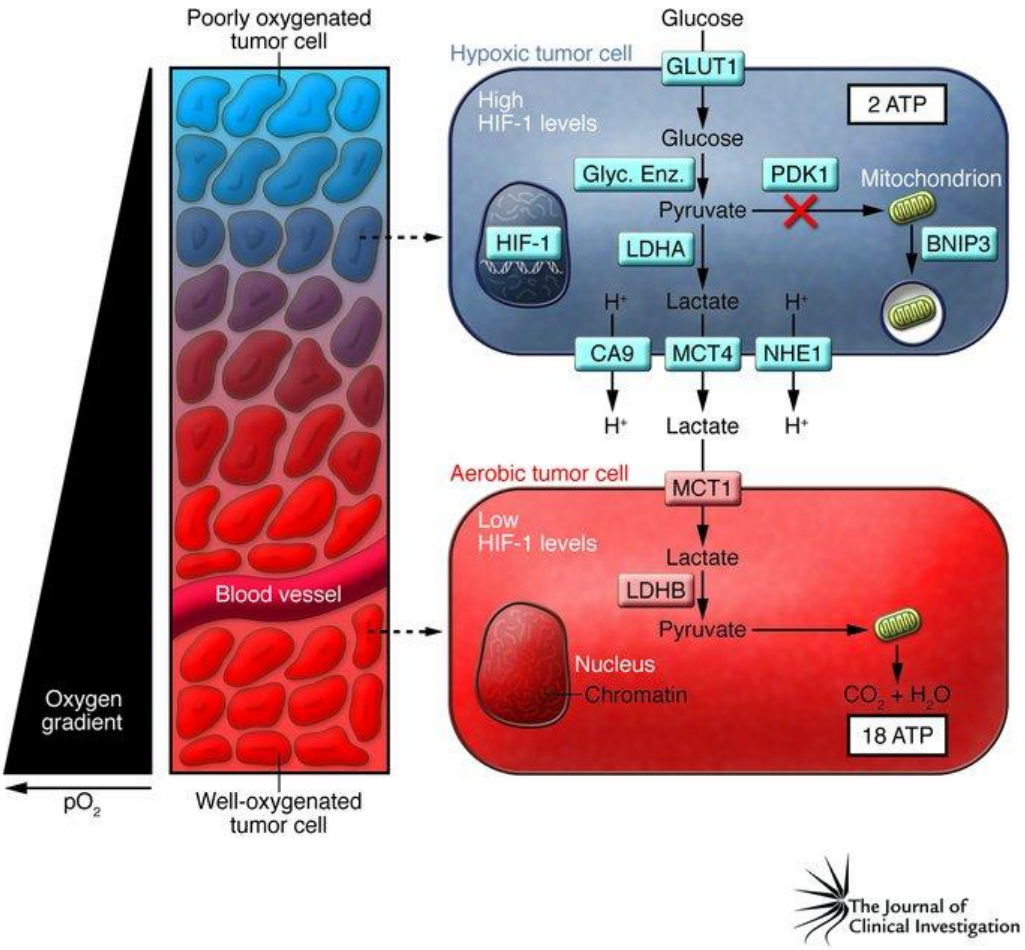

Figure 5.1: a model of cooperativity between LDH-A and LDH-B (Semenza, G.L., 2008).

5.1.3: AIMS

With these literature observations in mind, the aims of this chapter were threefold: one, to uncover whether lactate could fuel growth in either MCF-7 or MDA-MB-231 cells; two, to reveal whether this lactate-fuelled growth was dependent upon LDH-B; and three, to uncover what is controlling the selectivity between the reduction of pyruvate and the oxidation of lactate in these cells.

5.2: RESULTS

5.2.1: MCF-7 AND MDA-MB-231 GROW AT DIFFERENT RATES IN THE PRESENCE AND ABSENCE OF GLUCOSE

The first experiment was very simply to grow both MCF-7 and MDA-MB-231 cells in full DMEM (4.5g/L glucose) and glucose-free DMEM to see how much of these cell lines growth was attributable to glucose/how much glucose free growth occurred. Both cell lines grow robustly in full DMEM with MDA-MB-231 cells growing at a faster rate as previously described (**Figure 5.2**). Nevertheless, both cell lines in full DMEM achieve over-confluence from around day 10 onwards and thereafter begin to die.

The story in glucose free media is slightly more nuanced; MCF-7 cells remain static in number until day 4 before beginning to die. MDA-MB-231 on the other hand, whilst growing considerably more slowly than their counterparts in full DMEM, achieve a moderate level of growth up until day 13, at which point presumably their source of alternative growth is approaching exhaustion.

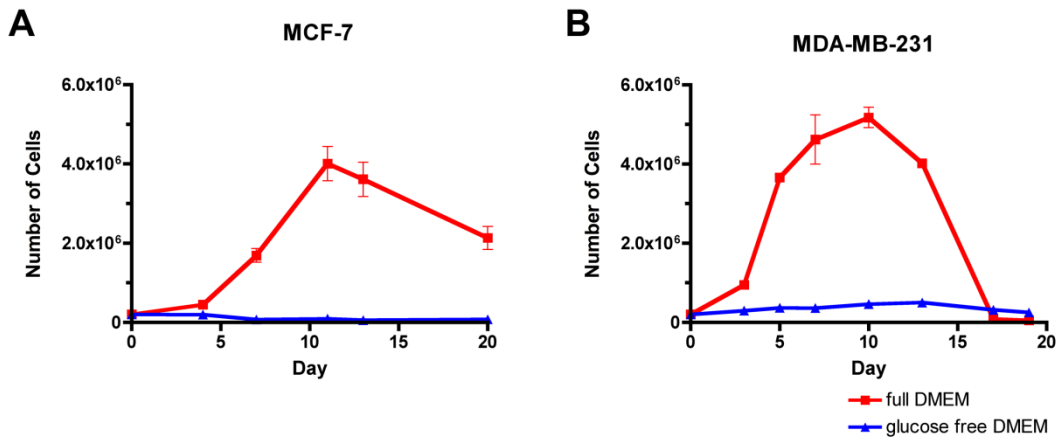

Figure 5.2: growth is more robust in full DMEM than glucose free DMEM in both [A] MCF-7 and [B] MDA-MB-231. N=3.

This source of alternative growth would appear to be lactate. Repeating the experiment and sampling the media reveals a basal level of lactate of around 0.5mM (**Figure 5.3**). The source of this lactate is likely to be FCS. The full DMEM experiments show an expected lactate relationship with an increase that matches the growth profiles; in short, more glucose consumption is leading to greater lactate production.

However, in the glucose free DMEM replicate the lactate level for MDA-MB-231 show a slight decrease indicating that there is a degree of lactate uptake and utilisation.

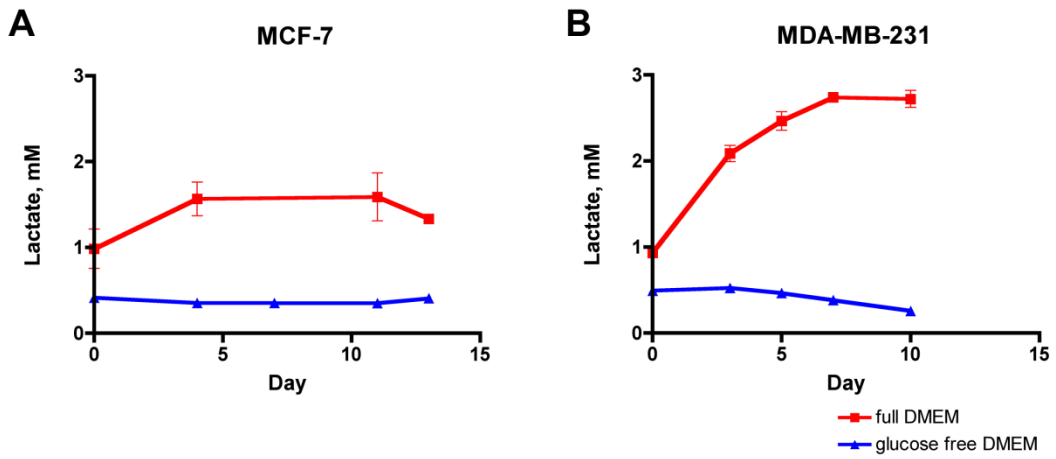

Figure 5.3: [A] lactate levels increase in MCF-7 cells in full DMEM and flatline in glucose free DMEM; [B] lactate levels increase in MDA-MB-231 cells in full DMEM and fall in glucose free DMEM. N=3.

5.2.2: MCF-7 AND MDA-MB-231 RESPOND DIFFERENTLY TO THE WITHDRAWL OF GLUCOSE AND GLUTAMINE

Given that there was a different response between MCF-7 and MDA-MB-231 cells to glucose-free DMEM, it was important to establish whether this effect was due to glutamine. The cells were therefore grown over varying time periods and with lystates collected for immunoblotting and media samples taken to analyse lactate levels. **Figure 5.4** is representative of the trend in that cells grown in glutamine-free DMEM demonstrate a similar lactate production profile to those grown in full DMEM. Whilst it is possible to infer from this that the bulk of lactate carbons in both MCF-7 and MDA-MB-231 derive from glucose, there is evidence that suggests that glutamine uptake is glucose-dependent (Wellen, K.E., *et al*, 2010). In either case, the critical result is this; that in the absence of glucose, glutamine will not fuel

growth. Furthermore, MDA-MB-231 produced more lactate than MCF-7 under all conditions tested.

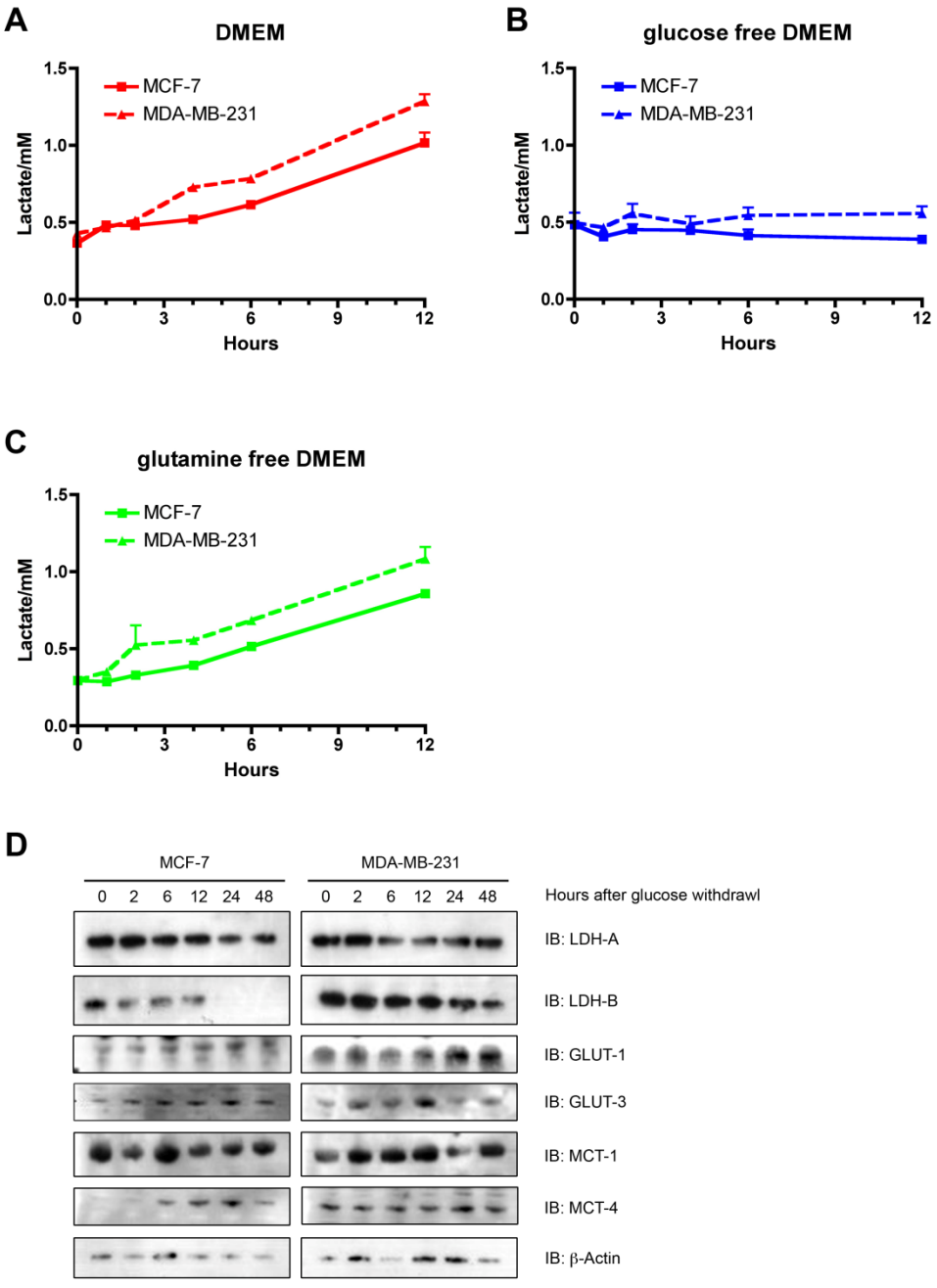

Figure 5.4: lacate production in [A] MCF-7; [B] MDA-MB-231; [C] in full DMEM; in [D] glucose free DMEM; [E] in glutamine free DMEM; [F] immunoblot reveals changes in protein expression levels after changing to glucose free DMEM. N=3.

In this instance, questions arise concerning the precise identity of any lactate source given that it cannot be glutamine alone. However, it must be stated that these experimental conditions are necessarily false and that *in vivo* differences in metabolite concentrations are likely to be both localised and transient.

In line with the model outlined above, where LDH-A is responsible for pyruvate reduction and LDH-B is responsible for lactate oxidation, the next step was to look at what happened to protein expression when MCF-7 and MDA-MB-231 were deprived of glucose.

The levels of glucose transporters GLUT1 and GLUT3 does not vary, though this does not account for the fact that their activity may be altered under glucose-free conditions. What is interesting is that in relation to LDH-B, there is a pseudo-hypoxic phenotype with a pattern of down-regulation over time. This is most pronounced in the MCF-7 cells, where there is also an up-regulation of MCT-4, the transporter protein responsible for lactate export. These last two observations taken together appear counterintuitive and there is no easy explanation.

That said, both LDH-B and MCT-4 are geared towards clearing lactate from the cell, albeit in different directions (the former back to pyruvate and the latter out of the cell completely). This may indicate a level of cooperativity between LDH-B and MCT-4 expression. The down-regulation of LDH-B in particular suggests that any role in lactate-fuelled growth may be overstated.

5.2.3: LDH-A INHIBITION IN MCF-7 AND MDA-MB-231 REDUCES GROWTH IN THE ABSENCE OF GLUCOSE

If the effect of LDH-A inhibition arises through a downstream inhibition of glycolysis then in the absence of glucose, LDH-A inhibition should have no effect. Likewise, if LDH-B has a role in maintaining growth in a glucose-free environment, then LDH-B knockdown in glucose-free DMEM should have a significant effect in the presence of background media lactate levels (~0.5 mM). However, the data is in stark contrast to these predictions (**Figure 5.5**).

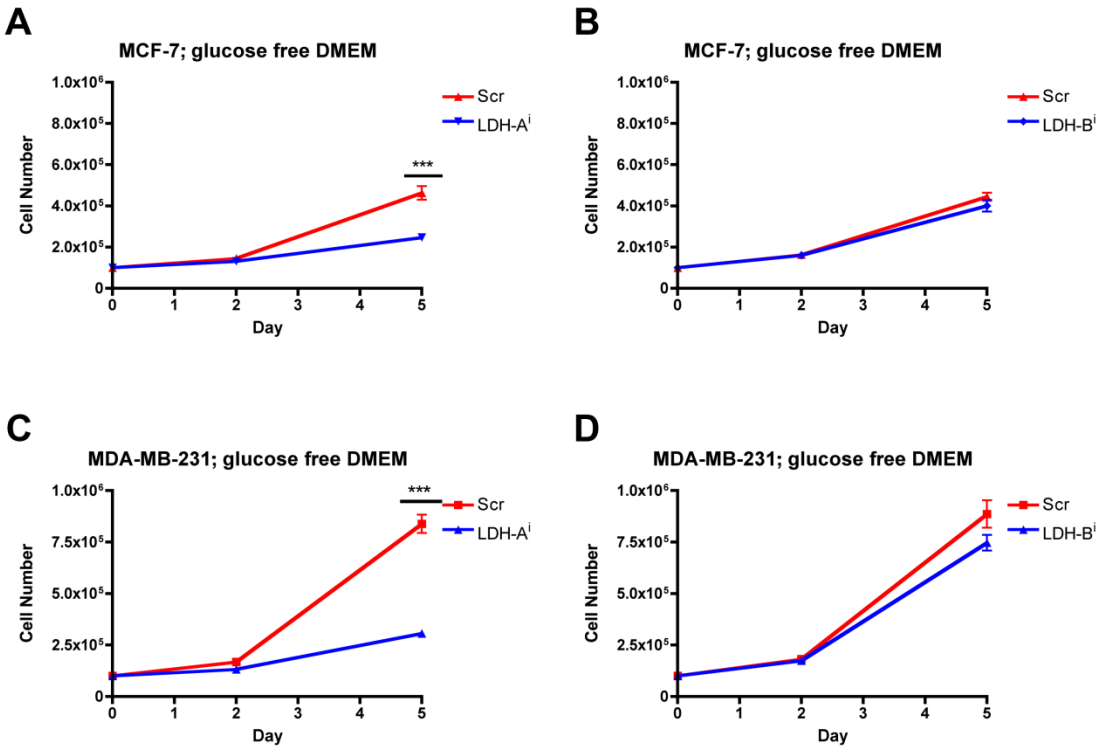

Figure 5.5: in glucose free DMEM[A] LDH-A knockdown in MCF-7 reduces growth; [B] LDH-B knockdown has no effect; [C] LDH-A knockdown in MDA-MB-231 reduces growth; [D] LDH-B knockdown in MDA-MB-231 has no effect. N=3 * = P <0.05; ** = P<0.01; *** = P<0.001.

Indeed, what is interesting is that the effects are, whilst scaled down to account for less growth in glucose-free DMEM, similar to the data for LDH-A and LDH-B knockdown in full DMEM seen in **Chapters 3 and 4**. Chiefly, LDH-A knockdown produces less growth when compared to the scramble control whilst LDH-B knockdown has no effect. Specifically, there is a 47% reduction in cell number in MCF-7 and a 63% reduction in cell number in MDA-MB-231 when the LDH-A knockdown is compared to the control.

This data implies that there is a level of metabolic activity occurring in the absence of glucose that is LDH-A dependent. The outstanding question then was whether this activity was confined to a residual level of glutaminolysis utilizing the TCA cycle and producing pyruvate as a by-product or extended to lactate-fuelled growth.

5.2.4: MDA-MB-231 CAN USE LACTATE AS A FUEL SOURCE UNDER STARVATION CONDITIONS

In order to establish whether MCF-7 and MDA-MB-231 cells could use lactate as a fuel source, cells were plated and grown in glucose free DMEM. At day 1, 10 mM lactate was added alongside a blank (media only) control and cell counts were taken at set points (**Figure 5.6**). For MCF-7, the cells died quickly in both the lactate-treated and lactate-free media. This correlated with the earlier data in **Figure 5.2** showing weak glucose free growth in MCF-7.

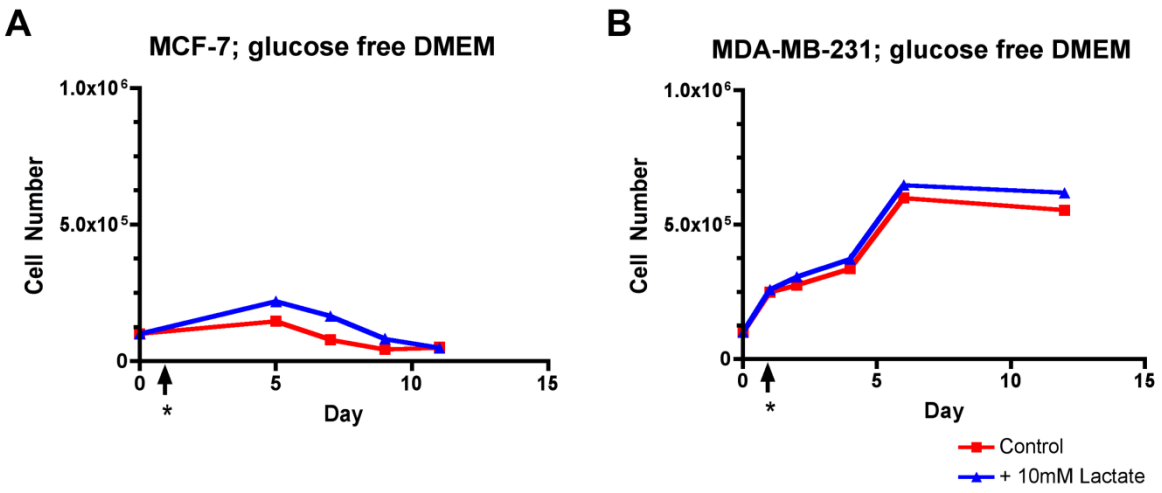

Figure 5.6: treating cells with 10mM lactate at day 1 has no effect on [A] MCF-7 or [B] MDA-MB-231. N=3.

The MDA-MB-231 cells showed stronger growth under glucose withdrawal but lactate treatment still had no effect. To rule out a role for glutamine, the experiment was repeated with the cells being grown in glucose free medium for a week prior to seeding in order to deplete any background metabolites (**Figure 5.7A**). Once again, this showed no effect for lactate and so a reverse approach was attempted using glutamine-free DMEM and the small molecule 2-deoxy glucose (2-DG), a known inhibitor of glycolysis, to modulate glucose flux (**Figure 5.7B**). Again, the effect of lactate at day 1 is negligible in glutamine-free DMEM in the absence of 2-DG, whilst the effects of 2-DG on those cells treated was so profound it suppressed growth to a large extent in both lactate treated and untreated cells. This data also seemed to confirm that any impact glutamine may have on growth is glucose-dependent.

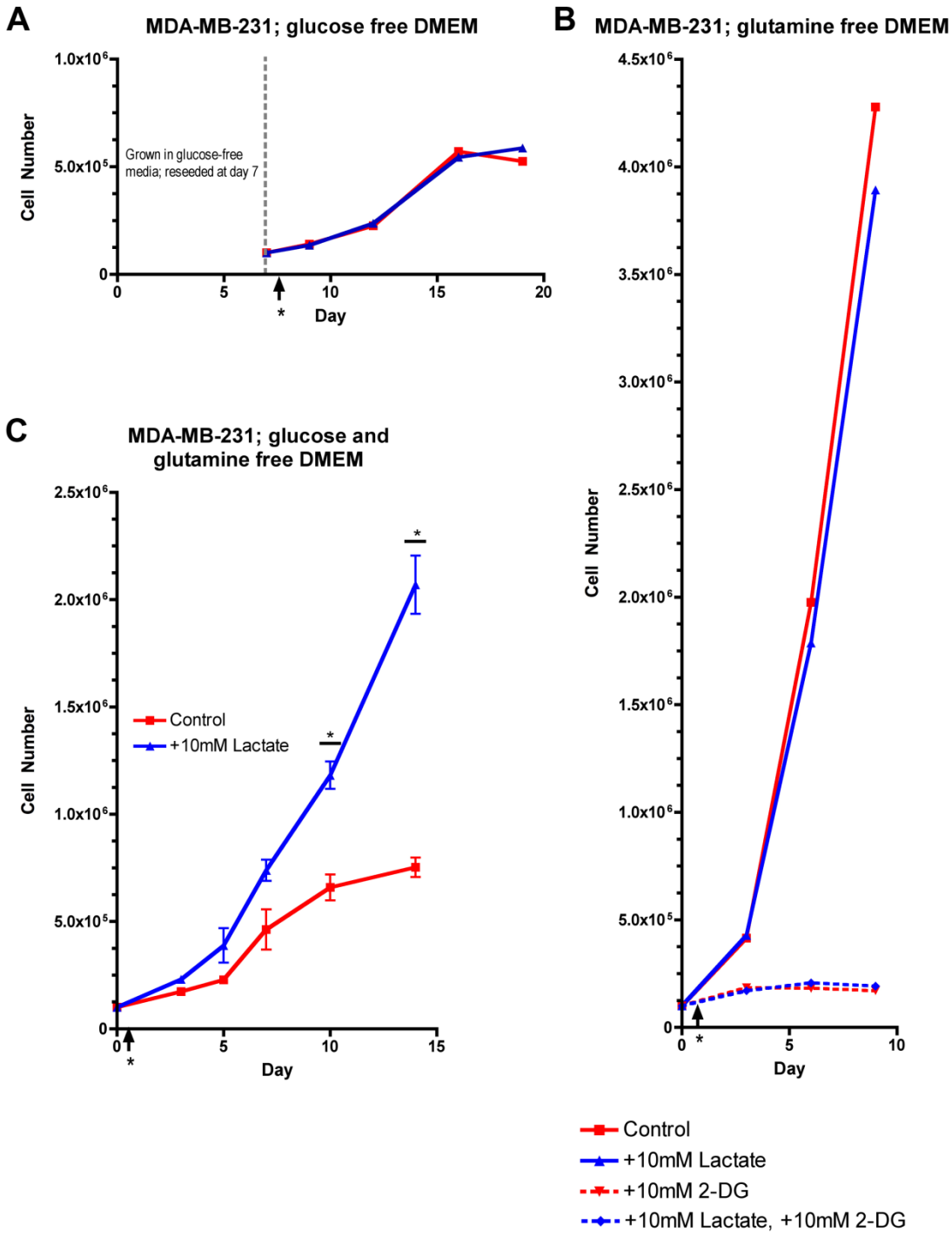

Figure 5.7: treating MDA-MB-231 cells with 10mM lactate at day 1 [A] has no effect after growing cells in glucose free DMEM for 7 days; [B] does not rescue cells treated with 10mM 2-DG in glutamine free DMEM; [C] produces a significant difference in growth in glucose and glutamine free DMEM. N=3 * = P <0.05; ** = P<0.01; *** = P<0.001.

The last approach, to discount the possibility of non-specific effects of 2-DG, was to reconstitute DMEM from powder without glucose or glutamine. In this experiment, treating cells with 10mM lactate at day 1 increased growth of MDA-MB-231 cells by 3 fold after 15 days when compared to the untreated (blank DMEM) control (**Figure 5.7C**).

5.2.5: LACTATE-FUELLED TUMOUR GROWTH IS LDH-A DEPENDENT AND OCCURS IN THE MITOCHONDRIA

Having arrived at conditions under which lactate could be used to fuel tumour growth, it was important to see if this lactate-fuelled growth was dependent upon either LDH-A or LDH-B. This was achieved by repeating the previous experiment in the presence of MDA-MB-231 cells in glucose and glutamine free media with LDH-A and LDH-B knocked down by siRNA.

As can be seen, lactate fuelled growth was LDH-A dependent and not, as suggested by models in the literature, LDH-B dependent (**Figure 5.8A**). This result manifests itself as not only lower growth in the LDH-A knockdown but also when lactate consumption is looked at. The level of reduction in growth in the lactate-treated LDH-A knockdown is stark, with a 44% reduction in cell number. This compares to a 51% reduction in cell number between the lactate treated and untreated controls. Moreover, media collected at day 5 shows that the consumption of lactate in the LDH-A knockdown had been markedly diminished (**Figure 5.8B**) with 1.3 fold and 1.6 increases in media lactate in the untreated and treated cells respectively.

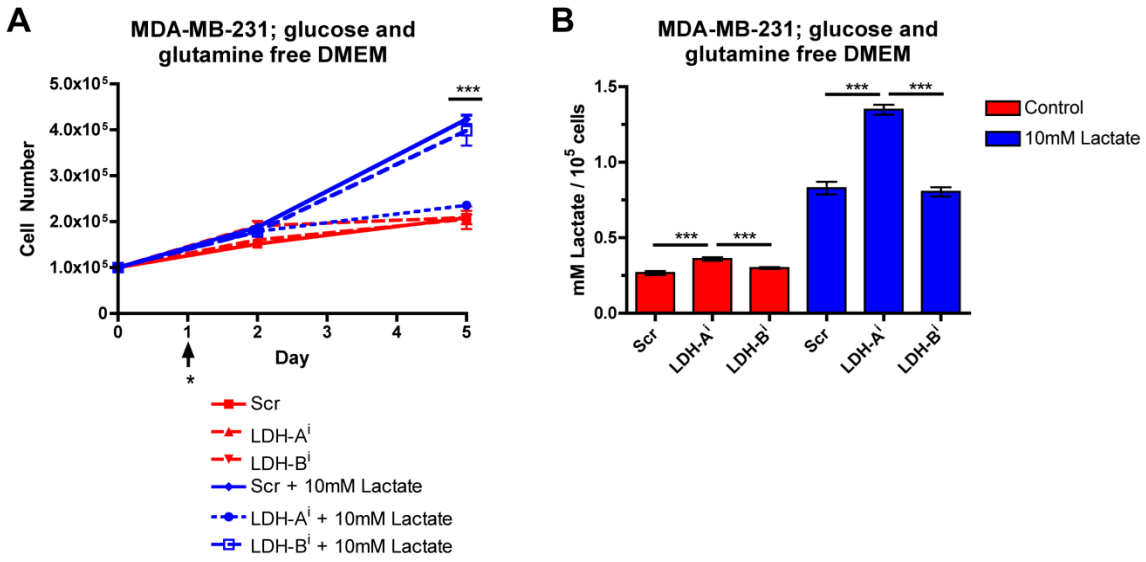

Figure 5.8: [A] LDH-A knockdown reveals that in MDA-MB-231 cells lactate fuelled tumour growth is LDH-A dependent; [B] lactate levels at day 5 show that LDH-A knockdown reduces lactate uptake and therefore increase the concentration remaining in the media. t = 120 h. N=3 * = P <0.05; ** = P<0.01; *** = P<0.001.

This surprising discovery brings an even greater focus upon the third aim of this chapter. Uncovering what mediates the selectivity between the interconversion of pyruvate to lactate assumed even greater importance now that it appeared that this interconversion was not being operated by different isoforms of the same enzyme but rather LDH-A alone.

A recourse to the literature revealed that another model for lactate oxidation had been proposed (Hussein, R., *et al*, 1999). The main feature of this model is that within different tissues, single isoforms of LDH could exist as either cytosolic LDH (cLDH) or mitochondrial LDH (mLDH) and that it was the latter that was

responsible for lactate oxidation whilst the former took control of the forward reduction of pyruvate.

As a preliminary step, an analysis was undertaken of both the LDH-A and LDH-B sequences using mitoprot to assess whether either gene contained a mitochondrial targeting sequence. The results, seen in **Appendix A**, show that neither gene has a high probability of mitochondrial export. This in itself is not conclusive however, as chaperone proteins may be responsible for the mitochondrial translocation of LDH. However, characterising the identity and nature of these putative chaperones is outside the remit of this project.

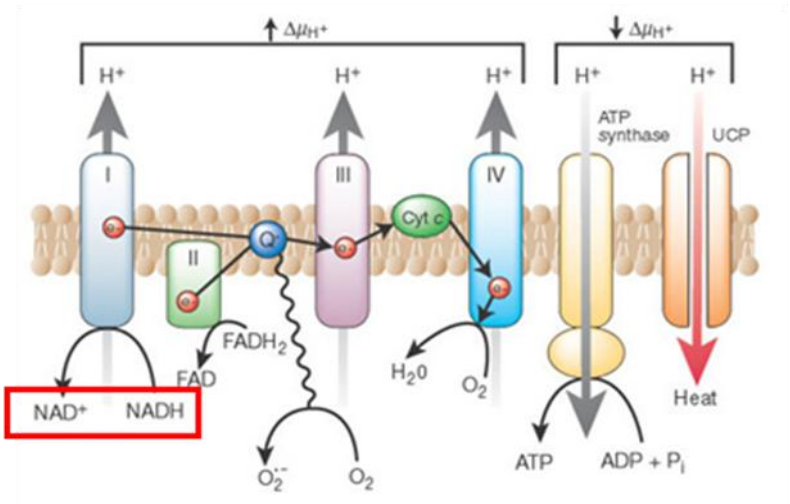

Figure 5.9: the mitochondrial electron transport chain (Brownlee, M., 2001).

In order to verify the existence of otherwise of mLDH-A, two experiments were planned. Firstly, for LDH-A to oxidize lactate it requires a source of NAD^+; in the mitochondria this is generated by the electron transport chain, specifically complex I (**Figure 5.9**). In the first instance then, MDA-MB-231 cells were grown and treated with 10mM lactate as previously. However, both the treated and

untreated were further divided in half and exposed to rotenone, a small molecule inhibitor of complex I.The results show that treatment with rotenone suppresses growth in the presence and absence of lactate (**Figure 5.10).**Though this data may imply a dependence upon OXPHOS under all conditions, previous data in this thesis and in the literature (Fantin, V.R., *et al*, 2006) (Le., A., *et al*, 2010) that suggests that mitochondrial activity is downregulated in highly glycolytic cells would appear to rule out such an interpretation.

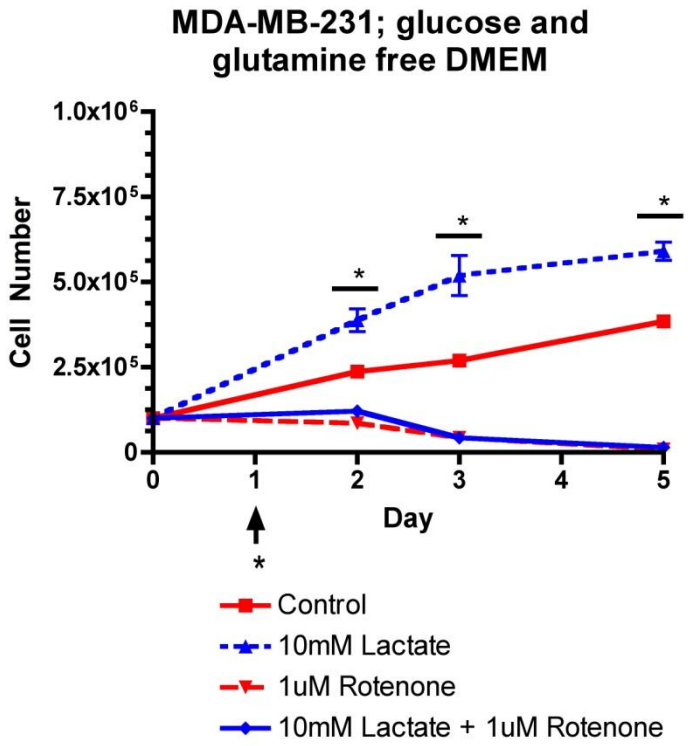

Figure 5.10: treating MDA-MB-231 cells with lactate at day 1 does not rescue cells from the effect of rotenone. N=3 * = P <0.05; ** = P<0.01; *** = P<0.001.

Finally, immunofluorescent staining was undertaken to see if LDH-A could be co-localised with the mitochondria using mitochondrial marker TOM20. This was performed using standard glucose enriched DMEM initially in order to get a

background picture. Nevertheless, the result is clear; there is a large degree of colocalisation when the signals are merged indicating a degree of mitochondrial localisation. This colocalisation disappears completely from the merged image when LDH-A is knocked down (**Figure 5.11**).

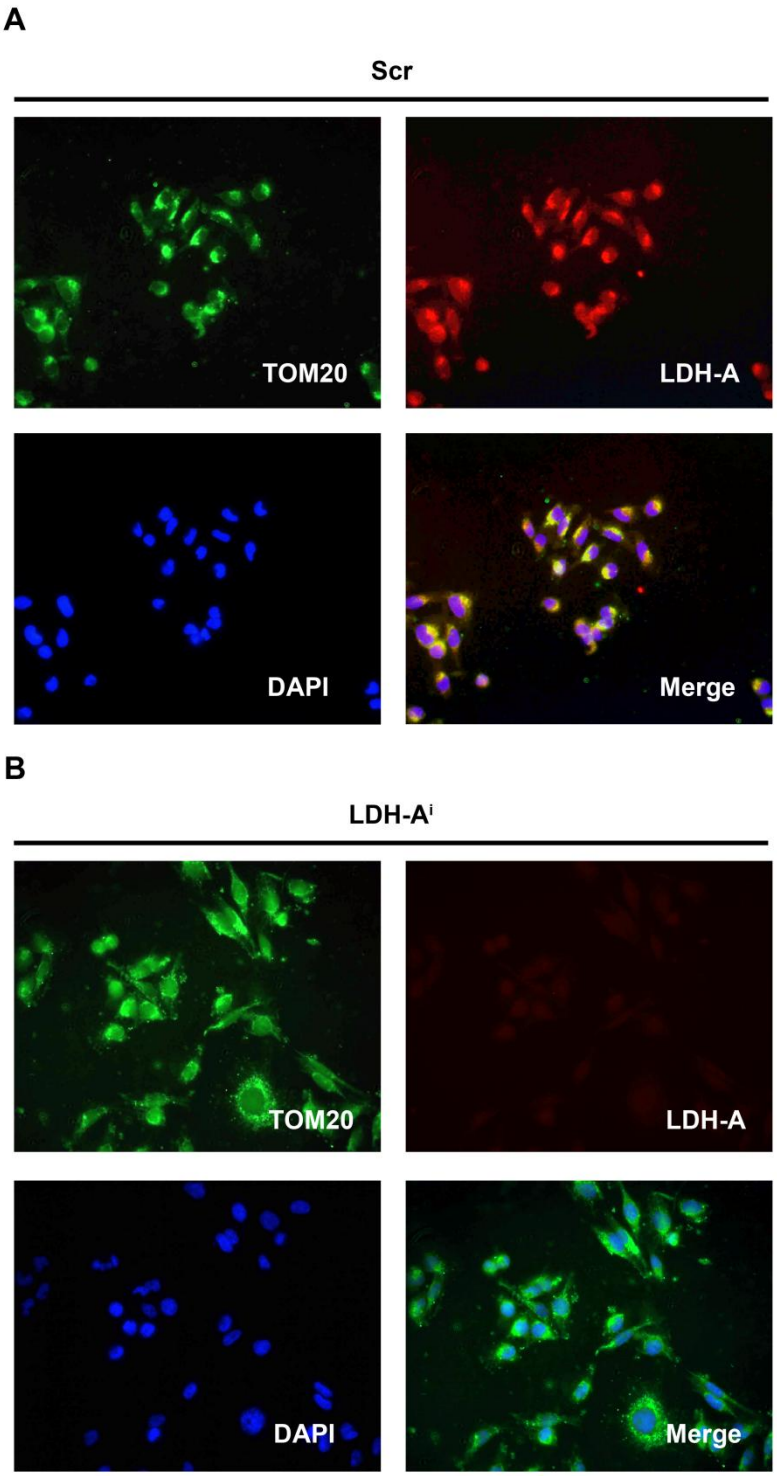

Figure 5.11: [A] immunofluorescence shows that LDH-A can be co-localised to the mitochondria in MDA-MB-231 cells; [B] LDH-A knockdown reduces the LDH-A signal verifying the specificity of the antibody. t = 48h. N=3.

5.3: DISCUSSION

5.3.1: LDH-A IS A SUITABLE TARGET FOR DRUG DEVELOPMENT

The broader remit of this thesis is to determine whether LDH-A is a suitable target for drug development. Having broadly established in previous chapters that in isolation, LDH-A knockdown achieves the desired effect of increased cytotoxicity, it was important to explore any other roles it performed, what role (if any) LDH-B had in maintaining tumour growth, whether there was any conflict between these isoforms and roles that would necessitate a degree of selectivity towards LDH-A, or whether indeed there was a degree of cooperation that hinted at synergy (which would therefore militate against selectivity).

This chapter then set out to uncover whether LDH-A is a suitable candidate for drug development in a more global sense. Considering that LDH-A has a role in maintaining lactate-fuelled tumour growth in addition to maintaining a Warburg phenotype and defending against ROS accumulation (and therefore cell death) it is possible to consider that LDH-A is a particularly attractive target for the development of small molecule inhibitors.

This lactate-fuelled tumour growth appears to be mediated by LDH-A that is localized in the mitochondria. The data has taken steps towards identifying the mechanism of this mitochondrial lactate-oxidation to be dependent upon complex I as a source of NAD^+: a model of lactate fuelled tumour growth is described by **Figure 5.12.**

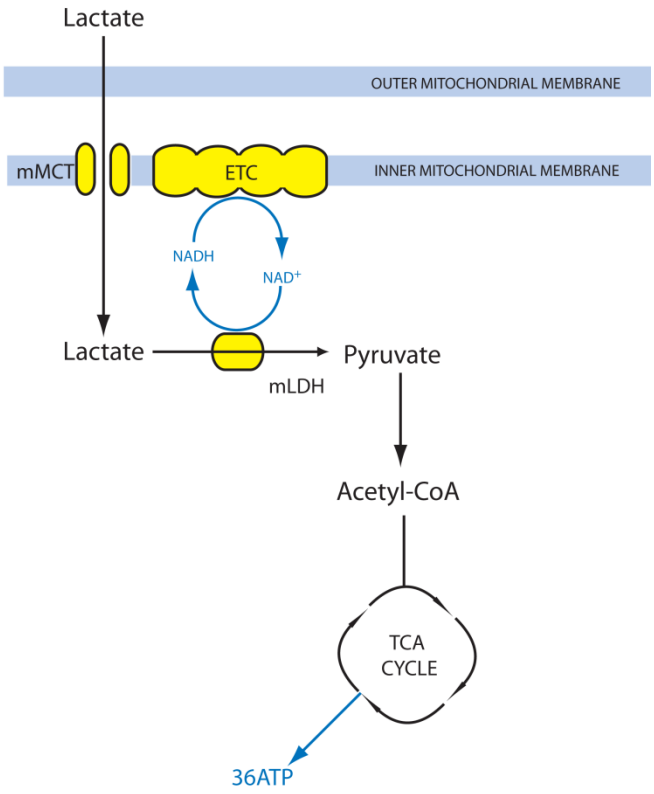

Figure 5.12: a model of mLDH-A dependent lactate oxidation.

What has yet to be elucidated is how the activity of LDH-A is controlled and how mitochondrial import and export is mediated. There is the further question of whether, as in the case of hexokinase, mLDH-A is integrated into broader mitochondrial physiology or whether its expression and activity are isolated within the mitochondria.

The role of lactate itself also begs the question 'what other carbon sources?' If cells possess the ability to oxidise a molecule usually considered as cellular waste, it is highly likely that mechanisms and pathways exist to utilize other carbon sources in times of starvation. Identifying and understanding these pathways is critical if

LDH-A is to be targeted as other pathways may offer LDH-A incompetent cells an escape route.

5.3.2: Future Work

The fact that LDH-A is responsible for more than one pathway places new emphasis on its earlier designation as a metabolic chokepoint. However, that lactate-fuelled growth can only occur in the absence of glutamine and glucose in this model is worthy of comment.

Other studies (Sonveaux, P., *et al*, 2008) have shown that lactate can be used preferentially even in the presence of glucose; this may remain the case in MDA-MB-231, but this speculation highlights the limits of basing metabolic models on cells grown in 2D culture. In order to get a better understanding of the flux of metabolites in 3D, 3D models need to be used. Techniques exist for quantitative metabolic analysis by spectroscopic means either by mass spectroscopy, which means disrupting the sample, or in real time using hyper-polarised nuclear magnetic resonance techniques (Wiechert, W., 2001) (Schroeder, M.A., *et al*, 2009). In reality, a combination of both approaches is likely to yield a fuller picture than any in isolation.

Moreover, to be absolutely confident of the role of mLDH-A several further experiments might be worthwhile. Firstly, a simple mitochondrial fraction using known mitochondrial proteins such as cytochrome-C would give a qualitative grip on approximate distribution of LDH between the cytosol and the mitochondria. Further, a time course could be attempted to see if this distribution changes over time or in reaction to any environmental stresses such as hypoxia or low glucose.

Lastly, to completely verify the mechanism of lactate oxidation, an oxygen consumption experiment should be undertaken in the presence and absence of both lactate and rotenone in order to determine whether lactate treatment increases oxygen consumption.

CHAPTER 6: TOWARDS A SMALL-MOLECULE INHIBITOR OF LDH-A

6.1: INTRODUCTION

This chapter will focus on applying the tools of medicinal chemistry and molecular pharmacology to the data generated by molecular biology techniques so far in order to produce small-molecule structures that have clinical application.

6.1.1: SMALL-MOLECULES WITH AFFINITY FOR LDH-A

LDH has been the focus of a fair degree of interest in medicinal chemistry terms, though this in large part has focused on *plasmodium falciparium* (*pf*) LDH, a bacterial isoform implicated in malaria. LDH-A as an anti-cancer target however, whilst experiencing a recent increase in interest, has in the large part not been fully exploited.

The best known LDH inhibitor is oxamate (**Figure 6.1**), which is a pyruvate mimic and is non-specific between isoforms. It also displays broader non-specific activity, inhibiting a range of other enzymes including aspartate aminotransferase (AAT) (Thornburg, J.M., *et al*, 2008).

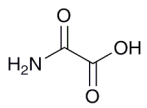

Figure 6.1: Oxamate.

If Oxamate is a very small small-molecule with only two carbons then gossypol (**Figure 6.2**), a natural product derived from cotton plants, is a much larger beast. Gossypol, and a variety of gossylic analogues are known LDH-A inhibitors (Yu, Y., *et al*, 2001). Again, there are a range of non-specific targets that gossypol also acts on; gossypol is pro-apoptotic, a mitochondrial toxin and also inhibits protein kinase D (Wang, X., *et al*, 2009).

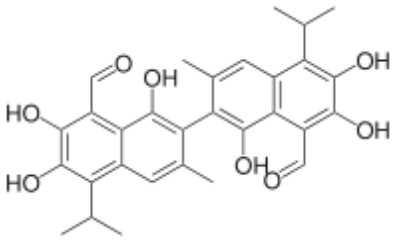

Figure 6.2: gossypol.

The final notable class of compounds are the heterodiazoles (Cameron, A., *et al*, 2004) of which the oxadiazoles (furazans) are one. These can also be seen as pyruvate mimics with the two C=N bonds looking like the 1,2 dicarbonyl motif of pyruvate locked into the conformation pyruvate adopts in the active site by heteroatom X (oxygen in the case of furazan).

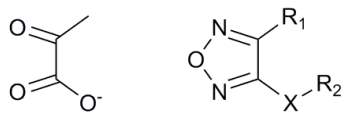

pyruvate furazan

Figure 6.3: Furazans are strucutural analogues of pyruvate.

6.1.2: AIMS

With known structures to hand, the challenge is to build on existing inhibition in *pf*LDH to create inhibitors of human LDH-A that recapitulate the previous cytotoxicity obtained using RNA interference. With this in mind, the aims can be refined as follows: firstly, to understand more fully the interactions of small molecules in the LDH active site, how they can potentially interfere with the mechanism of oxidation/reduction, and how this may be exploited structurally; secondly, to select and validate an appropriate screen to identify these structure activity relationships (SAR) and quantify inhibition; and thirdly, to bring this together to propose a synthetic strategy that will generate potential small-molecule inhibitors of LDH-A.

6.2: Results

6.2.1: Computational analysis can be used to describe the interaction of small molecules with the active site of LDH-A

Understanding interactions on a molecular level is important in order to build a structure-based idea of how small molecules interact with key residues in the active site of LDH. In the first instance, the molecular imaging and docking package GOLD was used to dock oxamate and the cofactor NADH in the substrate and cofactor binding sites (**Figure 6.4**).

What is stark is that active site itself is deeply buried. Moreover, the substrate binding site also appears as a deep cleft that would strongly impair anything but a small degree of steric freedom.

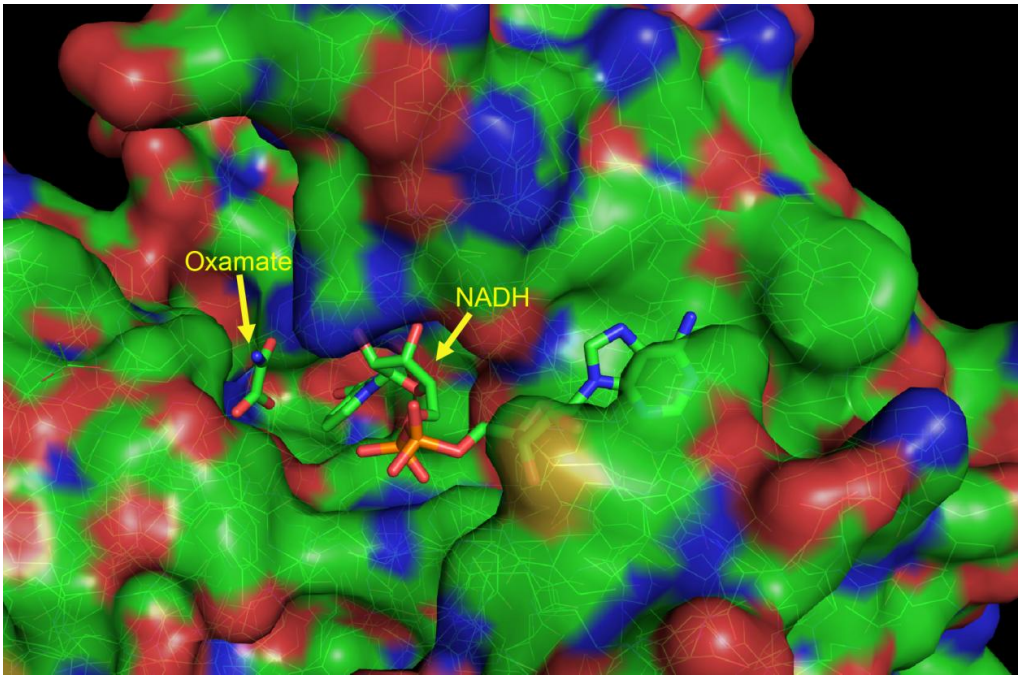

Figure 6.4: Oxamate and NADH (stick representation) docked into the active site of LDH-A (space-filling). Red represents oxygen, blue nitrogen, and green carbon (or the electron denisty of these atoms in the case of the space-filled LDH-A.

Stripping away the electron shells and large parts of the protein structure reveals several key residues and how they interact with a substrate like inhibitor and the cofactor NADH (**Figure 6.5**). These include several arginines (99, 106, 169), asparagine (138), threonine (248) and a criticial histidine (193) that is responsible for the proton transfer that reduces pyruvate to lactate. Several of these interactions have hydrogen-bonding distances in the order of 3 angstroms, a distance equivalent to the span of H-C-H.

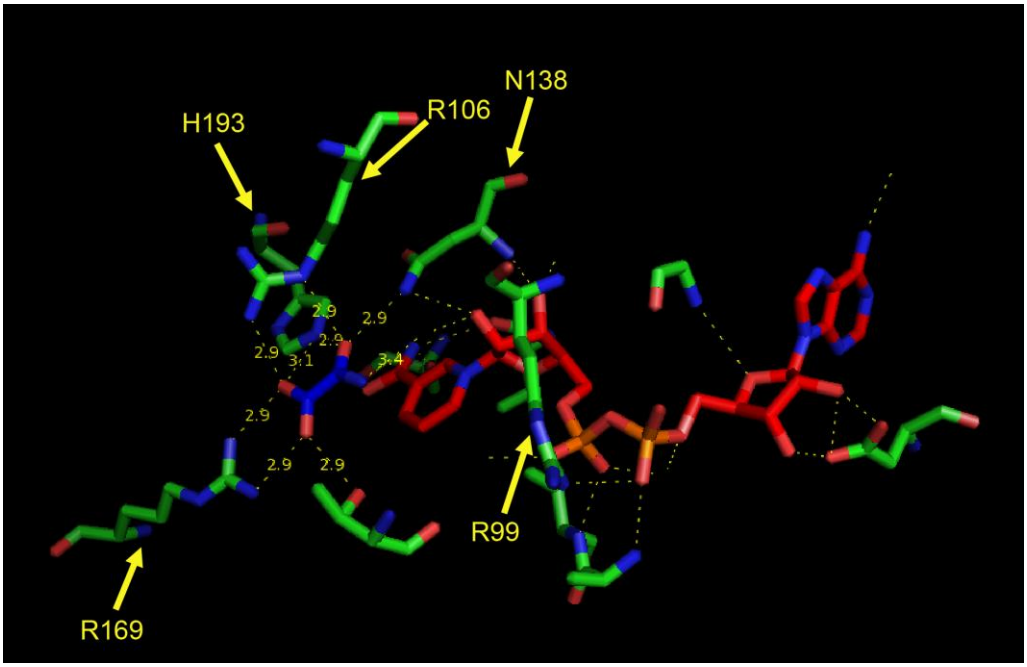

Figure 6.5: Oxamate and NADH interacting with key residues in the LDH-A active site.

If H193 is important for protonating the C-2 carbonyl in pyruvate, then NADH is critical in providing a source of hydride equivalents to reduce the C-2 oxygen from a ketone to an alcohol thus converting pyruvate to lactate.

6.2.2: A MEDIUM THROUGHPUT SCREEN REVEALS SOME PROMISING POTENTIAL INHIBITORS OF LDH-A

Tovalidate the enzymatic source and assay methodology, LDH-A and LDH-B were tested at a range of pyruvate concentrations. The assay, as used, was modified from a version used by (Hewitt, C.O., *et al*, 1999). The basic principle centres on monitoring the change in absorbance in NADH at 340nm which in turn indicates the amount of pyruvate that has been reduced. This is revealed best by **Figure 6.6**, where the decrease in absorbance from a 200:0mM NADH/NAD^+ ratio to a 0:200mM NADH/NAD^+ follows a linear relationship. The library compounds, (structures given in **Appendix B**) which will be introduced in more detail shortly, were tested for background absorbance (**Appendix C**) and the most highly absorbing compound APL091 was also tested under the same conditions to ensure that there was no interference between the library and the assay signal.

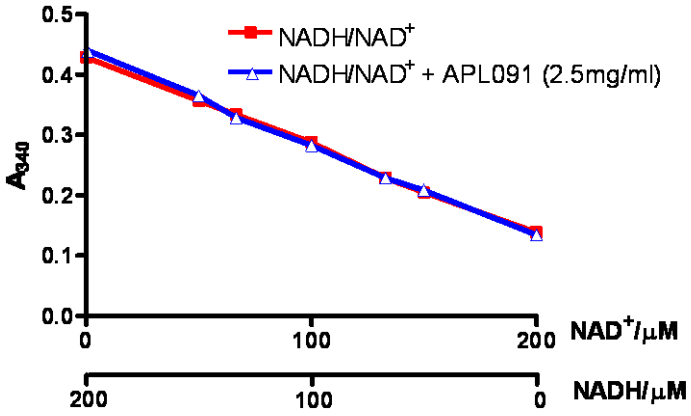

Figure 6.6: the absorbance of NADH:NAD^+ as the former decreases and the latter increases decays in a linear fashion.

Given that the signal for NADH oxidation at 340nm remained robust in the presence of absorbant small molecules, the next step was to validate the enzymatic source.

The K_M for pyruvate is different for LDH-A and LDH-B (**Figure 6.7A**), something that is reflected in the literature (Read, J.A., *et al*, 2001). Whilst the initial data displayed a level of variance with the recorded K_Ms for LDH-A and LDH-B, the non-linear regression was repeated with the respective K_Ms fixed at the literature value. From this analysis, it is clear that the data points collected also describe points along this fitted curve (**Figure 6.7B and 6.7C**), though both literature curves demonstrate a greater activity at lower concentrations of pyruvate. Nevertheless, the order of magnitude different in K_M is the same and from this it is possible to say with confidence that the enzyme source will display a relationship between LDH-A and LDH-B that reflects their slightly differing enzymologies.

On this basis, 200μM, a relatively high but non-saturating concentration of pyruvate was adopted for use when testing other variables. 200μM was also the concentration adopted for NADH.

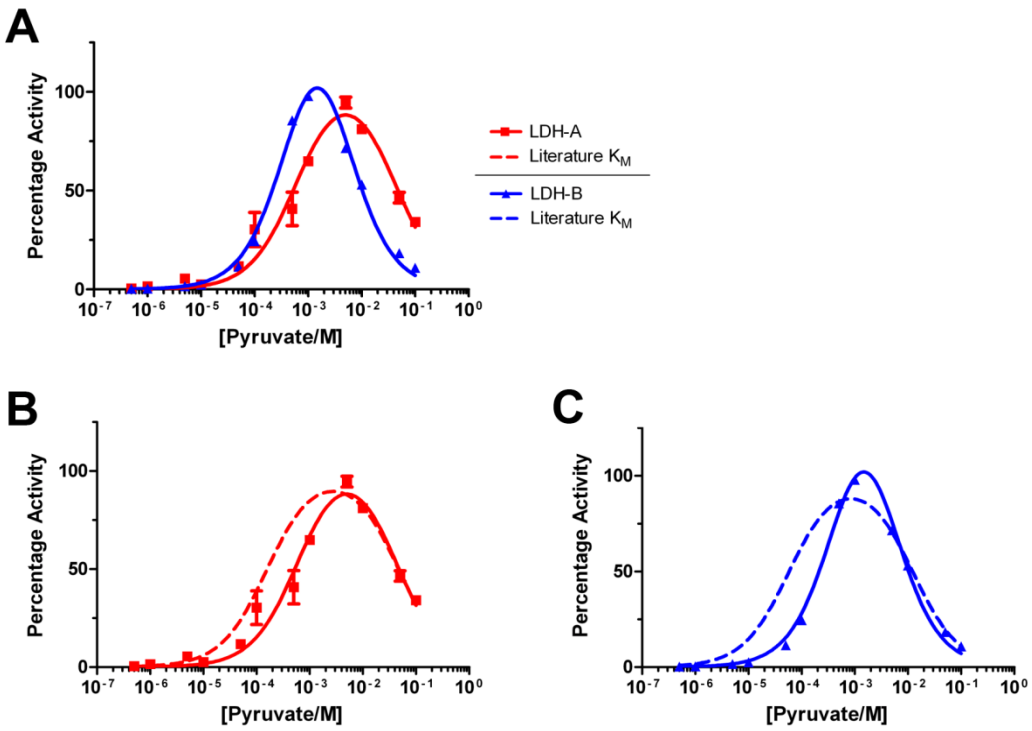

Figure 6.7: validating the enzymatic sources reveals [A] different K_Ms for pyruvate when reduced to lactate by LDH-A or LDH-B; these values compared favourably to the literature values for both [B] LDH-A and [C] LDH-B.

Following this, both isoforms were exposed to a range of oxamateconcentrations to produce a dose-response curve. Again, this corresponded with known data that suggests that oxamate is not specific between isoforms of LDH, with the IC_{50} the same for both isoforms at 46.5μM and 52.5μM for LDH-A and LDH-B respectively.

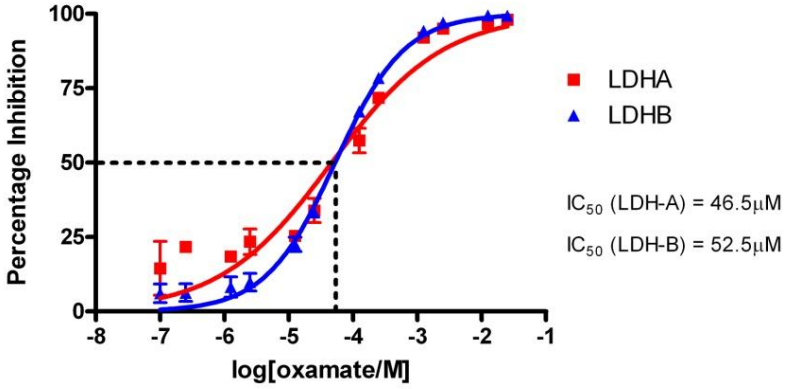

Figure 6.8: Oxamate is not selective between LDH-A and LDH-B.

With a robust assay in place, it was important to design a library to better understand the structure-activity relationship small molecules have with the LDH active site. Moreover, given that many reported inhibitors are active against bacterial forms of LDH, it was critical to understand whether these structures could be modified to improve their activity against the human isoforms or whether new strategies and structures are required all together.

With this in mind, the library was constructed around compounds that contained one of a series of key structural motifs: α,β unsaturated hydroxy-carbonyls, as a moiety that resembles at pyruvate-lactate transition state; furazans, for the aforementioned reasons of appearing as a promising compound class in the literature, and furans as a simpler derivative; lastly, N-benzyl piperazines as a motif that crops up repeatedly and was therefore deemed worthy of probing. This library was exclusively sourced from a larger Chembridge library and no synthesis was undertaken at this stage.

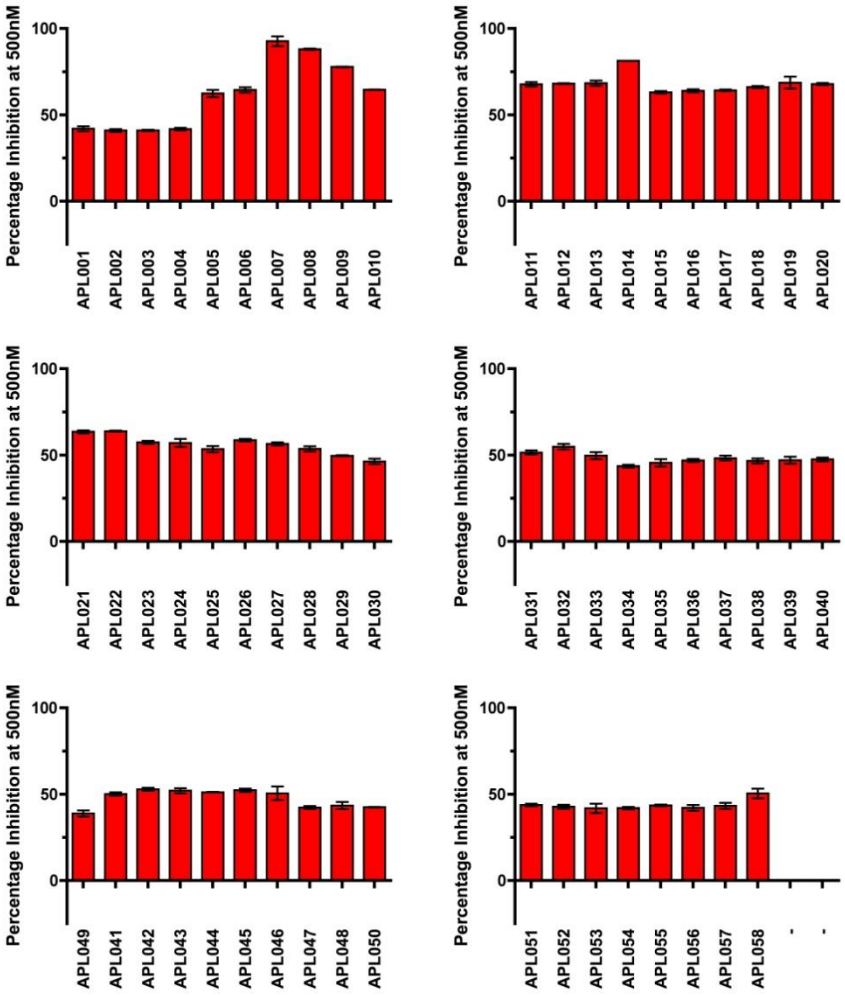

Figure 6.9: Screen results for compounds APL001-APL058.

These compounds were then tested using the previously validated assay. The format adopted initially was to monitor the reaction kinetically for 5 minutes at 3 concentrations of inhibitor (5, 0.5 and 0.05μM inhibitor) and then plot the endpoints as a dose-response curve. This approach was adopted for the first 58 compounds, APL001-APL058. As can be seen in **Figure 6.9** these results either reveal an improbably well-designed library with most compounds registering at least 50% inhibition at 500nM, or most likely the level of inhibition was being

overestimated. At any rate, from this subset only 16 compounds returned a dose-response relationship over 3 concentrations. To both validate these compounds and obtain a proper IC_{50}, the dose-response experiment was repeated over a greater range of concentrations. The screen was refined to use the initial rate data (the gradient of the curve at it's steepest) rather than endpoint. Encouragingly, 7 out of 16 reproduced a dose-response curve using the refined assay method though none had significantly greater efficacy than oxamate (**Figures6.10-6.11**).

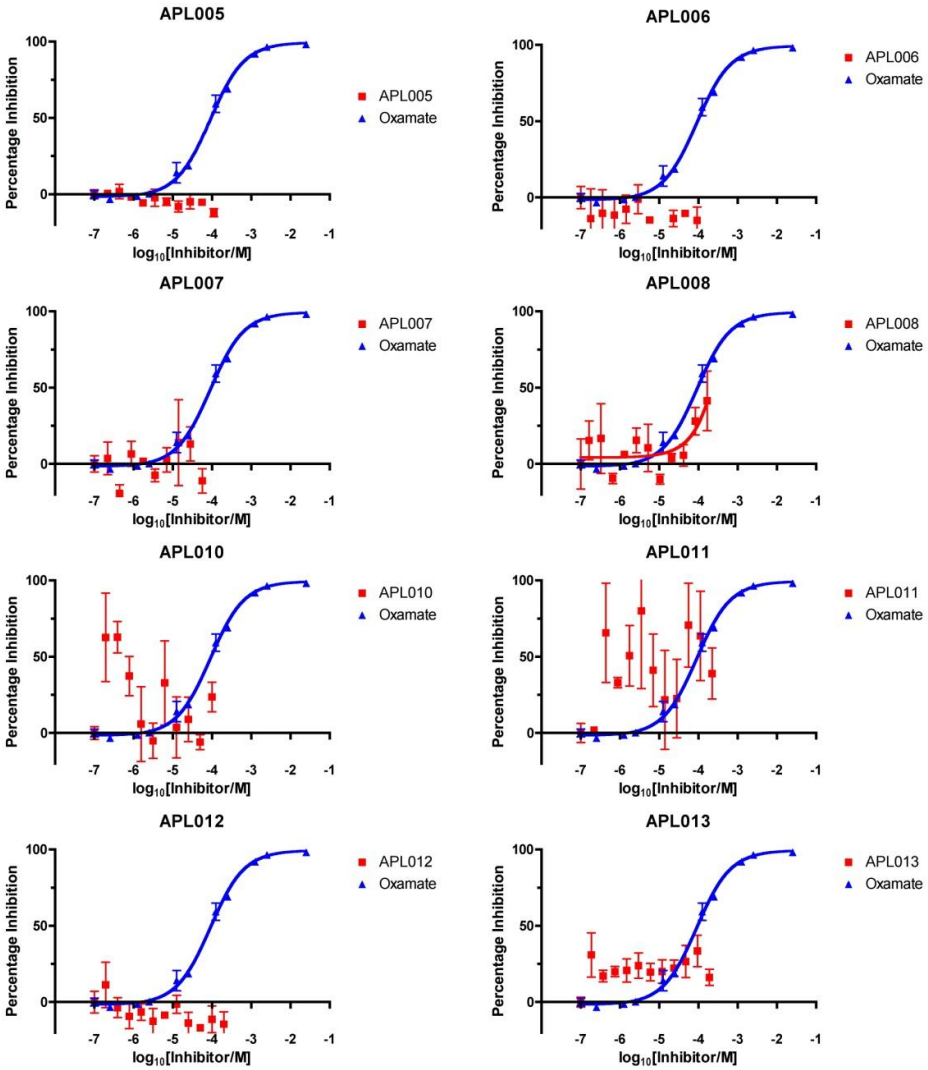

Figure 6.10: Retest for compounds APL005, APL006, APL007, APL008, APL010, APL011, APL 012 and APL013 reveal that only APL008 has a dose-response relationship and that this is not as potent as oxamate.

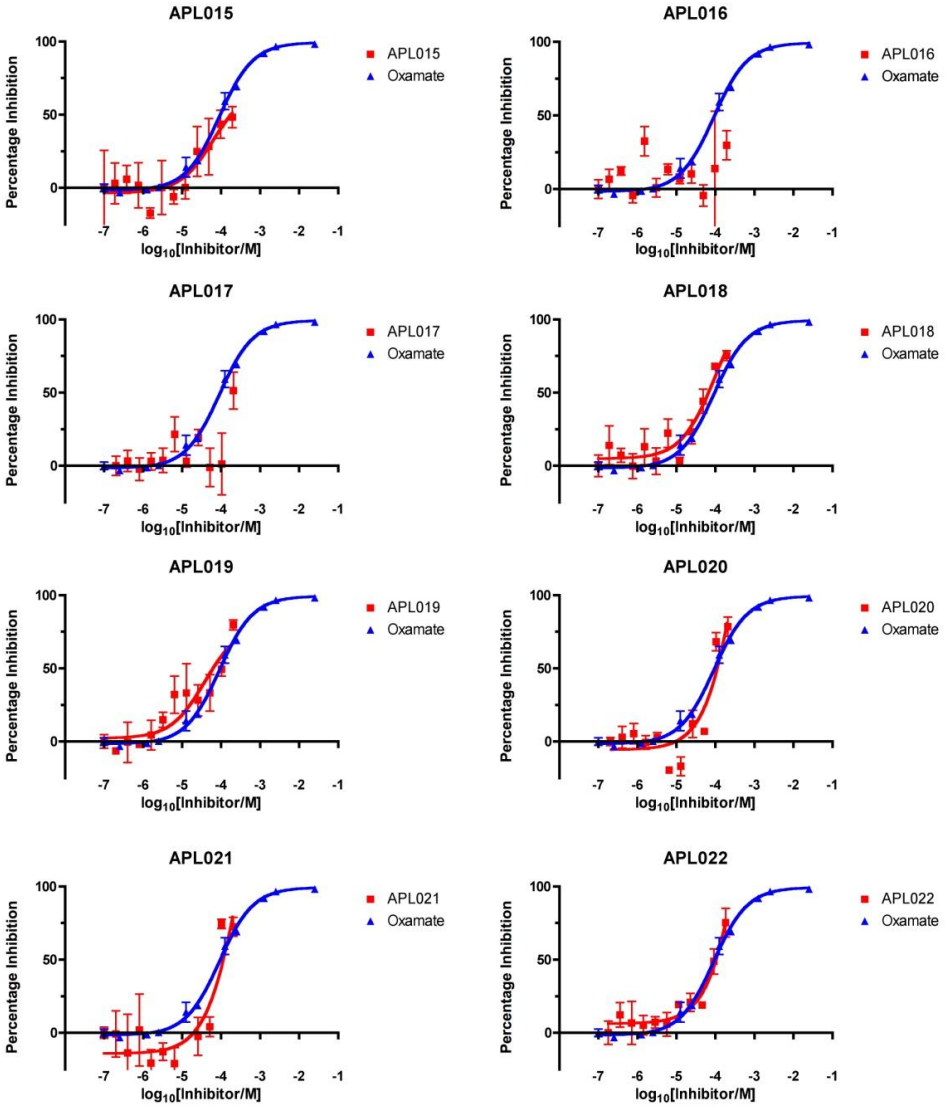

Figure 6.11: Retest for compounds APL015, APL016, APL017, APL018, APL019, APL020, APL021 and APL022 reveal that all but APL016 and APL017 had a dose-response relationship as potent as oxamate.

The remaining compounds in the library were therefore tested according to the refined method of using the raw reaction kinetics and the data for compounds APL058-APL172 is represented in **Figures6.12-6.13**. This produced a much lower hit rate; the threshold for retesting compounds was initially adjusted to 25% inhibition at 500nM with a correct dose-response relationship over the three concentrations acting as a second qualifier for whether a compound should be retested.

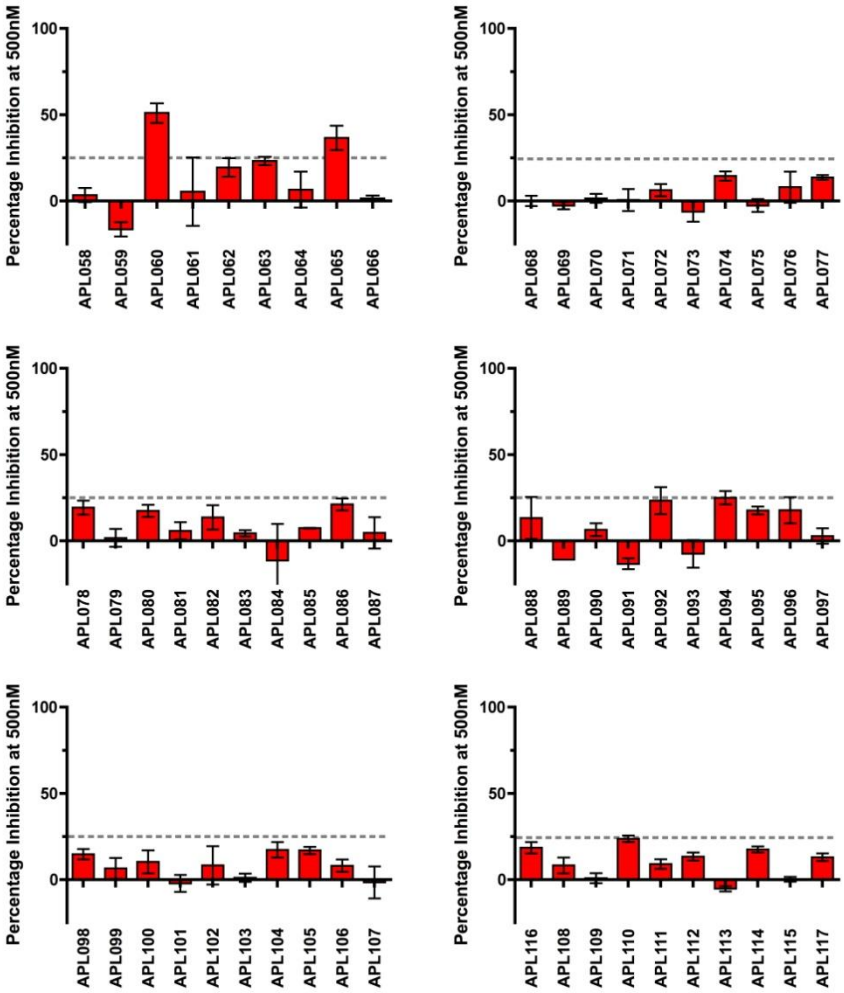

Figure 6.12: Screen results for APL058-APL172

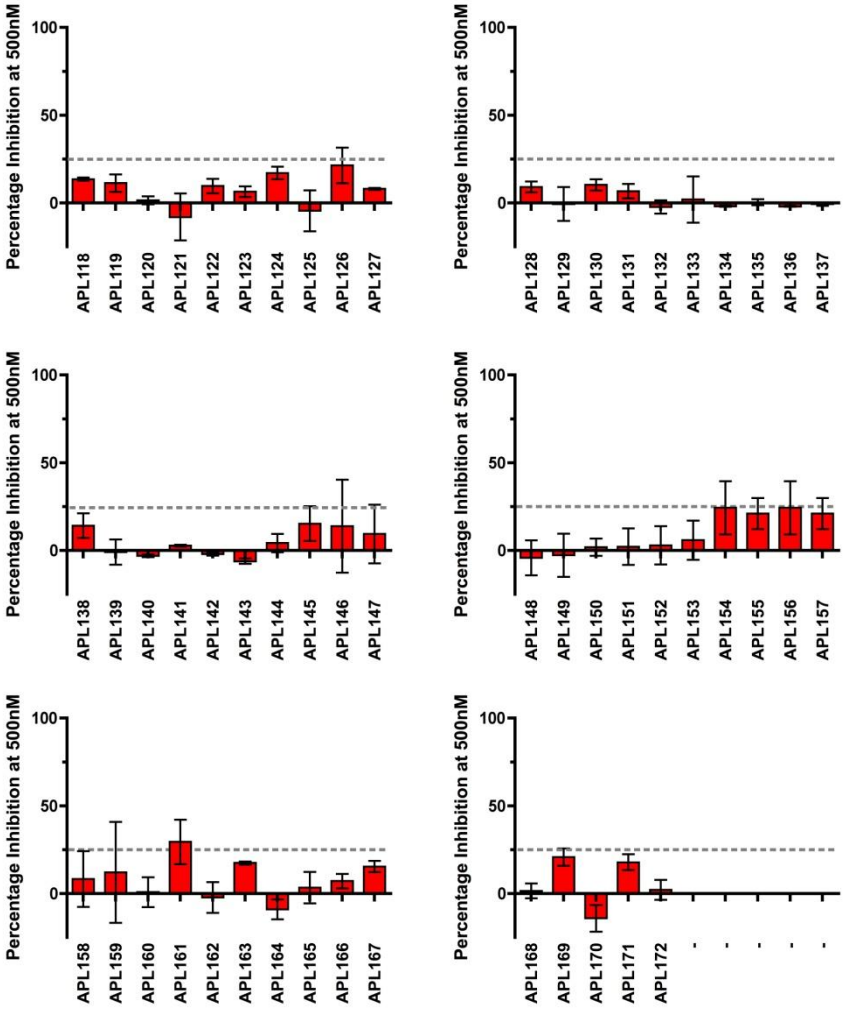

Figure 6.13: Screen results for APL058-APL172

However, many of the compounds above 25% inhibition did not demonstrate a dose response relationship over the initial 3 concentrations; therefore, the criteria were lowered and 7 compounds returned a dose-response relationship. These were APL064, APL065, APL152, APL153, APL154, APL155 andAPL165, which were subsequently retested over a broader range of concentrations. This time, none of the retested compounds returned a dose-response relationship (**Figure 6.14**).

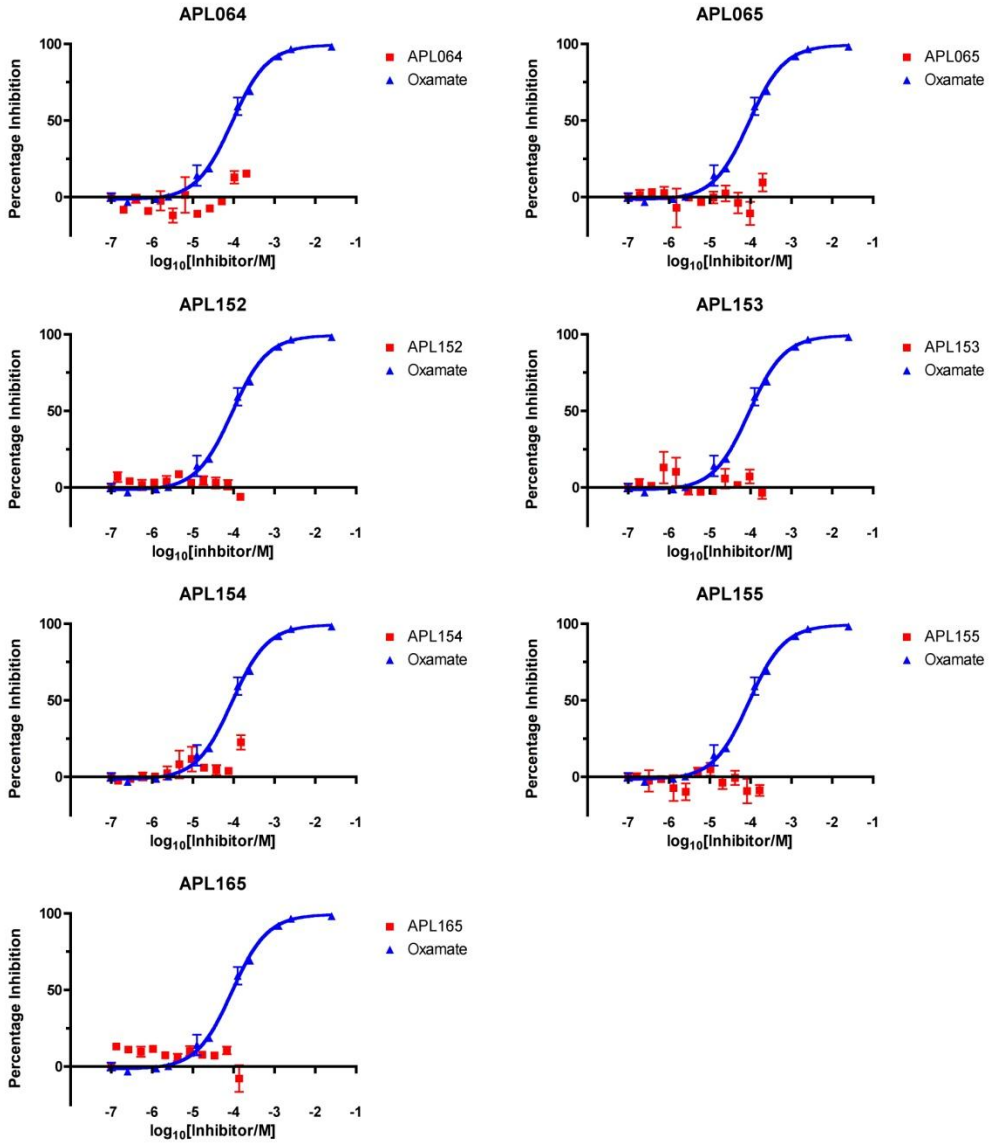

Figure 6.14: Retest for compounds APL064, APL065, APL152, APL153, APL154, APL155, and APL165 reveal that none display a dose-response relationship.

On the basis of the screen data, which was in turn supported by structural classes in the literature, two classes of compounds were identified as being worthy of pursuing by means of parallel syntheses to generate a panel of analogues.

6.2.3: A STRATEGY FOR SYNTHESISING DERIVATISED FURAZANS AS LDH-A INHIBITORS

To date, the majority of literature inhibitors of LDH have not been specifically synthesised to inhibit human LDH-A. A class of compounds with particular promise was identified as 1,2,5-oxadiazoles (furazans) (**Figure 6.15**). Literature reports had shown that a range of heterodiazoles, including the furazans, displayed activity against *pf*LDH (Cameron, A., *et al*, 2004).

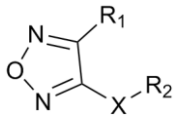

Figure 6.15: 1,2,5-oxadiazoles (furazans) are a class of LDH-A inhibitors.

In order to assess the veracity of the library furazan structures, attempts were started to resynthesise the early hit compounds. Literature precedent (Cameron, A., *et al*, 2004)(Ponzio, G., 1932) existed for the synthesis of furazans. The common first step to all of these procedures is the generation of a bis-oxime from the corresponding 1,2-dicarbonyl (**Scheme 6.1**)

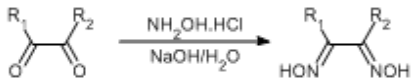

Scheme 6.1: generation of a bis-oxime.

From here, there are two options: cyclise the ring then install a handle for further functionalisation or install the handle first and then cyclise. The former strategy is represented by **Scheme 6.2** with a cyclisation followed by either by using an alkyl lithium to generated a carbon nucleophile or a haloform-type reaction that seeks to replace a methyl with an alcohol.

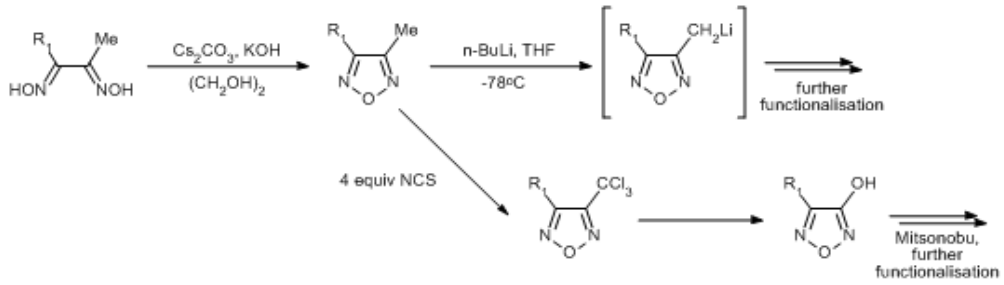

Scheme 6.2: cyclisation with caesium carbonate followed by functionalisation either via a lithiation or pseudo-haloform reaction.

The alternative route is to functionalise first by installing a chloro-group and then cyclise with phosphorous pentachloride (PCl_5) before replacing the chlorine atom with an alkoxy group. This route is represented in **Scheme 6.3**.

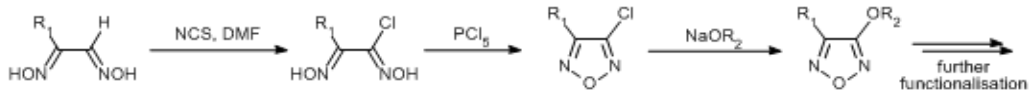

Scheme 6.3: chlorination of the bis-oxime with N-chloro succinimide followed by cyclisation with phosphorous pentachloride

6.2.4: THE SYNTHESIS OF FUNCTIONALISED FURAZANS IS NOT FACILE

Progress on this synthesis to date has been slow. Cyclisation has been achieved following the formation of the bis-oxime that varies between 31%-83% yields. 3-methyl-4-phenyl-1,2,5-oxadiazole and 3,4-dimethyl-1,2,5-oxadiazole have subsequently been successfully isolated at yields of 20-25% (**Figure 6.16**).

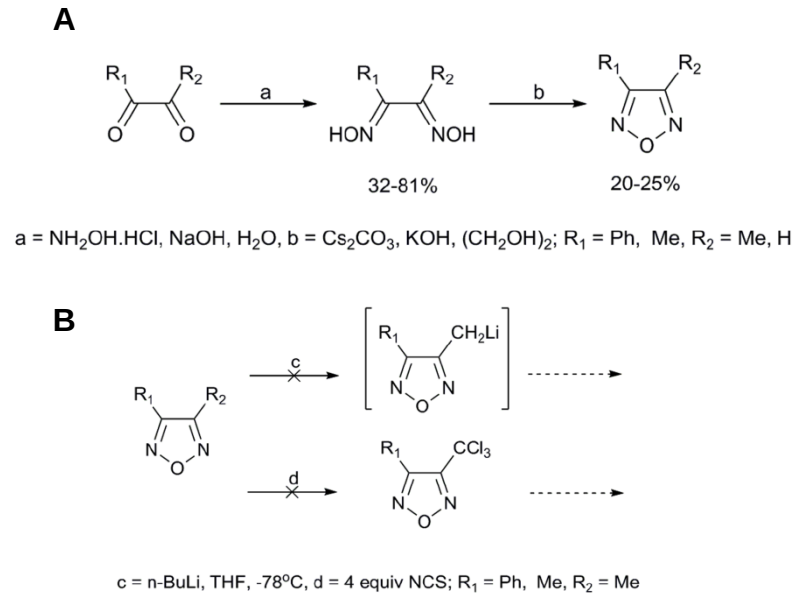

Figure 6.16: synthesis of furazans to date have had mixed results with [A] cyclisation possible but [B] further functionalisation elusive

However, issues surrounding attempts to functionalise the ring remain suggesting that other routes need to be considered. Specifically, neither alkyl lithium or pseudo-haloform reactions have succeeded in generating a reaction mixture containing anything other than starting material. Furthermore, using thiocyanate followed by phosphorous pentachloride has also not yet been successful though may be achievable on refinement.

With this in mind, it is important to return to the literature. Other synthetic routes to functionalised furazans are available and characterised in some depth elsewhere; however, there are significant issues with other types of cyclisation reaction in that they are potentially explosive which precludes there wider use in reactions above a certain scale (Talawar, M.B., *et al*, 2004). For the purposes of this thesis, it was therefore decided to proceed with the second class of compounds for synthesis and analysis.

6.2.5: A STRATEGY FOR SYNTHESISING DERIVATISED OXAMIC ESTERS AND ACIDS AS LDH-A INHIBITORS

Another structural class that came out of the screen were the substituted N-benzyl piperazines. In particular, there seemed a heavy prevalence of N-phenyl,N-benzyl piperazines as represented by hits APL021 and APL022 which are similar to ethyl 2-(4-benzylpiperazin-1-yl)-2-oxoacetate (**Figure 6.17**).

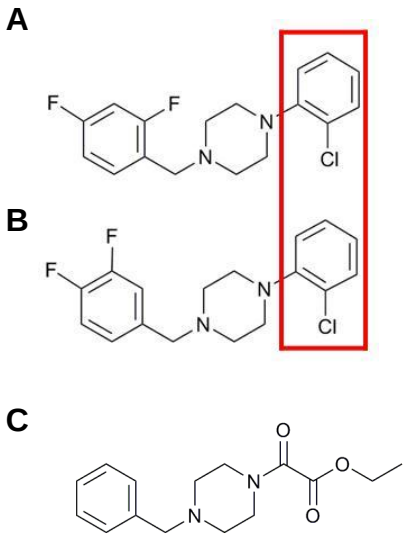

Figure 6.17: [A] APL021 amd [B] APL022 are structurally similar to [C] ethyl 2-(4-benzylpiperazin-1-yl)-2-oxoacetate once the chlorophenyl group has been substituted for an oxamic ester.

Given that there was literature precedent for bacterial LDH inhibitors (Choi, S., *et al*, 2007) that were oxamic esters and acids derivatised with N-benzyl piperazine, it seemed that a sensible approach would be to synthesise a series of analogues of oxamic N-benzyl piperazines where the hit compounds' N-phenyl substituent made way instead for an oxamic acid or ester.

Firstly, N-benzyl piperazine on its own was tested at a range of concentrations to determine whether there was any inhibitory effect from underivatised molecule (**Fig 6.18**). As can be seen, there is no dose-response relationship with N-benzyl piperazine.

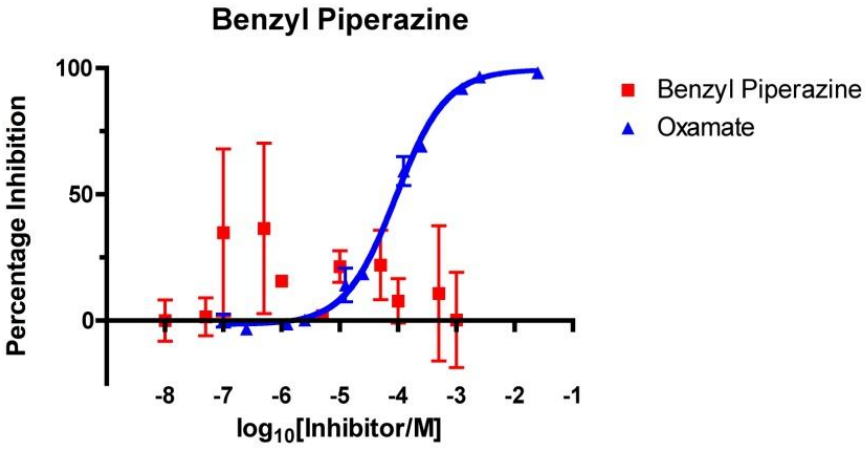

Figure 6.18: [A] N-benzyl piperazine has no inhibitory effect on LDH-A

The strategy taken was to select a range of derivatised N-benzyl piperazines alongside similarly derivatised N-phenyl piperazines to determine whether the benzylic carbon was critical. The reference compound in this regard was ethyl 2-

(4-benzylpiperazin-1-yl)-2-oxoacetate which is represented in the active-site in **Figure 6.19**.

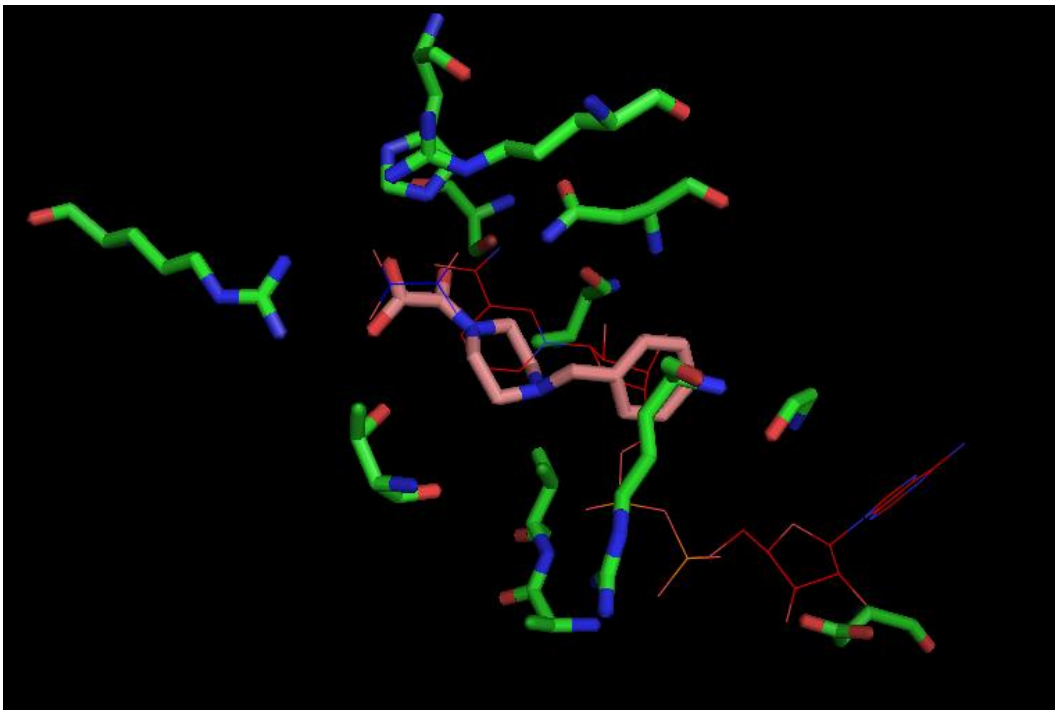

Figure 6.19: ethyl 2-(4-benzylpiperazin-1-yl)-2-oxoacetate modeled in the active site of LDH-A overlain on oxamate and NADH (thin wire model).

What is of note is that the oxamic group lies roughly where oxamate lies with the two ring systems of the N-benzyl piperazine coinciding with the ring systems of the nucleotide cofactor. This suggests that the right substituents in the right place could markedly improve the affinity of any small molecule and would militate towards an approach to probing SAR that varies ring substituents as much as possible.

With this in mind, a range of amines were selected to generate a comprehensive SAR picture. The full range is shown in **Figure 6.20**.

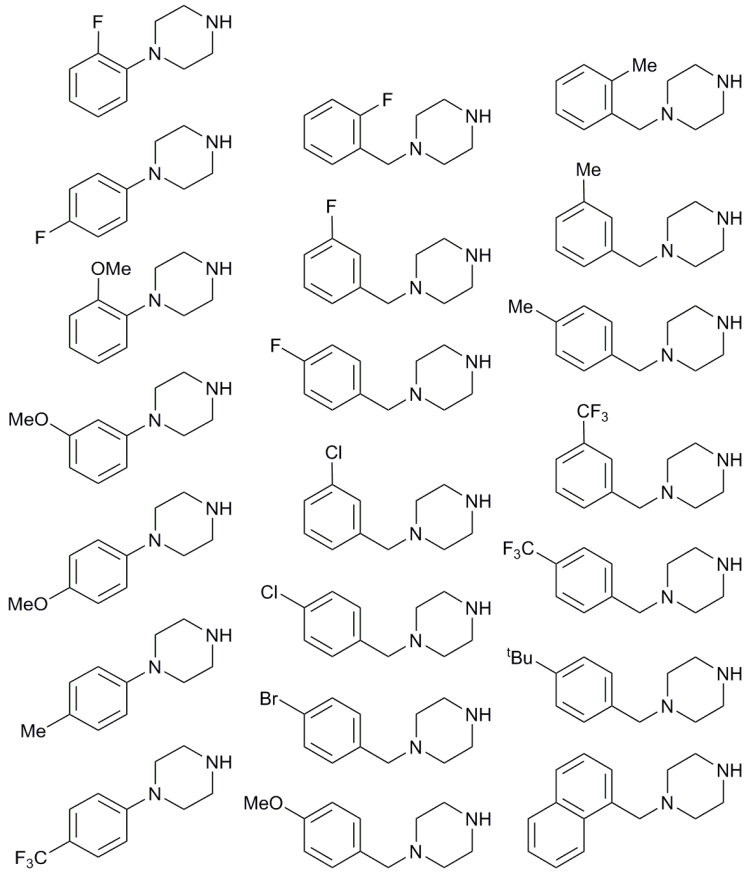

Figure 6.20: a range of differently substituted phenyl and benzyl piperazines.

The range encapsulates the range of steric and electronic differences amongst the substituents attached to the benzene ring. Halogens, alkyls, alkoxy and tri-fluoro groups were selected at *ortho*, *meta* and *para* positions so that as well as modifying the basic steric profile of the molecule, there would also be a change in the charge dispositions. Taken together, this was deemed to be a strategy that would best offer insight into a comprehensive structure activity relationship.

With the amines selected, the formation of the amide bond from the amine and the oxamic ester was relatively easy, as outlined in **scheme 6.4**.

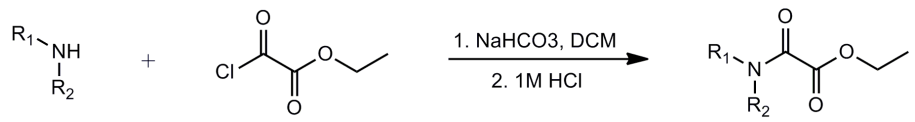

Scheme 6.4: the synthesis of derivatised oxamic esters.

The amines initially formed are outlined in **Figure 6.21** and their respective dose-response curves are represented in **Figure 6.22**. As can be seen, the results were disappointing. Further work needs to be undertaken to identify a way to cleave the ester to the acid, as this may be providing a steric obstacle. Unfortunately, methods used to date have only succeeded in cleaving the amide bond and returning the original starting materials.

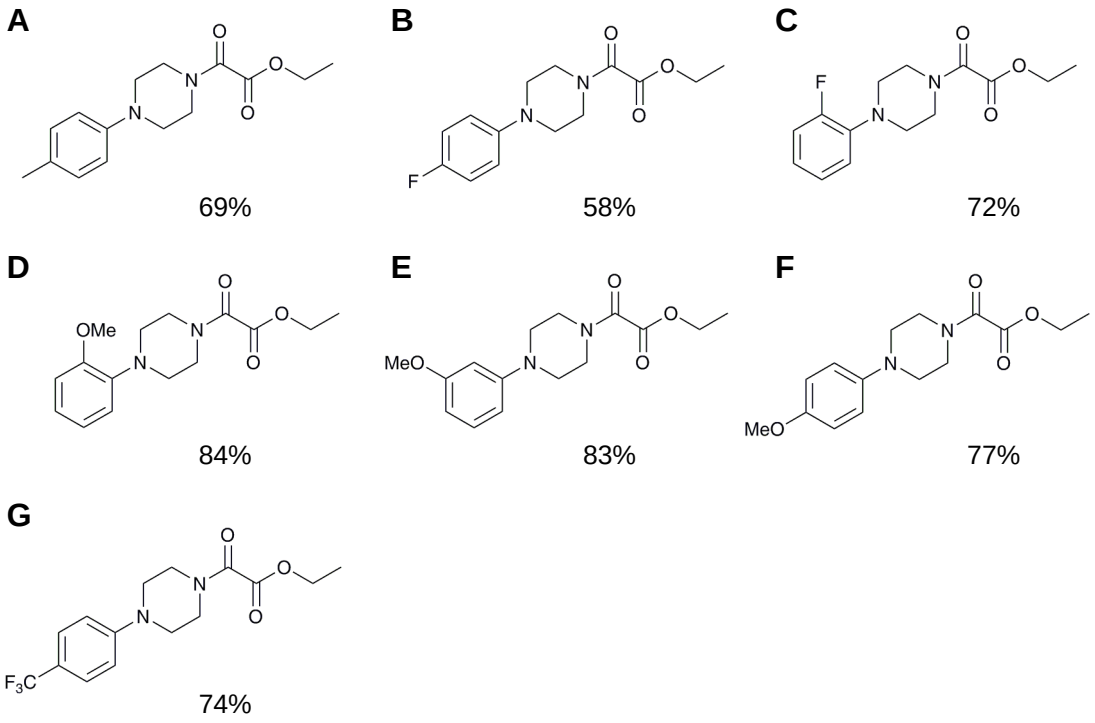

Figure 6.21: Oxamic esters synthesized and yields obtained: [A] (Ester A); [B] (Ester B); [C] (Ester C); [D] (Ester D); [E] (Ester E); [F] (Ester F); [G] (Ester G).

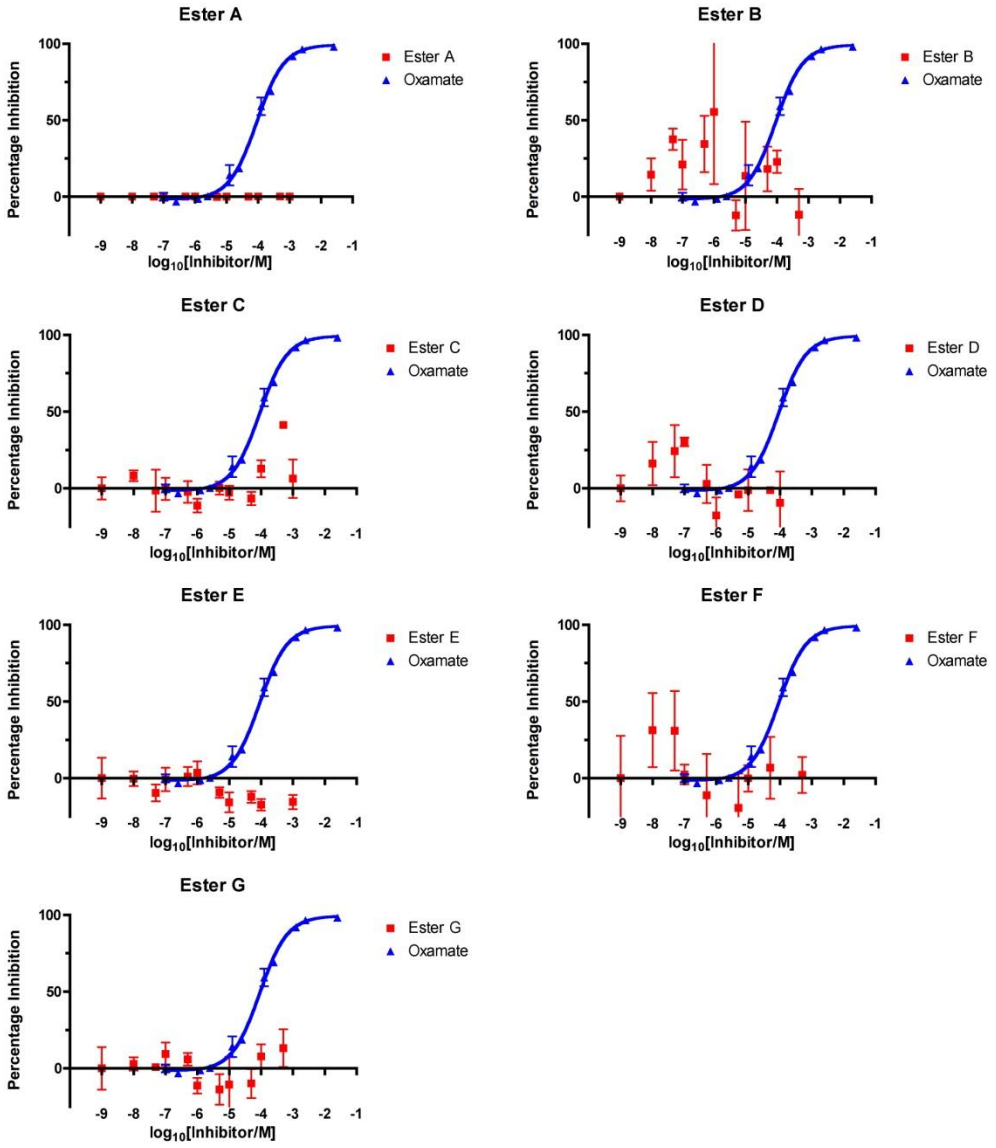

Figure 6.22: Esters A-G do not return a dose response relationship in terms of LDH-A inhibition.

6.2.6: FX11, A REPORTED LDH-A INHIBITOR, DISPLAYS NON-SPECIFIC CYTOTOXICITY

Given the slow pace of progress in generating a novel small-molecule inhibitor, FX11 (3-dihydroxy-6-methyl-7-(phenylmethyl)-4-propylnaphthalene-1-carboxylic acid), a reported (Yu, Y., *et al*, 2001) low concentration inhibitor was obtained and tested (**Figure 6.23**) to give an indication of the spectrum from poor inhibitor to strong inhibitor and also to carry out some preliminary work in cell culture to ascertain whether the assay data was transferable to another model. As can be seen in the figure, FX11 is a more potent inhibitor of LDH-A than oxamate with an IC_{50} of 1.8μM.

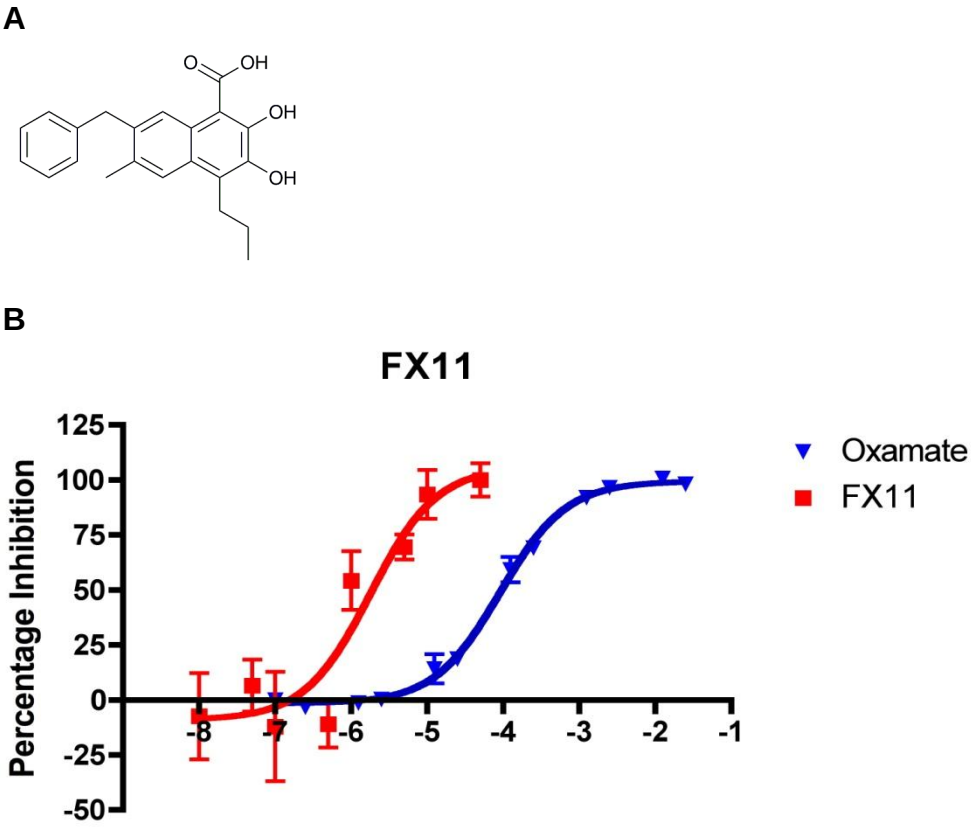

Figure 6.23: [A] FX-11 a reported LDH-A inhibitor [B] demonstrates greater potency (IC_{50} = 1.8μM) than oxamate against LDH-A.

To validate whether activity of FX-11 in cells was specifically related to its reported LDH-A inhibition, a simple dose-response experiment was conducted in a proliferation assay in MCF7 cells where LDH-A had been knocked down. Interestingly, whilst the cell-free assay data demonstrated that FX-11 is a highly potent LDH-A inhibitor, the cell data suggests that FX-11's cytotoxicity is in large part due to non-specific effects, with the IC50 falling from 76 μM to 26 μM when LDH-A is knocked down.

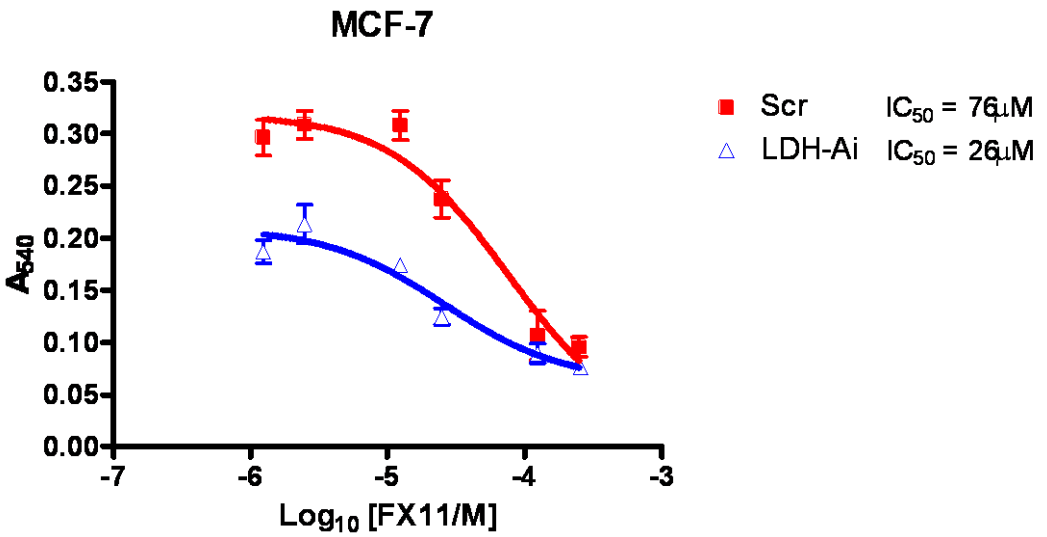

Figure 6.24: FX-11 a reported LDH-A inhibitor suppresses proliferation in an SRB assay beyond that of siRNA LDH-A knockdown. N=1

6.3 Discussion and future work

Organic synthesis is a painstaking and time-consuming process and unfortunately no novel small-molecule inhibitors of human LDH-A have yet been discovered.

Given the specific issues surrounding furazan synthesis, work is now being undertaken to identify other routes to heterodiazole rings and also other structural classes that may offer yet more potent inhibition of LDH-A. Again, literature precedent would suggest that varying the heteroatom in the ring between the two nitrogens can be done without impacting heavily on inhibition.

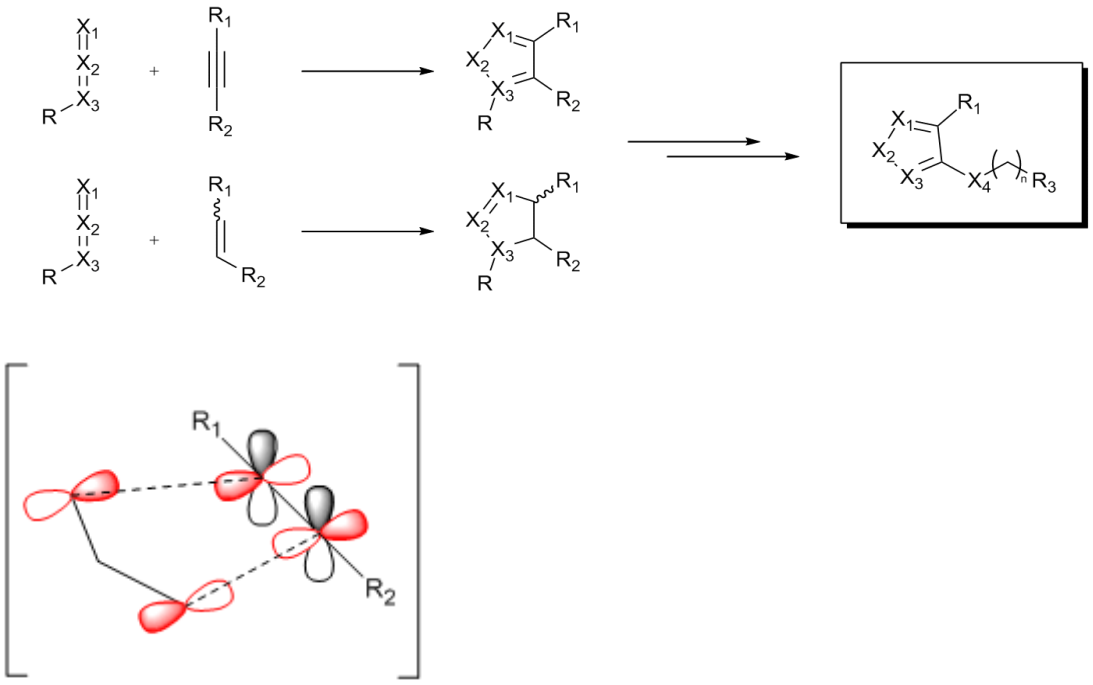

Scheme 6.5: 1, 3 dipolar cycloadditions can be used to generate substituted heterodiazoles.

Chief amongst other azole ring systems with potential applicability to the search for novel human LDH-A inhibitors are the triazoles which can be synthethised rapidly using functionalized alkynes (**Scheme 6.5**) (Huisgen, R., 1984) via a 1,3

cycloaddition that can be done in one pot. The advantages and potential novel applications of this approach are vast and an independent project is now under way to deal with them in depth. Future work in this regard should focus on methods to generate a library of heterodiazoles in order to probe the structure activity relationship of this class of compounds.

The lack of inhibitory potential of the oxamic esters is disappointing. However, work needs to be undertaken to synthesise the remaining compounds from the initial amine batch and to further cleave the esters to their corresponding acids.

Interestingly, the data for FX11 shows that whilst a compound may demonstrate impressive LDH-A inhibition in a cell free assay, that any cytotoxicity in cell culture can arise from completely non-specific inhibition.

Moving forward then, the strategy adopted is broadly right. However, identifying a small-molecule inhibitor will require drawing even further on the patience and perseverance of the investigator. In short, efforts to synthesise a highly active LDH-A inhibitor are likely to be measured in years rather than months.

CHAPTER 7: FINAL DISCUSSION

7.1: OVERVIEW

This thesis started with three aims:

1. to validate LDH-A inhibition and elucidate its full nature in terms of the implications for tumour survival.

2. to ascertain the role of LDH-B in order to determine whether selectivity towards LDH-A would be a necessary feature of any small molecule inhibitor.

3. to recapitulate siRNA mediated LDH-A inhibition with small molecule inhibitors that have the potential for clinical application.

In terms of these aims then, the following can be briefly stated. Firstly, LDH-A inhibition is now better understood to have a therapeutically useful effect on the survival and proliferation of breast cancer cells *in vitro*. Secondly, the role of LDH-B remains indeterminate; however, the reason for investigating LDH-B in parallel to LDH-A was to determine whether selectivity was required for inhibitors of LDH-A. Significantly, the data suggests that selectivity will not be a critical issue as LDH-B inhibition has marginal effects on growth. Lastly, work has begun on several classes of compound that possess the potential to be developed into high efficacy inhibitors.

7.2: TUMOUR METABOLISM REAPPRAISED

When work started on this thesis, the paradigm in which cancer biology operated was defined by Hanahan and Weinberg's seminal 2000 paper which identified six hallmarks of cancer (Hanahan, D., *et al*, 2000). Since then, several fields have asserted their claim to be researching the 'seventh hallmark' (Colotta, F., *et al*, 2009) (Yeung, S.J., *et al* , 2008), as if this label would lend added credibility to any work beyond its intrinsic scientific value.

Ultimately, Hanahan and Weinberg have returned to their original paper and revised it, adding several new 'hallmarks' of which reprogrammed tumour metabolism is one. Whether this new interpretation complicates rather than refines the picture is beyond the remit of this thesis to comment upon. The important point is not that scientists in a review believe tumour metabolism to be more important than it was previously, but that rather the increased interest in the field has lead to a greater breadth and depth of inquiry that has uncovered data that points to the importance of altered metabolism to tumour cells.

Warburg initially postulated that elevated aerobic glycolysis arose due to mitochondrial defects and was a necessary component of oncogenesis (Warburg, O., 1956). Whilst the mitochondria in transformed cells are silenced they remain competent and the role of altered metabolism in oncogenesis has not been revealed (regardless of its inclusion in a new list of hallmarks) it is interesting that Warburg's initial idea, having since been seemingly discredited, was not too far off the mark. So whilst the mitochondria remain competent, this thesis demonstrates that there is a definite benefit for transformed cells in down-regulating OXPHOS.

7.3: INCREASED TUMOUR LDH-A ACTIVITY CONFERS SEVERAL ADVANTAGES

More specifically, LDH-A inhibition can now be described as having an effect on tumour survival that is predicated upon its role in determining the fate of pyruvate. Whilst previous studies have suggested that a Warburg phenotype arises due to the greater biosynthetic requirements of transformed cells(DeBerardinis, R.J., *et al* , 2007) or because the increased extracellular acidity associated with elevated glycolysis promotes invasion (Gattenby, R.A., *et al*, 2004), the data in this thesis, along with recently published work (Le, A., *et al*, 2010) suggests that diverting pyruvate through LDH-A and away from the mitochondria confers a survival advantage by reducing oxygen consumption, and by corollary ROS production. An emerging picture seems to be developing then of LDH-A playing an integral role in reducing cellular oxidative stress.

That transformed cells could also be benefiting from the greater biosynthetic capacity and extracellular acidity is not within the remit of this thesis. In the case of the former, greater carbon flux into the pentose phosphate pathway will be attributable to the up-regulation of proteins well upstream of LDH-A; whilst greater biosynthetic capacity will benefit proliferating cells, this in itself does not point to a role for LDH-A as this upstream flux could be upregulated with OXPHOS remaining the primary means of ATP generation. With the latter, the effect of greater lactic acid production is not the primary benefit of greater LDH-A activity; besides, there is significant evidence that the bulk of extracellular acidity derives from carbonic acid.

Amongst this it is important to note that whilst OXPHOS is significantly down-regulated in aerobically glycolytic cells indicative of reduced ATP-sythase proton transport, the TCA cycle (and thereby the broader biosynthetic role of the mitochondria) remains largely intact. This is unsurprising as TCA cycle intermediates are critical for lipid synthesis. However, as pyruvate is being trafficked away from the mitochondria, there must be other sources of carbon to feed the TCA cycle. Evidence would suggest that glutamine provides the bulk of this carbon (Vander Heiden, M.G., *et al*, 2009); up to 60% of this glutamine is further converted to lactate, signalling a critical role for LDH-A as a chokepoint for several processes.

Bioenergetically, flux through LDH-A is important as it permits a cell to down-regulate OXPHOS and therefore reduce the oxidative stress it is under. Bioreductively the pyruvate to lactate reaction is one of the few sources of NAD^+ in the cell which permits other processes to continue in the absence of other sources if oxidative intermediates. Finally, biosynthetically, elevated LDH-A activity provides a means of clearing excess pyruvate, the accumulation of which is toxic (Thangaraju, M., *et al*, 2009).

Pulling these threads together it is therefore possible to see why attenuating LDH-A expression using siRNA had such a dramatic effect on growth. The reduction in proliferation as measured by ki-67 expression; the reduced tumour spheroid volume; the increase in cell death; and the increase in oxygen consumption when LDH-A is knocked down: all are likely to derive from pressures being brought to bear on the bioenergetic, biosynthetic, and bioreductive capacity available to the cell. Specifically, LDH-A knockdown depletes ATP whilst increasing oxygen

consumption; this points to an intolerance to the ROS that elevated OXPHOS generates as ordinarily mitochondrial respiration is produces significantly more ATP. It is therefore this intolerance to ROS that is triggering programmed cell death.

The most interesting observation was the dependence of lactate-fuelled tumour growth on LDH-A rather than LDH-B as previously thought. This adds an additional incentive to inhibiting LDH-A as impeding the ability to oxidise lactate is likely to impact on the capacity of a tumour to grow beyond a certain size.

7.5: FUTURE DIRECTIONS

In order to better determine the interplay between all of these factors there are several lines of inquiry any future investigator should pursue.

Firstly, a significant impediment to the range of experiments available was to lack of a stable knockdown. During the course of the thesis attempts were made using both retroviral and lentiviral systems that were either constitutive or inducible with limited success. The extent to which LDH-A knockdown diminishes growth precludes the use of a constitutive knockdown- work surrounding this was impeded by the large fraction of cells that died post-transfection.

Work then must focus on creating a stable inducible construct; even in the time since such attempts were made the technology has been refined and as a result has become far more robust and less prone to the accumulation of plasmid secondary structure and other issues that marred initial attempts. Besides these steps forward, there are significant benefits to an inducible approach, such as controlling

the point at which LDH-A is down-regulated *in vivo* that makes the extra effort worthwhile; *in vivo* work is certainly a necessary next step for understanding how LDH-A inhibition works in the context of a whole organism.

Beyond *in vivo* work, significant information could be gleaned by using spectroscopic techniques to probe metabolic flux beyond the sampling of cultured media at discrete endpoints used to date. Precedent now exists for using either mass spectroscopy or NMR to monitor and model changes in carbon flow (Wiechert, W., 2001) and two experiments in particular stand out as being worthwhile.

Firstly, using predesigned matrices it is possible to model carbon flux by assigning specific vector values to the key reactions of glycolysis, glutaminolysis, the pentose phosphate pathway and the TCA cycle (Forbes, N.S., *et al*, 2006). Whilst this is a more fundamental approach, combined with an LDH-A knockdown would give insight into how inhibiting LDH-A affects carbon flux, specifically whether there is an accumulation of any metabolites or, indeed, whether the potential exists for cells to bypass the effects of LDH-A knockdown over time. Mass spectroscopy or NMR have been used to collect the necessary data to input into the flux matrices; the predominant disadvantage of using mass spectroscopy is the sheer number of cells required to generate a sufficient pellet whilst any NMR technique will undoubtedly require the enrichment of the cells, media and any buffers/solutions with ^{13}C.

Secondly, a collaboration has recently been entered in to in order to utilise existing hyper-polarised NMR techniques (Schroeder, M.A., *et al*, 2009). This approach usesmicrowaves to hyperpolarise pyruvate (thereby overcoming the problem with

traditional ^{13}C NMR in that it does not provide quantitative spectra) which can then be injected into an animal and monitored, or isolated perfused heart which itself provides a powerful technique for quantifying any cardiotoxicity arising from LDH-A knockdown. This is a particularly elegant way of combining *in vivo* work and monitoring changes in metabolic fluxes.

A stable LDH-A knockdown might also shed light on the function on LDH-B; for example, attempts at a double LDH-A/LDH-B knockdown have foundered to date as a reasonable transfection efficiency cannot be achieved without significant non-specific effects.

Lastly, the mechanism of lactate-fuelled tumour growth, and its dependence upon LDH-A, would be conclusively verified by performing oxygen consumption experiments. Specifically, these experiments would be able to monitor, in real time, whether the addition of lactate leads to an increase in oxygen consumption in both LDH-A knock-down and control cell lines.

Taken together, these experiments constitute the next necessary steps in continuing an inquiry into the expression, function and activity of LDH-A with particular relevance to cancer.

7.6: THE ELUSIVE SILVER BULLET

In parallel, several steps forward have been taken towards the discovery of a small molecule inhibitor. Having moved on from an approach that favoured general cytotoxicity, drug discovery now focuses on rational drug design; a significant amount of time and effort is expended on research into finding new small molecule

inhibitors of defined biological targets. Nevertheless, the level of understanding of complex and intertwined molecular systems, whilst improving almost boundlessly, remains immature. Whilst this is more of a note of caution than pessimism, it must be in this context that any new agents are assessed.

In particular, despite a medicinal chemistry culture predicated on finding silver bullets, the reality is that both the tools used and the products generated remain blunt instruments. Alongside this, a broader shift in technology is taking place where biological molecules such as antibodies and peptides are becoming both cheaper to develop and easier to deliver, putting pressure on medicinal chemists whose small molecules will never be able to compete with the selectivity of biologicals.

That notwithstanding, small molecule therapies will remain more versatile, more deliverable, and more cost-effective for some time to come. With that in mind, what utility will an LDH-A inhibitor have in a clinical context?

Firstly, it is important to note that as this thesis has shown, LDH-A is upregulated in a broad range of cancers. Not only this but transformed metabolism, specifically increased aerobic glycolysis is a feature of many tumours. The points considered, LDH-A inhibition looks like an attractive option for killing transformed cells.

What barriers must be overcome then to develop an inhibitor of LDH-A? What strengths has this thesis identified that enhance the chances of designing a highly potent LDH-A inhibitor? Firstly, potential inhibitors remain in several structural classes; this structural diversity provides a great strength as the potential for exhausting possible leads is reduced. Furthermore, a common theme across these

structural classes is that the synthesis is pretty non-complex. This in turn allows a range of derivates to be quickly synthesised (and tested) and a fuller SAR picture to be developed. With the chemical space containing an estimated 10^{64} possible drug-like molecules (Bohacek, R.S., *et al*, 1996) the search for a high potency inhibitor remains much like finding a needle in a haystack. However, the screen is robust and easy to perform, permitting a quick feedback in the synthesise-screen-derivatise- rescreen loop, which in combination with the previous points at least makes the haystack smaller and gives the investigator a magnet. Whilst the end process might not produce a silver bullet, there is a significant chance of generating an agent that either sensitizes cells to other agents or synergises with other treatments.

7.7: A WINNING COMBINATION

In the end then, LDH-A inhibitors are likely to find the greatest utility when used in combination with other agents. This approach could either seek to reinforce a single effect, or act at several pressure points in a cell. In either case, the desired aim would be to reduce the dosage of any single agent and therefore reduce side-effects (and any compliance issues).

Firstly, given that LDH-A inhibition increases oxidative stress (Le. A., *et al*, 2010), co-treating with a DNA-damaging simple cytotoxic might have some use, as might radiation. This is because PARP activation and DNA damage depletes sources of NAD^+(Zong, W., *et al*, 2004) that are required for glycolysis which in turn will not be able to produce the ATP required to perform DNA repair.

Secondly, LDH-A inhibition depletes ATP and so co-treating a tumour with an LDH-A inhibitor and an ATP depleting agent is likely to have a strong combined effect. Indeed, this approach has been demonstrated as having some utility with other glycolytic inhibitors (Maschek, G., *et al*, 2004).

Finally, the possibility of co-administering glycolytic inhibitors with antiangiogenics has been mooted (Houston, S.K., *et al*, 2011). However, extensive work would have to be performed on this approach to validate it as it is unclear whether there would be a desirable synergy; LDH-A inhibition increase oxidative stress whereas an antiangiogenic reduces oxygen supply to the tumour making it more hypoxic and potentially able to sidestep the problem of ROS accumulation.

7.8: THE LAST WORD…

All told, significant progress has been made towards developing an increased understanding of the role LDH-A plays in maintaining tumour cells and the effect that inhibiting it has on proliferation and survival. A new role has been found for LDH-A in maintaining lactate-fuelled tumour growth and steps have been taken towards identifying structural classes of LDH-A inhibitors. The final question therefore, bluntly, is so what?

For many patients, cancer is no longer the death sentence it once was. This is in no small part due to the slow, iterative process of understanding the underlying biology and then refining treatments to match. Given the painfully slow progress on coming up with solutions to diseases where only one gene is defective, the reality of treating a disease where over a hundred mutations have occurred will

continue to be constrained by the number and type of agents available to target different specific pathways.

Our knowledge, whilst undoubtedly continuing to improve with each passing year, is likely to remain imperfect and incomplete. With this in mind, anything that increases or improves the toolkit available to the clinician to tackle individual tumours must be considered a worthwhile exercise.

APPENDIX A: FULL

IMMUNOHISTOCHEMICAL STAINING

KI67 – SCR

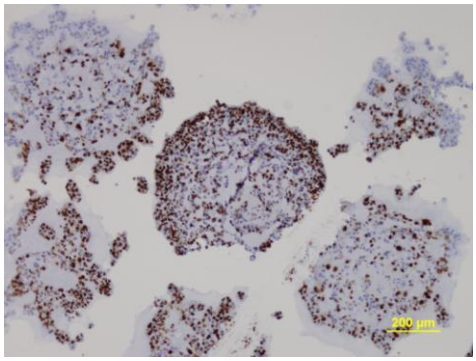

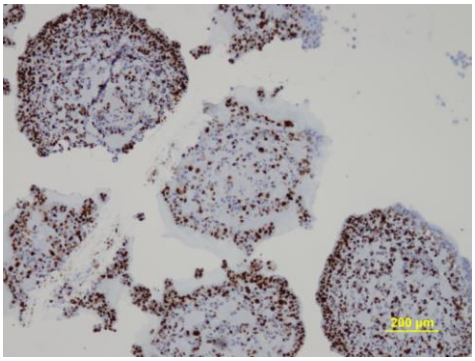

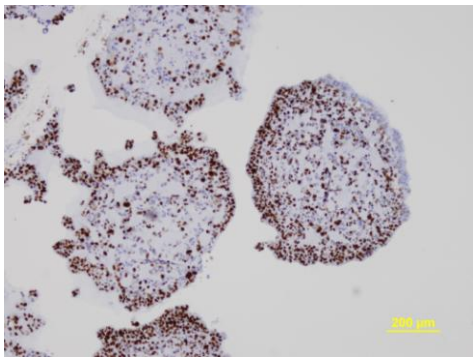

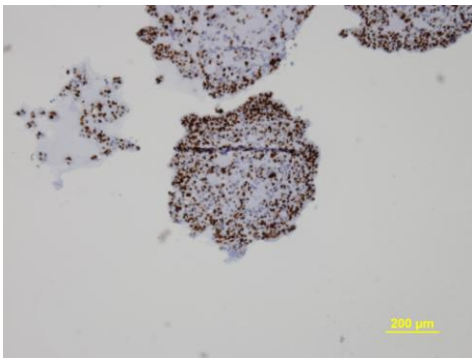

KI67 – LDH-A

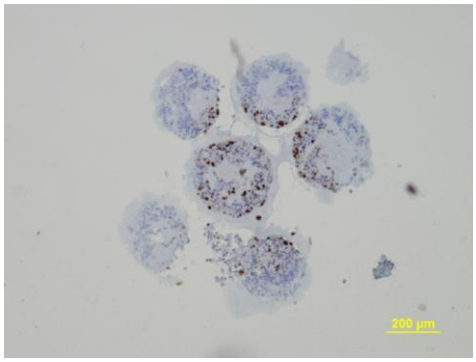

KI67 – LDH-B

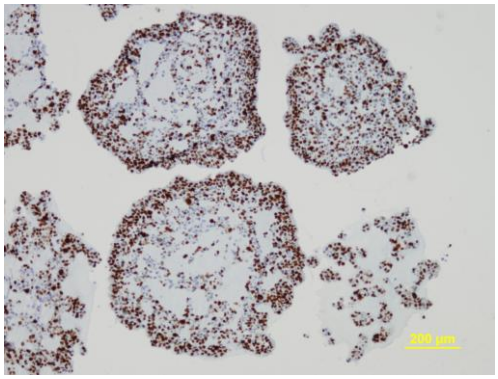

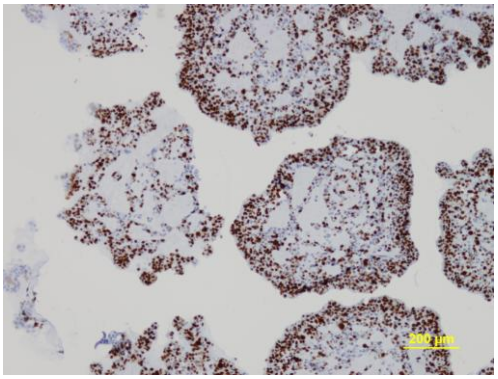

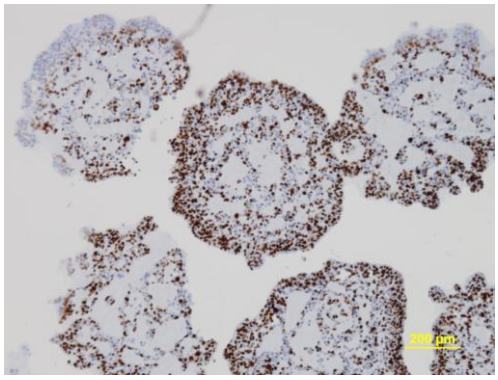

CLEAVED CASPASE-3 – SCR

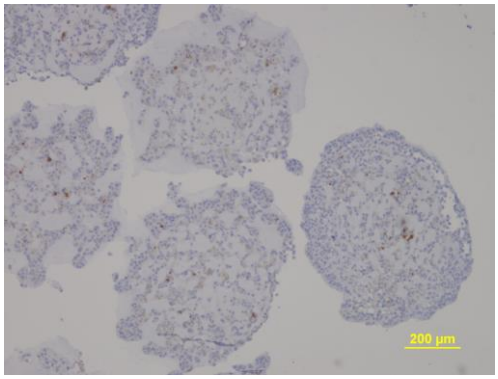

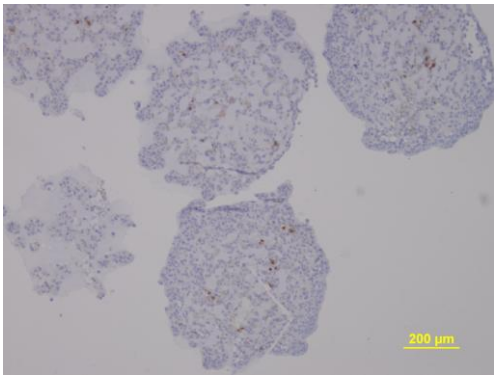

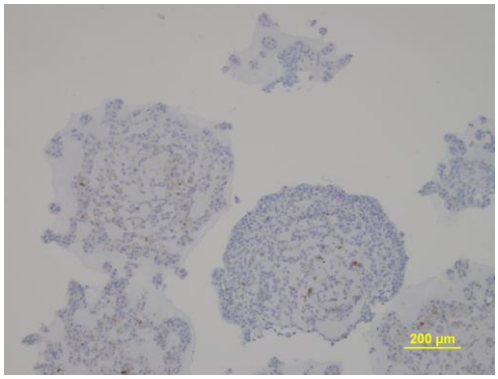

CLEAVED CASPASE-3 – LDH-A

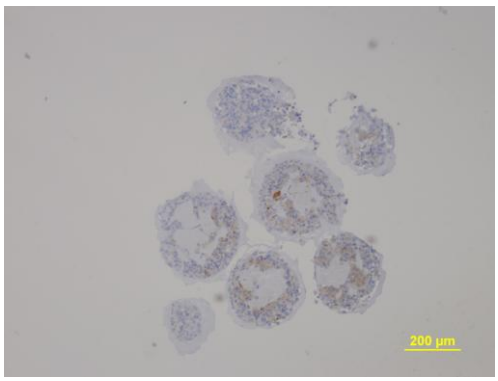

CLEAVED CASPASE-3 – LDH-B

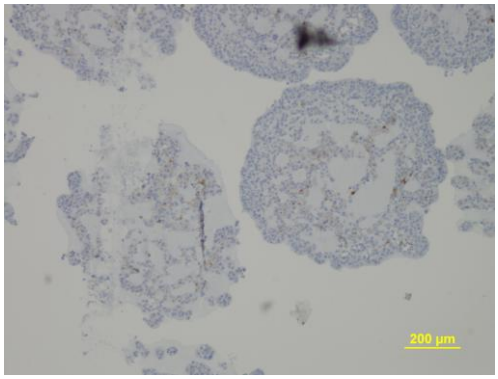

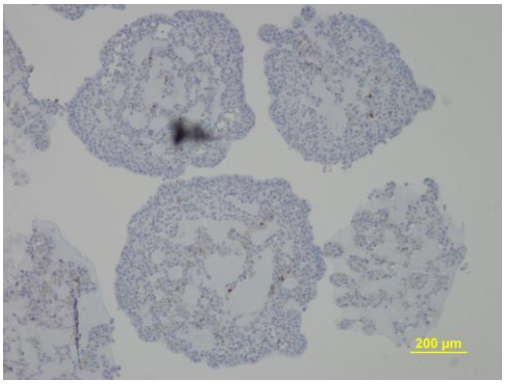

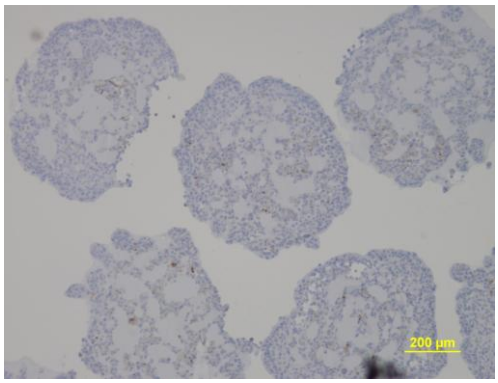

CA9 – SCR

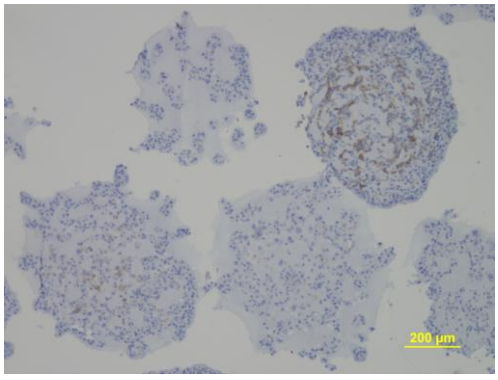

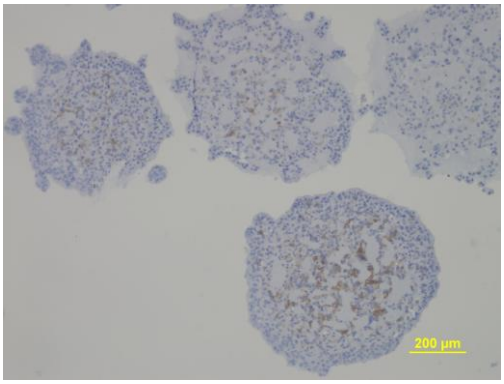

CA9 – LDH-A

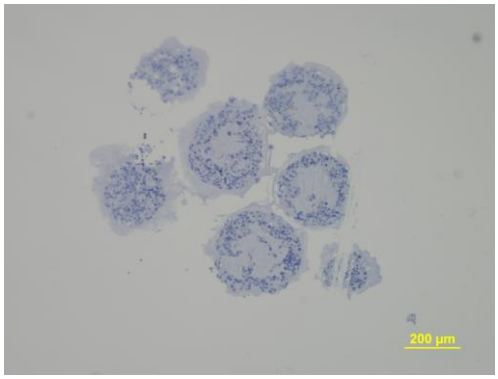

CA9 – LDH-B

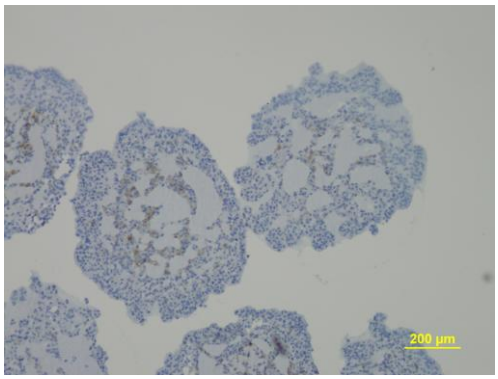

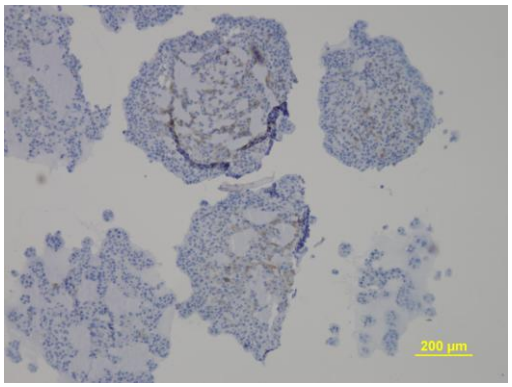

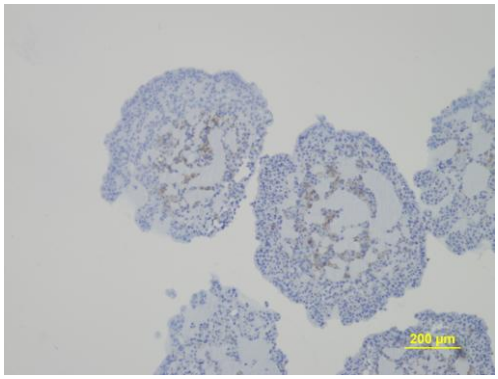

PIMO – SCR

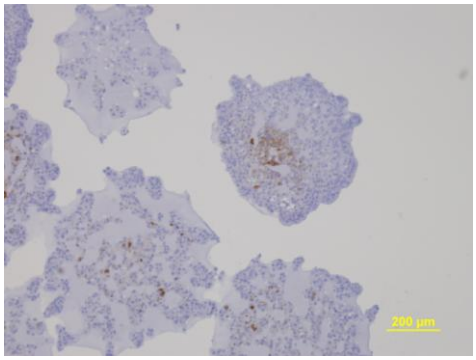

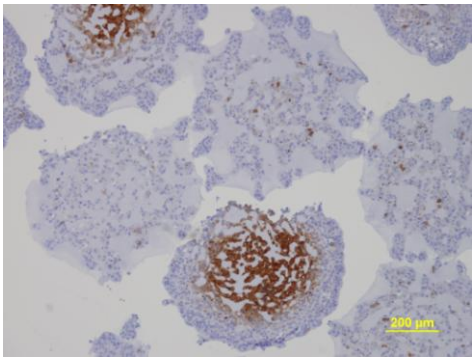

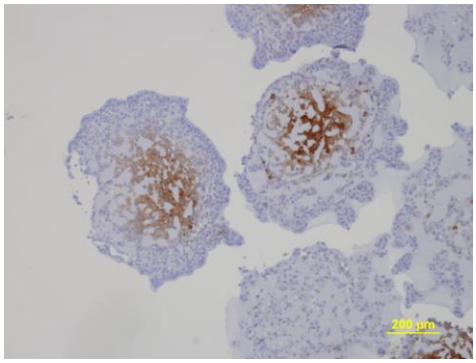

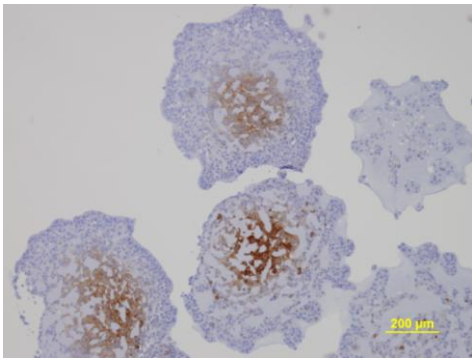

PIMO – LDH-A

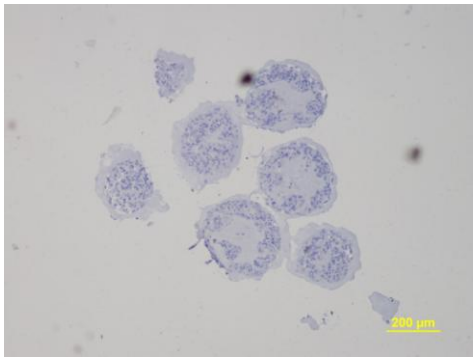

PIMO – LDH-B

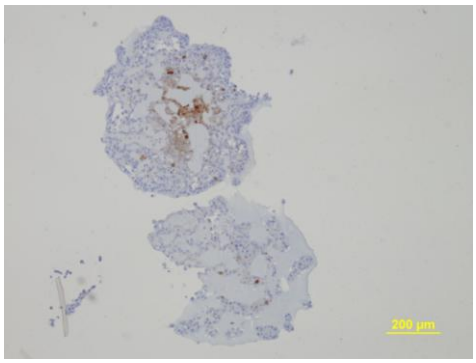

H&E – SCR

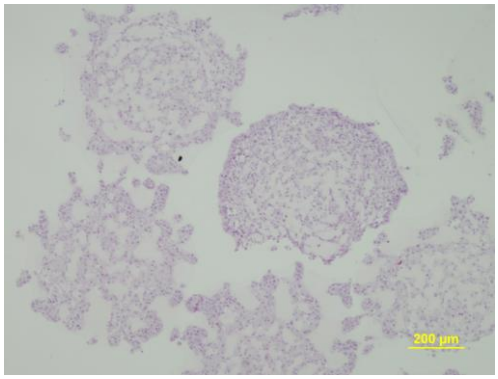

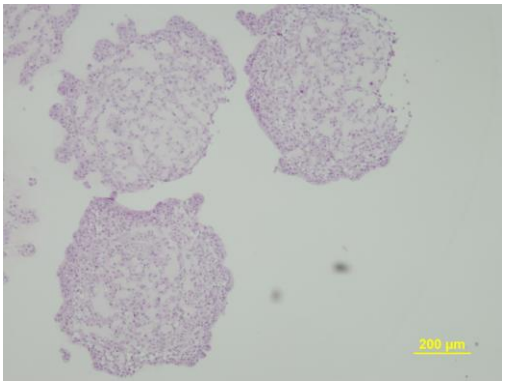

H&E – LDH-A

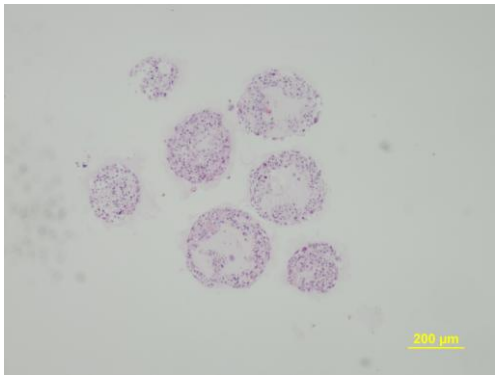

H&E – LDH-B

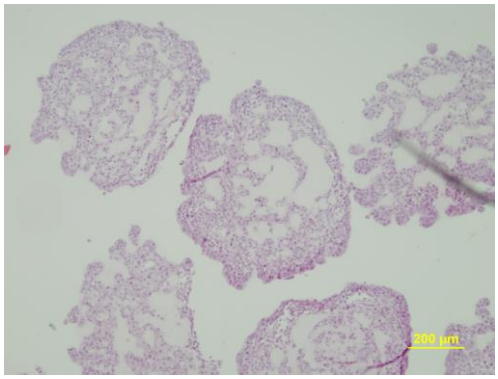

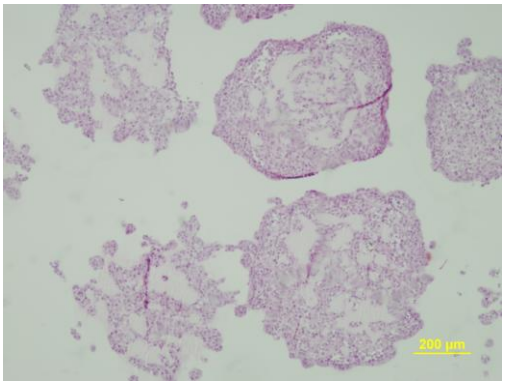

APPENDIX B: MITOPROT ANALYSIS ON LDH-A AND LDH-B SEQUENCES

MitoProt II - v1.101

Sequence name: LDH-A
Input sequence length : 332 aa

VALUES OF COMPUTED PARAMETERS

Net charge of query sequence	:	+3
Analysed region	:	5
Number of basic residues in targeting sequence	:	1
Number of acidic residues in targeting sequence	:	0
Cleavage site	:	**not predictable**
Cleaved sequence	:	

HYDROPHOBIC SCALE USED

		GES	KD	GVH1	ECS
H17	:	2.153	2.312	0.519	0.764
MesoH	:	-0.506	0.532	-0.342	0.233
MuHd_075	:	34.791	21.882	9.831	5.497
MuHd_095	:	14.951	19.713	4.653	4.968
MuHd_100	:	10.254	17.079	3.605	4.299
MuHd_105	:	5.224	12.777	3.007	3.235
Hmax_075	:	9.800	13.183	0.860	3.750
Hmax_095	:	0.612	12.425	-1.609	3.675
Hmax_100	:	0.000	8.400	-2.508	2.620
Hmax_105	:	-3.300	8.400	-2.638	3.010

PROBABILITY

of export to mitochondria: **0.0364**

MitoProt II - v1.101

Sequence name: LDH-B
Input sequence length : 334 aa

VALUES OF COMPUTED PARAMETERS

Net charge of query sequence	:	-6
Analysed region	:	5
Number of basic residues in targeting sequence	:	1
Number of acidic residues in targeting sequence	:	0
Cleavage site	:	**not predictable**
Cleaved sequence	:	

HYDROPHOBIC SCALE USED

		GES	KD	GVH1	ECS
H17	:	1.706	1.888	0.396	0.668
MesoH	:	-0.379	0.526	-0.308	0.257
MuHd_075	:	30.034	18.805	9.037	4.766
MuHd_095	:	13.020	16.402	3.951	3.928
MuHd_100	:	5.475	11.037	2.009	2.589
MuHd_105	:	3.391	5.390	0.658	1.249
Hmax_075	:	14.300	14.300	2.585	4.740
Hmax_095	:	-0.613	11.025	-1.835	3.255
Hmax_100	:	4.400	8.800	-0.486	3.270
Hmax_105	:	-3.500	8.800	-2.720	2.637

PROBABILITY

of export to mitochondria: **0.0460**

APPENDIX C: BACKGROUND ABSORBANCE OF LIBRARY COMPOUNDS

APPENDIX D: SMALL MOLECULE LIBRARY

APL001

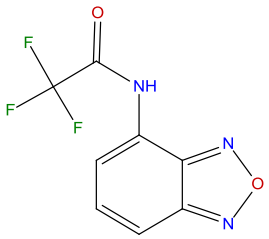

APL002

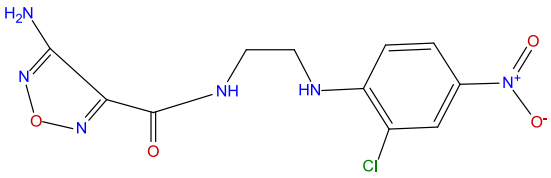

APL003

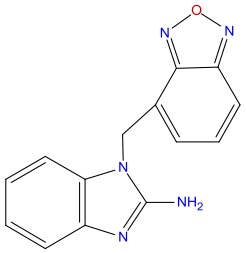

APL004

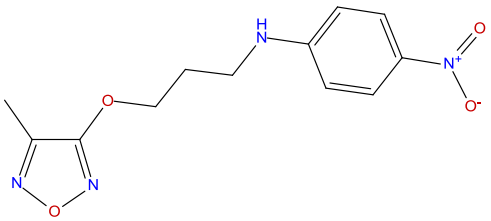

APL005

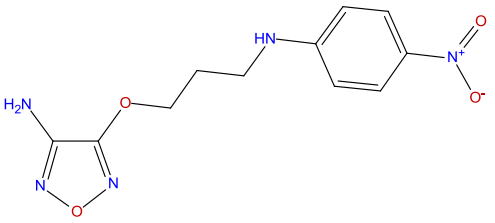

APL006

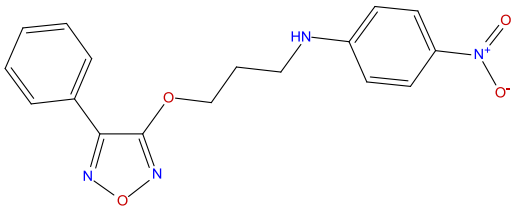

APL007

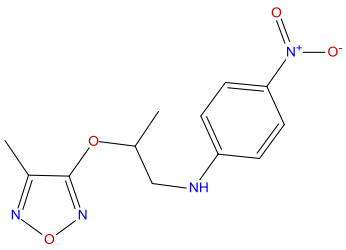

APL008

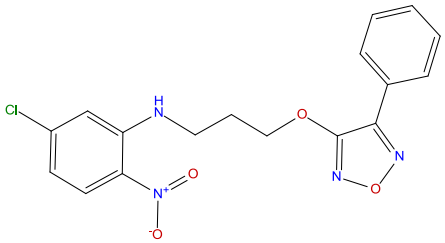

APL009

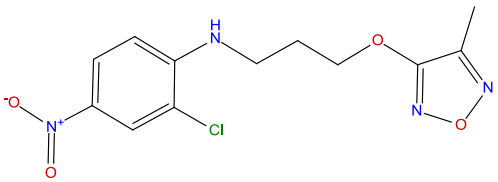

APL010

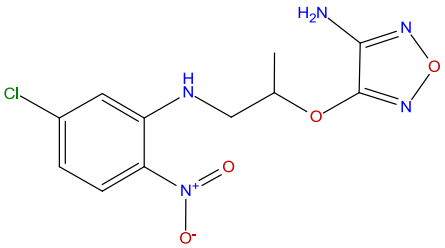

APL011

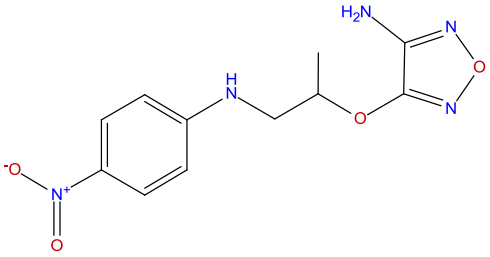

APL012 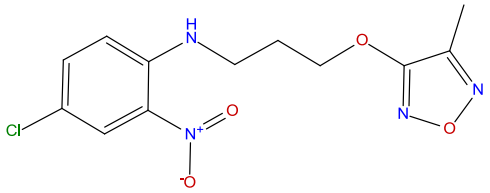

APL013 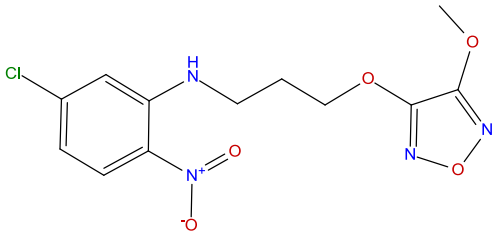

APL015 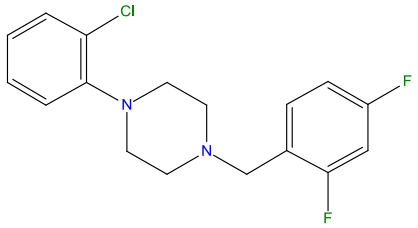

APL016 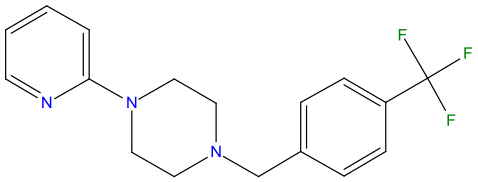

APL017 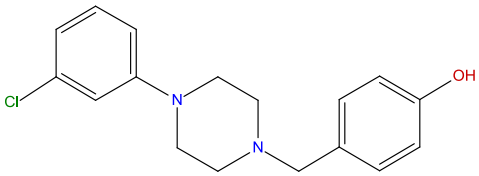

APL018 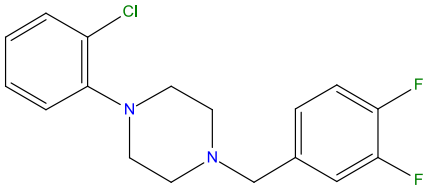

APL019 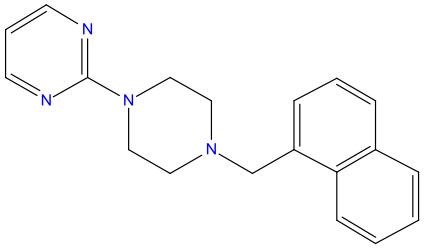

APL020 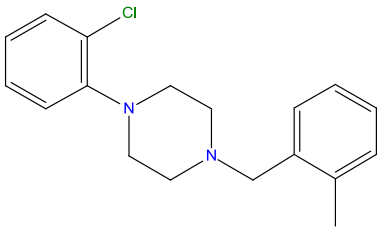

APL021 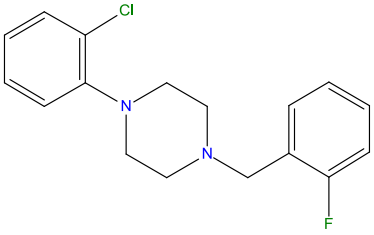

APL022 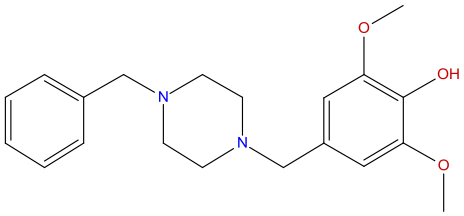

APL023 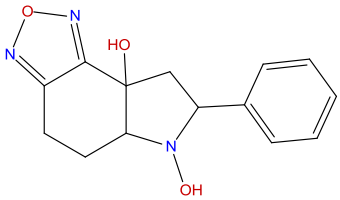

APL024 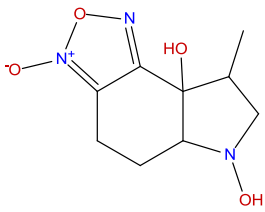

APL025

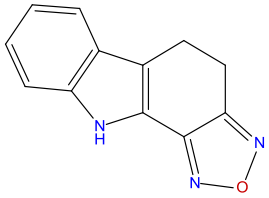

APL026

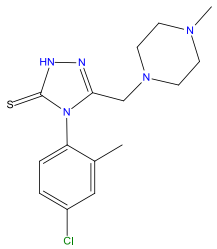

APL027

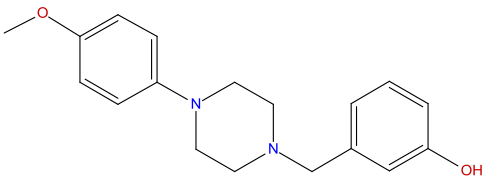

APL028

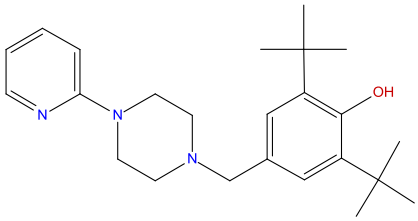

APL029

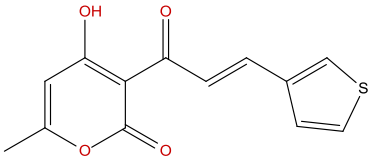

APL030

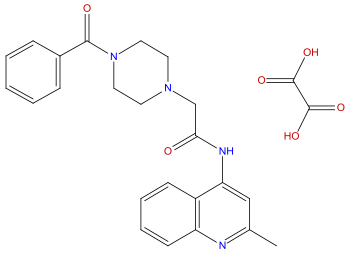

APL031 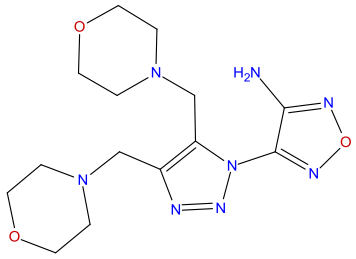

APL032 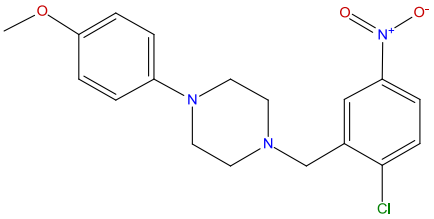

APL033 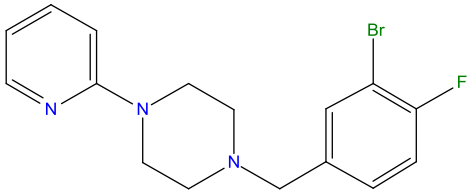

APL034 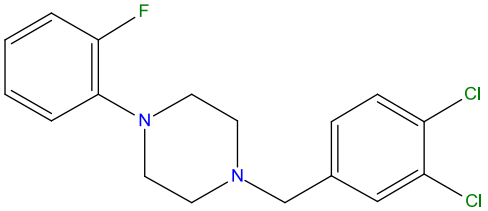

APL035 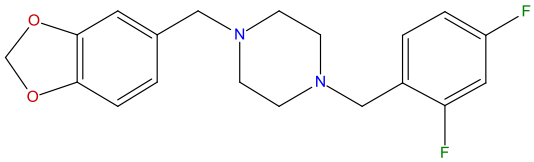

APL036 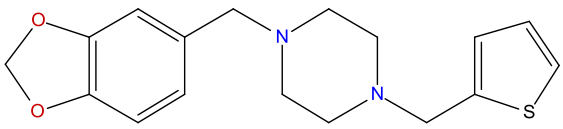

APL037

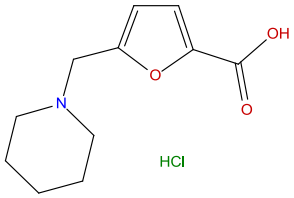

APL038

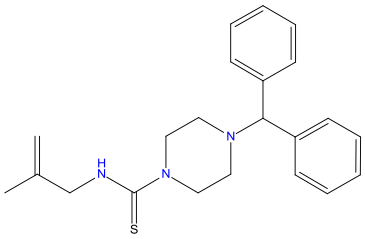

APL039

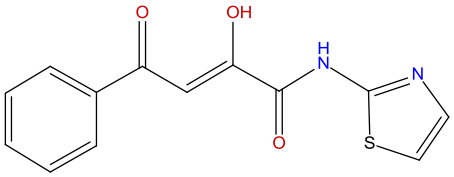

APL040

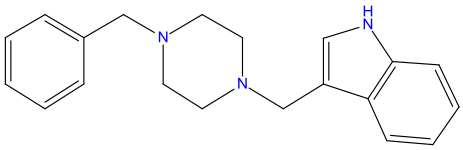

APL041

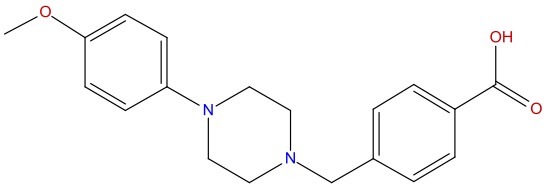

APL042

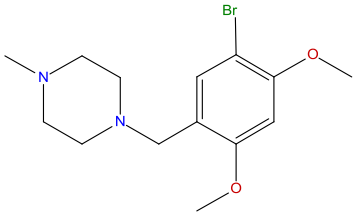

APL043

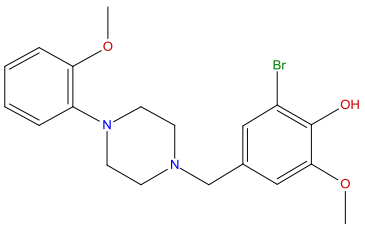

APL044

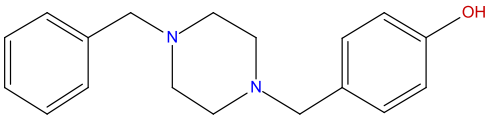

APL045

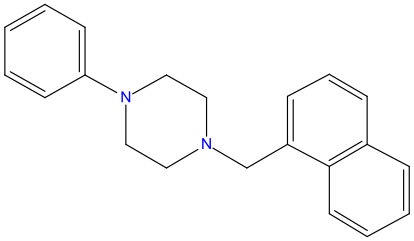

APL046

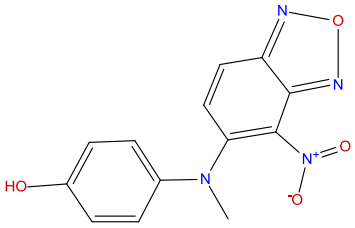

APL047

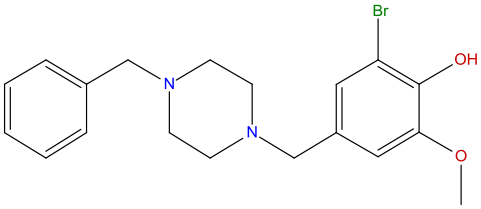

APL048

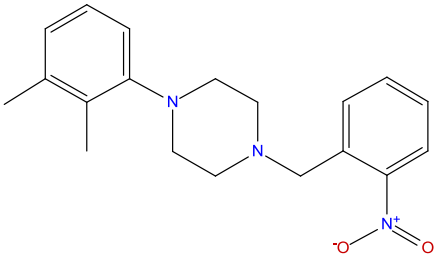

APL049 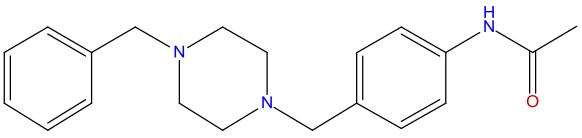

APL050 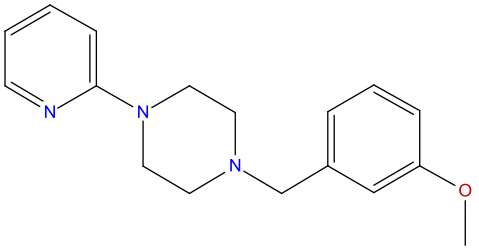

APL051 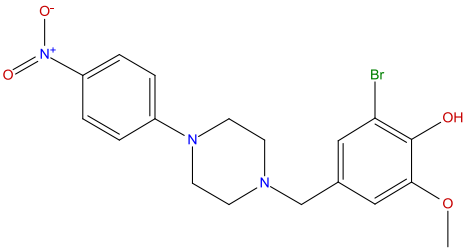

APL052 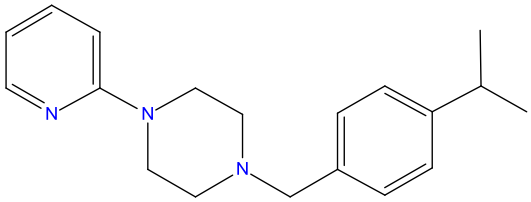

APL053 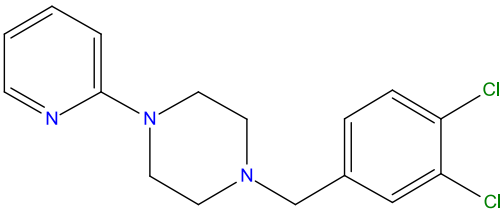

APL054 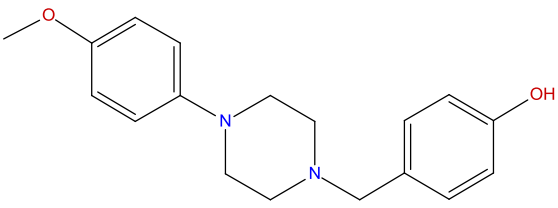

APL055 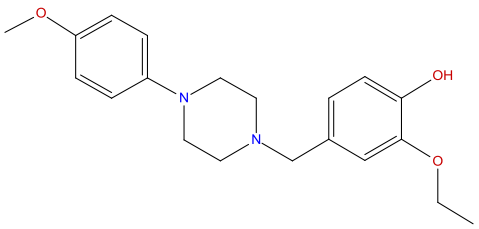

APL056 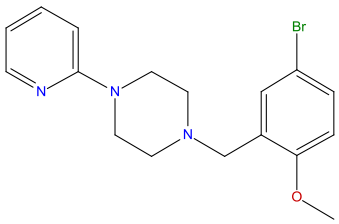

APL057 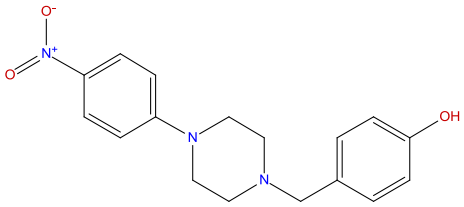

APL058 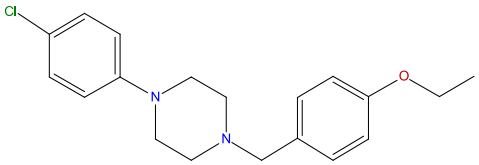

APL059 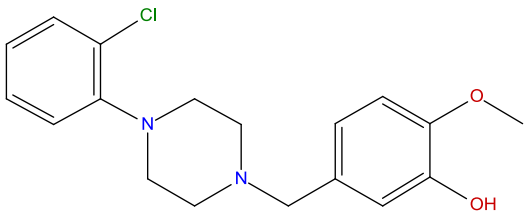

APL060 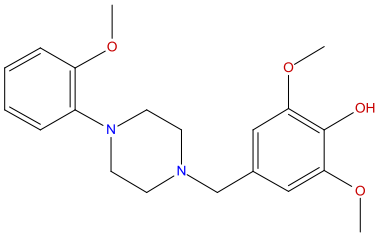

APL061 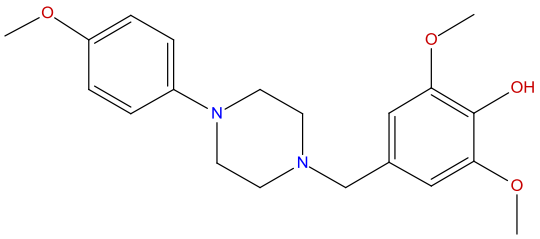

APL062 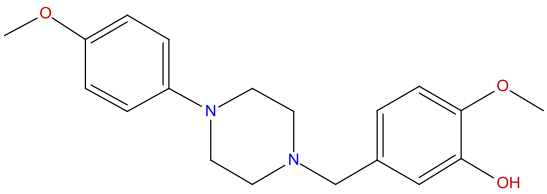

APL063 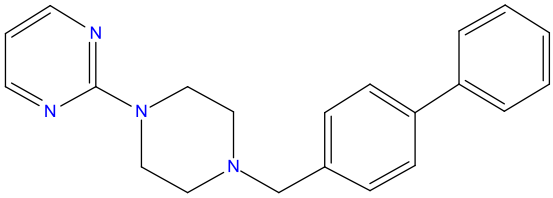

APL064 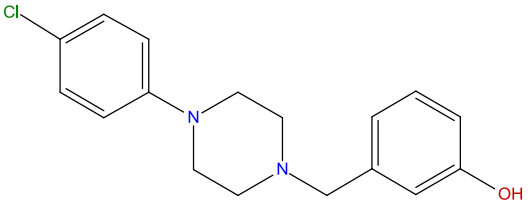

APL065 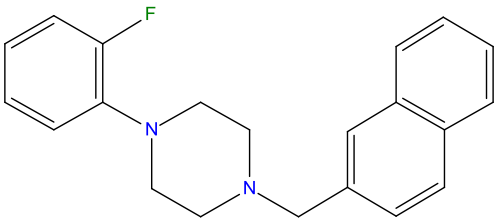

APL066 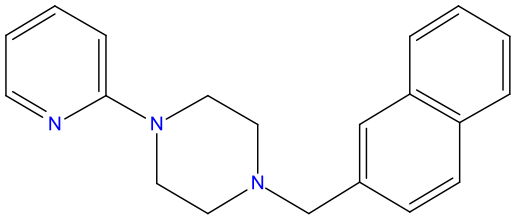

APL067 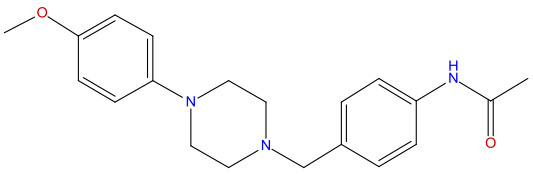

APL068 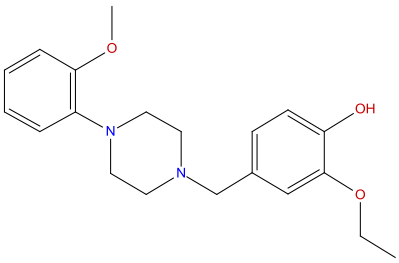

APL069 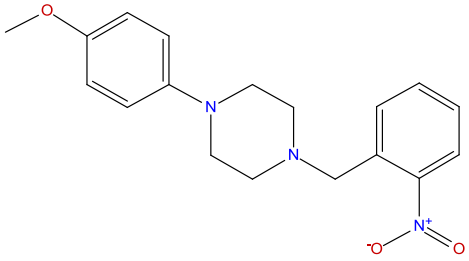

APL070 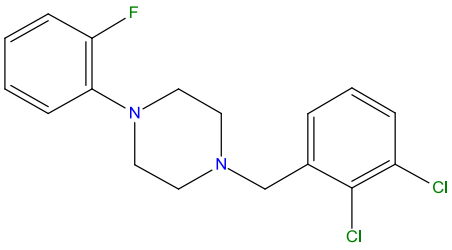

APL071 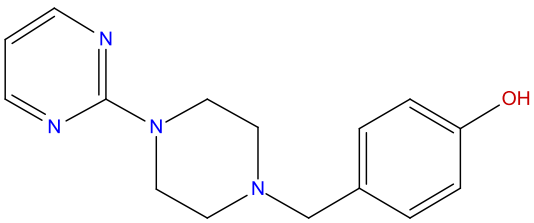

APL072 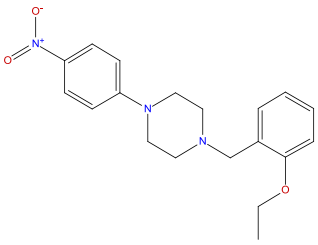

APL073 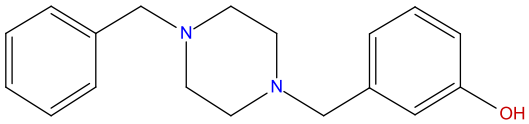

APL074 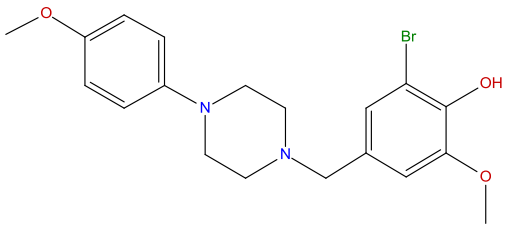

APL075 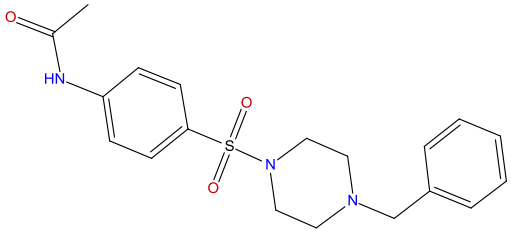

APL076 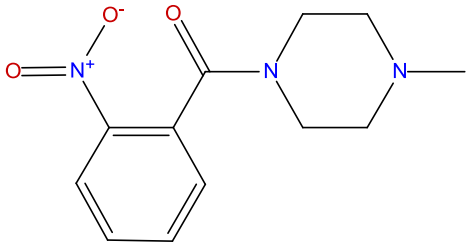

APL077 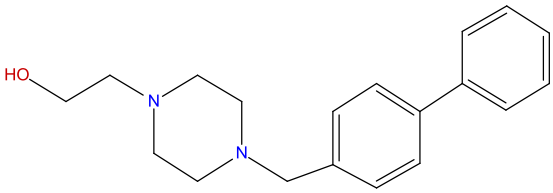

APL078 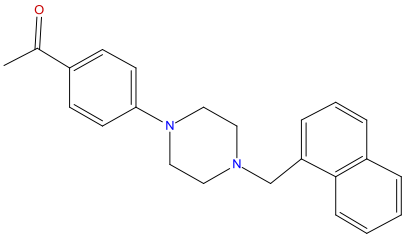

APL079 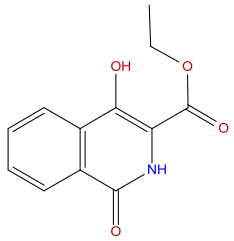

APL080 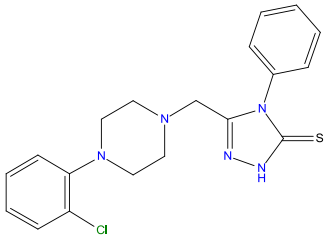

APL081 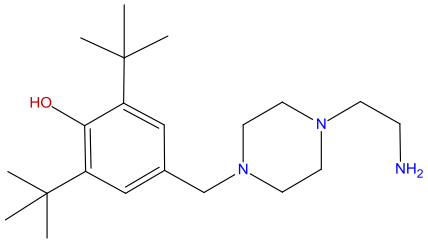

APL082 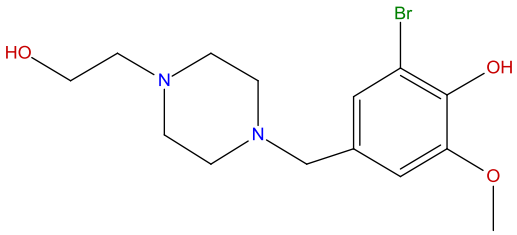

APL083 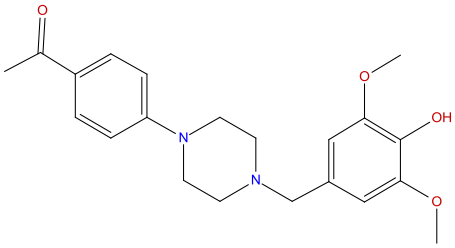

APL084 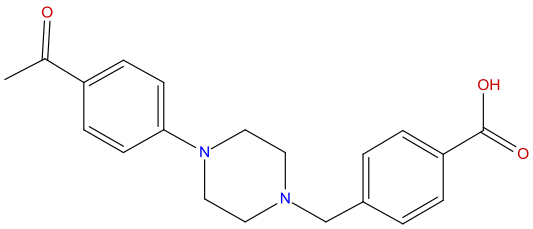

APL085 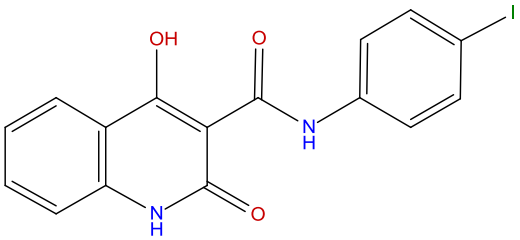

APL086 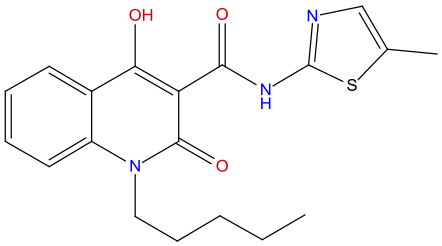

APL087 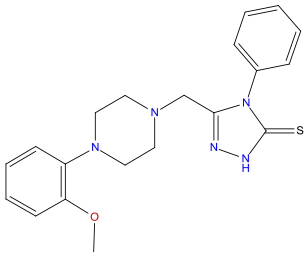

APL088 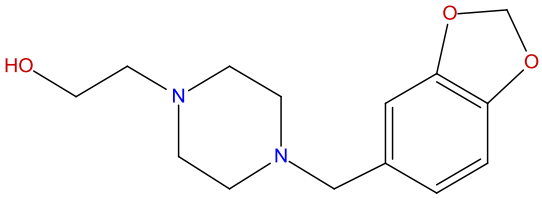

APL089 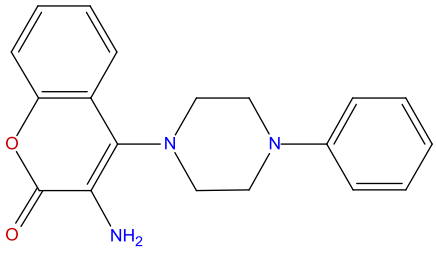

APL090 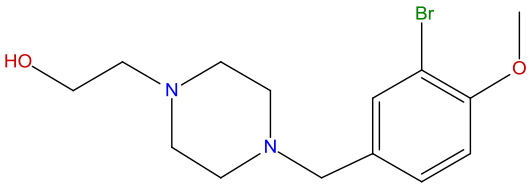

APL091 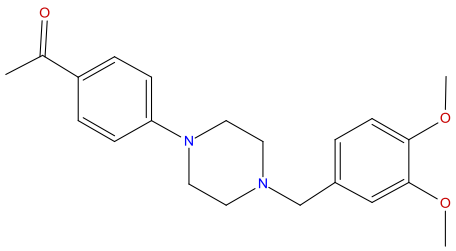

APL092 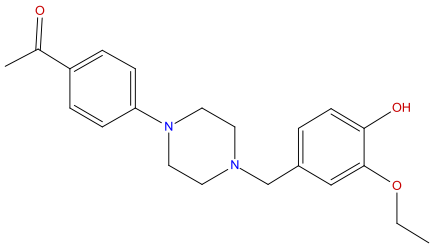

APL093 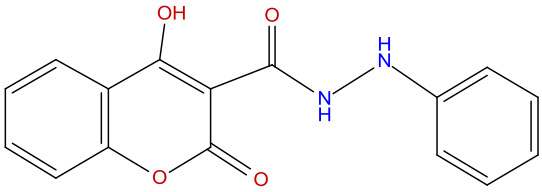

APL094 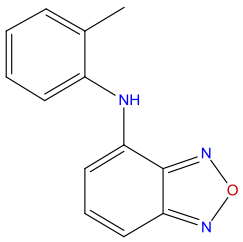

APL095 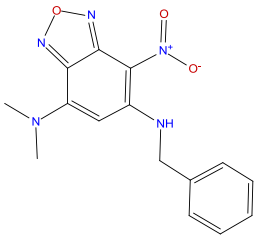

APL096 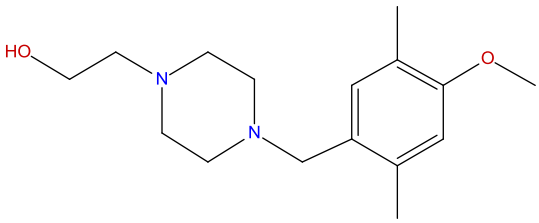

APL097 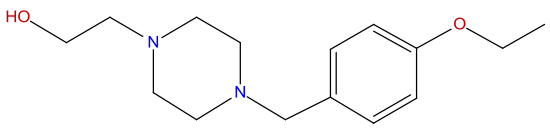

APL098 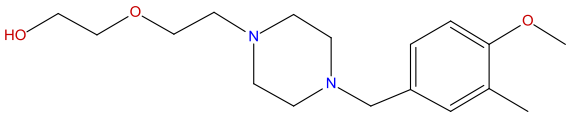

APL099 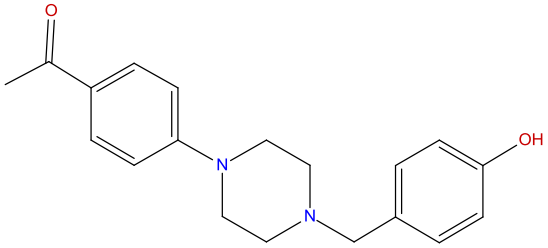

APL100 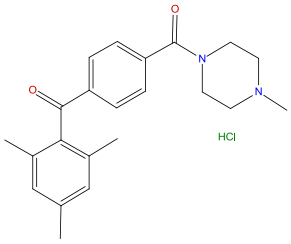

APL101 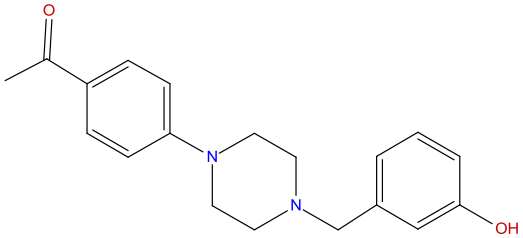

APL102 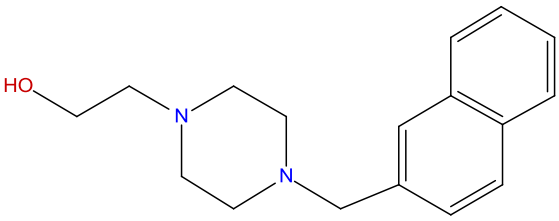

APL103

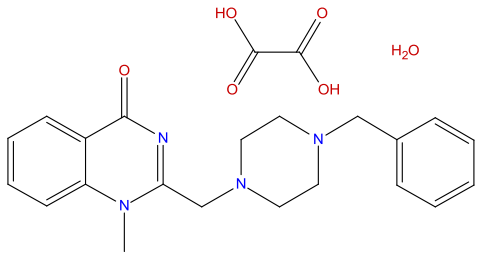

APL104

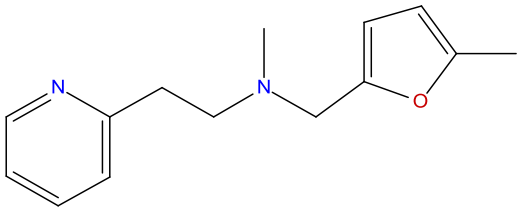

APL105

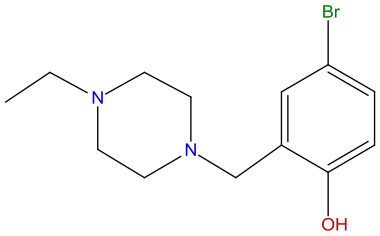

APL106

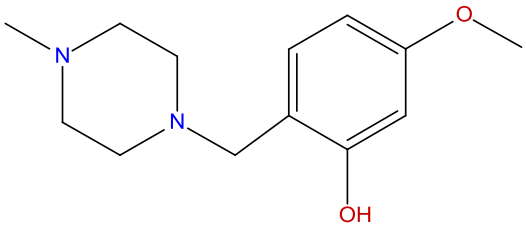

APL107

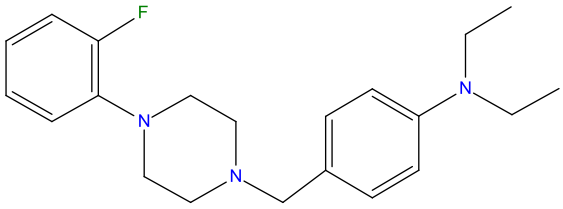

APL108

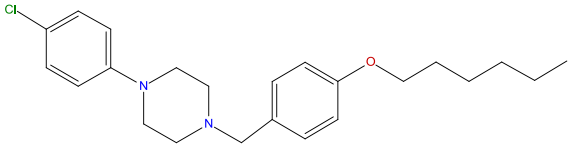

APL109 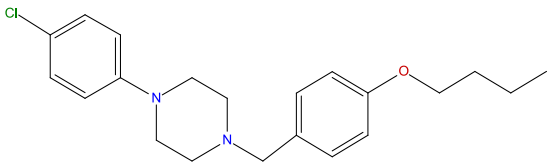

APL110 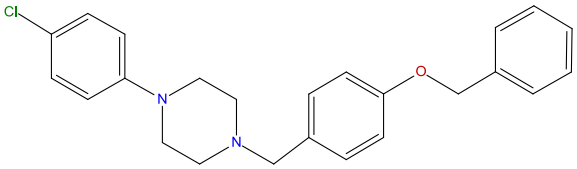

APL111 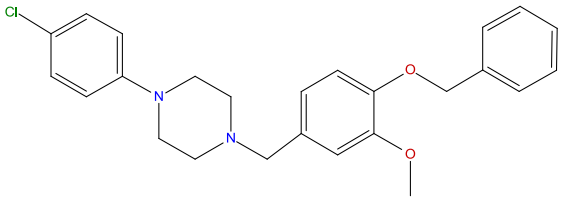

APL112 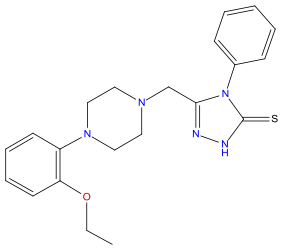

APL113 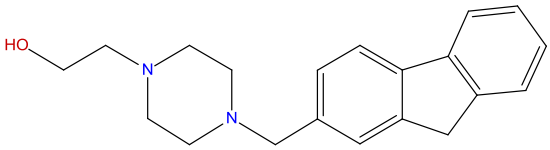

APL114 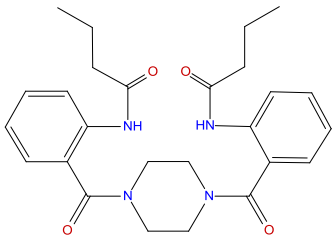

APL115 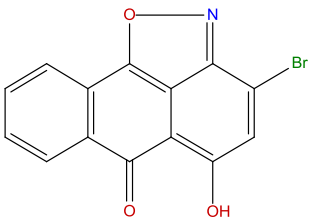

APL116 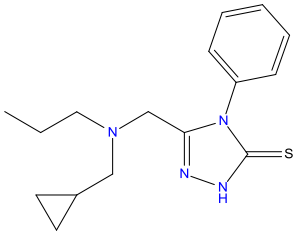

APL117 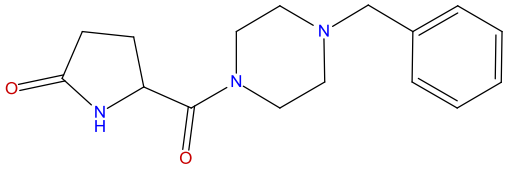

APL118 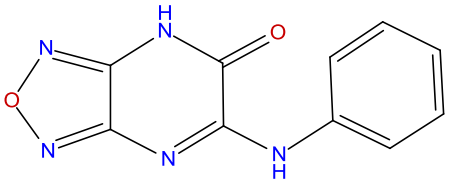

APL119 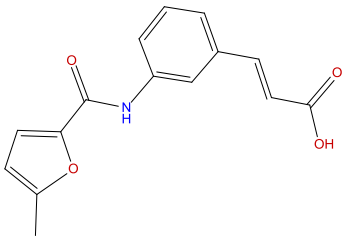

APL120 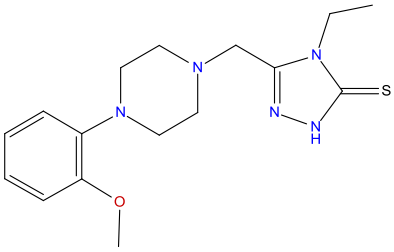

APL121 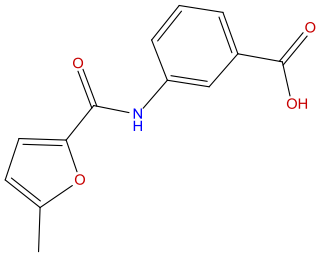

APL122 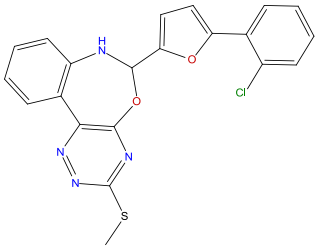

APL123 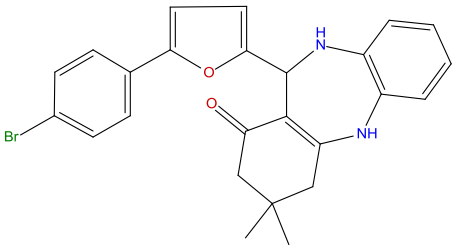

APL124 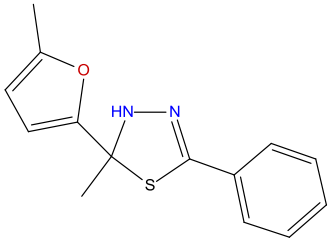

APL125 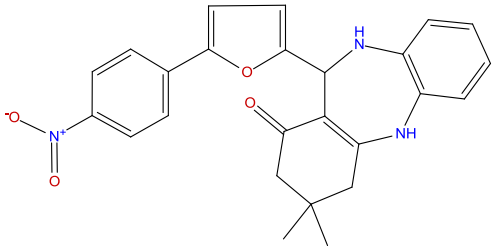

APL126 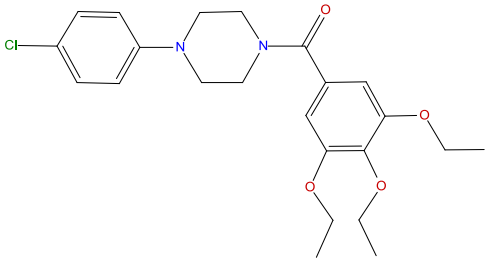

APL127

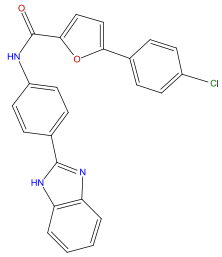

APL128

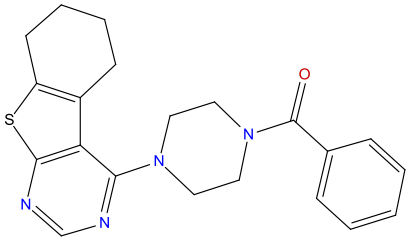

APL129

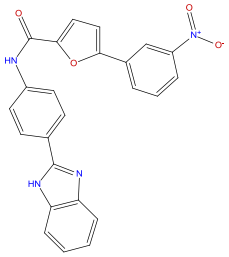

APL130

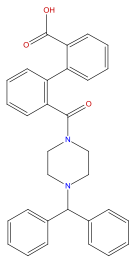

APL131

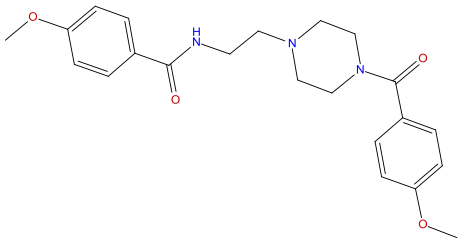

APL132

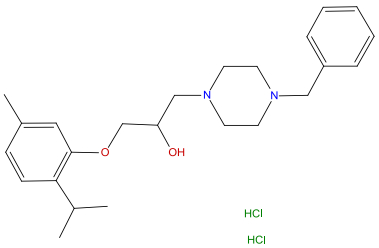

APL133 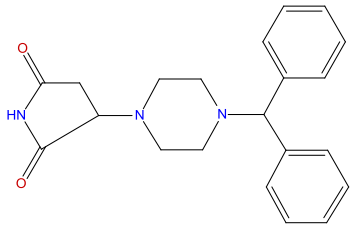

APL134 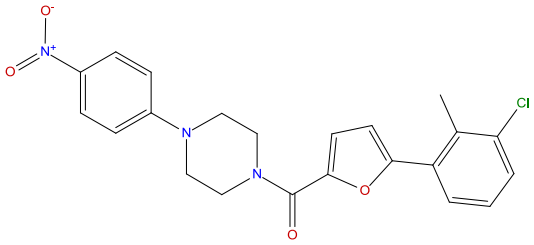

APL135 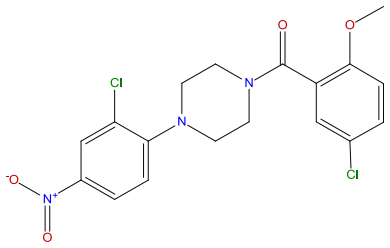

APL136 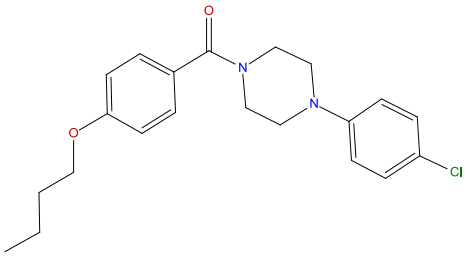

APL137 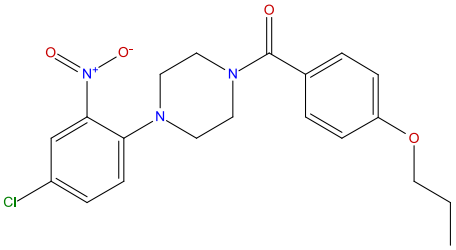

APL138 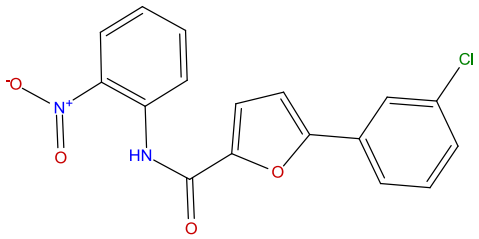

APL139 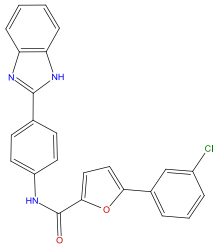

APL140 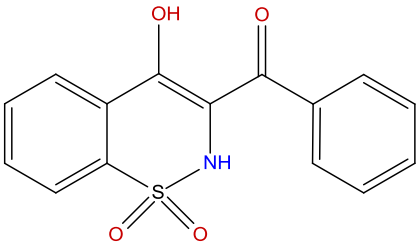

APL141 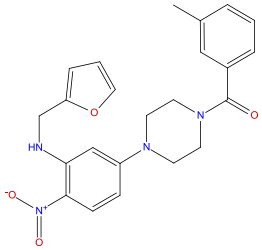

APL142 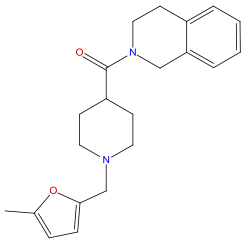

APL143 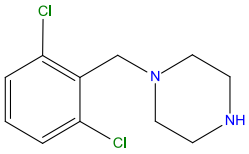

APL144 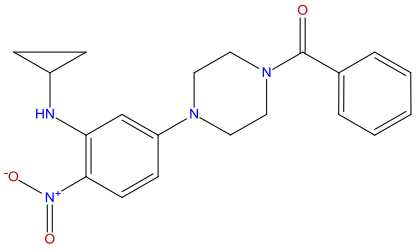

APL145 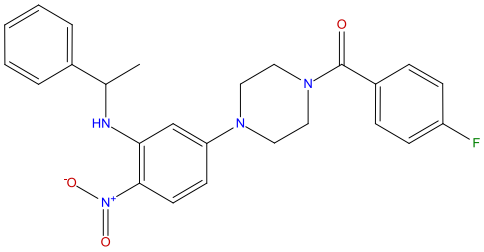

APL146 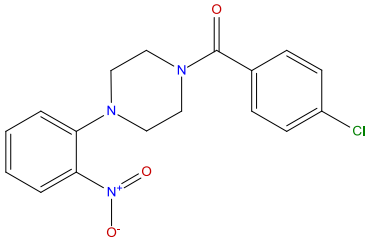

APL147 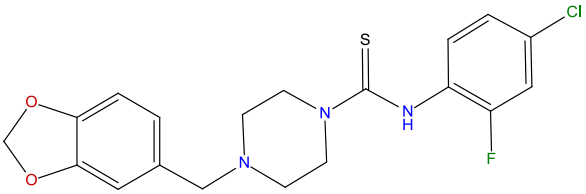

APL148 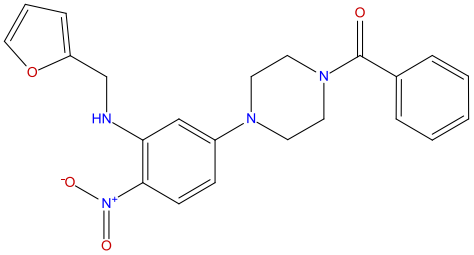

APL149 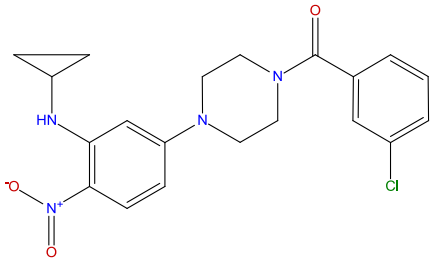

APL150 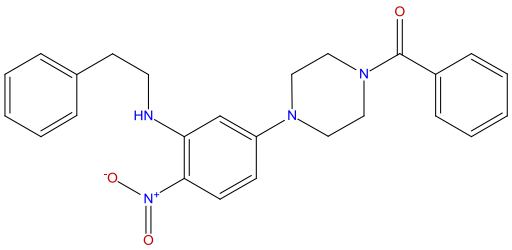

APL151 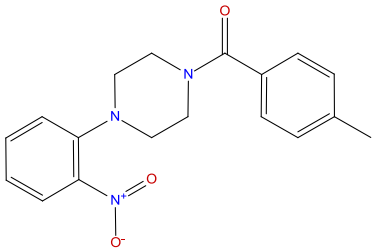

APL152 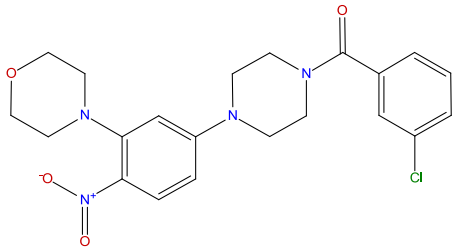

APL153 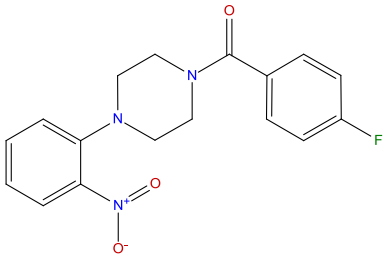

APL154 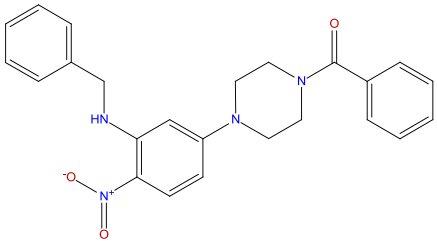

APL155 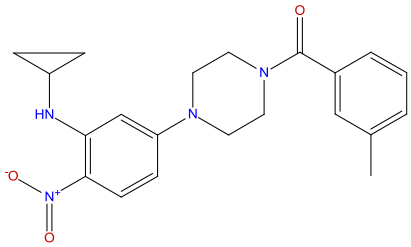

APL156 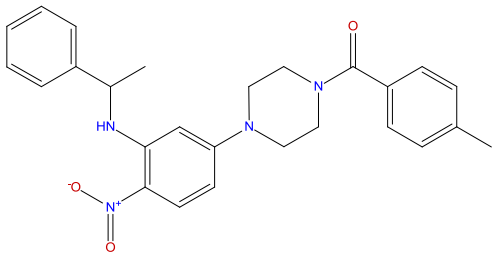

APL157 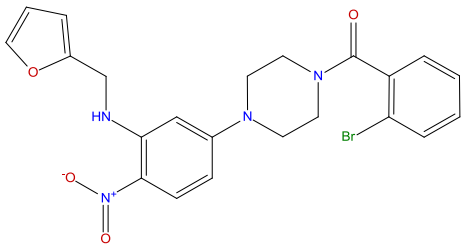

APL158 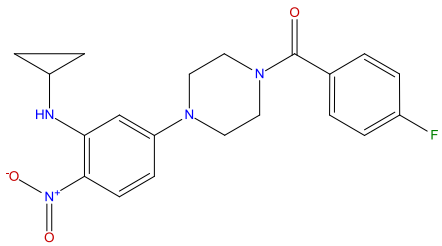

APL159 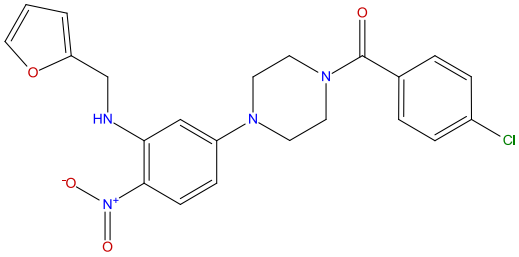

APL160 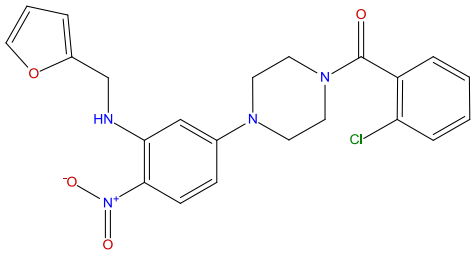

APL161 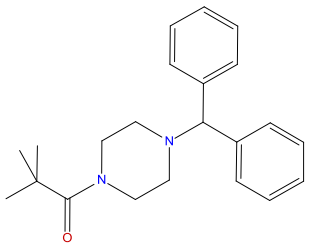

APL162 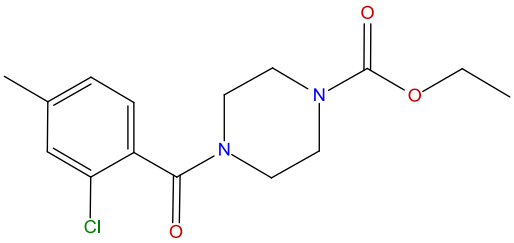

APL163

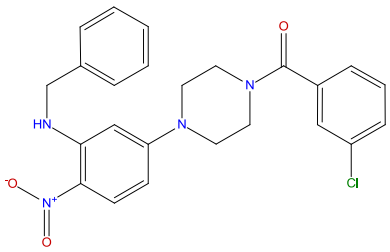

APL164

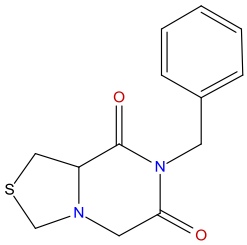

APL165

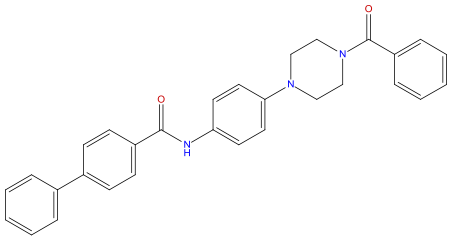

APL166

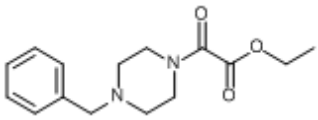

APL167

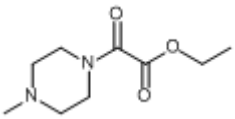

APL168

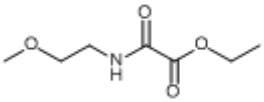

APL169

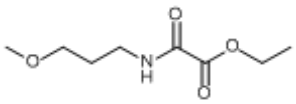

APL170

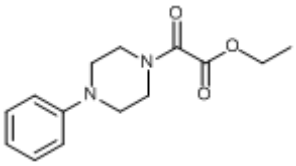

APL171

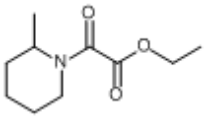

APL172

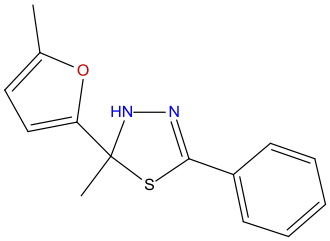

REFERENCES

An WG, Kanekal M, Simon MC, Maltepe E, Blagosklonny MV, Neckers LM. Stabilization of wild-type p53 by hypoxia-inducible factor 1alpha. Nature 1998;392(6674):405-8.

Arai T, Ogawa T, Nakamura M, Hosoya M, Ohnishi Y. Changes in hepatic enzyme activities in transgenic mice carrying human prototype c-Ha-ras gene treated with diethylnitrosamine. J Vet Med Sci 2002;64:1065 - 7.

Arnone A, Rogers PH, Hyde CC, et al. Crystallographic and chemical studies on cytosolic aspartate aminotransferase. Prog Clin Biol Res 1984;144B:171 - 93.

Arora KK, Pedersen PL. Functional significance of mitochondrial bound hexokinase in tumor cell metabolism. Evidence for preferential phosphorylation of glucose by intramitochondrially generated ATP. J Biol Chem 1988;263(33):17422-8.

Atsumi T, Chesney J, Metz C, et al. High expression of inducible 6-phosphofructo-2-kinase/fructose-2,6-bisphosphatase (iPFK-2; PFKFB3) in human cancers. Cancer Res 2002;62(20):5881-7.

Avril N, Menzel M, Dose J, et al. Glucose metabolism of breast cancer assessed by 18F-FDG PET: histologic and immunohistochemical tissue analysis. J Nucl Med 2001;42:9 - 16.

Balinsky D, Platz CE, Lewis JW. Isozyme patterns of normal, benign, and malignant human breast tissues. Cancer Res 1983;43:5895 - 901.

Baron-Delage S, Mahraoui L, Cadoret A, et al. Deregulation of hexose transporter expression in Caco-2 cells by ras and polyoma middle T oncogenes. Am J Physiol 1996;270(2 Pt 1):G314-23.

Bensaad K, Tsuruta A, Selak MA, et al. TIGAR, a p53-Inducible Regulator of Glycolysis and Apoptosis. Cell 2006;126(1):107-20.

Bensaad K, Vousden KH. p53: new roles in metabolism. Trends in cell biology 2007;17(6):286-91.

Bhaskar PT, Hay N. The Two TORCs and Akt. Developmental Cell 2007;12(4):487-502.

Bild AH, Yao G, Chang JT, et al. Oncogenic pathway signatures in human cancers as a guide to targeted therapies. Nature 2006;439:353 - 7.

Blamey RW. The design and clinical use of the Nottingham Prognostic Index in breast cancer. The Breast 1996;5:156 - 7.

Blancher C, Moore JW, Robertson N, Harris AL. Effects of ras and von Hippel-Lindau (VHL) gene mutations on hypoxia-inducible factor (HIF)-1alpha, HIF-2alpha, and vascular endothelial growth factor expression and their regulation by the phosphatidylinositol 3'-kinase/Akt signaling pathway. Cancer Res 2001;61(19):7349-55.

Bogaerts J, Cardoso F, Buyse M, et al. Gene signature evaluation as a prognostic tool: challenges in the design of the MINDACT trial. Nat Clin Pract Oncol 2006;3:540 - 51.

Bohacek RS, McMartin, C., Guida, W. C. The art and practice of structure-based drug design:a molecular modelling perspective. Med Res Rev 1996;16:3-50.

Borisov VV, Borisova SN, Kachalova GS, et al. Three-dimensional structure at 5 A resolution of cytosolic aspartate transaminase from chicken heart. J Mol Biol 1978;125:275 - 92.

Borisov VV, Borisova SN, Kachalova GS, Sosfenov NI, Voronova AA. [X-ray-structural study of aspartate transaminase at 5 A resolution]. Dokl Akad Nauk SSSR 1977;235:212 - 5.

Bos R, van Diest PJ, Groep P, Shvarts A, Greijer AE, Wall E. Expression of hypoxia-inducible factor-1alpha and cell cycle proteins in invasive breast cancer are estrogen receptor related. Breast Cancer Res 2004;6:R450 - 9.

Bosca L, Mojena M, Ghysdael J, Rousseau GG, Hue L. Expression of the v-src or v-fps oncogene increases fructose 2,6-bisphosphate in chick-embryo fibroblasts. Novel mechanism for the stimulation of glycolysis by retroviruses. Biochem J 1986;236(2):595-9.

Bowker-Kinley MM, Davis WI, Wu P, Harris RA, Popov KM. Evidence for existence of tissue-specific regulation of the mammalian pyruvate dehydrogenase complex. Biochem J 1998;329 (Pt 1):191-6.

Braunshtein AE, Arutiunian EG, Malashkevich VN, Kochkina VM, Torchinskii Iu M. Cytosol aspartate aminotransferase from the chicken heart: three-dimensional structure at 2.8 angstroms resolution and the characteristic conformation of various enzyme forms. Mol Biol (Mosk) 1985;19:196 - 208.

Brooks GA, Dubouchaud H, Brown M, Sicurello JP, Butz CE. Role of mitochondrial lactate dehydrogenase and lactate oxidation in the intracellular lactate shuttle. Proceedings of the National Academy of Sciences 1999;96(3):1129-34.

Brownlee, M., biochemistry and molecular cell biology of diabetic complications, Nature 2001; 414, 813-820

Buffa FM, Harris AL, West CM, Miller CJ. Large meta-analysis of multiple cancers reveals a common, compact and highly prognostic hypoxia metagene. Br J Cancer 2010;102(2):428-35.

Buyse M, Loi S, van't Veer L, et al. Validation and clinical utility of a 70-gene prognostic signature for women with node-negative breast cancer. J Natl Cancer Inst 2006;98:1183 - 92.

Calza S, Hall P, Auer G, et al. Intrinsic molecular signature of breast cancer in a population-based cohort of 412 patients. Breast Cancer Res 2006;8:R34.

Cameron A, Read J, Tranter R, et al. Identification and activity of a series of azole-based compounds with lactate dehydrogenase-directed anti-malarial activity. J Biol Chem 2004;279(30):31429-39.

Cao X, Fang L, Gibbs S, et al. Glucose uptake inhibitor sensitizes cancer cells to daunorubicin and overcomes drug resistance in hypoxia. Cancer Chemother Pharmacol 2007;59(4):495-505.

Cederbaum AI, Lieber CS, Beattie DS, Rubin E. Characterization of shuttle mechanisms for the transport of reducing equivalents into mitochondria. Arch Biochem Biophys 1973;158:763 - 81.

Chan DA, Sutphin PD, Denko NC, Giaccia AJ. Role of prolyl hydroxylation in oncogenically stabilized hypoxia-inducible factor-1alpha. J Biol Chem 2002;277(42):40112-7.

Chang HY, Nuyten DS, Sneddon JB, et al. Robustness, scalability, and integration of a wound-response gene expression signature in predicting breast cancer survival. Proc Natl Acad Sci USA 2005;102:3738 - 43.

Chang HY, Sneddon JB, Alizadeh AA, et al. Gene expression signature of fibroblast serum response predicts human cancer progression: similarities between tumors and wounds. PLoS Biol 2004;2:E7.

Chen C, Pore N, Behrooz A, Ismail-Beigi F, Maity A. Regulation of glut1 mRNA by hypoxia-inducible factor-1. Interaction between H-ras and hypoxia. J Biol Chem 2001;276(12):9519-25.

Chen LB. Mitochondrial membrane potential in living cells. Annu Rev Cell Biol 1988;4:155-81.

Cheng EH, Sheiko TV, Fisher JK, Craigen WJ, Korsmeyer SJ. VDAC2 inhibits BAK activation and mitochondrial apoptosis. Science 2003;301(5632):513-7.

Chesney J. 6-phosphofructo-2-kinase/fructose-2,6-bisphosphatase and tumor cell glycolysis. Curr Opin Clin Nutr Metab Care 2006;9(5):535-9.

Chesney J, Mitchell R, Benigni F, et al. An inducible gene product for 6-phosphofructo-2-kinase with an AU-rich instability element: role in tumor cell glycolysis and the Warburg effect. Proc Natl Acad Sci U S A 1999;96(6):3047-52.

Chesney J, Telang S, Yalcin A, Clem A, Wallis N, Bucala R. Targeted disruption of inducible 6-phosphofructo-2-kinase results in embryonic lethality. Biochem Biophys Res Commun 2005;331:139 - 46.

Chevrollier A, Loiseau D, Chabi B, et al. ANT2 isoform required for cancer cell glycolysis. J Bioenerg Biomembr 2005;37(5):307-16.

Chiaretti B, Casciaro A, Minotti G, Eboli ML, Galeotti T. Quantitative evaluation of the activity of the malate-aspartate shuttle in Ehrlich ascites tumor cells. Cancer Res 1979;39:2195 - 9.

Choi S-r, Beeler AB, Pradhan A, et al. Generation of Oxamic Acid Libraries: Antimalarials and Inhibitors of Plasmodium falciparum Lactate Dehydrogenase. Journal of Combinatorial Chemistry 2007;9(2):292-300.

Christofk HR, Vander Heiden MG, Harris MH, et al. The M2 splice isoform of pyruvate kinase is important for cancer metabolism and tumour growth. Nature 2008;452(7184):230-3.

Christofk HR, Vander Heiden MG, Wu N, Asara JM, Cantley LC. Pyruvate kinase M2 is a phosphotyrosine-binding protein. Nature 2008;452(7184):181-6.

Colotta F, Allavena P, Sica A, Garlanda C, Mantovani A. Cancer-related inflammation, the seventh hallmark of cancer: links to genetic instability. Carcinogenesis 2009;30(7):1073-81.

Cooper AJL, Meister A. New York: John Wiley and Sons; 1985.

Curthoys NP, Watford, M. Regulation of glutaminase activity and glutamine metabolism. Annu Rev Nutr 1995;15:133–59.

Czerniak B, Chen R, Tuziak T, et al. Expression of ras oncogene p21 protein in relation to regional spread of human breast carcinomas. Cancer 1989;63:2008-13.

Daly EB, Wind T, Jiang XM, Sun L, Hogg PJ. Secretion of phosphoglycerate kinase from tumour cells is controlled by oxygen-sensing hydroxylases. Biochim Biophys Acta 2004;1691(1):17-22.

Dang CV, Semenza GL. Oncogenic alterations of metabolism. Trends Biochem Sci 1999;24(2):68-72.

DeBerardinis RJ, Lum JJ, Hatzivassiliou G, Thompson CB. The Biology of Cancer: Metabolic Reprogramming Fuels Cell Growth and Proliferation. Cell Metabolism 2008;7(1):11-20.

DeBerardinis RJ, Mancuso A, Daikhin E, et al. Beyond aerobic glycolysis: transformed cells can engage in glutamine metabolism that exceeds the requirement for protein and nucleotide synthesis. Proc Natl Acad Sci U S A 2007;104(49):19345-50.

Deberardinis RJ, Sayed N, Ditsworth D, Thompson CB. Brick by brick: metabolism and tumor cell growth. Curr Opin Genet Dev 2008;18(1):54-61.

Deming SL, Nass SJ, Dickson RB, Trock BJ. C-myc amplification in breast cancer: a meta-analysis of its occurrence and prognostic relevance. Br J Cancer 2000;83:1688 - 95.

Desai KV, Xiao N, Wang W, et al. Initiating oncogenic event determines gene-expression patterns of human breast cancer models. Proc Natl Acad Sci USA 2002;99:6967 - 72.

Espinosa E, Vara JA, Redondo A, et al. Breast cancer prognosis determined by gene expression profiling: a quantitative reverse transcriptase polymerase chain reaction study. J Clin Oncol 2005;23:7278 - 85.

Fan C, Oh DS, Wessels L, et al. Concordance among gene-expression-based predictors for breast cancer. N Engl J Med 2006;355:560 - 9.

Fantin VR, St-Pierre J, Leder P. Attenuation of LDH-A expression uncovers a link between glycolysis, mitochondrial physiology, and tumor maintenance. Cancer Cell 2006;9(6):425-34.

Farmer P, Bonnefoi H, Becette V, et al. Identification of molecular apocrine breast tumours by microarray analysis. Oncogene 2005;24:4660 - 71.

Feliu JE, Hue L, Hers HG. Hormonal control of pyruvate kinase activity and of gluconeogenesis in isolated hepatocytes. Proc Natl Acad Sci U S A 1976;73(8):2762-6.

Fitzpatrick SM, Cooper AJ, Duffy TE. Use of beta-methylene-D, L-aspartate to assess the role of aspartate aminotransferase in cerebral oxidative metabolism. J Neurochem 1983;41:1370 - 83.

Foekens JA, Atkins D, Zhang Y, et al. Multicenter validation of a gene expression-based prognostic signature in lymph node-negative primary breast cancer. J Clin Oncol 2006;24:1665 - 71.

Forbes NS, Meadows AL, Clark DS, Blanch HW. Estradiol stimulates the biosynthetic pathways of breast cancer cells: Detection by metabolic flux analysis. Metabolic Engineering 2006;8(6):639-52.

Ford GC, Eichele G, Jansonius JN. Three-dimensional structure of a pyridoxal-phosphate-dependent enzyme, mitochondrial aspartate aminotransferase. Proc Natl Acad Sci USA 1980;77:2559 - 63.

Funasaka T, Yanagawa T, Hogan V, Raz A. Regulation of phosphoglucose isomerase/autocrine motility factor expression by hypoxia. Faseb J 2005;19(11):1422-30.

Gallagher SM, Castorino JJ, Wang D, Philp NJ. Monocarboxylate transporter 4 regulates maturation and trafficking of CD147 to the plasma membrane in the metastatic breast cancer cell line MDA-MB-231. Cancer Res 2007;67:4182 - 9.

Gatenby RA, Gillies RJ. Why do cancers have high aerobic glycolysis? Nat Rev Cancer 2004;4(11):891-9.

Gauthier T, Denis-Pouxviel C, Murat JC. Mitochondrial hexokinase from differentiated and undifferentiated HT29 colon cancer cells: effect of some metabolites on the bound/soluble equilibrium. Int J Biochem 1990;22(4):419-23.

Gelbfish GA, Davidson, A.L., Kopel, S., Schreibman, B., Gelbfish, J.S., Degenshein, G.A., Herz, B.L., Cunningham, J.N. Relationship of estrogen and progesterone receptors to prognosis in breast cancer. Ann Surg 1988;207(1):75-9.

Giatromanolaki A, Sivridis E, Gatter KC, Turley H, Harris AL, Koukourakis MI. Lactate dehydrogenase 5 (LDH-5) expression in endometrial cancer relates to the activated VEGF/VEGFR2(KDR) pathway and prognosis. Gynecol Oncol 2006;103(3):912-8.

Goldberg EB, Colowick SP. The role of glycolysis in the growth of tumor cells. 3. Lactic dehydrogenase as the site of action of oxamate on the growth of cultured cells. J Biol Chem 1965;240:2786 - 90.

Goldberg EB, Nitowsky HM, Colowick SP. The role of glycolysis in the growth of tumor cells. Iv. The basis of glucose toxicity in oxamate-treated, cultured cells. J Biol Chem 1965;240:2791 - 6.

Goodrich DW. The retinoblastoma tumor-suppressor gene, the exception that proves the rule. Oncogene 2006;25(38):5233-43.

Gordan JD, Thompson CB, Simon MC. HIF and c-Myc: Sibling Rivals for Control of Cancer Cell Metabolism and Proliferation. Cancer Cell 2007;12(2):108-13.

Gould GW, Holman GD. The glucose transporter family: structure, function and tissue-specific expression. Biochem J 1993;295 (Pt 2):329-41.

Granchi C. BS, Macchia M., Minutolo F. Inhibitors of Lactate Dehydrogenase Isoforms and their Therapeutic Potentials Current Med Chem 2010;17(7):672-97.

Graven KK, Bellur D, Klahn BD, Lowrey SL, Amberger E. HIF-2alpha regulates glyceraldehyde-3-phosphate dehydrogenase expression in endothelial cells. Biochim Biophys Acta 2003;1626(1-3):10-8.

Greenhouse WV, Lehninger AL. Occurrence of the malate-aspartate shuttle in various tumor types. Cancer Res 1976;36:1392 - 6.

Greiner EF, Guppy, M., Brand, K. Glucose is essential for proliferation and the glycolytic enzyme induction that provokes a transition to glycolytic energy production. J Biol Chem 1994;269:31484-90.

Gudi R, Melissa MB-K, Kedishvili NY, Zhao Y, Popov KM. Diversity of the Pyruvate Dehydrogenase Kinase Gene Family in Humans. Journal of Biological Chemistry 1995;270(48):28989-94.

Halestrap AP, Doran E, Gillespie JP, O'Toole A. Mitochondria and cell death. Biochem Soc Trans 2000;28(2):170-7.

Halestrap AP, Gillespie JP, O'Toole A, Doran E. Mitochondria and cell death: a pore way to die? Symp Soc Exp Biol 2000;52:65-80.

Hanahan D, Folkman J. Patterns and Emerging Mechanisms of the Angiogenic Switch during Tumorigenesis. Cell 1996;86(3):353-64.

Hanahan D, Weinberg RA. The Hallmarks of Cancer. Cell 2000;100(1):57-70.

Hanahan D, Weinberg Robert A. Hallmarks of Cancer: The Next Generation. Cell 2011;144(5):646-74.

Hara MR, Agrawal N, Kim SF, et al. S-nitrosylated GAPDH initiates apoptotic cell death by nuclear translocation following Siah1 binding. Nat Cell Biol 2005;7(7):665-74.

Harris AL. Hypoxia--a key regulatory factor in tumour growth. Nat Rev Cancer 2002;2(1):38-47.

Harris CC. p53 tumor suppressor gene: From the basic research laboratory to the clinic - An abridged historical perspective. Carcinogenesis 1996;17(6):1187-98.

Hedges LV, Olkin I. London: Academic Press; 1985.

Heidelberger C, Chauduri, N.K., Danneberg, P., Mooren, D., Griesbach, L., Duschinsky, R., Schnitzer, R.J., Pleven, E., Scheiner, J. Fluorinated Pyrimidines, A New Class of Tumour-Inhibitory Compounds. Nature 1957;179:663-6.

Hennipman A, Smits J, van Oirschot B, et al. Glycolytic enzymes in breast cancer, benign breast disease and normal breast tissue. Tumour Biol 1987;8(5):251-63.

Hennipman A, van Oirschot BA, Smits J, Rijksen G, Staal GE. Glycolytic enzyme activities in breast cancer metastases. Tumour Biol 1988;9(5):241-8.

Hewitt CO, Eszes CM, Sessions RB, et al. A general method for relieving substrate inhibition in lactate dehydrogenases. Protein Engineering 1999;12(6):491-6.

Higgins GS, Harris, A.L., Prevo, R., Helleday, T., McKenna, W.G., Buffa, F.M. Overexpression of POLQ confers a poor prognosis in early breast cancer patients. Oncotarget 2010;1(3):175-84.

Hilf R, Rector WD, Orlando RA. Multiple molecular forms of lactate dehydrogenase and glucose 6-phosphate dehydrogenase in normal and abnormal human breast tissues. Cancer 1976;37:1825 - 30.

Hirono Y, Fushida S, Yonemura Y, Yamamoto H, Watanabe H, Raz A. Expression of autocrine motility factor receptor correlates with disease progression in human gastric cancer. Br J Cancer 1996;74(12):2003-7.

Houston SK, Piña, Y., Murray, T.G., Boutrid, H., Cebulla, C., Schefler, A.C., Shi, W., Celdran, M., Feuer, W., Merchan, J., Lampidis, T.J. Novel retinoblastoma treatment avoids chemotherapy: the effect of optimally timed combination therapy with angiogenic and glycolytic inhibitors on LHBETATAG retinoblastoma tumors. Clin Opthalmol 2011;5:129-37.

Hu Z, Fan C, Oh DS, et al. The molecular portraits of breast tumors are conserved across microarray platforms. BMC Genomics 2006;7:96.

Huang E, Ishida S, Pittman J, et al. Gene expression phenotypic models that predict the activity of oncogenic pathways. Nat Genet 2003;34:226 - 30.

Hue L, Rousseau GG. Fructose 2,6-bisphosphate and the control of glycolysis by growth factors, tumor promoters and oncogenes. Adv Enzyme Regul 1993;33:97-110.

Huisgen R. 1,3 Dipolar Cycloaddtions- Introduction, Survey, Mechanism. Book, ed Padwa 1984.

Hussien R, Brooks GA. Mitochondrial and plasma membrane lactate transporter and lactate dehydrogenase isoform expression in breast cancer cell lines. Physiological Genomics 1999;43(5):255-64.

Ivascu A, Kubbies M. Rapid Generation of Single-Tumor Spheroids for High-Throughput Cell Function and Toxicity Analysis. Journal of Biomolecular Screening 2006;11(8):922-32.

Ivshina AV, George J, Senko O, et al. Genetic reclassification of histologic grade delineates new clinical subtypes of breast cancer. Cancer Res 2006;66:10292 - 301.

Jager J, Moser M, Sauder U, Jansonius JN. Crystal structures of Escherichia coli aspartate aminotransferase in two conformations. Comparison of an unliganded open and two liganded closed forms. J Mol Biol 1994;239:285 - 305.

Jeffery CJ, Barry T, Doonan S, Petsko GA, Ringe D. Crystal structure of Saccharomyces cerevisiae cytosolic aspartate aminotransferase. Protein Sci 1998;7:1380 - 7.

Jiang BH, Agani F, Passaniti A, Semenza GL. V-SRC induces expression of hypoxia-inducible factor 1 (HIF-1) and transcription of genes encoding vascular endothelial growth factor and enolase 1: involvement of HIF-1 in tumor progression. Cancer Res 1997;57(23):5328-35.

Jones, G.; Willet, P.; Glen, R. C.; Leach, A. R.; Taylor, R. J. Mol. Biol 1997;267:727-748.

Jurica MS, Mesecar A, Heath PJ, Shi W, Nowak T, Stoddard BL. The allosteric regulation of pyruvate kinase by fructose-1,6-bisphosphate. Structure 1998;6(2):195-210.

Kamitori S, Okamoto A, Hirotsu K, et al. Three-dimensional structures of aspartate aminotransferase from Escherichia coli and its mutant enzyme at 2.5 A resolution. J Biochem 1990;108:175 - 84.

Kanno T, Sudo K, Takeuchi I, et al. Hereditary deficiency of lactate dehydrogenase M-subunit. Clin Chim Acta 1980;108(2):267-76.

Ke Q, Costa M. Hypoxia-inducible factor-1 (HIF-1). Mol Pharmacol 2006;70(5):1469-80.

Kim JW, Dang CV. Multifaceted roles of glycolytic enzymes. Trends Biochem Sci 2005;30(3):142-50.

Kim JW, Dang CV. Cancer's molecular sweet tooth and the Warburg effect. Cancer Res 2006;66(18):8927-30.

Kim J-w, Tchernyshyov I, Semenza GL, Dang CV. HIF-1-mediated expression of pyruvate dehydrogenase kinase: A metabolic switch required for cellular adaptation to hypoxia. Cell Metabolism 2006;3(3):177-85.

Knight ZA, Lin H, Shokat KM. Targeting the cancer kinome through polypharmacology. Nat Rev Cancer 2010;10(2):130-7.

Ko YH, Smith BL, Wang Y, et al. Advanced cancers: eradication in all cases using 3-bromopyruvate therapy to deplete ATP. Biochem Biophys Res Commun 2004;324(1):269-75.

Kole HK, Resnick RJ, Van Doren M, Racker E. Regulation of 6-phosphofructo-1-kinase activity in ras-transformed rat-1 fibroblasts. Arch Biochem Biophys 1991;286(2):586-90.

Kolobova E, Tuganova A, Boulatnikov I, Popov KM. Regulation of pyruvate dehydrogenase activity through phosphorylation at multiple sites. Biochem J 2001;358(Pt 1):69-77.

Korkola JE, DeVries S, Fridlyand J, et al. Differentiation of lobular versus ductal breast carcinomas by expression microarray analysis. Cancer Res 2003;63:7167 - 75.

Koukourakis MI, Giatromanolaki A, Sivridis E, et al. Lactate dehydrogenase-5 (LDH-5) overexpression in non-small-cell lung cancer tissues is linked to tumour hypoxia, angiogenic factor production and poor prognosis. Br J Cancer 2003;89(5):877-85.

Koukourakis MI, Giatromanolaki A, Sivridis E, et al. Lactate dehydrogenase-5 (LDH-5) overexpression in non-small-cell lung cancer tissues is linked to tumour hypoxia, angiogenic factor production and poor prognosis. Br J Cancer 2003;89(5):877-85.

Koukourakis MI, Giatromanolaki A, Sivridis E, Gatter KC, Harris AL. Pyruvate dehydrogenase and pyruvate dehydrogenase kinase expression in non small cell lung cancer and tumor-associated stroma. Neoplasia 2005;7(1):1-6.

Koukourakis MI, Giatromanolaki A, Sivridis E, Gatter KC, Harris AL. Lactate dehydrogenase 5 expression in operable colorectal cancer: strong association with survival and activated vascular endothelial growth factor pathway--a report of the Tumour Angiogenesis Research Group. J Clin Oncol 2006;24(26):4301-8.

Krumbhaar EB. Role of the blood and bone marrow in certain forms of gas poisoning. JAMA 1919;72:39-41.

Lawen A, Ly JD, Lane DJ, Zarschler K, Messina A, De Pinto V. Voltage-dependent anion-selective channel 1 (VDAC1)--a mitochondrial protein, rediscovered as a novel enzyme in the plasma membrane. Int J Biochem Cell Biol 2005;37(2):277-82.

Le A, Cooper CR, Gouw AM, et al. Inhibition of lactate dehydrogenase A induces oxidative stress and inhibits tumor progression. Proceedings of the National Academy of Sciences 2010;107(5):2037-42.

Levine AJ, Oren M. The first 30 years of p53: growing ever more complex. Nat Rev Cancer 2009;9(10):749-58.

Lewis BC, Prescott JE, Campbell SE, Shim H, Orlowski RZ, Dang CV. Tumor induction by the c-Myc target genes rcl and lactate dehydrogenase A. Cancer Res 2000;60:6178 - 83.

Lim K-H, Counter CM. Reduction in the requirement of oncogenic Ras signaling to activation of PI3K/AKT pathway during tumor maintenance. Cancer Cell 2005;8(5):381-92.

Liotta LA, Mandler R, Murano G, et al. Tumor cell autocrine motility factor. Proc Natl Acad Sci U S A 1986;83(10):3302-6.

Lobo C, Ruiz-Bellido MA, Aledo JC, MÃ¡rquez J, NÃºÃ±ez De Castro I, Alonso FJ. Inhibition of glutaminase expression by antisense mRNA decreases growth and tumourigenicity of tumour cells. Biochem J 2000;348(2):257-61.

Loncaster JA, Harris AL, Davidson SE, et al. Carbonic anhydrase (CA IX) expression, a potential new intrinsic marker of hypoxia: correlations with tumor oxygen measurements and prognosis in locally advanced carcinoma of the cervix. Cancer Res 2001;61(17):6394-9.

Lopez-Alarcon L, Eboli ML. Oxidation of reduced cytosolic nicotinamide adenine dinucleotide by the malate-aspartate shuttle in the K-562 human leukemia cell line. Cancer Res 1986;46:5589 - 91.

Lu H, Dalgard CL, Mohyeldin A, McFate T, Tait AS, Verma A. Reversible inactivation of HIF-1 prolyl hydroxylases allows cell metabolism to control basal HIF-1. J Biol Chem 2005;280(51):41928-39.

Ma XJ, Wang Z, Ryan PD, et al. A two-gene expression ratio predicts clinical outcome in breast cancer patients treated with tamoxifen. Cancer Cell 2004;5:607 - 16.

Macheda ML, Rogers S, Best JD. Molecular and cellular regulation of glucose transporter (GLUT) proteins in cancer. J Cell Physiol 2005;202(3):654-62.

Maglott D, Ostell J, Pruitt KD, Tatusova T. Entrez Gene: gene-centered information at NCBI. Nucleic Acids Res 2007(35 Database):D26 - 31.

Maqc C, Shi L, Reid LH, et al. The MicroArray Quality Control (MAQC) project shows inter- and intraplatform reproducibility of gene expression measurements. Nat Biotechnol 2006;24:1151 - 61.

Markert CL, Shaklee JB, Whitt GS. Evolution of a gene. Multiple genes for LDH isozymes provide a model of the evolution of gene structure, function and regulation. Science 1975;189:102 - 14.

Maschek G, Savaraj N, Priebe W, et al. 2-Deoxy-d-glucose Increases the Efficacy of Adriamycin and Paclitaxel in Human Osteosarcoma and Non-Small Cell Lung Cancers In Vivo. Cancer Research 2004;64(1):31-4.

Mathupala SP, Heese C, Pedersen PL. Glucose catabolism in cancer cells. The type II hexokinase promoter contains functionally active response elements for the tumor suppressor p53. J Biol Chem 1997;272(36):22776-80.

Mathupala SP, Ko YH, Pedersen PL. Hexokinase II: cancer's double-edged sword acting as both facilitator and gatekeeper of malignancy when bound to mitochondria. Oncogene 2006;25(34):4777-86.

Mathupala SP, Rempel A, Pedersen PL. Aberrant glycolytic metabolism of cancer cells: a remarkable coordination of genetic, transcriptional, post-translational, and mutational events that lead to a critical role for type II hexokinase. J Bioenerg Biomembr 1997;29(4):339-43.

Matsuno T, Hirai, H. Glutamine synthetase and glutaminase activities in various hepatoma cells. Biochem Int 1989;19(2):219-25.

Mazurek S. The Tumour Metabolome. Anticancer Res 2003;23(2A):1149-54.

Mazurek S, Boschek CB, Hugo F, Eigenbrodt E. Pyruvate kinase type M2 and its role in tumor growth and spreading. Seminars in Cancer Biology 2005;15(4):300-8.

McKenna MC, Waagepetersen HS, Schousboe A, Sonnewald U. Neuronal and astrocytic shuttle mechanisms for cytosolic-mitochondrial transfer of reducing equivalents: current evidence and pharmacological tools. Biochem Pharmacol 2006;71:399 - 407.

McLachlan G, Peel D. New York: John Wiley & Sons, Inc; 2000.

McNeill LA, Hewitson KS, Gleadle JM, et al. The use of dioxygen by HIF prolyl hydroxylase (PHD1). Bioorganic & Medicinal Chemistry Letters 2002;12(12):1547-50.

Miccoli L, Oudard S, Sureau F, Poirson F, Dutrillaux B, Poupon MF. Intracellular pH governs the subcellular distribution of hexokinase in a glioma cell line. Biochem J 1996;313 (Pt 3):957-62.

Miller LD, Smeds J, George J, et al. An expression signature for p53 status in human breast cancer predicts mutation status, transcriptional effects, and patient survival. Proc Natl Acad Sci USA 2005;102:13550 - 5.

Minchenko A, Leshchinsky I, Opentanova I, et al. Hypoxia-inducible factor-1-mediated expression of the 6-phosphofructo-2-kinase/fructose-2,6-bisphosphatase-3 (PFKFB3) gene. Its possible role in the Warburg effect. J Biol Chem 2002;277(8):6183-7.

Minchenko O, Opentanova I, Caro J. Hypoxic regulation of the 6-phosphofructo-2-kinase/fructose-2,6-bisphosphatase gene family (PFKFB-1-4) expression in vivo. FEBS Lett 2003;554(3):264-70.

Minotti G, Menna P, Salvatorelli E, Cairo G, Gianni L. Anthracyclines: Molecular Advances and Pharmacologic Developments in Antitumor Activity and Cardiotoxicity. Pharmacological Reviews 2004;56(2):185-229.

Miyakis S, Sourvinos G, Spandidos DA. Differential expression and mutation of the ras family genes in human breast cancer. Biochem Biophys Res Commun 1998;251:609 - 12.

Mori N, Glunde K, Takagi T, Raman V, Bhujwalla ZM. Choline kinase down-regulation increases the effect of 5-fluorouracil in breast cancer cells. Cancer Res 2007;67:11284 - 90.

Muesch A, Hartmann E, Rohde K, Rubartelli A, Sitia R, Rapoport TA. A novel pathway for secretory proteins? Trends Biochem Sci 1990;15(3):86-8.

Murakami T, Nishiyama T, Shirotani T, et al. Identification of two enhancer elements in the gene encoding the type 1 glucose transporter from the mouse which are responsive to serum, growth factor, and oncogenes. J Biol Chem 1992;267(13):9300-6.

Naderi A, Teschendorff AE, Barbosa-Morais NL, et al. A gene-expression signature to predict survival in breast cancer across independent data sets. Oncogene 2007;26:1507 - 16.

Nagai MA, Sonohara S, Brentani MM. Estrogen control of lactate dehydrogenase isoenzyme-5 in human breast cancer. Int J Cancer 1988;41:10 - 6.

Nagy E, Henics T, Eckert M, Miseta A, Lightowlers RN, Kellermayer M. Identification of the NAD(+)-binding fold of glyceraldehyde-3-phosphate dehydrogenase as a novel RNA-binding domain. Biochem Biophys Res Commun 2000;275(2):253-60.

Nagy I, Hirka G, Kurcz M, Anda E, Baranyai P. The role of estrogens in the regulation of lactate dehydrogenase activity and its submolecular organization in rat anterior pituitary. Endokrinologie 1978;71:1 - 12.

Okamoto A, Higuchi T, Hirotsu K, Kuramitsu S, Kagamiyama H. X-ray crystallographic study of pyridoxal 5'-phosphate-type aspartate aminotransferases from Escherichia coli in open and closed form. J Biochem 1994;116:95 - 107.

Okar DA, Lange AJ. Fructose-2,6-bisphosphate and control of carbohydrate metabolism in eukaryotes. Biofactors 1999;10(1):1-14.

Okar DA, Manzano A, Navarro-Sabate A, Riera L, Bartrons R, Lange AJ. PFK-2/FBPase-2: maker and breaker of the essential biofactor fructose-2,6-bisphosphate. Trends Biochem Sci 2001;26(1):30-5.

Okar DA, Wu C, Lange AJ. Regulation of the regulatory enzyme, 6-phosphofructo-2-kinase/fructose-2,6-bisphosphatase. Adv Enzyme Regul 2004;44:123-54.

Onodera, K; Satou, K; Hirota, HJ, Chem Inf Model 2007; 47(4); 1609-18.

Paik S, Shak S, Tang G, et al. International Genomics Consortium. A multigene assay to predict recurrence of tamoxifen-treated, node-negative breast cancer. N Engl J Med 2004;351:2817 - 26.

Paik S, Tang G, Shak S, et al. Gene expression and benefit of chemotherapy in women with node-negative, estrogen receptor-positive breast cancer. J Clin Oncol 2006;24:3726 - 34.

Pangborn, A. B.; Giardello, M. A.; Grubbs, R.H.; Rosen, R. K.; Timmers, F. J

Organometallics;1996, 15, 1518.

Papaconstantinou J, Colowick SP. Published abstract. Federation Proc 1957;16:230.

Papaconstantinou J, Colowick SP. The role of glycolysis in the growth of tumor cells. II. The effect of oxamic acid on the growth of HeLa cells in tissue culture. J Biol Chem 1961;236:285 - 8.

Parkkila S, Rajaniemi H, Parkkila AK, et al. Carbonic anhydrase inhibitor suppresses invasion of renal cancer cells in vitro. Proc Natl Acad Sci U S A 2000;97(5):2220-4.

Pastorino JG, Hoek JB. Hexokinase II: the integration of energy metabolism and control of apoptosis. Curr Med Chem 2003;10(16):1535-51.

Pawitan Y, Bjohle J, Amler L, et al. Gene expression profiling spares early breast cancer patients from adjuvant therapy: derived and validated in two population-based cohorts. Breast Cancer Res 2005;7:R953 - 64.

Pedersen PL, Mathupala S, Rempel A, Geschwind JF, Ko YH. Mitochondrial bound type II hexokinase: a key player in the growth and survival of many cancers and an ideal prospect for therapeutic intervention. Biochim Biophys Acta 2002;1555(1-3):14-20.

Pelicano H, Martin DS, Xu RH, Huang P. Glycolysis inhibition for anticancer treatment. Oncogene 2006;25(34):4633-46.

Pérez de Heredia F, Wood I, Trayhurn P. Hypoxia stimulates lactate release and modulates monocarboxylate transporter (MCT1, MCT2, and MCT4) expression in human adipocytes. Pflügers Archiv European Journal of Physiology 2010;459(3):509-18.

Perou CM, Sorlie T, Eisen MB, et al. Molecular portraits of human breast tumours. Nature 2000;406:747 - 52.

Perucho M, Salas J, Salas ML. Study of the interaction of glyceraldehyde-3-phosphate dehydrogenase with DNA. Biochim Biophys Acta 1980;606(2):181-95.

Pfaffl MW. A new mathematical model for relative quantification in real-time RT-PCR. Nucleic Acids Research 2001;29(9):45.

Pinheiro C, Reis RM, Ricardo S, Longatto-Filho A, Schmitt F, Baltazar F. Expression of monocarboxylate transporters 1, 2, and 4 in human tumours and their association with CD147 and CD44. Journal of biomedicine & biotechnology 2010;2010:427694.

Ponzio G. Dioximes XCVII. Gazzetta Chimica Italiana 1932;62:1025-34.

Pretsch W, Chatterjee B, Favor J, Merkle S, Sandulache R. Molecular, genetic and biochemical characterization of lactate dehydrogenase-A enzyme activity mutations in Mus musculus. Mamm Genome 1998;9(2):144-9.

Price JT, Tiganis T, Agarwal A, Djakiew D, Thompson EW. Epidermal growth factor promotes MDA-MB-231 breast cancer cell migration through a phosphatidylinositol 3'-kinase and phospholipase C-dependent mechanism. Cancer Res 1999;59(21):5475-8.

Price NT, Jackson, V.N, Halestrap, A.P. Cloning and sequencing of four new mammalian monocarboxylate transporter (MCT) homologues confirms the existence of a transporter family with an ancient past. Biochem J 1998;329(2):321-8.

Ramanathan A, Wang C, Schreiber SL. Perturbational profiling of a cell-line model of tumorigenesis by using metabolic measurements. Proc Natl Acad Sci USA 2005;102:5992 - 7.

Rankin EB, Giaccia AJ. The role of hypoxia-inducible factors in tumorigenesis. Cell Death Differ 2008;15(4):678-85.

Read JA, Winter VJ, Eszes CM, Sessions RB, Brady RL. Structural basis for altered activity of M- and H-isozyme forms of human lactate dehydrogenase. Proteins: Structure, Function, and Bioinformatics 2001;43(2):175-85.

Rej R. Measurement of aspartate aminotransferase activity: effects of oxamate. Clin Chem 1979;25:555 - 9.

Rempel A, Bannasch P, Mayer D. Differences in expression and intracellular distribution of hexokinase isoenzymes in rat liver cells of different transformation stages. Biochim Biophys Acta 1994;1219(3):660-8.

Rempel A, Mathupala SP, Griffin CA, Hawkins AL, Pedersen PL. Glucose catabolism in cancer cells: amplification of the gene encoding type II hexokinase. Cancer Res 1996;56(11):2468-71.

Richardson AL, Wang ZC, De Nicolo A, et al. X chromosomal abnormalities in basal-like human breast cancer. Cancer Cell 2006;9:121 - 32.

Rider MH, Bertrand L, Vertommen D, Michels PA, Rousseau GG, Hue L. 6-phosphofructo-2-kinase/fructose-2,6-bisphosphatase: head-to-head with a bifunctional enzyme that controls glycolysis. Biochem J 2004;381(Pt 3):561-79.

Robey RB, Hay N. Is Akt the "Warburg kinase"?--Akt-energy metabolism interactions and oncogenesis. Seminars in Cancer Biology 2009;19(1):25-31.

Rogers S, Macheda ML, Docherty SE, et al. Identification of a novel glucose transporter-like protein-GLUT-12. Am J Physiol Endocrinol Metab 2002;282(3):E733-8.

Romond EH, Perez EA, Bryant J, et al. Tamoxifen for early breast cancer: an overview of the randomised trials. Early Breast Cancer Trialists' Collaborative Group

Trastuzumab plus adjuvant chemotherapy for operable HER2-positive breast cancer. Lancet 1998;351:1451 - 67.

Rosenberg BVC, L.; Krigas, T. Inhibition of cell division in Escheria coli by electrolysis products from a platinum electrode. Nature 1965;205(4972):698-9.

Sakaki T, Yamada K, Otsuki H, Yuguchi T, Kohmura E, Hayakawa T. Brief exposure to hypoxia induces bFGF mRNA and protein and protects rat cortical neurons from prolonged hypoxic stress. Neurosci Res 1995;23(3):289-96.

Sakakibara R, Kato M, Okamura N, et al. Characterization of a human placental fructose-6-phosphate, 2-kinase/fructose-2,6-bisphosphatase. J Biochem 1997;122(1):122-8.

Sakakibara R, Uemura M, Hirata T, Okamura N, Kato M. Human placental fructose-6-phosphate,2-kinase/fructose-2,6-bisphosphatase: its isozymic form, expression and characterization. Biosci Biotechnol Biochem 1997;61(11):1949-52.

Sanchez-Martinez C, Aragon JJ. Analysis of phosphofructokinase subunits and isozymes in ascites tumor cells and its original tissue, murine mammary gland. FEBS Lett 1997;409(1):86-90.

Saunders PA, Chen RW, Chuang DM. Nuclear translocation of glyceraldehyde-3-phosphate dehydrogenase isoforms during neuronal apoptosis. J Neurochem 1999;72(3):925-32.

Schroeder MA, Atherton HJ, Ball DR, et al. Real-time assessment of Krebs cycle metabolism using hyperpolarized 13C magnetic resonance spectroscopy. The FASEB Journal 2009;23(8):2529-38.

Seagroves TN, Ryan HE, Lu H, et al. Transcription factor HIF-1 is a necessary mediator of the pasteur effect in mammalian cells. Mol Cell Biol 2001;21(10):3436-44.

Seidner G, Alvarez MG, Yeh JI, et al. GLUT-1 deficiency syndrome caused by haploinsufficiency of the blood-brain barrier hexose carrier. Nat Genet 1998;18(2):188-91.

Semenza GL. Tumor metabolism: cancer cells give and take lactate. The Journal of Clinical Investigation 2008;118(12):3835-7.

Semenza GL, Jiang BH, Leung SW, et al. Hypoxia response elements in the aldolase A, enolase 1, and lactate dehydrogenase A gene promoters contain essential binding sites for hypoxia-inducible factor 1. J Biol Chem 1996;271(51):32529-37.

Semenza GL, Roth PH, Fang HM, Wang GL. Transcriptional regulation of genes encoding glycolytic enzymes by hypoxia-inducible factor 1. J Biol Chem 1994;269:23757 - 63.

Shay JW, Bacchetti S. A survey of telomerase activity in human cancer. European Journal of Cancer 1997;33(5):787-91.

Sheremetev, A.B., Organometallic Synthesis in the Furazan Series. Part 2. Furazanylethanes. ChemInform, 2003, 34(41)

Shi Y, Massagué J. Mechanisms of TGF-[beta] Signaling from Cell Membrane to the Nucleus. Cell 2003;113(6):685-700.

Shim H, Dolde C, Lewis BC, et al. c-Myc transactivation of LDH-A: implications for tumor metabolism and growth. Proc Natl Acad Sci U S A 1997;94(13):6658-63.

Shinohara Y, Ishida T, Hino M, Yamazaki N, Baba Y, Terada H. Characterization of porin isoforms expressed in tumor cells. Eur J Biochem 2000;267(19):6067-73.

Sirover MA. New insights into an old protein: the functional diversity of mammalian glyceraldehyde-3-phosphate dehydrogenase. Biochim Biophys Acta 1999;1432(2):159-84.

Sirover MA. New nuclear functions of the glycolytic protein, glyceraldehyde-3-phosphate dehydrogenase, in mammalian cells. J Cell Biochem 2005;95(1):45-52.

Smith DL, Almo SC, Toney MD, Ringe D. 2.8-A-resolution crystal structure of an active-site mutant of aspartate aminotransferase from Escherichia coli. Biochemistry 1989;28:8161 - 7.

Sonveaux P, Vegran F, Schroeder T, et al. Targeting lactate-fueled respiration selectively kills hypoxic tumor cells in mice. J Clin Invest 2008.

Sorlie T, Perou CM, Tibshirani R, et al. Gene expression patterns of breast carcinomas distinguish tumor subclasses with clinical implications. Proc Natl Acad Sci USA 2001;98:10869 - 74.

Sorlie T, Tibshirani R, Parker J, et al. Repeated observation of breast tumor subtypes in independent gene expression data sets. Proc Natl Acad Sci USA 2003;100:8418 - 23.

Sotiriou C, Neo SY, McShane LM, et al. Breast cancer classification and prognosis based on gene expression profiles from a population-based study. Proc Natl Acad Sci USA 2003;100:10393 - 8.

Sotiriou C, Wirapati P, Loi S, et al. Gene expression profiling in breast cancer: understanding the molecular basis of histologic grade to improve prognosis. J Natl Cancer Inst 2006;98:262 - 72.

Sparano JA. TAILORx: trial assigning individualized options for treatment (Rx). Clin Breast Cancer 2006;7:347 - 50.

Sporn MB. The war on cancer. The Lancet 1996;347(9012):1377-81.

Starling D. Two ultrastructurally distinct tubulin paracrystals induced in sea-urchin eggs by vinblastine sulphate. J Cell Sci 1976;20(1):79-89.

Sum EY, Peng B, Yu X, et al. The LIM domain protein LMO4 interacts with the cofactor CtIP and the tumor suppressor BRCA1 and inhibits BRCA1 activity. J Biol Chem 2002;277:7849 - 56.

Sun AQ, Yuksel KU, Jacobson TM, Gracy RW. Isolation and characterization of human glucose-6-phosphate isomerase isoforms containing two different size subunits. Arch Biochem Biophys 1990;283(1):120-9.

Sundararaj KP, Wood RE, Ponnusamy S, et al. Rapid shortening of telomere length in response to ceramide involves the inhibition of telomere binding activity of nuclear glyceraldehyde-3-phosphate dehydrogenase. J Biol Chem 2004;279(7):6152-62.

Szucs G, Toth I, Barna T, Nagy Z, Horvath G, Kiss JI. [Role of surgery, its results and complications, in the combined treatment of primary gastric non-Hodgkin lymphoma]. Magy Seb 2000;53(6):253-8.

Taetle R, Rosen F, Abramson I, Venditti J, Howell S. Use of nude mouse xenografts as preclinical drug screens: in vivo activity of established chemotherapeutic agents against melanoma and ovarian carcinoma xenografts. Cancer Treat Rep 1987;71:297 - 304.

Talawar MB, Sivabalan R, Senthilkumar N, Prabhu G, Asthana SN. Synthesis, characterization and thermal studies on furazan- and tetrazine-based high energy materials. Journal of Hazardous Materials 2004;113(1-3):11-25.

Talmadge JE, Fidler IJ. AACR Centennial Series: The Biology of Cancer Metastasis: Historical Perspective. Cancer Research 2010;70(14):5649-69.

Telang S, Yalcin A, Clem AL, et al. Ras transformation requires metabolic control by 6-phosphofructo-2-kinase. Oncogene 2006;25(55):7225-34.

Telang S, Yalcin A, Clem AL, et al. Ras transformation requires metabolic control by 6-phosphofructo-2-kinase. Oncogene 2006;25:7225 - 34.

Tennant DA, Duran RV, Gottlieb E. Targeting metabolic transformation for cancer therapy. Nat Rev Cancer 2010;10(4):267-77.

Terenius L. Anti-oestrogens and breast cancer. Eur J Cancer 1971;7(1):57-64.

Teschendorff AE, Miremadi A, Pinder SE, Ellis IO, Caldas C. An immune response gene expression module identifies a good prognosis subtype in estrogen receptor negative breast cancer. Genome Biol 2007;8:R157.

Teschendorff AE, Naderi A, Barbosa-Morais NL, et al. A consensus prognostic gene expression classifier for ER positive breast cancer. Genome Biol 2006;7:R101.

Thangaraju M, Carswell KN, Prasad PD, Ganapathy V. Colon cancer cells maintain low levels of pyruvate to avoid cell death caused by inhibition of HDAC1/HDAC3. Biochem J 2009;417(1):379-89.

Therneau TM. Rochester, MN: Mayo Clinic Foundation; 1999.

Thornburg J, Nelson K, Clem B, et al. Targeting aspartate aminotransferase in breast cancer. Breast Cancer Research 2008;10(5):R84.

Tsutsumi S, Hogan V, Nabi IR, Raz A. Overexpression of the autocrine motility factor/phosphoglucose isomerase induces transformation and survival of NIH-3T3 fibroblasts. Cancer Res 2003;63(1):242-9.

Van Schaftingen E, Hue L, Hers HG. Fructose 2,6-bisphosphate, the probably structure of the glucose- and glucagon-sensitive stimulator of phosphofructokinase. Biochem J 1980;192(3):897-901.

van Wijk R, van Solinge WW. The energy-less red blood cell is lost: erythrocyte enzyme abnormalities of glycolysis. Blood 2005;106(13):4034-42.

Vander Heiden MG, Cantley LC, Thompson CB. Understanding the Warburg Effect: The Metabolic Requirements of Cell Proliferation. Science 2009;324(5930):1029-33.

van't Veer LJ, Dai H, Vijver MJ, et al. Gene expression profiling predicts clinical outcome of breast cancer. Nature 2002;415:530 - 6.

Vijver MJ, He YD, van't Veer LJ, et al. A gene-expression signature as a predictor of survival in breast cancer. N Engl J Med 2002;347:1999 - 2009.

Voet D, Voet J. Metabolism: Glycolysis. Biochemistry. 1995:444 - 76.

Vora S, Halper JP, Knowles DM. Alterations in the activity and isozymic profile of human phosphofructokinase during malignant transformation in vivo and in vitro: transformation- and progression-linked discriminants of malignancy. Cancer Res 1985;45(7):2993-3001.

Walker RA, Wilkinson N. p21 ras protein expression in benign and malignant human breast. J Pathol 1988;156:147 - 53.

Wang X, Howell CP, Chen F, Yin J, Jiang Y, Steve LT. Chapter 6 Gossypol-A Polyphenolic Compound from Cotton Plant. In: Advances in Food and Nutrition Research: Academic Press; 2009:215-63.

Wang Y, Klijn JG, Zhang Y, et al. Gene-expression profiles to predict distant metastasis of lymph-node-negative primary breast cancer. Lancet 2005;365:671 - 9.

Wani M, Taylor, H., Wall, M., Coggon, P., McPhail, A. Plant antitumor agents. VI. The isolation and structure of taxol, a novel antileukemic and antitumor agent from Taxus brevifolia. J Am Chem Soc 1971;93(9):2325-7.

Warburg O. On the origin of cancer cells. Science 1956;123(3191):309-14.

Watanabe H, Takehana K, Date M, Shinozaki T, Raz A. Tumor cell autocrine motility factor is the neuroleukin/phosphohexose isomerase polypeptide. Cancer Res 1996;56(13):2960-3.

Watson DM, Elton RA, Jack WJ, Dixon JM, Chetty U, Miller WR. The H-ras oncogene product p21 and prognosis in human breast cancer. Breast Cancer Res Treat 1991;17:161 - 9.

Wellen KE, Lu C, Mancuso A, et al. The hexosamine biosynthetic pathway couples growth factor-induced glutamine uptake to glucose metabolism. Genes & Development 2010;24(24):2784-99.

Whitfield ML, George LK, Grant GD, Perou CM. Common markers of proliferation. Nat Rev Cancer 2006;6:99 - 106.

Wiechert W. 13C Metabolic Flux Analysis. Metabolic Engineering 2001;3(3):195-206.

Wigfield SM, Winter SC, Giatromanolaki A, Taylor J, Koukourakis ML, Harris AL. PDK-1 regulates lactate production in hypoxia and is associated with poor prognosis in head and neck squamous cancer. Br J Cancer 2008;98(12):1975-84.

Wilkinson JH, Walter SJ. Oxamate as a differential inhibitor of lactate dehydrogenase isoenzymes. Enzyme 1972;13:170 - 6.

Wirapati P, Sotiriou C, Kunkel S, et al. Meta-analysis of gene expression profiles in breast cancer: toward a unified understanding of breast cancer subtyping and prognosis signatures. Breast Cancer Research 2008;10(4):R65.

Wu G, Aoyama C, Young SG, Vance DE. Early embryonic lethality caused by disruption of the gene for choline kinase alpha, the first enzyme in phosphatidylcholine biosynthesis. J Biol Chem 2008;283:1456 - 62.

Xie H, Valera VA, Merino MJ, et al. LDH-A inhibition, a therapeutic strategy for treatment of hereditary leiomyomatosis and renal cell cancer. Molecular Cancer Therapeutics 2009;8(3):626-35.

Xu W, Seiter K, Feldman E, Ahmed T, Chiao JW. The differentiation and maturation mediator for human myeloid leukemia cells shares homology with neuroleukin or phosphoglucose isomerase. Blood 1996;87(11):4502-6.

Yamagata M, Hasuda K, Stamato T, Tannock IF. The contribution of lactic acid to acidification of tumours: studies of variant cells lacking lactate dehydrogenase. Br J Cancer 1998;77(11):1726-31.

Yeung S, Pan J, Lee MH. Roles of p53, Myc and HIF-1 in Regulating Glycolysis — the Seventh Hallmark of Cancer. Cellular and Molecular Life Sciences 2008;65(24):3981-99.

Younes M, Lechago LV, Somoano JR, Mosharaf M, Lechago J. Wide expression of the human erythrocyte glucose transporter Glut1 in human cancers. Cancer Res 1996;56(5):1164-7.

Yu AC, Schousboe A, Hertz L. Metabolic fate of 14C-labeled glutamate in astrocytes in primary cultures. J Neurochem 1982;39:954 - 60.

Yu Y, Deck JA, Hunsaker LA, et al. Selective active site inhibitors of human lactate dehydrogenases A4, B4, and C4. Biochemical Pharmacology 2001;62(1):81-9.

Zaid H, Abu-Hamad S, Israelson A, Nathan I, Shoshan-Barmatz V. The voltage-dependent anion channel-1 modulates apoptotic cell death. Cell Death Differ 2005;12(7):751-60.

Zamora-Leon SP, Golde DW, Concha, II, et al. Expression of the fructose transporter GLUT5 in human breast cancer. Proc Natl Acad Sci U S A 1996;93(5):1847-52.

Zha X, Wang F, Wang Y, Lactate Dehydrogenase B Is Critical for Hyperactive mTOR-mediated Tumorigenesis, Cancer Research, 2011;71:13-18

Zheng L, Roeder RG, Luo Y. S phase activation of the histone H2B promoter by OCA-S, a coactivator complex that contains GAPDH as a key component. Cell 2003;114(2):255-66.

Zong W-X, Ditsworth D, Bauer DE, Wang Z-Q, Thompson CB. Alkylating DNA damage stimulates a regulated form of necrotic cell death. Genes & Development 2004;18(11):1272-82.